Intra and inter individual variation of the 3-D scapulo-humeral rhythm during elevation of the arm in 'the scapular plane'

J.H. de Groot, Lab. of Measurement and Control, Delft Un. of Technology, Mekelweg 2, 2628CD, Delft, The Netherlands.

The scapulo-humeral rhythm is a clinical parameter used to quantify kinematic disorders or to determine the success of medical treatment. Inman et al., Poppen and Walker and others, published 2-D scapulo-humeral rhythms. The rhythms range from $2.27 \leq \Delta\theta_A/\Delta\theta_{TH} \leq 3.25$ ($\Delta\theta_A$: arm elevation, $\Delta\theta_{TH}$: scapular rotation). It can be shown that the resolution of this scapulo-humeral rhythm is very low, due to the projection from 3-D movements to 2-D planes (De Groot 1995).

In this study the 3-D scapulo-humeral rhythm is recorded during the elevation of the arm in the (scapular-)plane, rotated 30° anterior from the frontal (coronal) plane. The accuracy of the applied palpation method (Pronk and Van der Helm) is determined. The intra-individual motoric noise and the inter-individual variance is estimated.

Methods

The subjects (n=5, male, average age 25 years), standing with feet, hips and head in fixed positions, performed an arm elevation in the scapular plane (10 positions). The three-dimensional position of the skeletal landmarks of the humerus (Medial and lateral condyles [Em,El] and the glenoid [GH]) and the scapula (Acromioclavicular joint [AC], Angulus Acromialis [AA], Trigonum Spinae [TS], Angulus Inferior [AI]) are determined by means of palpation and subsequent digitization of the landmarks except for GH. The position of GH is estimated from the scapular skeletal landmarks (Rozendaal 1995). The scapular axes are defined by AA, TS and AI (figure 1).

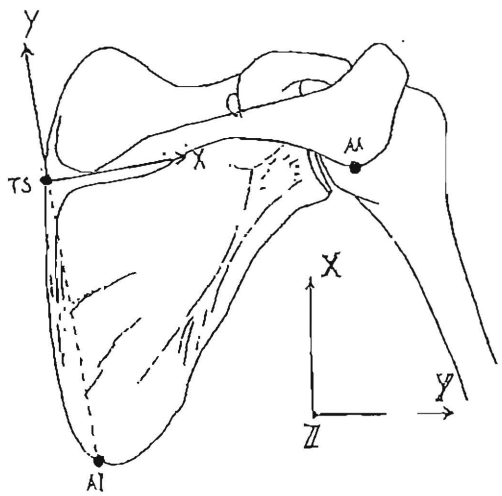

Figure 1: Definition of the local and the global axes. The scapular skeletal landmarks are in the plane of the paper.

Cardanic angles are calculated subsequently around the Y *(AA-protraction)*, Z' *(spinal elevation)* and X''-axis *(spinal rotation)*. The reference position is aligned with the right-handed global co-ordinate system.

The palpation error E_p, expressed in the local scapular co-ordinates is experimentally determined. The scapula orientation $[O_s]$ is determined by the 9 co-ordinates of AA,TS and AI.

$$O_s = f(p_i) \text{ for } i = 1, \ldots, 9 \text{ co-ordinates} \qquad (1)$$

The variance on the O_s due to the palpation error E_p is calculated from $f(p)$ by:

$$\text{var}(O_s) = \sum_{i=1}^{9} \left(\frac{\partial f}{\partial p_i} \right)^2 \times E_i^2 \qquad (2)$$

Intra-individual and inter-individual variance on the cardanic angles is determined at 4 intervals of 45° humerus elevation.

Results

The standard error on the individual coordinates of the skeletal landmarks are about 4mm or smaller resulting in a s.d. of less then 3°.

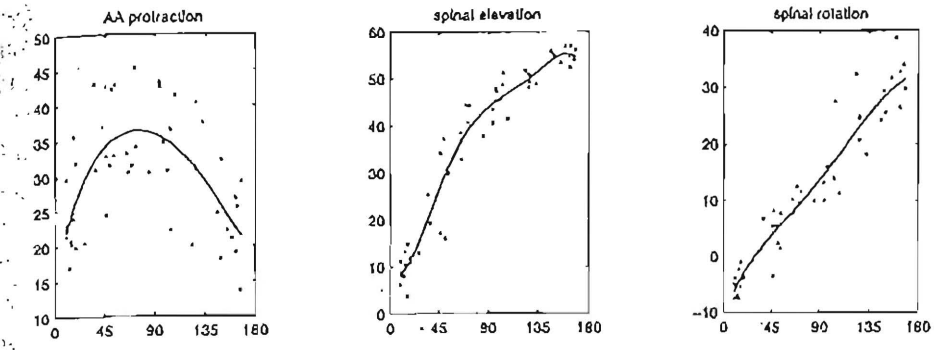

Figure 2: Average movement [deg] of the scapula during arm elevation [0-180°] expressed in 3 cardanic angles [Y,Z',X"] for n=1 subjects.

The dots in figure 2 show the results of five recordings of a single subject. A fifth order polynomial is estimated (solid line) and the intra-individual variance is calculated at 4 equal intervals of 45°. The same procedure is used to calculate the inter-individual variance. The results are shown in figure 3.

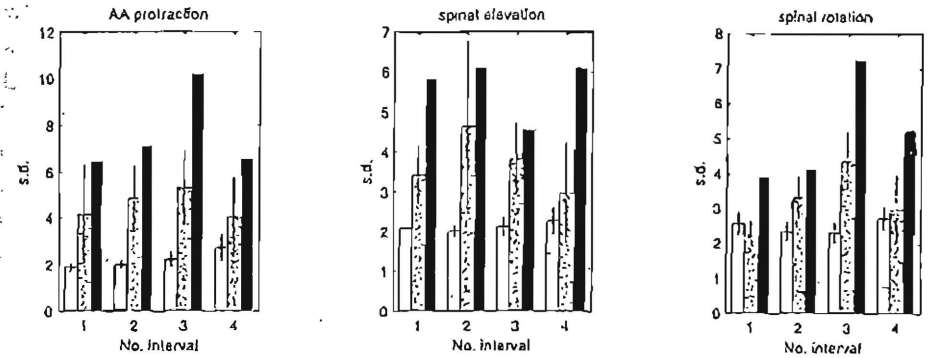

Figure 3: The overall results of the standard error (s.d.) on each of the cardanic rotations at 4 intervals of 45° arm elevation. white: palpation inaccuracy; dotted: intra-individual variance; solid: inter-individual variance.

When assumed that variances (sd^2) add linearly, it can be concluded that about 20% of the inter-individual variance is explained by the palpation error, 35% is explained by motoric noise and the residual 45% is caused by morphologic and motoric differences between the subjects.

Conclusions

The three dimensional digitization of skeletal landmarks by means of palpation is an accurate means of determining the spatial scapulo-humeral rhythm. Each of the three cardanic angles can be used as a clinical parameter in the follow up a treatment. Due to major inter-individual differences of scapulo-humeral rhythms, a deviation of a 'normal pattern' must be relatively large in order to classify a kinematic disorder.

References

De Groot J.H. 1995. Scapulo-humeral rhythm: A dynamic study. Submitted to J. Clinical Biomechanics.

Inman VT, Saunders JB, Abbot LC, 1944. Observations on the function of the shoulder joint. J. Bone and Joint Surgery 26A: 1-30

Poppen NK, Walker PS, 1976. Normal and abnormal motion of the shoulder. J.Bone and Joint Surgery 58A: 195-200

Pronk GM, Van der Helm FCT, 1991. The palpator, an instrument for measuring the 3-D positions of bony landmarks in a fast and easy way. J.Med.Eng.Techn. 15(1): 15-20.

Rozendaal L. 1995. Estimation of the geometrical centre of the glenohumeral joint from bony landmarks of the scapula. (in prep.

THE ANALYSIS OF GAIT DATA USING PRINCIPAL COMPONENTS

K.J. Deluzio, U.P. Wyss, P.A. Costigan, B. Zee

Clinical Mechanics Group, Kingston General Hospital
Kingston, Canada

INTRODUCTION

Osteoarthritis (OA) occurs world-wide (Altman, 1987), and is probably the most common rheumatic condition that causes disability (Dieppe, 1992). Experimental and clinical evidence suggests that maintaining normal joint loading, articular geometry and lower limb alignment are important factors supporting normal knee function (Kamibayashi, 1994). Gait analysis is slowly becoming recognised as a useful tool in understanding joint problems such as OA, and in the discerning changes after therapeutical and surgical interventions, and in artificial joint development. However, the analysis and interpretation of gait data is varied, controversial, and has hindered its application to clinical decision making (Brand 1992).

Gait data is often in temporal waveforms such as joint angles, forces, and moments measured in two or three dimensions. A common way to analyse these waveforms is to extract predefined parameters (maximums, minimums, ranges, etc.) from them and then attempt to discriminate between subject groups using statistical tests on these individual parameters. Consequently, many values from the waveforms are discarded along with potentially useful discriminatory information. As well, the choice of these parameters is somewhat arbitrary and investigators are often left with many parameters that may or may not contain useful information which leads to significant interpretation difficulties.

The proposed Modified Principal Components Method takes advantage of the complete gait waveform instead of a few individual predefined gait parameters. This method was developed in such a way that it accounts for the majority of the waveform variation through the entire gait cycle and from subject to subject so as to statistically distinguish between subjects.

METHODS

It is important to develop a method for comparing the complete gait curve between old asymptomatic subjects and OA patients in such a way that the results can be interpreted directly. The proposed modified principal components method is developed with this characteristic in mind.

Principal components analysis (PCA) simply transforms p correlated variables $\mathbf{X}=x_1,x_2,...,x_p$ (as in a time normalised gait curve sampled at each 1% from 0 to 100% of the cycle) into p new uncorrelated principal components $\mathbf{Z}=z_1,z_2,...,z_p$. The transformation is $\mathbf{Z}=\mathbf{XP}$ where the columns of $\mathbf{P}=p_1,p_2,...,p_p$ are the eigenvectors of the covariance (or correlation) matrix of $\mathbf{X}$. These eigenvectors are also called the loadings of the principal components since each z_i is a product of the original variables $\mathbf{X}$ and the loadings p_i. New observations on $\mathbf{X}$ can be transformed into principal components using these same loadings. The power of PCA is its potential to adequately represent a p-variable data set in $k<p$ dimensions. For example, a 100 point gait waveform can be reduced to 3 to 4 principal components that account for much of the variation in the original waveform. A measure variation explained is provided by the eigenvalues of the decomposition.

The reduction in dimension coupled with the removal of collinearity has eliminated two of the main difficulties in analysing gait data. The principal components can now be used to calculate multivariate confidence limits on the database $\mathbf{X}$. Hotelling's T^2 is a multivariate generalisation of the squared distance from the sample mean to an observation. If the generalised distance is too large-that is the observation is too far from

the sample mean-then that observation is rejected as being an estimate of that mean. The T^2 statistic can be calculated directly from the principal components as a weighted sum of squares.

Twenty-eight asymptomatic older subjects (ages 55-80,avg 65)were used to establish a principal component model of the flexion moment throughout the gait cycle. This model was then used to evaluate the preoperative gait of a single prospective hemi-arthroplasty patient. We demonstrate that we could, with statistical significance, identify the hemi-arthroplasty patient.

RESULTS

The flexion moment was chosen in this analysis because it has shown to reveal discriminatory information between normals and preoperative OA patients (Mikosz et al. 1994). Figure 1 displays the flexion moment for 28 older normals and 1 OA patient who later received a hemi-arthroplasty. The one and two standard deviation curves indicate the well-known significant variation in gait variables among normals. It is quite apparent that the patient's flexion moment waveform differs dramatically from the normals, yet this is difficult to indicate statistically. Only at a few point does this waveform depart beyond two standard deviation limits. Rather than choosing parameters from this curve the principal components method allowed us to describe the entire flexion moment waveform and then discriminate based on the overall pattern.

The analysis resulted in three principal components that explained 80% of the variation in the asymptomatic's flexion moment waveforms. These three principal components were then used to calculate the T^2 statistic for each subject as well as a 95% confidence limit. The flexion moment for the OA patient was introduced to the model and the T^2 statistic for this patient was found to exceed the 95% limit (Figure 2).

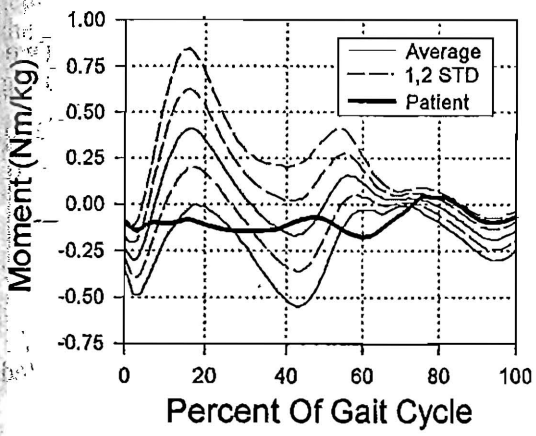

Figure 1.Moment normalised to bodymass

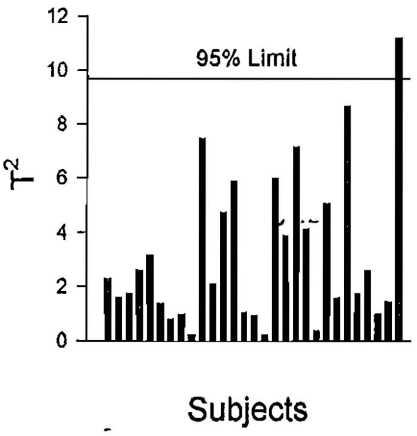

Figure 2. Hotelling's T^2 per subject

DISCUSSION

Gait analysis will find application in clinical decision making only when analysis methods can reduce the enormous quantity of data down to parsimonious measures that provide clinical interpretation. The modified principal components method described here easily identifies the patient as having an abnormal flexion moment waveform. Further examination of the loadings can then reveal the portions of the gait cycle that account for these differences.

References

Altman RD (1987) Am.J.Med. 83:65-69.

Brand RA (1992) Proceedings European Society of Biomech. Rome, Italy, 257-259.

Dieppe P (1992) "Osteoarthritis". Br.J.Rheumatol. 31:132-133.

Kamibayashi L. (1994) PhD thesis, Queen's University, Kingston, Canada.

Mikosz RP et al. (1994) Proceedings Orthopaedic Research Society, New Orleans, USA.

A NEW *IN VIVO* FINGER TENDON FORCE TRANSDUCER: CALIBRATION ISSUES

Jack Dennerlein†,††, Joel Miller‡, C.D. Mote Jr.†, and David Rempel††.

† University of California, Berkeley, Dept. of Mechanical Engineering, USA
†† University of California, San Francisco, Ergonomics Program, USA
‡ Smith Kettlewell Eye Research Institute, San Francisco, USA

INTRODUCTION:

Knowledge of *in vivo* tendon force is a useful tool for study of musculo-skeletal biomechanics (Komi, 1990; Hahs, 1990). The development of tendon tension (buckle) transducers has been discussed by An, *et. al.,* (1990) and Komi (1987 & 1990); however, discussions of device calibration have not considered the dynamic response of the transducer or the effects of seating of the viscoelastic tendons on the transducer. We describe a buckle transducer for finger flexor tendons and summarize its static and transient performance, addressing the issue of tendon viscoelastic properties in developing a model to predict tendon tension from the transducer output.

BUCKLE TRANSDUCER DESIGN

The transducer consisting of a 9 x 16 x 4.5 mm stainless steel frame and a removable stainless steel fulcrum, fits tendons up to 5 mm wide, 3 mm thick. Its slim profile allows easy fits inside the wrist during surgery (Fig 1). The tendon rests and self-aligns in the semicircular arches (r=2.5 mm) in the frame and fulcrum. The transducer operates by measuring the deformation of the frame through increased tension in the tendon passing over the fulcrum (Fig 1). Bending of the frame is measured with strain gauges. Because the bending load depends on tendon thickness, the calibration requires correlation between the transducer output, the applied tension and the tendon thickness (An, *et. al.,* 1990). Two 500 Ω silicon strain gauges placed on opposites sides of the frame form a half Wheatstone bridge increasing the measurement of strain created from the bending load and summing the components from both sides.

METHODS:

A 3-post caliper was fabricated to measure tendon thickness in the transducer. Two reference posts rest on the transducer and a central sliding post with a spring and locking mechanism is lowered to the top of the tendon indicating its thickness at the fulcrum.

To assess linearity, repeatability and drift, the device was supported at the ends and weights (0-14 N) were hung from the fulcrum. These direct loading tests were repeated with the transducer at 37°C. Differences were tested at 95% confidence levels with sample *t*-tests. The dynamic response of the transducer was tested by tapping the transducer with a hammer instrumented with an accelerometer with no applied load.

IN VITRO LOADING

The conversion factor (CF) model was developed using 12 fresh frozen human finger flexor tendons of different thicknesses taken from 5 hands. The tendons, mounted in a uni-axial loading machine and submerged in a 0.9% saline solution (20°C), were preconditioned with 10 loading cycles (0-50N). Data were collected during three additional loadings. Five tendon thickness measurements were recorded immediately.

The first calibration attempts indicated that tendon thickness changed during tests, affecting the CF. To study this tendon seating effect, a fresh frozen human finger flexor tendon, in a 0.9% saline solution, was loaded over 100 sinusoidal cycles. The tendon thickness was measured once every 20 cycles.

RESULTS

The transducer's output is linear ($r \geq 0.99$), repeatable (s.d.≤1%) and has no noticeable drift over 5 minutes. Difference in the gains measured at the different temperature range were not significant. The magnitude of the empirical transfer function estimation is flat until resonance at 660 rad/sec (105 Hz).

Variations in tendon thickness measurements were small (s.d.≤ 0.07 mm). The transducer's output for the three additional loading cycles was linear ($r \geq 0.99$). Over the three cycles the variation in CF was small (<1%). A least squares fit of the linear model relating CF to thickness (t) data provides the prediction $CF = 42.8 - 9.9*t$, (r=0.93) (Fig 2) with unbiased errors from 0% to 16% ($\mu = 6\%$).

This error in the CF creates a biased error in predicting the tension. Average and maximum relative errors calculated for each tendon tested ranged from 1% to 15% of scale (μ = 6%) and from 6% to 23% of scale (μ = 11%) respectively. The absolute maximum errors ranged from 0.8 N to 8.3 N (μ =3.2 N).

Figure 3 shows the change in the CF over the 100 loading cycles along with the six predicted gains based on the thickness measurements every 20 cycles. The CF increases 21% over the first 20 cycles and then 4%, 4%, 2%, and 3% for the second, third, fourth and fifth 20 cycles intervals respectively. The thickness measurements predicts an increase of 30%, 6%, 1%, 3%, and 0% for the same 20 cycles intervals.

DISCUSSION

Several processes are involved in measuring tendon tension with a buckle transducer. Of course, it is the complete input/output relationship which is of interest, but examination of the processes highlight limitations in the transducer concept. For example, it provides insight to a possible source of creep (viscoelastic properties of tendon) reported by An, *et. al.* (1990), while providing evidence that the transducer is working properly.

The assumption that tendon thickness is uniform within the transducer can contribute error in predicting the CF. One of our tendons did not have constant thickness, its twisted geometry resulting in a reduced thickness at one end. The predicted CF error for this tendon was large (13 %). Because tendons deform around the buckle during loading, thickness measurement within the transducer differ from those outside. Tendon seating (fig. 3) illustrates the necessity to measure the tendon thickness in the transducer to reduce the error.

The testing of tendons in tension requires preconditioning the tendon so that repeatable data are obtained (Woo, 1982, Viidik, 1987). Calibration of the transducer or seating of the tendon in the transducer requires similar preconditioning. The change in CF is greatly reduced after 10 cycles, and the change over the next three cycles (the ones used to create the model) is small (<1%). Over the next ten cycles it is within 6%, the error of the conversion factor prediction. Therefore pre-seating or preconditioning reduces the cycle to cycle variation in the conversion factor. The *in vivo* tendon requires the transducer to seat and therefore should be exposed to several loading cycles before thickness measurements. Future *in vivo* procedures will include pre-seating the tendon with 10 loading cycles. Ideally the design of the calibration procedure should be matched with the load cycles planned for *in vivo* testing. *In vivo* experiments will have only four loading cycles and monitoring the thickness during these experiment, as planned, can predict similar changes in the CF.

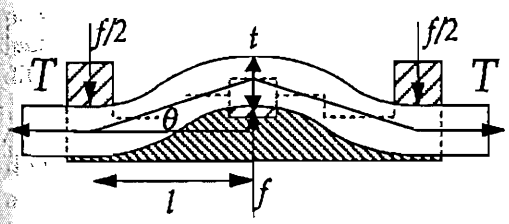

Figure 1: Cross-sectional view of a tendon inserted in the transducer. $f = T\sin(\theta)$

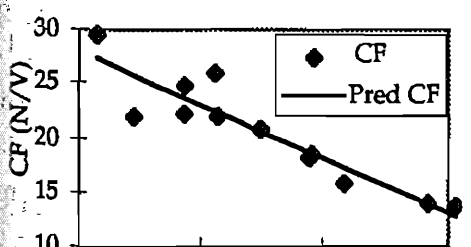

Figure 2: The measured and predicted conversion factors for the 12 tendons.

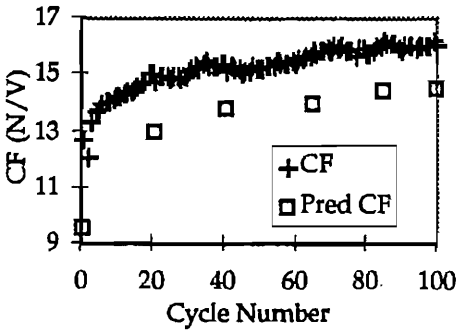

Figure 3: The measured and predicted conversion factors for 100 loading cycles.

ACKNOWLEDGMENTS:
UCSF School of Medicine REAC Cason Fund,
UCSF Orthopedic Bioengineering Laboratory

REFERENCES:

An, *J. Biomech*, 1990, 23(12), 1269-71.
Hahs, *J. Biomech*, 1989, 22(2) 165-6.
Komi, *J. Biomech*, 1990, 23(1), 23-34.
Miller, *Vision Research*, 1992, 32(6),1099-113.
Viidik, *Hdbk of Bioengineering*, 1987,6.1-19.
Woo, S. *Biorheology*, 1982, 19, 385-96.

FINGER EXTENSOR MECHANISM PASSIVE RESISTANCE FOR DIFFERENT INTERPHALANGEAL JOINT POSITIONS

Dennerlein J T †,††, Hollister AM †, Rempel DM †
† University of California, San Francisco, Ergonomics Program, USA
†† University of California, Berkeley, Dept. of Mechanical Engineering, USA

INTRODUCTION

An accurate mechanical model of the finger extensor mechanism is needed to understand normal and pathologic finger function. Previous workers have demonstrated that the extensor mechanism is a single structure distal to the metacarpophalangeal (MP) joint[2,3], that the moment arms for the proximal interphalangeal (PIP) joint vary with joint position[4,5], and that the function of the mechanism is dependent on the positions of the two interphalangeal (IP) joints[2]. Attempts to determine the moment arms for the mechanism by anatomical studies have been frustrated by the fine structure of the mechanism[1,5]. We have extended the technique of measuring the joint torque for different loads[4] to determine the passive resistance and the mechanical advantage at both IP joints in different positions.

METHODS

The middle fingers of three fresh frozen intact cadaver hands were mounted on a frame by pins through the middle metacarpal. Sutures were attached to four tendons, the extrinsic extensor, both interossei, and the lumbrical, proximal to the MP joints. Weights were hung from the sutures to load the fingers. The skin and flexor tendons were removed to reduce passive resistance. Care was taken to preserve the volar plate structures and the oblique and lateral retinacular ligaments. A self centering goniometer made with a precision potentiometer recorded joint motion. Torque was measured by strain gauges on the moving arm of the goniometer. The device was fixed to the lateral aspect of the finger by fine pins drilled into the bones. The output of the strain gauges was calibrated by placing weights on the arm of the goniometer creating a torque (0-15 N-cm). The output was linear ($r \geq 0.98$). The potentiometer was calibrated using a manual goniometer and its output was linear for 0 to 180° ($r \geq 0.98$). Prior to testing each loading configuration and with the joint extended (0° flexion) the instrument was zeroed.

Data from the PIP and distal interphalangeal (DIP) joints were measured for the following load configurations: unloaded, 0.6 N, 1.4 N, 2.8 N and 4.5 N on all tendons and 4.5 load on each tendon with all others at 1.4 N. The lumbrical was not loaded at the higher loads due to its fine tendon of insertion. The PIP joint was measured in all load configurations with the DIP free, pinned in extension, 30°, 60°, and 90° of flexion. The DIP joint was measured in all load configurations with the PIP free, pinned in extension, 30°, 60°, and 90° of flexion. The joint was moved passively from extension to flexion and back while the torque and angle were continuously recorded at 30 Hz. Three measurements were made for each configuration and averaged every 5 degrees (Fig 1).

RESULTS

The method's repeatability for measuring torque and angle for a single unloaded finger is show in figure 1. The standard error over the three trials shown in figure 1 was on average 0.5 N-cm with extreme values at the maximum joint angles. The average standard error for all configurations ranged from 0.1 to 0.7 N-cm.

The PIP joint passive torque changes as the DIP joint is flexed (Fig 2). The characteristic shape changes from a flat curve (similar to [4]) to a double humped curve as DIP flexion increases. The lateral bands of the extensor mechanism would tend to bow string above the PIP joint when the DIP was flexed and the PIP extended. The bands would then "pop" to a position next to the PIP joint as it was flexed. This is seen as the first hump, at about 20° flexion, in figures 1 and 2. Therefore the preferred PIP position is a function of DIP angle. This was observed on all three fingers.

The muscles exhibit different load curves when the same load was applied to each muscle individually (Fig 3&4). This indicates that the three muscles have different mechanical advantages at the joint. These observed differences change for different PIP angles indicating that the moment arms are a function of both joint angles (Fig 3&4).

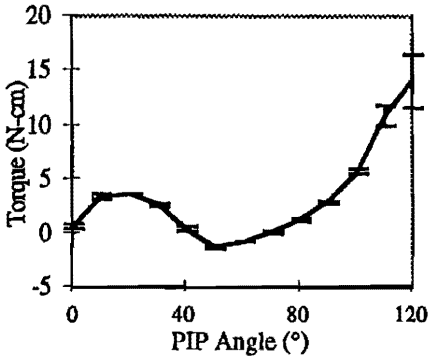

Fig. 1: The average PIP flexion torque with standard error bars (3 trials); finger 1, no load & 30° DIP flexion.

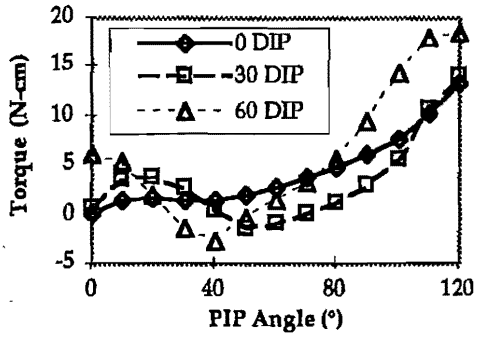

Fig. 2: PIP passive resistance for different DIP positions, finger 1 (flexion only).

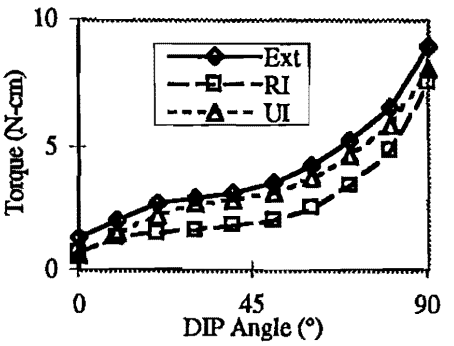

Fig. 3: DIP flexion torque for 4.5N on one tendon & 1.4N on others. (PIP = 0°)

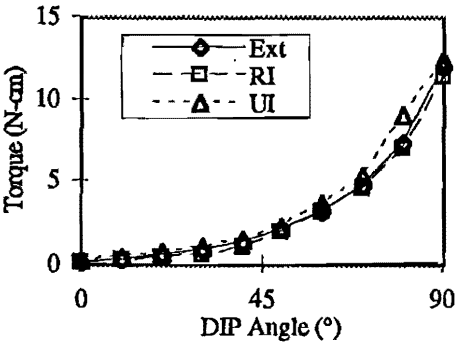

Fig. 4: DIP flexion torque 4.5N on one tendon & 1.4N on others. (PIP = 60°)

DISCUSSION

The new and repeatable method presented here allows us to study the effects of the IP joint positions on the mechanics of the finger and it's extensor mechanism. It has revealed that the extensor mechanism exerts a significant effect on passive finger resistance and furthermore this resistance is dependent upon the relative position of the IP joints. The area of lower passive resistance coordinates the positions of the IP joints, producing smooth opening and closing of the finger. The new method has also indicated that the mechanical advantage (moment arms) of the individual muscles are different and are a function of both PIP and DIP joint positions (Fig 3 & 4).

The combination of passive resistance and extensor mechanism moment arms at each joint determine the preferred sequences for finger opening and closing. When the finger is used in flexion such as for pinch or grip, low extensor moment arms and moments at each joint are desirable. When the finger is moved into extension, maximal extensor moment arms at each joint are needed. Models of the extensor mechanism derived from these measurements can be used to further analyze the function of and the forces in the finger.

REFERENCES

[1] Garcia-Elias M, An KN, Berglung L, Linscheid RL, Cooney WP, Chao EYS. Extensor mechanism of the fingers I: A quantitative geometric study *J Hand Surg*, 1991, 16(a), 1130-36.

[2] Harris C, Rutledge G. The Functional Anatomy of the Extensor Mechanism of the Finger, *J Bone Joint Surg*, 1972 54A(4), 713-26.

[3] Landsmeer JMF. Anatomical and Functional Investigations of the articulation of the human fingers, *Acta Anatomica*, supp 24, 1955, 1-65.

[4]Micks JE, Reswick JB. Confirmation of differential loading of lateral and central fibers of the extensor tendon *J Hand Surg* 1981, 6(5), 462-7.

[5] Sarrafian S, Kazarian LE, Topouzian LK, Sarrafian VK, Siegelman A. Strain Variations in the components of the extensor apparatus of the finger during flexion and extension *J Bone Joint Surg*, 1970, 52A(5), 980-990.

A METHOD TO QUANTIFY THE EFFICIENCY OF EXERCISES IN REHABILITATION OF ATROPHIED MUSCLE GROUPS

Denoth J, Doninelli A, Gerber H, Müller R, Stacoff A, Stüssi E

Laboratory for Biomechanics, Swiss Federal Institute of Technology (ETH), Schlieren, Switzerland

INTRODUCTION

Muscle atrophy is a serious problem affecting numerous 'bed-rest' patients. Human muscle biopsy studies have shown that, in general, it is mainly the type I fibres that undergoe atrophy with immobilisation. The cross-sectional area decreases and the potential for oxidative enzyme activity is reduced (e.g. Häggmark, 1978). In elite athletes, inactivity following injury, surgery, or immobilisation rapidly decreases the size and the aerobic capability of muscle fibres, particularly in the fiber type affected by the chosen sport: In endurance athletes, type I fibres are affected, while in athletes engaged in explosive activity such as sprinting type II fibres are affected (Arvison et al., 1984). In other words, immobilisation can affect both fiber types. Physical training increases the cross-sectional area of all muscle fibers; the fibers respond to the athlete's principal activity. To increase muscular force or muscular power for special sports activities different training techniques are used e.g. isometric, concentric or even eccentric physical training. In eccentric training more than maximum isometric muscle force is produced. This is due to (a) the force-velocity-relationship, a pure mechanical effect (Hill, 1970) and (b) an increased muscle activity as a consequence of a superposition of the reflex activity (Nichols and Houk, 1971) onto the voluntary nerve activation. Therefore an eccentric exercise is expected to be more efficient in training of muscle groups than isometric or concentric exercises.
The goal of this project is to evaluate a method to quantify the efficiency of exercises in rehabilitation of atrophied muscle groups.

METHODS

By use of a specific Torque-Velocity Dynamometer (Denoth et al., 1994) - which allows to deduct the intrinsic mechanical characteristics of muscle groups - experiments on the flexor and extensor muscles of the elbow and of the ankle are performed. The device allows to measure the angular velocity and the torque during predefined types of contractions. The following contraction types are studied: isometric, concentric and eccentric contractions under isovelocity or isotonic conditions. These types of experiments allow to deduct the force-velocity-relationship or the force-length-relationship for different levels of activity. From a neurological point of view the mechanical response of the muscle on the stretch or release has a delay of about 50 msec. Considering this fact, it is possible to separate the pure mechanical part of the resultant torque from the neurological part.

RESULTS

In Figure 1 the torque of the flexors of the elbow during concentric (top) and eccentric (bottom) contractions (release and stretch experiments) at an angular velocity of 1 rad/s (left) and 2 rad/s (right) respectively are shown. The maximal torque in the two eccentric experiments is comparable and reaches about 150% of maximal isometric torque. In concentric experiments the influence of the angular velocity on torque is evident; at 1 rad/s a reduction of about 15%, at 2 rad/s of about 30% of the maximal isometric torque. (Rem.: The oszillations in the torque-time-curve are due to a nonrigid fixation between arm and device for security reasons with the prototype of the TVD.)

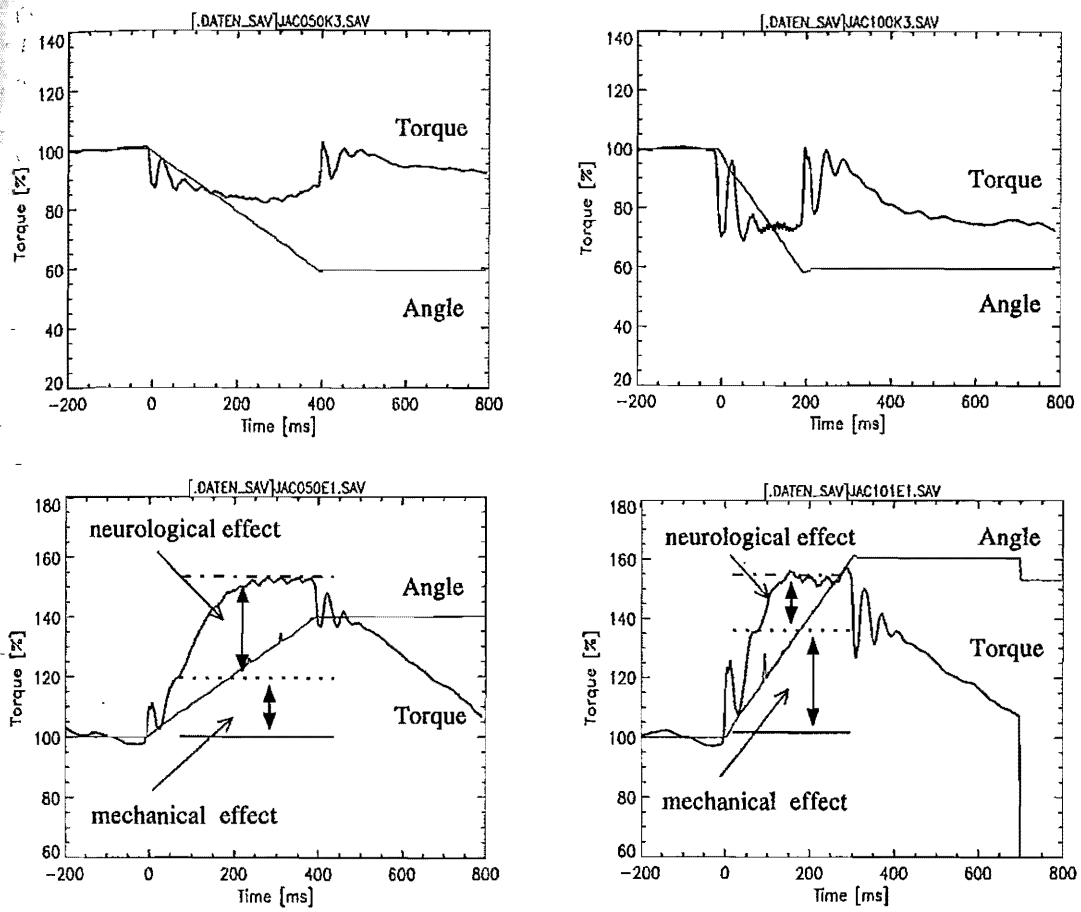

Figure 1 The torque of the flexors of the elbow and the elbow angle during concentric (top) and eccentric (bottom) contractions at an angular velocity of 1 rad/s (left) and 2 rad/s (right) respectively.

DISCUSSION

In concentric experiments these differences in torque are due to Hill's well known force-velocity-relationship of skeletal muscle. The torque developed during the eccentric experiments therefore is affected not only by the force-velocity-relationship but also by additional neurological reflex activity. This reflex activates additional muscle fibres. By this way a larger part of the muscle is stimulated, and the efficiency of the exercise in rehabilitation of muscle groups will be enlarged.

REFERENCES

Arvidson I, Eriksson E, Pitman M. Neuromuscular basis of rehabilitation. In: Rehabilitation of the Injured Knee. ed. E Hunter J. Funk. St Louis: CV Mosby, 1984: 214-234.

Denoth J, Stacoff A, Gerber H, Stüssi E. In vivo estimation of mechanical parameters of muscle groups. Abstracts of the Second World Congress of Biomechanics, Amsterdam, 1994: 1.

Häggmark T. A study of morphological and enzymatic properties of the skeletal muscles after injuries and immobilization in man. Thesis, Karolinska Institute, University of Stockholm, 1978.

Hill AV. First and Last Experiments in Muscle Mechanics. Cambridge: University Press, 1970.

Nichols TR, Houk JC. Improvement in linearity and regulation of stiffness that results from actions of stretch reflex. J. Neurophyiol. 1971; 39:119-142.

THE EFFECTS OF SIMULATED MUAP SHAPE, RATE AND VARIABILITY ON THE POWER SPECTRUM

T.R. Derrick, G.E. Caldwell and J. Hamill
University of Massachusetts, Amherst, MA, USA

INTRODUCTION

De Luca (1983) has modeled motor unit action potential (MUAP) trains by passing a series of impulses through a filter with an impulse response in the general shape of a MUAP. This process has the advantage of accurate replication of MUAP shape, but the MUAP waveform is then composed of multiple frequencies, making interpretation of the power spectral density (PSD) difficult. By modeling the MUAP as a sine wave, the interactions between shape frequency (F_s), rate frequency (F_r) and rate frequency variation (F_{rsd}), each of which may be influenced by physiological processes such as rate coding or fatigue, become clear. The purpose of this study was to determine the effects of F_s, F_r and F_{rsd} on the resulting PSD.

METHODS

A model of a MUAP train was created with independent parameters of MUAP shape, firing frequency and firing variability. PSD curves were then computed using a fast Fourier transform (FFT) algorithm. De Luca (1983) reported normally distributed interpulse interval histograms, thus the rate frequency was modeled as a series of independent and normally distributed values reflecting the natural variability in the interpulse interval. Values of 95.2, 35.1 and 7.8 Hz for F_s, F_r and F_{rsd} respectively were used as representative values of MUAP trains. Independent manipulation of each of these values revealed their contributions to shifts in the median frequency (MedF) of the PSD.

RESULTS AND DISCUSSION

Shape Frequency

Figure 1 shows that a change in F_s equivalent to a 10% reduction in conduction velocity produces a 7% reduction in MedF. Fatigue which produces such conduction velocity shifts has been associated with much larger shifts in MedF (Bigland-Ritchie et al., 1981). This model then agrees with their suggestion that other factors such as motor unit synchronization account for part of the spectral shift seen with fatigue.

Figure 1. Median frequency: a) 85.7 Hz; b)79.9 Hz.

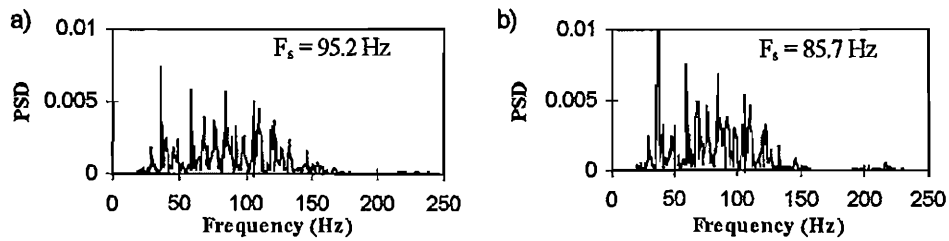

Rate Frequency

It would be expected that as F_r increases the median frequency of the PSD will also increase. However, because of the interaction between F_s and F_r this is not always the case. Increases in F_r can actually cause large decreases in the median frequency (Figure 2). F_r values of 20.0, 40.0 and 60.0 Hz produced MedF values of 84.0, 84.5 and 74.2 Hz respectively. These graphs show a progressive increase in the power of the initial peak in the PSD as the rate frequency gets closer to the shape frequency. The peak at 80.0 Hz in figure 2b is eliminated in figure 2c because only multiples of the 60.0 Hz rate

frequency appear. This elimination of the 80.0 Hz peak together with an increase in power of the initial peak causes the median frequency to shift from 84.5 Hz to 74.2 Hz. This occurs despite a 20 Hz increase in the rate frequency. Rate frequencies of 60.0 Hz are probably high for normal contractions but frequencies this high are not necessary for this type of interaction to occur. A decrease in the MedF will occur when F_r exceeds one half of F_s. This can occur as the firing frequency of the motor unit increases or when the conduction velocity causes a decrease in the shape frequency.

Figure 2. Median frequency: a) 84.0 Hz; b) 84.5 Hz; c) 74.2 Hz.

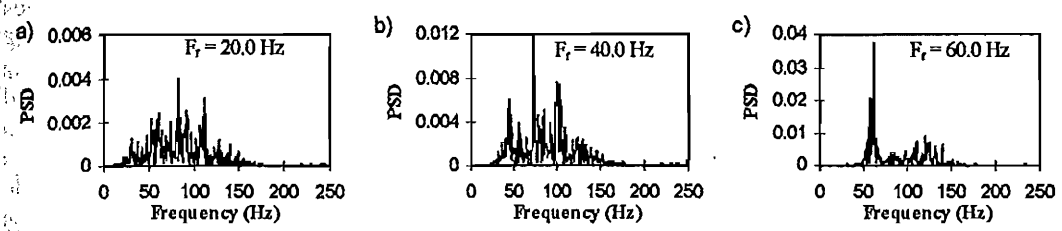

Rate Variability

By holding F_s and F_r constant and increasing F_{rsd} the median frequency also increases. Increasing F_{rsd} from 0.0 to 4.0 Hz increased the median frequency from 70.2 to 81.1 Hz (Figure 3). A further increase in F_{rsd} to 8.0 Hz resulted in a smaller shift in the median frequency from 81.1 to 84.1 Hz. The rate frequency did not change during these trials, thus the initial peak at 35.1 Hz did not shift even though it spreads out with increased variability. De Luca (1983) states that the interpulse interval statistics of a MUAP only noticeably alter the shape of an individual MUAP train power density spectrum between 0 and 40 Hz. These data do not support this statement.

Figure 3. Median frequency: a) 70.2 Hz; b) 81.1 Hz; c) 84.1 Hz.

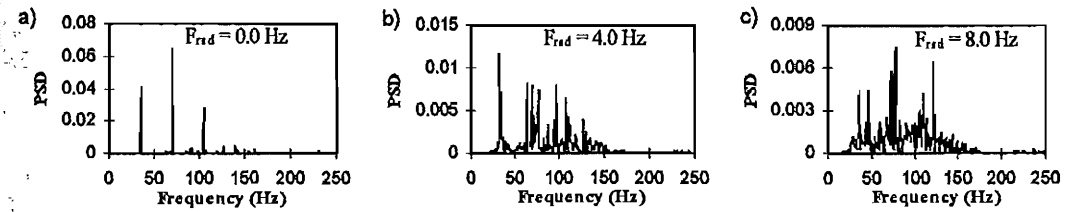

CONCLUSIONS

This project was an attempt to model the general properties of a MUAP train and to determine the effects of F_s, F_r and F_{rsd} on the resulting PSD. There is a high degree of interaction between F_s and F_r that can produce surprising effects on the median frequency of the PSD. In general, peaks in the PSD will occur at multiples of F_r with the greatest power near F_s. Increasing the variability of F_r will cause multiple peaks in the PSD near each F_r multiple and it will cause a slight increase in the median frequency of the PSD.

REFERENCES

Bigland-Ritchie, B., Donovan, E.F., Roussos, C.S. (1981). Conduction velocity and EMG power spectrum changes in fatigue of sustained maximal efforts. *J. Appl. Physiol.*, **51**:5, 1300-1305.

De Luca, C.J. (1983). Myoelectrical manifestations of localized muscular fatigue in humans. *Crit. Reviews in Biomed. Eng.*, **11**:4, 251-279.

KINEMATIC DIFFERENCES BETWEEN MALE AND FEMALE HIGH LEVEL SWIMMERS IN THE FRONT CRAWL TRAJECTORIES

[1]Deschodt V.J., [1]Rouard A.H., [1]Monteil K.M., and [2]Bonifazi M.
[1]Centre de Recherche et d'Innovation sur le Sport, University of Lyon, France; [2]Istituto di Fisiologia Umana, Siena, Italia

INTRODUCTION

Some physiological studies have been conducted on energetic cost of the upper limb, of the lower limb on the front crawl (Adrian & al., 1966), or in regard to the velocities range (Pendergast & al., 1977). Few studies observed the kinematics difference. East (1970) analysed films from the men and women 100-yd events in all 4 stroke styles. The shorter distances per stroke accounted for the lower velocities. Craig & al. (1985) noted that although the faster women had greater length, they were more dependent than men on faster stroke rates to achieve superiority. Rouard (1990) noted that the best swimmers (males or females), at the same relative effort, had a greater hip displacement. The swimmer's technique, especially the position of the upper arm during the push phase was an important parameter of the performance. This study aimed to compare the maximal and the minimal values of the underwater trajectory of each joint, in each dimension (distance, percentage of time) between female and male high level swimmers.

METHODS

Twenty-eight swimmers have been studied during the 100 m and 200 m freestyle races of the World Championships. Their characteristics were reported in the table 1.Two video camcorders (30 Hz) filmed the swimmers on 15 meters, at the extremity of the length of the swimming pool, before the turn. They were synchronised and fixed in underwater boxes (60 cm deep) with an angle of 90° between themselves. Each view was digitized frame by frame, according to Schleihauf (1979). From this digitalisation, coordinates in each of the 3 dimensions were obtained for the wrist, the elbow and the shoulder joints during the cycle. One cycle was defined by the hand entry to the water to the same hand exit.

Table 1: Characteristics of the population (N=18)

Subjects (N=18)		Weight (kg)	Stature (m)	Age(y)	Velocity ($m.s^{-1}$)
Males (N=10)	mean	78,94	1,85	20,4	1,97
	SD	±14,98	±0,02	±2,58	±0,04
Females (N=8)	mean	61,24	1,71	19,01	1,79
	SD	±15,02	±0,23	±4,01	±0,05

The trajectories of each joint was observedin a descriptive way. Each maximal and minimal values of the coordinates in each dimension was used to obtain the maximal progression in the antero-posterior axis, the maximal lateral deviation and the maximal depth of each joint on the aquatic stroke. The time of the stroke was determined and the time when the maximal and the minimal values appeared, were calculated in regard to the total time in order to compare the swimmers between themselves.

RESULTS

The duration of the total cycle was not significantly different between males and females (males: 0,84s ±0,03 and females: 0,83s ±0,05). The minimal and the maximal coordinates of the wrist and of the elbow for the aquatic stroke were described (Fig 1.), in each dimension. The females moved their wrist more forward and more backward than the males in the horizontal axis. The elbow had a greater maximal value (M(x)) of displacement for the males than for the females. In regard to the minimal coordinate (m(x)), for all the swimmers, the elbow joint never slipped backward the x-coordinate corresponding to the begimming on the aquatic stroke. For the lateral axis, the maximal coordinates (M(y)) for the two joints were less important, and the subjects (males and females) were very dispersed. The male swimmers seemed to have greater lateral deviation than the female. For the vertical axis, the minimal values of the coordinates (m(z)) were more important for the males than the females, the two population being very homogeneous.

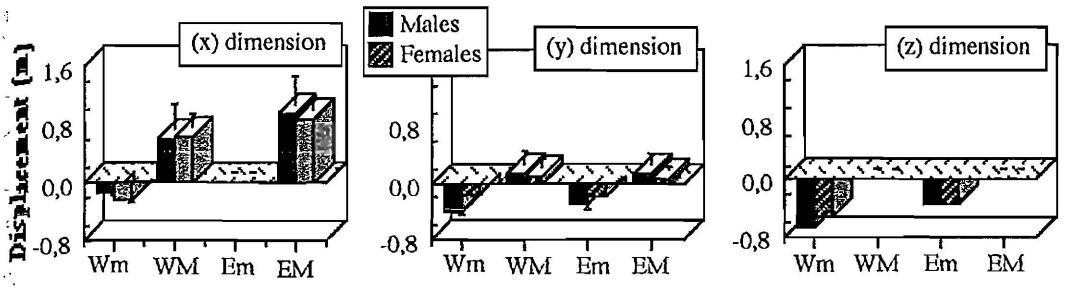

Figure. 1. Mean and standard deviation of the minimal (m) and maximal (M) coordinates of the wrist (W) and of the elbow (E) in each dimension (x, y, z) on the aquatic stroke for males and females.

Concerning the percentage of the time (Fig.2.), the males were dispersed for the time of the minimal coordinate in the antero posterior axis (Tm(x)), contrary to the females and presented a minimal coordinates for the wrist at the end of the stroke. For this axis, the maximal value of the coordinates appeared at the same time (TM(x)) for the two genders: at 50% of the total stroke for the wrist and at the end of the stoke for the elbow. For the lateral dimension, the population was very heterogeneous for the time of the minimal (Tm) and the maximal (TM) coordinates of the wrist and of the elbow. Finally, for the vertical axis, the same relative time (Tm(z)) have been observed for the minimal values of the coordinates of the two joints (about 60% of the total time of the stroke), the population being homogeneous.

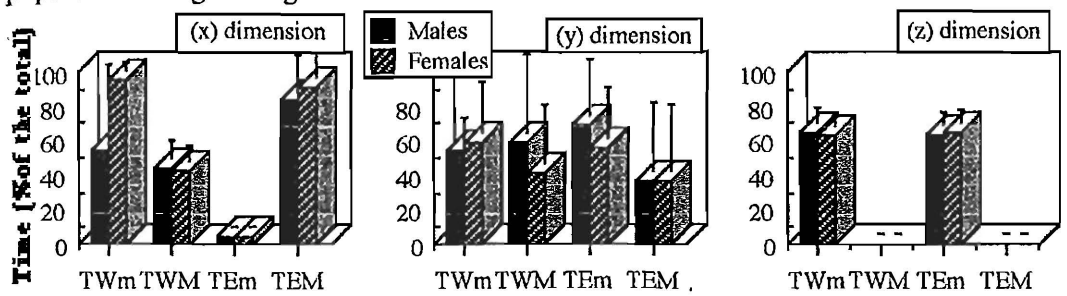

Figure.2. Mean and SD of the time (%) of the appearance of the maximal (M) and minimal (m) coordinates, for the wrist (W) and the elbow (E) for each dimension.

DISCUSSION

The total time of the stroke did not differ between the males ans the females, but some differences emerged in studying each dimension of the upper limb joints aquatic trajectory. The females presented more variations of the wrist in the antero posterior axis. The relative time of the minimal value of this joint for the same axis showed that the wrist of the women slipped backward at the end of the stroke. The elbow did not glided backward like for the men. Even if important lateral variations was observed for the both groups, no relation was obtained with the performance because of the heterogeneity of the swimmers. The males presented greater deep of the wrist and of the elbow than the females. This results suggested that the males would presente a greatr extension of their arm during the aquatic stroke than the females.

REFERENCES

1. Adrian J.A., Singh M., and Karpovitch P.V. (1966) Energy cost of leg kick, arm stroke, and whole crawl stroke. J. Appl. Physiol., 21(6), p1763-1766.
2. Pendergast D.R., Di Prampero P.E., Craig A.B., Wilson D.R., and Rennie D.W. (1977) Quantitative analysis of the front crawl in men and women. J. Appl. Physiol., 43, p475-479.
3. East D.J. (1970) Swimming: an analysis of stroke frequency, stroke length and performance. New Zealand J.of Health, Phys. Educ. and Recreation, 3(3), p16-27.
4. Craig A.B., Skehan P.L., Pawelczyk J.A., and Boomer W.L. (1985) Velocity, stroke rate, and distance per stroke during elite swimming competition. Med. Sci. Sports Exerc., 17(6), p625-634.
5. Rouard A.H. Influences of sex and level of performance on freestyle stroke: an EMG and kinematic study. International Journal of Sports Medicine, 2, 11, 150-155, 1990.

COMPUTER SIMULATION OF THE IMPACT DYNAMICS DURING THE TENNIS STROKE

C. Detlefs, U. Glitsch
Institute of Biomechanics, German Sport University Cologne, Germany

INTRODUCTION

The dynamic process of the tennis stroke is rather complex because the different segments of the arm connected by joints interact with each other and the angle of those joints change already during the contact phase of the ball with the racket. Many mathematical models have described the arm with the racket fixed tightly at the hand as a pendulum consisting of three segments. Because of the enormous calculative work which would be required for the solution of the whole equation-system of motion they have assumed for the transfer of impulse an infinitesimal short time.
The experimental approach to look into the dependence of the ball rebound velocity from the grip force have registered muscle activities during the stroke by EMG. As a calibration is impossible only qualitative results but no information about applied muscle forces are obtained there. The results of our computer simulation make it possible to calculate the kinetics of the pendulum and the ball as well as the effective forces and torques in the grip and in the joints during the whole contact phase. The exact knowledge of the impulse transfer during the period of the contact between racket and ball is useful for the optimisation of the stroke technique (e.g. reduction of the grip force) and will in all probability give an explanation for arm injuries especially for the well known widespread tennis elbow.

METHODOLOGY

In our two-dimensional computer simulation of the tennis impact the three-dimensional human model of GLITSCH, FARKAS (1993) has been modified. The hand, the forearm the upper arm and the immovable body are assumed to be connected by frictionless revolute joints so that the arm is movable without any resistance whereas the remaining part of the body is fixed. Calculations have been carried out by the software package DADS (Dynamic Analysis and Design System) of CADSI (Computer Aided Design Software Incorporation). Up to now no muscle activities have been considered. The racket is assumed to be fixed tightly in prolongation of the outstretched arm. The arm-racket-system rotates with an angular velocity of 17,45 rad/s around the shoulder joint according with values of real tennis strokes reported by ELLIOT et al. (1989). The racket area hits the resting ball. The impact process itself has been described as a elastic spring with a spring constant to the effect that the contact period is about 3 ms.

RESULTS

The results presented here focus on the transition between hand and racket. The resulting grip force consisting of an axial and a radial component must be expended by the tennis player to avoid the racket not to slip out of his hand when striking. The simulation of the tennis impact calculates a resulting grip force about 100 N. If the ball hits the racket in the sweet point it varies between 0 N and 130 N, if the hitting point is located at the edge of the racket the resulting force raises to values between 60 N to 170 N.
Figure 1 shows the time history of the **normal** force component at the grip effective perpendicular to the racket. Distal impacts induce normal grip forces in one direction. If the racket hits the ball in the centre area or more proximal to the grip the appearing forces have an opposite effect. As shown in figure 1 there exists one point on the racket where the normal grip force disappears during the whole impact phase. Because the impulse transfer at this spot is soft it is called 'sweet point'. It is worth mentioning that

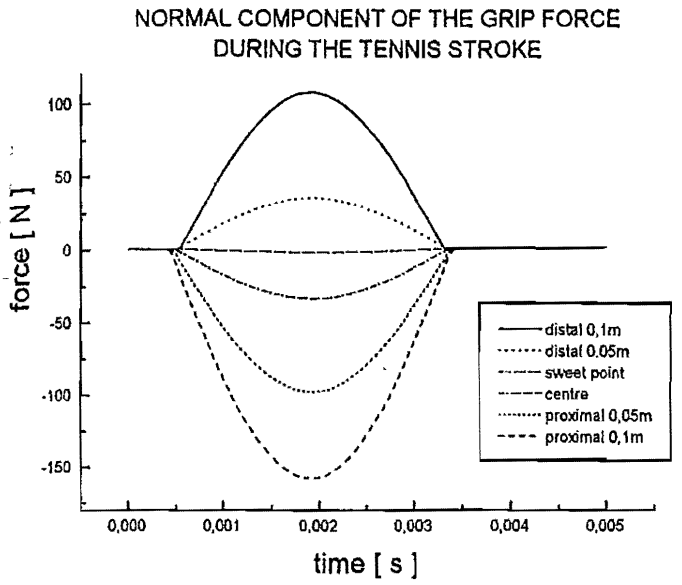

Figure 1: *Normal component of the grip force for different contact points along the longitudinal axis of the racket area*

Table 1: *Ball kinetics in dependency of the impact point on the longitudinal axis of the racket area*

distance from centre of racket area in m	ball velocity in m/s	angle of trajectory in degree
distal 0,1	31,95	0,132
distal 0,05	31,56	0,0792
distal 0,0235 (sweet point)	31,18	0,14
centre 0,0	31,2	0,052
proximal 0,05	30,69	0,0424
proximal 0,1	30,02	0,035

the centre of the racket area and the sweet point must not be identical as already found out by Hatze (1993) in practice.

If the hitting point is located more distally the ball velocity after impact increases from 30 m/s to 32 m/s as can be seen in table 1 which is apparently caused by the distally higher trajectory velocity. Nevertheless we get a paradoxical result here. Though the sweet point is located more distally than the centre point of the area the ball is accelerated to the same velocity at both points. A similar phenomen we obtained when considering the angular deviation of the ball trajectory during the impact. The further distally the hitting point is located the bigger the angle of trajectory is. But if the ball is hit in the sweet point the deviation reaches the highest value with 0,14 degrees. As the spring acts only in one direction it is effective in the connecting line between racket impact point and the ball centre. Therefore the racket position relative to the ball must be responsible for the deviation.

CONCLUSION

The two-dimensional computer simulation calculates the movement of the arm described by a pendulum of three segments during a tennis stroke as well as the joint and the grip forces. Though it is assumed that the impulse values are higher in the sweet point it is more convenient for tennis players to hit the ball there. Because of the disappearing normal component of the grip force they only have to apply the radial component. Results of experimental investigations show that excellent tennis players are able to play with less effort. This computer simulation will be extended to the flexibility of the racket frame as well as muscular activities.

REFERENCES

Glitsch, U., Farkas, R. (1993) Applications of a multi-body simulation model in human movement studies. Proc. Int. Soc. of Biomech., XIVth congress, Paris.

Hatze, H. (1993) The relationship between the coefficient of restitution and energy losses in tennis rackets. J. Appl. Biomech., **9**, 124-142

Elliot, B., Marsh, T., Overheu, P. (1989) A biomechanical comparison of the multisegment and single unit topspin forehand drives in tennis. Int. J. Sport Biomech., **5**, 350-364

REPRODUCIBILITY OF TRUNK EXTENSOR ENDURANCE AND RELATED ELECTROMYOGRAM PARAMETERS

Dieën JH van[1,2]; Heijblom P[2]
IMAG-DLO, Wageningen, The Netherlands[1];
Faculty of Human Movement Sciences, Amsterdam, The Netherlands[2]

INTRODUCTION

Various authors have suggested that low back pain (LBP) has a muscular component either as a cause or as a consequence of the primary etiological process. Prospectively, subjects with less trunk extension endurance have been shown to have a larger chance of attracting LBP[1]. In addition, in transversal studies evidence of a faster development of fatigue in LBP patients, as compared to healthy subjects, has been found [2]. Slope estimates of the time-series of the amplitude and spectral parameters of the electromyogram (EMG) of the trunk extensor muscles have been shown to be related to their endurance [3,4]. Consequently, it has been suggested that fatigue related changes of the EMG of the back muscles might be clinically used to diagnose and monitor the muscular component of LBP [5]. The EMG parameters would have the major advantage of being objective in contrast with endurance time measurements, and they would allow for less strenuous tests to be used. However, a further prerequisite for the clinical use of these parameters is that the slope estimates are sufficiently reproducible. The present study was aimed at determining the test-retest reliability of trunk extension endurance time and related EMG parameters at high force levels and to interpret these findings in terms of the clinical applicability of the parameters.

METHODS

9 healthy young male subjects participated in the experiment. After determination of the maximum extension torque (MVC), they performed a contraction at 80% MVC, till the limit of endurance. During the test the EMG of the bilateral longissimus thoracis, iliocostalis lumborum and multifidus muscles was continuously recorded. Each test was repeated several days later. The EMG data were digitized at 1024 Hz, divided into 3-second samples and subsequently time-series of the mean power frequency (MPF) and median frequency (MDF) were determined using a 1024-point Fast Fourier Transformation averaging the spectra of 90% overlapping windows from each 3-second sample. The amplitude (AMP) of the signal was determined by calculating the rectified and averaged value of each of the samples. Linear regression analysis was performed to obtain estimates of the slope of the 3 parameters. In all subsequent analyses only slope estimates significantly different from 0 were used. Their relation to the endurance time was evaluated by means of regression analysis. To evaluate the reproducibility intra-class correlation coefficients (ICC) and the smallest detectable difference (SDD) were calculated. The ICC expresses the inter-subject variation as a proportion of the total variation in the complete data-set. The smallest detectable difference expresses the amount of change in a parameter, when repeatedly measuring on one subject, that is just large enough to be ascribed (with 95% certainty) to a real change instead of being due to test-retest errors [6].

RESULTS

85% of the slope estimates of the AMP differed significantly from 0. For the MPF this amounted to 82% and for the MDF to 79%. Based on these results it was decided to use the MPF to describe the spectral changes of the EMG. Using only non-zero slope estimates the logarithm of the endurance time appeared to be significantly related to 11 out of 12 AMP slopes and 8 out of 12 MPF slopes. When correlating the slope estimates for those muscles showing the steepest slope to the logarithm of the endurance time, coefficients of correlation of 0.8 and 0.7 were found for the AMP and 0.9 and 0.7 for the MPF in the first and second test, respectively.
The ICC of the MVC was as high as 0.9, whereas it was only 0.7 for the endurance time. For the AMP slope estimates it was on average 0.7 (0.3 - 0.9) and for the MPF slope estimates 0.6 (-0.6 - 0.9). The SDD's for MVC and endurance time were 18 and 67%, respectively. For the amplitude estimates the SDD was on average 119% (61 - 188%) and for the MPF 89% (60 - 101%).

DISCUSSION

The ICC of the endurance time in the present study was with a value 0.7 at most reasonable. In a similar setup, but without redetermining the MVC in the second test, Jørgensen and Nicolaisen[7] found an ICC of 0.8 for the endurance time, which seems well comparable to our results. Using a somewhat different endurance test they found an ICC of 0.9, whereas Mannion and Dolan [4] even found an ICC of 1 for the latter test, using only 5 subjects, however.
The relatively short duration of the contractions used (45s, SD 18s) could cause poor reproducibility of the EMG parameters by yielding inaccurate slope estimates. Mannion and Dolan [4] found an ICC of the normalized median frequency of lumbar trunk extensors of 0.98 in a test which resulted in an endurance time of about 200s. However, from the r^2 values of those observations included in the present analysis 72% for the time versus AMP regression and 88% for the time versus MPF regression were above 0.7. Therefore, the slope estimates can be considered fairly accurate, consequently this has probably not caused the low ICC values for some muscles.
In conclusion, reproducibility of the parameters used in this study was in general not satisfactory for use in clinical settings. In spite of generally satisfactory values of the ICC, the EMG parameters can not be considered well repeatable. Even though confidence intervals for SDD estimates are rather wide, the high values for the SDD imply that only major changes in a patient's condition can be detected reliably. The present results suggest that an evaluation of a patient based on more than one parameter and more than one muscle might be necessary in order to obtain a valid and reliable judgement.

REFERENCES

1. Biering-Sørensen F. *Spine* 1984;9:106-119
2. Nicolaisen T, Jørgensen K. *Scand J Rehab Med* 1985;17:121-127
3. Dieën JH van, et al. *Eur J Appl Physiol* 1993;66:388-396
4. Mannion AF, Dolan P. *Spine* 1994;19:1223-1229
5. De Luca CJ. *Muscle and Nerve* 1993;16:210-216
6. Roebroeck ME, et al. *Phys Ther* 1993;73:386-401
7. Jørgensen K, Nicolaisen T. *Eur J Appl Physiol* 1986;55:639-644

Noninvasive Diagnostic of Neuromuscular Disorders by a Quantitative Evaluation of the High Spatial Resolution EMG (HSR-EMG)

C. Disselhorst-Klug, J. Silny, G. Rau

Helmholtz-Institute for Biomedical Engineering
Aachen, University of Technology
Pauwelsstr. 20, 52074 Aachen, Germany

Introduction

Neuromuscular disorders are often related to typical changes in the structure of single motor units (MUs). Therefore, is the information about the electrical activity of single MUs essential for the diagnosis of those disorders. The conventional surface EMG is, due to it's low spatial resolution, not suitable for this diagnostic purpose. That is why regardless to it's painfulness the invasive Needle-EMG methodology is used in clinical practice.

A newly developed EMG procedure with a high spatial resolution (HSR-EMG) allows in contrast to the standard EMG methodologies the detection of the single MU activity in a noninvasive way [1]. First clinical investigations have shown that the HSR-EMG allows the detection of typical changes in the electrical activity of the MUs in neuronal and muscular disorder (Fig.1) [2]. Here we want to describe a quantitative evaluation of the typical changes in the HSR-EMG pattern.

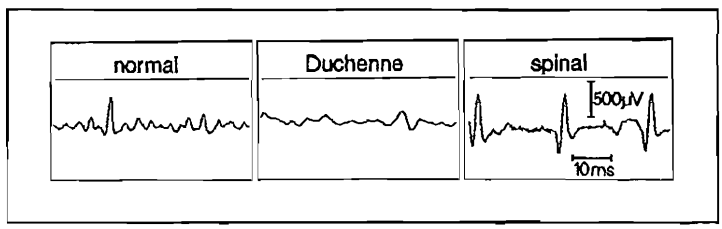

Fig.1: Spatial filtered EMG-signal of children with different kinds of neuromuscular disorders

Method

The HSR-EMG procedure is based on the used of a multi-electrode array in combination with a spatial filter processing [1]. The multi-electrode array consists of 32 pin-electrodes in a two-dimensional arrangement (inter-electrode distances 0.25 mm). Using a special, spatial filter procedure [1] the EMG-signals of MUs located directly beneath the skin surface have been amplified and the signals of more distantly located sources have been reduced.

The HSR-EMG has been recorded during maximal voluntary contraction of the *m. abductor pollicis brevis* in 117 volunteers (61 healthy children, 35 patients with muscular disorders, 21 patients with neuronal disorders) aged between the infancy and 25 years.

The typical differences in the HSR-EMG pattern have been evaluated by 9 parameters regarding the excitation spread, the signal course in long signal segments, the shape of isolated peaks and the frequency distribution of all peaks within the signal (Tab.1). For each parameter a 'reference range' has

been determined which contains at least 44 of the investigated 61 healthy volunteers. Afterwards, the probability that a parameter in a specific patient group is higher, the same or lower than the 'reference range' has been calculated.

Results

The results show a distinct difference between the parameter sets of volunteers, patients with muscular and patients with neuronal disorders (Tab.1).

Parameter	Muscular Disorders		Neuronal Disorders	
	higher than reference	lower than reference	higher than reference	lower than reference
Conduction velocity	0	34	0	13
Entropy	0	23	1	8
Root mean square (RMS)	1	17	4	3
Dwell Time over RMS	22	1	0	16
First zero crossing of ACF	35	0	4	3
Maximal peak amplitude	0	29	3	7
Peak -Energy/Gap-Energy	2	10	18	0
Gradient of Peak Edge	0	32	9	5
CHI-Value of the χ^2-Test	1	28	1	9

Tab.1: Parameters for a quantitative evaluation of the typical HSR-EMG patterns and the number of patients belonging to an interval higher or lower than the 'reference range'.

Using the typical parameter sets 97% of all healthy children, 94% of all children with muscular disorders and 71% of all children with neuronal disorders can be correctly identified by a classification based on the Bayes-Theorem. On the average the diagnosis by means of the noninvasive HSR-EMG was in 92% of all investigated children correct.

Conclusion

HSR-EMG allows the noninvasive detection of the activities of single, superficial MUs. It also detects changes in the electrical activities of the MUs which are typical for muscular and neuronal disorders. Using a special parameter set it was possible to classify 92% of all investigated children correctly. In this way, the noninvasive HSR-EMG, derived from the *m. abductor pollicis brevis*, becomes in children the same diagnostic selectivity as the commonly used invasive Needle-EMG.

References

[1] Reucher H., Silny J., Rau G. 1987 Spatial Filtering of Noninvasive Multielectrode EMG Part I: Introduction to Measuring Technique and Application; Part II: Filterperformance in Theory and Modelling.
IEEE Trans. on Biomed. Eng. BME-34, No. 2, 98-113

[2] Ramaekers V., Disselhorst-Klug C., Schneider J., Silny J., Forst J., Forst R., Kottlarek F., Rau G. 1993 Clinical Application of a Noninvasive Multi-Electrode-Array EMG for the Recording of Single Motor Units. Neuropaediatrics 24, 134-138.

THE INFLUENCE OF FIRM HEEL LIFTS ON MAXIMUM ACHILLES TENDON FORCE DURING BAREFOOTED RUNNING

S.J.Dixon and D.G.Kerwin
Loughborough University, Loughborough, U.K.

INTRODUCTION

Achilles tendon injury is common in middle and long distance runners (Leach et al, 1981). The use of heel inserts made from Sorbothane, a shock-absorbing visco-elastic polymer, has been demonstrated to reduce Achilles tendon pain (Maclellan and Vyvyan, 1981). In a previous study, of a subject running with a rearfoot ground strike (Dixon and Kerwin, 1994), it was demonstrated that attaching shock-absorbing heel inserts to the plantar surface of the foot decreased the maximum Achilles tendon force. The use of running shoes with a relatively high heel has been demonstrated to have a similar effect (Subotnick, 1979). When prescribing heel inserts, practitioners have used two distinctly different types of heel lift: lifts constructed from a firm material, designed to raise the heel; and those made from a shock-absorbing material, designed to raise the heel and cushion some of the impact shock.

The aim of the present study was to investigate the influence of firm heel lifts on maximum Achilles tendon force during barefooted running.

METHODS

Running trials were performed at seven minute mile pace (3.8 $m.s^{-1} \pm 5\%$), for two subjects demonstrating distinctly different running styles at this speed. Subject A exhibited a rearfoot strike. Subject B made initial ground contact at the forefoot, with the heel not contacting the ground at any stage. Three running conditions were used: barefooted; barefooted with one heel lift; and barefooted with two heel lifts. Heel lifts were made from a high density EVA material tapered at a 5 degree angle along a length of 88 mm. These were attached to the plantar surface of the foot using surgical tape.

A "single subject" approach was taken using a randomised block design. Single trials for each of the three conditions in 10 blocks were recorded for each subject. Video recordings at 100 fields per second were made of movement in the sagittal plane using two 50 Hz video cameras genlocked out of phase (Panasonic F15 camera and AG7350 sVHS recorder; MS2 video camera). Synchronised ground reaction force data were collected at 1000 Hz using a force plate (Kistler 9281B12). Four reference points, a point representing the ankle joint centre, and two points on the skin surface over the Achilles tendon were digitised.

Using the methods of Dixon and Kerwin (1993), the line of action of the Achilles tendon was estimated as a straight line joining the two digitised tendon points. It was assumed that the ankle moment was generated entirely by the triceps surae muscle group, and was thus transmitted by the Achilles tendon (Figure 1, Equation 1). Maximum Achilles tendon force was estimated for each subject for each of the conditions.

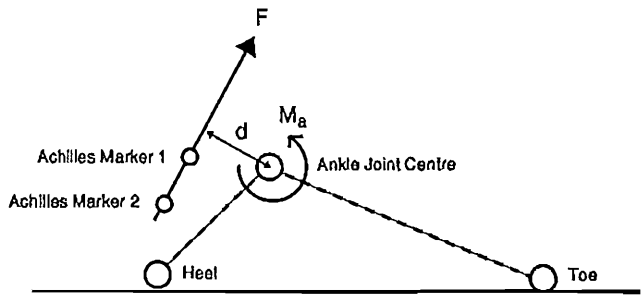

Figure 1. Moments about the ankle joint

$$M_a = F.d \qquad 1$$

RESULTS

The maximum Achilles tendon force values are presented in Table 1. A t-test for correlated data was used to identify significant differences between conditions for each subject. For Subject A, a significant increase in maximum Achilles tendon force was demonstrated for the one heel lift ($p<0.05$) and two heel lift ($p<0.01$) conditions, compared to barefooted running. No difference in maximum Achilles tendon force was found when comparing one and two heel lifts. For Subject B, the use of heel lifts had no influence on the maximum Achilles tendon force.

Table 1. Maximum Achilles tendon force in bodyweights (SD)

	Barefoot	Barefoot 1 lift	Barefoot 2 lifts
Subject A	9.3 (0.5)	9.9 (0.5)	10.2 (0.5)
Subject B	17.8 (0.5)	18.2 (1.0)	18.3 (1.6)

DISCUSSION

It has been suggested, (Subotnick, 1979), that raising the heel in relation to the forefoot, decreases the incidence of Achilles tendon injury, by reducing the tendon loading. In a previous study using Subject A (Dixon and Kerwin, 1993), a reduction in maximum Achilles tendon force was demonstrated using heel lifts constructed from a visco-elastic material. No significant changes in ground reaction force magnitude were observed at the time of maximum Achilles tendon force. It was therefore suggested that the reduction in maximum Achilles tendon force was a result of raising the heel. To isolate this effect, heels lifts constructed from a firm, rather than visco-elastic material, were used in the present study.

The results of the present study demonstrate that, for Subject A, firm heel lifts caused an increase in the maximum Achilles tendon force. This is contrary to the indications of the previous study, demonstrating the complexity of the mechanism by which heel lifts may influence maximum Achilles tendon force.

Subject B demonstrated a forefoot ground strike. When running barefoot, this subject did not contact the ground with the heel. Despite this fact, this subject had independently been prescribed a corrective device placed in the rear of the shoe, in an attempt to reduce Achilles tendon pain. It was therefore of interest to see that the attachment of firm heel lifts did not influence the maximum Achilles tendon force for this subject.

In conclusion, for prediction of the influence of heel lifts on maximum Achilles tendon force, detailed consideration of each individual case is clearly required. This suggestion has implications for the practitioners who routinely prescribe heel lifts to individuals suffering from Achilles tendon injury.

REFERENCES

Dixon, S.J. and Kerwin, D.G. (1993). Estimating Achilles tendon force using quasi-static moments. *J. Sports Science*, 170 (abstract).

Dixon, S.J. and Kerwin, D.G. (1994). The influence of heel raises on Achilles tendon force in running. *Proceedings of the Second World Congress of Biomechanics, abstract #* I-255B. Amsterdam.

Cavanagh, P.R. and Lafortune, M.A. (1980). Ground reaction forces in distance running. *J. Biomechanics* **13**, 397-406.

Leach, R.E., James, S. and Wasilewski, S. (1981). Achilles tendinitis. *Am. J. Sports Med.* **9**, 93-98.

Maclellan, G.E. and Vyvyan, B. (1981). Management of pain beneath the heel and Achilles tendinitis with visco-elastic heel inserts. *Brit. J. Sports. Med.* **15**, 117-121.

Subotnick, S.I. (1979). *The Running Foot Doctor.* World Publications.

Subotnick, S.I. and Sisney, P. (1986). Treatment of Achilles tendinopathy in the athlete. *J. Am. Podiatric Med. Assoc.* **76**, 552-557.

A SO-FAR UNDESCRIBED ISOMETRIC BIOMECHANICAL FUNCTION OF THE HUMAN HIP-JOINT MUSCLES, PRESENTING ORTHOPAEDIC TREATMENT OF THE HIP-JOINT PATHOLOGY IN A NEW LIGHT

Dobrev R., D. Djerov, B. Vladimirov
University Hospital of Orthopaedics at Medical University in Sofia, Bulgaria

INTRODUCTION

While doing our research on the failures in hip-joint prosthesizing, we were quite impressed by the large number of cases published of the so-called "illogical" breakage's of the femoral stem of total endoprostheses. In 1986 Mözer and Hein [1] published their study on 25 similar breakage's, where the "illogical" element was expressed in that the cracks in the stem metal had begun spreading from medially towards laterally. Such a direction of the crack is incompatible with the classical conception as to the console nature of the femur. The contradiction between clinical practice and the fundamental theory was obvious. The basic of this theory is to be found in the generally accepted ever since 1867 analogy of Meyer and Culmann, postulating that the proximal femur is assumed to act as a console, known as "Culmann's crane". The contradiction between theory and practice gave us grounds to feel some doubt as to this console analogy. It would have been much more probable that the self-organising organisms had found some more affective solution, which is yet unravelled by science. The purpose of the investigation was to establish a more realistic model of human hip joint biomechanics, with the view to enhancing effectivity of joint pathology treatments. The study of the trabecular structure in proximal femur bone sections with different spatial orientations, carried out by us for the purpose, points to the existence of a new, so-far undescribed isometric biomechanical function of the iliacus, obturator externus, obturator internus and vastus lateralis muscles. We named this function "active supportive function", and the physiological phenomenon - "active supportive bone-and- muscle synergy". Here only the new function of obturator externus and vastus lateralis muscles will be discussed.

METHODS

Cadaver materials were used of bone and muscle fragments of adults and newly born humans, as well as other biped and quadruped vertebral animals. The methods applied were: a study of the architectonics of cancellous tissue in the proximal femur and pelvic bones; comparative-anatomy studies of the pelvic bones and muscles; histological studies of bone-and-muscle preparations; biomechanical reinterpretation of the known anatomical data.

RESULTS

As a result of the investigation, several facts were settled: At the lower end of the femoral head, where the furrow-like-shaped end of the femoral neck begins, a zone was discovered where the trabecular beams ware directed perpendicularly to the outer surface of the bone. Just through this furrow-like-shaped canal underlying the femoral head slide the upper fibres of the obturator externus muscle before reaching their terminal insertion site within fossa trochanterica; At an oblique bone section through fossa trochanterica and trochanter minor we discovered a parallel trabecular chain, connecting fossa trochanterica to the front base of the trochanter major. The anterior end of the proximal insertion of m. vastus lateralis is located at this point; The obturators externus and internus are the only hip-joint muscles, whose initial insertion sites in the lesser pelvis are situated at a level below their terminal insertion site to fossa trochanterica.

The biomechanical interpretation of the above-mentioned facts gave us grounds to build up the following model of the active supportive bone-and-muscle synergy within the human hip-joint region: By the obturator externus muscle isometric action, excited by osteoreceptor signals coming from the loaded femoral neck, the upper fibres of the

muscle, taut as a bowstring underlying the femoral neck, generate a lifting force, acting on the furrow-like-shaped canal as an active support of the femoral head (thence the name of "active supportive" function of the muscle"). The lower part of the muscle, whose initial insertion site is spatially lying lower down than its final insertion point is, absorbs from the lesser pelvis part of the pelvic load and transmits it directly into fossa trochanterica. Through the muscle fibres of the lower part of this muscle, a practically "hanging" pelvis results, suspended on the femoral tip in fossa trochanterica. After the discussion the inference is reached that the pelvic force is divides into three branches before reaching the acetabulum. Only one of the latter exerts a direct stress on the femoral head. The other two branches of the force "used up" through os pubis and os ischium, and then, taken up by obturator externus thanks to its isometric action, are transmitted to its insertion point in fossa trochanterica. From this place, the pressure component of the transmitted force is shifted to the powerful femoral calcar, while the tensile component is transmitted to the front base of the trochanter major through a parallel trabecular chain. From that site it is taken up by the vastus lateralis muscle. This defines the latter as a supportive muscle of the hip-joint too. The fossa itself is situated in the longitudinal axis of the femoral dyaphysis. Thus, this part of the pelvic load does not cause bending of the femoral neck and of the proximal femur. The suspension of the pelvis upon the lower part of the obturator externus muscle could be compared to the suspension of the royal carriages of olden times. The analogy (Fig. 1., given up by Dr. K. Klaue from Bern) is complete, as to the above-mentioned two components of the pelvic load that have been deflected away from the acetabulum.

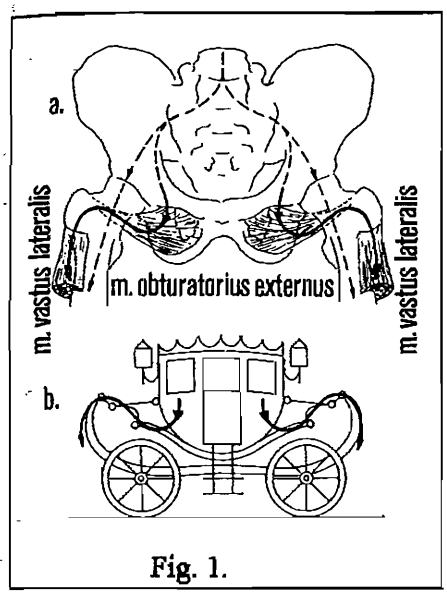

Fig. 1.

DISCUSSION

A so-far undescribed additional isometric supportive function of the obturator externus and vastus lateralis muscles was revealed. These muscles are involved in an active supportive bone-and-muscle synergy through this function, thus redistributing the loads upon the femoral head and providing for the high load-bearing capacity of the hip joint. The pelvis is practically partially 'hung' upon the supportive muscle. It has turned out that the femoral neck is enjoying much more favourable biomechanical conditions than our contemporary science has so far taken for granted. The bending loads upon the neck as well as upon the dyaphysis are being brought down to a minimum. This is also being facilitated by the vastus lateralis muscle, which takes on the supportive reaction of the obturator externus muscle and also plays the part of a supportive muscle to the hip joint. The new knowledge of the active supportive bone-and-muscle synergy in a normal hip joint has made it necessary to reconsider the methods and means of treatment in pathologic joints. When replacing the injured joint with an artificial one, the conceptually new type of endoprosthesis ought to provide an 'endoprosthesis-and-muscle' synergy that is closest to the natural bone-and-muscle synergy. In cases of congenital hip dislocation the pelvis is almost entirely hung upon the obturator externus muscle - something that necessitates an adequate change of methods in surgical treatment.

REFERENCES

1. Mözer, M. und Hein, W. (1986) Bestimmung der Hüftkraftrichtung aus Bruchflächen von Hüftgelenksprothesen. *Beitr. Orthop. Traumatol.* **33**, H. 6, S. 286-295.

LIGAMENT STRAIN MEASUREMENTS IN CADAVERIC FEET DURING SIMULATED FUNCTIONAL ACTIVITIES.

A.W. Donn and A.C. Nicol.
Bioengineering Unit, University of Strathclyde, Glasgow, Scotland, UK.

INTRODUCTION

The mechanisms of load support in the foot have been the subject of investigation for many years. Electromyography studies have revealed that the principal mechanisms of load support are ligamentous, the muscles forming a dynamic reserve called upon during periods of excessive loading (Basmajian and Stecko, 1983; Walker, 1991). Several investigators have used a selective dissection process to explore the relative contributions of the plantar ligaments of the foot to normal load support (Ker *et al.*, 1982; Huang *et al.*, 1993). While such tests provided broad conclusions of the relative importance of each of the plantar structures, the precise functional interrelationships in the intact foot could not be found. The aim of the present study was to gain a detailed, quantitative, understanding of the biomechanics and function of the plantar ligaments and passive support mechanisms of the human foot. The information rendered would be of great value not only to biomechanics researchers but to surgeons and other clinicians, orthotists, prosthetists and footwear designers amongst others. A method of direct instrumentation of the ligaments of cadaveric feet subjected to functional loads, positions and movements was adopted.

METHODS

All tests were carried out on unembalmed cadaveric foot specimens. Five liquid metal strain gauges (LMSGs) were used to monitor strain patterns in four selected test ligaments namely; plantar aponeurosis (PA), long plantar ligament (LPL), short plantar ligament (SPL) and calcaneonavicular ligament (CNL). The LMSGs were custom made and introduced with approximately 5% prestrain onto the ligaments using a set of normalised, reproducible placement parameters derived from detailed measurements of embalmed specimens (Stone *et al.*,1983). Access to the ligaments was gained through a small incision along the bony margins of the lateral border and small windows in the plantar fascia. Virtually no tissue was removed and the intrinsic musculature was not sacrificed during this process hence the anatomy was left essentially intact. The foot was placed in a specially designed loading rig which was mounted in an Instron® materials testing machine. The rig allowed the foot to be loaded dynamically in a variety of positions with either measured loads or fixed positions applied to five extrinsic muscle tendons namely; tendo achilles (TACH), tibialis anterior (TA), tibialis posterior (TP), peroneus longus (PL) and flexor digitorum longus (FDL). Physiological levels of force and loading rates, anatomical positions and small motions could be applied to each foot specimen. The following simulated functional activities were carried out:

1. Standing (with the foot in five different orientations).
2. Standing (with varying forces applied to four long extrinsic muscle tendons).
3. Effects of toe extension on ligament strain patterns ('windlass' mechanism).
4. Gait (simulated in three stages (i) heel strike, (ii) mid stance, (iii) toe off).

All tests were repeated as a dynamic cycle, at physiological loading rates, in order to take account of preconditioning and non-linear visco-elastic behaviour of the tissues.

RESULTS AND DISCUSSION

Initial results have confirmed the viability of the techniques as well as providing a valuable insight into the mechanics of the foot. The results presented below were obtained from a left foot of a 67 year old male subject. Ligament strains during standing with applied muscle forces and different foot positions are shown in tables 1 and 2. It can be seen from the values in table 1 that forces applied by the extrinsic musculature have a marked effect on the strain patterns of the ligaments. In particular it was concluded that the TA and TP muscles were able to reduce the levels of maximum strain in all the test ligaments, but especially for the LPL and SPL where reductions in strain of between 50 and 90% were

noted. This confirms earlier findings that the extrinsic muscles have an important role in functional load bearing of the foot (Basmajian and Stecko, 1963). During simulated standing with the foot in different positions, a wide range of ligament strains was experienced indicating a complex system of functional interactions. The strain in the CNL was seen to rise by around 40% in eversion compared to the neutral position. This has implications in the live subject for active eversion and incurred rearfoot motion during running. Applied extension to the toes confirmed the existence and generally accepted function of a 'windlass' mechanism with respect to the mechanics of the PA. In the simulated gait studies, maximum ligament strains were observed during the toe off phase where strain values of 3 times those experienced during standing were recorded. These results are being used in the development of a mathematical model of the structures of the foot which forms a continuing but separate project.

Ligament	Muscle Force Applied								
	None	TA		TP		PL		FDL	
		50N	100N	50N	100N	50N	100N	50N	100N
PA (Distal)	1.01	0.81	0.54	0.74	0.81	1.09	2.49	1.77	3.52
PA (Prox.)	2.51	2.05	1.24	1.84	1.47	2.51	3.86	1.96	3.02
LPL	2.96	1.58	1.10	1.92	1.38	1.99	1.80	1.50	1.05
SPL	7.21	5.61	3.80	3.93	0.61	3.04	3.40	4.52	3.11

Table 1. Percentage ligament strains in simulated standing in the neutral position with muscle forces applied to selected long extrinsic muscle tendons.

Ligament	Foot Position				
	Neutral	10^0 Invert.	10^0 Evert	10^0 D. Flex	20^0 P.Flex
PA (Distal)	0.65	0.82	0.36	0.54	0.49
PA (Prox)	1.34	1.44	0.72	1.05	1.43
LPL	1.34	2.09	1.09	1.09	1.40
SPL	3.05	4.26	-1.32	3.04	4.12
CNL	5.98	7.28	8.54	4.65	7.63

Table 2. Percentage ligament strains in simulated standing with the foot in different positions. Negative strain values indicate a contraction from the reference position but not laxity in the ligament.

ACKNOWLEDGEMENT

The principal author is supported by a studentship from the Medical Research Council.

REFERENCES

Basmajian, J.V. and Stecko, G. (1963) The role of muscles in arch support of the foot. *J. Bone Jt Surg.*, **45A**, 1184-1190.

Huang, C.H., Kitaoka, H.B., An, K.N. and Chao, E.Y.S. (1993) Biomechanical evaluation of longitudinal arch stability. *Foot Ankle*, **14**, 353-357.

Ker, R.F., Bennett, M.B., Bibby, S.R., Kester, R.C. and Alexander, R.McN. (1987) The spring in the arch of the human foot. *Nature*, **325**, 147-149.

Stone, J., Masden, N.H., Milton, J.L., Swinson, W.F. and Turner, J.L. (1983) Developments in the design and use of liquid metal strain gauges. *Exp. Mech.*, **23**, 331 -338.

Walker, L.T. (1991) The biomechanics of the human foot. PhD thesis, University of Strathclyde, Glasgow, Scotland.

INTERMUSCULAR CO-ORDINATION DURING FAST CONTACT CONTROL LEG TASKS

Caroline A.M. Doorenbosch, Gerrit Jan van Ingen Schenau
Faculty of Human Movement Sciences, Vrije Universiteit
Amsterdam, The Netherlands

INTRODUCTION

An analysis of cycling revealed that mono- and biarticular muscles may have different roles in the control of force and position during contact control tasks (Ingen Schenau *et al.*, 1992). Mono-articular muscles appeared to be mainly active when they could contribute to positive work, i.e. when they could shorten, whereas the biarticular muscles seem to provide the distribution of the net moments about the joints. To test this hypothesis, experiments had been executed on a special dynamometer (Figure 1), which allows independent change of force and position direction (e.g. Doorenbosch & Ingen Schenau, 1994). The results of these previous experiments showed that the activity of the biarticular antagonists behaved in a reciprocal way and thereby regulated the distribution of the net moments about the hip and knee joints. Following the proposed hypothesis very rigidly, the mono-articulars were supposed to be active independent of the required net moment. However, also the activity of the mono-articular muscles showed a positive relation with the corresponding net moment. Moreover, both mono- and biarticular muscles seemed to be related to the amount of muscle shortening. It was speculated that compared to cycling, the subjects performed rather novel tasks at very low velocities. It was suggested that an intensive training period of the same tasks, executed cyclical at much higher speeds, would reveal more clearly the proposed differences in activation of the mono- and biarticular muscles. The purpose of the present study was to examine the activation of mono- and biarticular muscles during such dynamic contact control leg tasks.

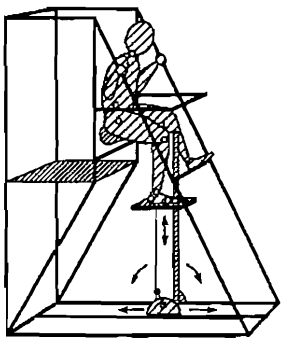

Figure 1. Illustration of the dynamometer, which was used for the experiments. Different movement directions can be adjusted according to the arrows.

METHODS

During two months prior to the actual experiments, all subjects (n=5) trained intensively for 1 hour twice a week, practising the required tasks. Each subject was seated in the dynamometer with the right foot on a forceplate (see Figure 1). For the tasks, subjects had to exert a force in a prescribed direction (see Figure 2) with a constant magnitude, while the forceplate moved five times down- and upwards with a velocity of 0.4 $m.s^{-1}$. The subjects were instructed to exert the prescribed force while the forceplate moved downwards and hold the force as constant as possible. On-line feedback of the direction and magnitude of the reaction force was given on a computer screen. During each trial joint position and reaction force were recorded and muscle

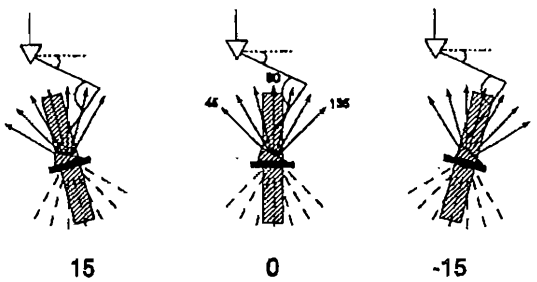

Figure 2. Illustration of the experimental protocol. Subjects had to exert the force in 7 force directions ranging from 45 to 135° relative to the forceplate in 3 different positions (-15 0 15).

activation was registered by using surface EMG.

For each task, the mean value of net moments and EMG, calculated over a period for which the knee angle was within 5 degrees of a reference position during the last two cycles, were used for further analysis. These datapoints were averaged for all subjects and used for statistical analysis.

DISCUSSION OF RESULTS

All subjects performed the tasks very accurately, for both force direction and force magnitude. In Figure 3A, the EMG-activity of the biarticular muscles is plotted as a function of the required net moment combination of hip and knee (Mk-Mh). A clear reciprocal activity is present for the biarticular antagonists. The EMG data of the monoarticular mm.vastii and gluteus maximus are shown in Figure 3B and 3C and showed an increase with increasing extending moments. However, the vastii also appear to be active at knee flexing moments.

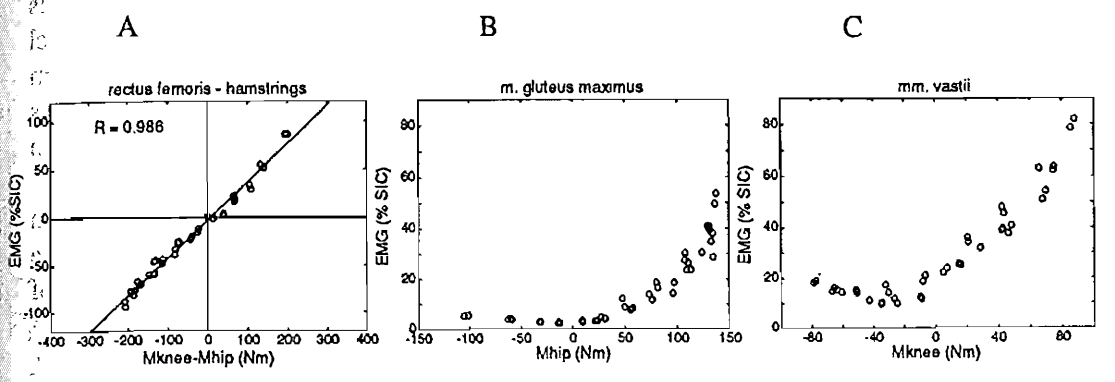

Figure 3. A. Mean values (n=5) of the difference in EMG (as % of SIC-level) between the rectus femoris and hamstrings as a function of net moment difference of knee and hip (Mknee-Mhip). Inset shows the correlation coefficient (R) for those datapoints. B.and C. The mean EMG-values (n=5) of gluteus maximus (B) and vastii (C) as a function of net hip and knee moment respectively.

Compared to the data of the slow dynamic experiments described recently (Doorenbosch & Ingen Schenau, 1994), the amount of variation of the EMGs as a function of the net moments is considerably less in the present study. The squared correlation coefficient between the EMG difference of rectus femoris and hamstrings during the slow tasks was .865, whereas this coefficient is .972 for the data of the 'fast' tasks. This means that in the present study less than 3% could not be explained by the amount of variation, whereas this was 13.2% for the slow movements.

Clearly, the tasks were executed more stereotyped in the last experiments, indicated by the higher squared correlation coefficient. This might be due to a more constraining movement speed and/or the longer training period. It is likely that this stereotyped muscle coordination is, at least in part, aimed at an optimization of the mechanical efficiency in these intensive movements. In comparison to our observations in cycling, the different roles between mono- and biarticular muscles are less pronounced. Although we found again a dominant role for the biarticular muscles in the fine regulation of the net hip and knee joint torques. The mono-articular muscles also appear to be activated as a function of the required net moments necessary to control the direction of the external force.

REFERENCES

Doorenbosch CAM, Ingen Schenau GJ van (1994) The activation of mono- and biarticular muscles during contact control leg tasks in man (submitted to Exp Brain Res)

Ingen Schenau van GJ, Boots PJM, Groot G de, Snackers RJ, Woensel WWLM van (1992) The constrained control of force and position in multi-joint movements. Neuroscience 46: 197-207

A NEW MODEL FOR AN ARTIFICIALLY ACTIVATED HUMAN NEUROMUSCULAR SYSTEM.

S.J.Dorgan, M.J.O'Malley,

Department of Electronic & Electrical Engineering,
University College Dublin,
Belfield, Dublin 4, Ireland

INTRODUCTION

Most muscle models presented to date have been macroscopic models of either the Black Box or Lumped Parameter Type, 'simple' model structures capable of relatively easy parameter identification. With a myriad of smaller inter-dependant systems switching in and out of various contractile states at different times, any attempt to model the underlying physiology of muscle increases model complexity. The apparent system complexity is such that many investigators abandon modelling the underlying processes in favour of macroscopic models, losing valuable insight into the actual biological system behaviour.

Functional Electrical Stimulation, FES, of human muscle offers a possible solution to some of the present modelling difficulties. As both the inputs and outputs of the system are well defined, it is possible to model the underlying physiological behaviour of artificially activated muscle. In doing so one can easily incorporate neural feedback from proprioceptors, and gain significant insight into the actual behaviour of FES muscle.

METHODS

A model for physiologically activated muscle proposed by Hatze, (1978), was taken as a basis for a new model of FES muscle. This new model utilises the well known inverse recruitment dynamics of FES activated muscle. The model may be categorised as being of an "activation type". It models Ca^{2+} ion concentration in the sarcoplasm and recruitment dynamics, in response to FES, to produce system outputs. The mathematics is very involved and will not be discussed here.

A specially designed computer controlled electrical stimulator, (McCoy, 1994), capable of producing any desirable stimulation pattern, and a Cybex machine capable of accurately measuring joint torque's have been used to experimentally validate this non-linear model.

A non-linear spindle model, (Hasan, 1983), has been added to transform the musculotendon model to a new neuromuscular model, enabling an investigation of the role proprioceptor feedback plays in a neuromuscular model.

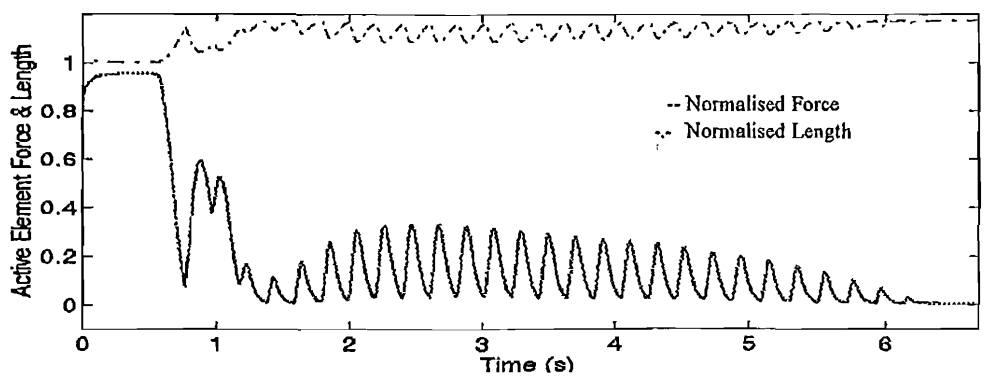

Figure 1

RESULTS

The newly derived FES muscle model is presented below. It is a highly non-linear and strongly coupled system that takes FES pulse amplitude and frequency as inputs. Variable definitions may be found in (Hatze, 1978).

$$\dot{n} = \bar{m}[z(a) - n] \tag{1}$$

$$\dot{r} = -\dot{n} - \frac{mr}{\ln(1 + 10^{-3}m + \phi/k_{2c})} \tag{2}$$

$$\dot{\psi} = m(cv - \psi) + \bar{c}\dot{n}\frac{[1 - e^{\rho_0(\psi-\phi)}]}{\rho_0[1 - e^{\bar{c}n}]} + \dot{\phi} \tag{3}$$

$$\dot{\phi} = -\phi m - \rho_0\frac{\dot{\psi}}{\psi}\phi + \bar{c}\dot{r}\frac{[1 - e^{\rho_0(\phi-\psi)}]}{[1 - e^{-\bar{c}r}]} \tag{4}$$

$$\dot{\epsilon} = -\frac{\dot{\bar{\lambda}}_0}{\bar{\lambda}}\left[a_2 + a_1^{-1}\tanh^{-1}\left[\frac{\left(F^c/\bar{F}\sin\theta(\epsilon) + b_1\exp[-a_6(\epsilon - 1)]\right)b_2}{\varepsilon k(\epsilon)} - 1\right]\right] \tag{5}$$

Equations (1) and (2) define the recruitment dynamics, describing the number of active and semi-active fibres in the system. Equations (3) and (4) describe the excitation dynamics primarily as functions of FES frequency, and muscular length. Equation (5) describes the contraction dynamics. Its structure is precisely that proposed for physiologically activated muscle, (Hatze, 1977), due to the fact that contraction dynamics are identical whether muscle be FES or physiologically activated. However, the excitation function 'ε' for FES muscle is different.

With the introduction of proprioceptor feedback a change in normal system behaviour is observed, with classic spastic phenomena being exhibited by the complete neuromuscular system as illustrated in the "Active Element Stretch" of Figure 1.

DISCUSSION

The newly derived musculotendon model gives further insight into the complex dynamics of a FES activated neuromuscular system. Further the assumptions made for tractability in the Hatze muscle model derivation, (Hatze, 1978), have been removed. All fundamental assumptions made in the development of this model reflect the physical reality of an FES activated system. The FES model displays great stability, while demonstrating a number of well known behaviours, both spastic and non-spastic.

Without linearisation, the new model also enables investigations to be made into the roles played by many elements involved in physiological feedback, such as input sensitivities and propagation delays.

REFERENCES

Hasan Z., *A Model of Spindle Afferent Response to Muscle Stretch,* J. Neurophysiol., Vol. 49, No. 4, 1983, pp. 989-1006.

Hatze H., *A Myocybernetic Control Model of Skeletal Muscle,* Biol. Cybernetics, Vol. 25, 1977, pp. 103-119.

Hatze H., *A General Myocybernetic Control Model of Skeletal Muscle,* Biol. Cybernetics, Vol. 28, 1978, pp. 143-157.

Mc Coy, D, *A Computer Controllable Stimulator and Its Use in FES Assisted Cycle Ergometry,* M.Eng.Sc. Dissert., National University of Ireland, 1994.

A DEVICE FOR THE MEASUREMENT OF FORCES AND MOMENTS IN THREE DIMENSIONS DURING NORDIC SKIING

P. Dorotich, W. Herzog, A. Stano, R. Jackson*

Human Performance Laboratory & *Sport Medicine Clinic
University of Calgary, Calgary, Canada

INTRODUCTION

Measuring ground reaction forces in skiing presents a technological challenge which only a few researchers have attempted to meet. Some (Komi, 1985; Leppävuori et al., 1993) have used multiple force platforms buried beneath a ski track. This approach, however, appears cumbersome, expensive, and does not allow the measurement of consecutive strides. Other researchers (Komi, 1987; Pierce et al., 1987) have tried an mounting small load cells between the bindings and the skis. Force transducers beneath the forefoot and the heel were used to measure the forces normal and longitudinal to the ski. Smith (1989) used three-dimensional video data to resolve forces normal to the ski into the components of an inertial reference frame. However, aside from a device constructed for roller skis (Street, 1988), no portable system has been designed to measure the forces lateral to the ski or the corresponding three-dimensional (3-D) moments. The purpose of this project was to build and evaluate a device for measuring forces and moments in three dimensions during on-snow Nordic skiing.

METHODS

A pair of transducers, capable of measuring forces and moments in three dimensions, was constructed to our specifications by Advanced Mechanical Technologies, Inc. The devices are essentially miniature force plates which have been inverted and mounted on a pair of Nordic skis (Fig. 1). Two strain gauge-based dynamometers are supported by hinges on L-shaped brackets mounted 50 cm apart on the skis. A 1 cm thick aluminum plate, on which the ski bindings are mounted, is suspended beneath the transducers such that the lower surface of the plate is 0.8 cm above the top deck of the ski. Each force platform weighs 1050 g and does not appear to impede the performance of a skier. Data from the six output channels on each ski are sent via cables to a portable data logger (Tattletale Model 6F), carried in a belt about the skier's waist. At a sampling frequency of 100 Hz per channel, it is possible to collect data continuously for three minutes before having to download the data to a micro computer. A 12 V battery pack provides the power for the data logger and a 5 V excitation voltage to the strain gauges of the force transducers. At room temperature, the battery lasts three hours. The total weight of the fanny pack with the data logger and battery pack is 1200 g.

The force transducers were calibrated primarily using an Instron loading device. An instrumented ski was clamped to a rigid steel beam and placed beneath the cross-head of the Instron. A series of incremental static and dynamic loads (0-1000 N) were applied vertically downward at various locations on the force plate. Voltage output from the force and moment channels was sampled for 1 s at 100 Hz for the static loads and for 10 s at 200 Hz for the dynamic tests. The ski was also turned on its side so that loads (0-500 N) could be applied to the medial aspect of the plate in the positive Fx direction. Loads in the negative Fy direction (0-100 N) were applied by orienting the ski vertically, and hanging weights

from a rigid L-shaped bracket attached to the force plate. These data were used to calculate the sensitivity and resolution, at a gain of 1500, and to examine the linearity and the cross-sensitivity of the system. The equipment was also tested in the field, using each of the three major skating techniques, to ensure operation in a cold, snowy environment. Output was sampled at 100 Hz and smoothed using a low pass, Butterworth filter.

RESULTS

The force transducers in all three directions were highly linear. Sensitivities were less than 5 mV/N for the force channels and ranged from 7 to 200 mV/Nm for the moment channels. The smallest measurable force was less than 1N and the resolution for moments ranged from .005 to .14 Nm. Test/re-test repeatability for various placements of an 800 N load in the Fz direction proved to be ±21 N, providing an accuracy of 2.6%. When loads in the Fz direction exceeded 700 N, some cross-talk (approximately 3.5%) in the Fy and Fx channels was observed. The aluminum force plate, however, did not show any hysteresis. Representative force output is presented for on-snow trials of one-skate technique (Fig. 2).

DISCUSSION

The accuracy and reliability of the ski-mounted force and moment transducers was good, suggesting that this device can be used to measure the forces and moments in three dimensions during Nordic skiing. Although there was evidence of some cross-talk, a stiffer plate would likely resolve this problem. However, given that Fz forces during our preliminary on-snow trials did not greatly exceed 800 N, the device may be used without modifications. Should it be necessary, a calibration correction factor could be used to account for the observed cross-talk. The portability of the system will allow for continuous measurement of the ground reaction forces and moments for complete analysis of skating techniques used in Nordic skiing.

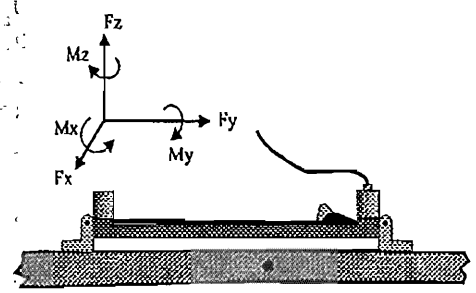

Figure 1: Schematics and local reference system of the ski-mounted force/moment transducer.

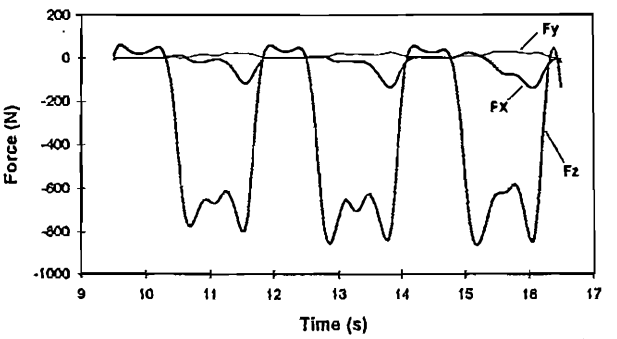

Figure 2: Force-time histories measured during three consecutive strides of the 1-skate technique.

Acknowledgments - This project was supported by Sport Canada.

REFERENCES

Komi, P. (1987). Force measurements during cross-country skiing. *I.J.S.B.* **3**, 370-381.

Leppävuori, A. et al. (1993) A new method of measuring 3-D ground reaction forces under the ski during skiing on snow. *J.A.B.* 9, 315-328.

Pierce, J. et al. (1987). Force measurement in cross-country skiing. *I.J.S.B.* **3**, 382-391.

Smith, G. (1989). *Unpublished doctoral dissertation*, Penn State Univ.

Street, G. (1988). *Unpublished doctoral dissertation*, Penn State Univ.

VARIABILITY OF TORQUE-ANGLE-VELOCITY RELATIONS IN HILL-TYPE MUSCLE MODELS

J.J. Dowling, J.R. MacDonald, G. Ioannidis, K.S. Davison
Department of Kinesiology, McMaster University, Ontario

INTRODUCTION

The use of Hill-type muscle models to estimate individual muscle forces has received wide spread interest in recent years. Often, literature values are chosen for parameters needed to define important functions such as the force-velocity and force-length relations of the muscle being modelled. Another method is to perform calibration experiments to establish torque-angle and torque-angular velocity relations on the specific subjects and then use anatomical information from the literature to convert to force, length and linear velocity. The latter method is quite time consuming and requires special dynamometers. A third method has been to use literature torque-velocity and torque-angle curves obtained from experiments on living subjects to estimate the model parameters. While this third method is convenient, the accuracy of the predictions is limited by the external validity of the literature functions.

The purpose of this study was to examine the variability in the torque angle and torque-angular velocity curves of the elbow flexors of four groups.

METHODS

The elbow flexors of 8 untrained men, 8 untrained women, 8 trained men and 8 trained women were examined on an isokinetic dynamometer (Biodex) that allowed both concentric and eccentric actions. The angular velocites were chosen to be -120, -90, -60, -30, 30, 60, 90, 120, 180, 270, 360 degrees per second (negative velocities indicate eccentric actions). Each of the 32 subjects was also tested isometrically at 90 and 120 degrees of elbow extension. The order in which the velocities were presented to each subject was random and each velocity was performed at least twice to insure that reliable results were obtained. The elbow torques and angular positions were converted to digital signals at a rate of 1500 samples per second and stored on computer disk. The joint angle data were differentiated to yield velocities which deviated slightly from those specified by the dynamometer. The actual velocities and elbow torques were calculated at every two degrees of elbow extension from 170° to 60° for each subject at each of the 11 speeds. In order to plot the three dimensional surface of joint torque by angle by angular velocity, the torque values for all velocities at each joint angle were linearly interpolated between each actual velocity to yield equispaced torque values in both angle and angular velocity. The torque values for each subject were normalized to the average maximum isometric torque at 90° and 120°. Means and standard errors of the means were determined.

RESULTS AND DISCUSSION

When the mean elbow torque data of the 32 subjects were plotted against angular velocity at joint angles of 90° and 120° (see Fig. 1), the data were similar to those reported previously (i.e. Westing et al., 1990). The standard errors of the means at each velocity were small which would indicate that a normalized function could be derived which would allow good predictions of velocity effects on torque in a Hill-type muscle model. The mean interpolated data for all joint angles and velocities are shown in Fig. 2. There were few systematic differences between the four groups of male and female, trained and untrained subjects.

In spite of the small standard errors of the means, the variance was actually quite large and would be best demonstrated with the standard deviations. As an example of possible

prediction errors, the data of a trained male (Fig. 3) were compared to the mean data of Fig. 2. The root mean square prediction error of using the group data on this subject was 13.4% of the maximum voluntary effort (12 N.m). These results suggest that caution should be exercised when normalized functions are used in Hill-type models that predict muscle forces during dynamic actions of individuals.

REFERENCE

Westing, S.H. et al. ACTA PHYSIOL. SCAND. 140:17-22, 1990.

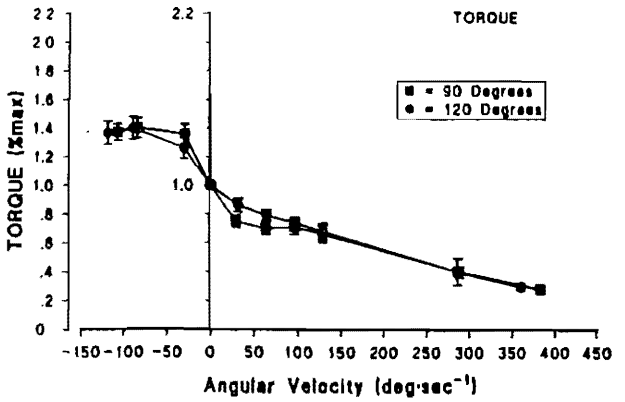

Figure 1. Mean ± SEM elbow torque vs. angular velocity of all 32 subjects at 90 and 120 degrees of elbow extension.

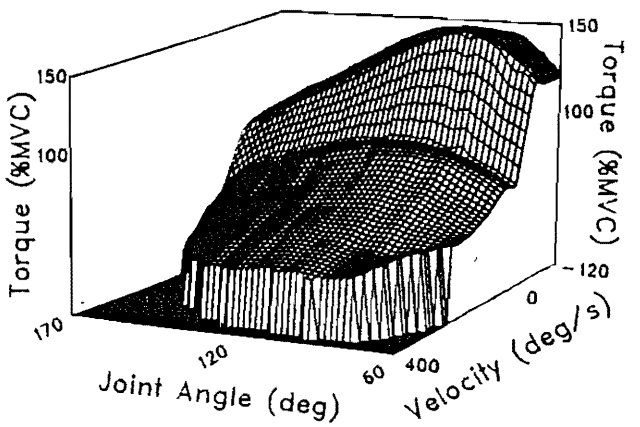

Figure 2. 3-D surface plot of mean elbow torque vs joint angle vs angular velocity of all 32 subjects.

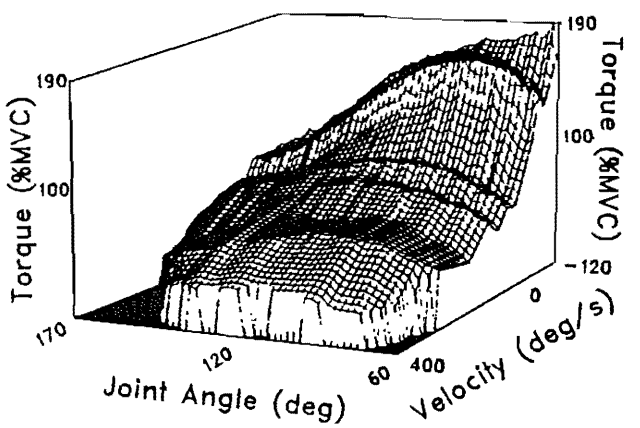

Figure 3. 3-D surface plot of elbow torque vs joint angle vs angular velocity of a single trained male subject.

THE ABILITY OF MECHANICAL POWER ESTIMATIONS TO IDENTIFY SOURCES OF RUNNING INEFFICIENCY IN CHILDREN

J.J. Dowling[1], G. Frost[2], O. Bar-Or[2]
[1]Department of Kinesiology, McMaster University, Canada
[2]Children's Exercise and Nutrition Center, McMaster University, Canada

INTRODUCTION

Older children consume less oxygen per kilogram of body weight than younger children when running at the same speed. This apparent increase in running economy with age cannot be accounted for simply by an increase in stride length and a decrease in stride rate associated with the greater height of the older children. We hypothesized that the running patterns of older children are more efficient and that a biomechanical analysis might reveal the reason for the increased economy.

Previous work that has assessed the ability of mechanical power and energy transfer estimations to elucidate the reasons for differences in running economy has concluded that neither kinematic nor kinetic modeling approaches can adequately explain interindividual differences (Martin et al. 1993). The previously cited study, as well as others, have used the correlation coefficient between mechanical and metabolic work rates as an indicator of the ability of the mechanical measure to identify causes of economy differences. While the square of these coefficients is an indicator of explained variance, a low coefficient does not necessarily mean that the biomechanical model has a low diagnostic value. A simple model that is missing several important characteristics could achieve a high correlation if some of the missing functions would cause an overestimation, and others an underestimation, of the dependent variable. Regardless of predictive value, simple models lack diagnostic value because many of the causal mechanisms have been replaced by more easily measured predictors.

The purpose of this study was to examine the ability of mechanical power and energy transfer equations to account for differences in the running economy of children.

METHODS

Nine children in each of two age groups ran on a treadmill at four different speeds. Metabolic power was calculated from the oxygen consumed (VO_2) and mechanical power was calculated from the digitized video using linked segment mechanics. The equation for mechanical power allowed energy transfer within each of the 12 segments and between segments of the same limb only (Wwb). The methods of calculating mechanical power did not take into account work wasted by cocontraction of antagonistic muscles, work recovered from elastic energy storage or isometric work against gravity. Each of these omissions would lead to an overestimation of economy and may be responsible for the relatively high values obtained. By scaling all of the values per kilogram of body weight, the differences between the two age groups in terms of isometric work against gravity may have been mostly accounted for.

RESULTS AND DISCUSSION

Figure 1 shows the relationship between mechanical and metabolic power for the nine subjects of the younger age group at each of the four speeds. The correlation coefficient of 0.38 explained only 14% of the variance in VO_2 which was similar to the relationship found by Martin et al. (1993). However, it can be seen in Figure 2 that a strong relationship between Wwb and VO_2 could exist for each child even though this relationship was different for each. Since each subject was tested at four different running speeds, a correlation value could be obtained for each child within the age

group. Table 1 shows that even though the group correlation value was low, each individual score was over 0.6 with an average of 0.85. Figure 2 shows that each child had a different economy and the economy changed with the speed of running, even within a child. These results show that even though a poor correlation between runners at the same speed may be achieved, the mechanical power calculations could be quite accurate.

Given that Wwb is a good measure of mechanical work and that it does explain most of the variance in metabolic measures for each individual, its diagnostic value still must be determined. In Figure 3, the data of the 7-8 year old children are compared with the 10-12 year olds when running at the same speed. A significant difference in VO_2 was observed but there were no significant differences in the amount of mechanical work performed. This means that oxygen cost savings of the older group cannot be accounted for by more energy transfered and indicates that older children are more muscularly efficient. It could also mean that the oxygen cost savings were due to factors not accounted for in the Wwb model. Such factors include utilization of stored elastic energy, less waste due to antagonistic cocontractions, and less relative isometric work against gravity.

Figure 3 shows the importance of energy transfers in running. Although it was not responsible for the differences in the age groups, the amount of energy transfered in running is about 30% of the total work done. Perhaps this importance causes children to learn the benefits early in the development of running patterns and that utilization of stored elastic energy and decreased cocontraction occurs later.

REFERENCE

Martin, P.E., et al. MED. SCI. SPORTS EXERC. 25:508-515, 1993.

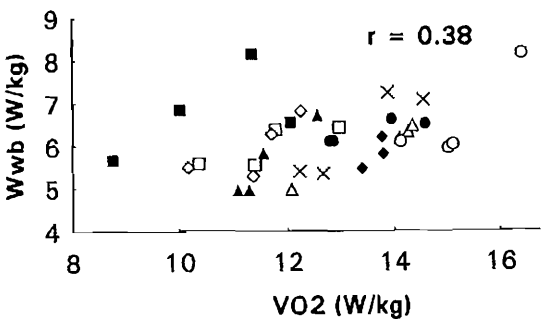

Fig. 1. Mechanical vs metabolic power of the 7-8 year olds at each speed.

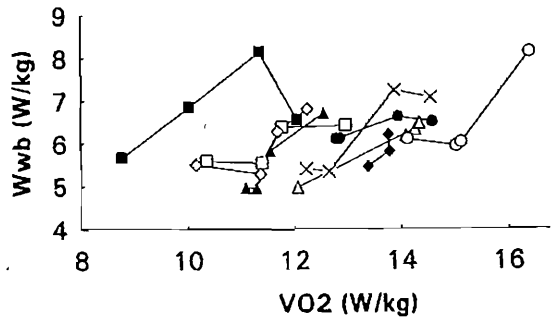

Fig. 2. Same data as Fig. 1. with connected points for each child.

Table 1. Correlation coefficients of the children in Fig. 2.

Subject	r
AF2	0.60
AF4	0.83
AM7	0.81
AM8	0.76
AF11	0.96
AM20	1.00
AF29	0.88
AM30	0.85
AM32	0.93

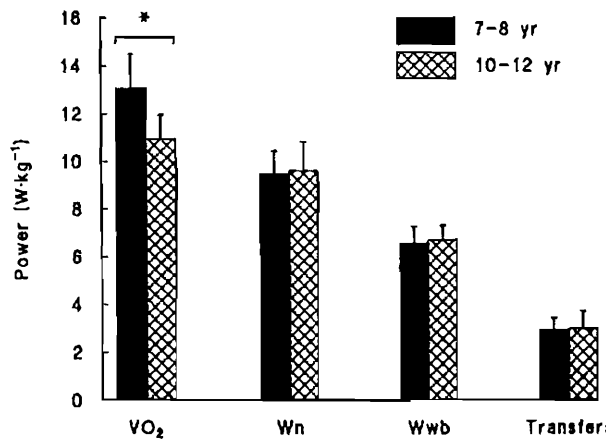

Fig. 3. Age group comparisons for metabolic power and mechanical powers with (Wwb) and without transfers (Wn).

MOTOR UNIT ACTIVATION ORDER DURING ELECTRICAL STIMULATION.

DUCHATEAU J., FEIEREISEN, P. AND HAINAUT K.

Laboratory of Biology , Université Libre de Bruxelles, Belgium.

INTRODUCTION

In the last two decades there has been quite some interest in the recruitment order of motor units (MUs) during voluntary and electrically induced contractions. It is now generally accepted that in voluntary isometric or dynamic concentric contractions, MUs are recruited according to Henneman's size principle (Milner-Brown et al, 1973). This means that small MUs are activated before larger ones. Conversely, it has been shown in animals that during electrically induced contractions MUs are recruited in the reverse order (Solomonow, 1984). A reversal in the order of MU activation during electrical stimulation has also been suggested in the case of humans (for a review see Hainaut and Duchateau, 1992), but the experimental approaches were indirect (Trimble and Enoka, 1991; Heyters et al, 1994)). The present study uses direct recording to compare the activation order of single MU during voluntary and electrically induced contractions in the human tibialis anterior.

METHODOLOGY

The experiments were performed on several occasions on 4 healthy male subjects aged between 22 and 39 and well accustomed to the experimental procedure. Each subject, who had given his consent, sat on a chair with his left foot strapped to a foot-plate connected to a strain-gauge transducer. In this position, the ankle and knee joints were set at about 90 and 100 respectively. Pairs of MUs were recorded by means of highly selective wire electrodes (40 µm in diameter) inserted into the distal part of the tibialis anterior. Under voluntary activation the recruitment order was assessed during isometric ramp contractions. The recruitment threshold, defined as the level of force at which the MU action potential appeared for the first time on the electromyographic (EMG) trace, was expressed as a percentage of the maximal voluntary contraction. Under electrical stimulation, rectangular pulses (0.1 and 1 ms in duration) were delivered over the muscle motor point at a frequency of 0.1 Hz. Once the motor nerve branch was located, the stimulus intensity was brought down to the level at which the first MU has been consistently recruited. The stimulus intensity was then gradually increased until the next small change in the EMG was seen, a change was considered to be the result of the recruitment of an additional MU. Single MU action potentials were then isolated by the subtraction of the preceding level. The action potential of these MUs was compared with those recorded in voluntary contraction on the basis of their shape and amplitude. The mechanical properties of single MU were studied using the spike triggered averaging method (Milner-Brown et al, 1973).

RESULTS

A total of 276 MUs were recorded with recruitment thresholds ranging from 1 to 88 % of the maximal voluntary contraction. The analysis of the MU population showed that during voluntary contractions of progressively increasing in force, MUs were recruited according to Henneman's size principle since a linear relationship ($r = 0.66$; $p < 0.001$) was found between the MU twitch force and their recruitment threshold. The comparison of the recruitment order between pairs of MUs showed a reversed sequence of activation in only 5% of our observations, and essentially when MU recruitment thresholds were very close. A reverse activation sequence appeared more frequently under electrical stimulation and its importance was related to the

duration of the stimulus. Indeed, while 25% of reversed MU recruitment was recorded for a pulse width of 1 ms, it was more frequent (33%) for the short (0.1 ms) pulse duration. Moreover, the percentage of reversed activation for both pulse durations was independent of the recruitment threshold difference of the two MUs.

DISCUSSION AND CONCLUSION

This work, performed on the tibialis anterior, confirms previous results obtained on hand and forearm muscles indicating that in voluntary contractions, MUs are activated according to the "size principle". The few reversals observed in MU activation were within the range reported in the literature and occurred only for close recruitment thresholds MUs. Under electrical stimulation the percentage of reverse activation between pairs of MUs was less than expected. This had already been suggested by indirect experiment approaches using both EMG power spectrum analysis and the measurement of the average muscle fibre conduction velocity recorded in the same muscle (Knaflitz et al, 1990). Our observation is also consistent with another indirect approach consisting of the analysis of the change in the twitch contraction time during graded stimulation intensity. The results of this study indicate that the reversal in the recruitment order should be less frequent in the tibialis anterior than in other muscles such as the vastus medialis, the gastrocnemius or the first dorsal interosseous (Trimble and Enoka, 1991; Heyters et al, 1994).

In conclusion, our direct observation of MU recruitment during electrical stimulation supports the view that MUs are activated in reverse order as compared to voluntary contractions. The evidence in the tibialis anterior is not as clear-cut as it is in the other muscles, possibly because more slow MUs are peripherally located (cf Henriksson-Larsen et al, 1985), and their proximity to the stimulating electrodes facilitates their activation.

REFERENCES

- Hainaut, K. and Duchateau, J. (1992) Neuromuscular electrical stimulation and voluntary exercise. Sports Med. 14(2):100-113.
- Henriksson-Larsen, K., Friden, J. and Wretling M.L. (1985) Distribution of fibre sizes in human skeletal muscle. An enzyme histochemical study in m. tibialis anterior. Acta Physiol. Scand. 123:171-177.
- Heyters, M., Carpentier, A., Duchateau, J. and Hainaut, K. (1994) Twitch analysis as an approach to motor unit activation during electrical stimulation. Can. J. Appl. Physiol. 19(4):456-4467.
- Knaflitz, M., Merletti, R. and De Luca, C.J. (1990) Inference of motor unit recruitment order in voluntary and electrically elicted contractions. J. Appl. Physiol. 68(4):1657-1667.
- Milner-Brown, H.S., Stein, R.B. and Yemm, R. (1973) The orderly recruitment of human motor units during voluntary isometric contractions. J. Physiol. 230:350-370.
- Solomonow, M. (1984) External control of the neuromuscular system. IEEE Trans. Biomed. Eng. 12:752-763.
- Trimble, M.H. and Enoka, R.M. (1991) Mechanisms underlying the training effects associated with neuromuscular electrical stimulation. Phys.Ther. 71(4):273-282.

This work was supported by the Université Libre de Buxelles and NATO (RG n 930261)

EFFECT OF POSTURE ON THE MECHANICAL IMPEDANCE OF UPPER AIRWAYS

[1]D'yachenko, Alexander I., [2]Nacke, Hans-G., [3]Konig, Joachim, [1]Baranov, Victor M., [1]Dorofeev, Yury G.

[1]Institute of Biomedical Problems, Moscow, Russia;
[2]Technical University, Dresden, Germany;
[3]EUROSPACE, Flöha, Germany

INTRODUCTION

The non-invasive forced oscillation technique is convenient for investigations of postural changes in the respiratory mechanics. Transition from the sitting position to the supine position increases resistance, elastance and inertance of the respiratory system. A theoretical analysis showed that these changes can not be explained only by changes in the lung volume, so we supposed that a substantial role in changes of respiratory impedance may belong to the shift of blood into the thorax [1]. Effect of posture on the mechanical properties of upper airways was not studied. We suppose that changes of upper airway dimensions and a shift of fluids in a head in a supine position are able to change an impedance of the upper airways. The objective of this paper was to study effects of posture and water immersion on the mechanical impedance of upper airways.

METHODS

We used a device designed for measuring the respiratory impedance under space conditions [2]. The pump produced small-amplitude forced oscillations at frequencies f = 7, 10, 13, 16, 19 Hz. An impedance of the upper airways Z(f) was measured for 6 s each frequency during the Valsalva maneuver with glottis closed. The parameters of a linear series resistance - inertance - elastance (R-I-E) model were identified. A resistance is a frequency-averaged Re Z(f). E, I and compliance C=1/E were identified by a list square algorithm for slope I and intercept E in the linear regression $\omega \cdot Im\ Z = \omega^2 \cdot I - E$; $\omega = 2\pi f$. The sitting-supine study in air was performed in 4 normal subjects. Measurements were made for 20-60 minutes after changing a posture. Effect of head-out sitting water immersion was measured on two subjects in 2 hours after the beginning of exposure. In each subject from 4 to 9 measurements in each position were made. Individual means of Z(f) were used for calculation R, I, E, C.

RESULTS

The supine position increased Re Z and decreased Im Z in all the subjects. Using the results of Z measurements in 4 subjects individual and mean R, E, C and I of upper airways were estimated. The mean of individual ratios of supine R to sitting R is equal 1.515±0.210SD. By t-test this value is significantly greater 1 ($P<0.02$). In the supine position R, E increased (Table 1).

Table 1. Effect of posture on parameters of upper airways

parameter	group mean±S.D.		P
	sitting	supine	
R, hPa/l/s	4.06±1.77	5.83±2.04	<0.05
E, hPa/l	636±130	899±151	<0.02
C, ml/hPa	1.62±0.35	1.13±0.17	<0.05
I, 10^{-2}hPa/s^2/l	2.86±0.46	3.50±0.71	NS
r	0.942±0.045	0.917±0.046	<0.005

r - correlation coefficient between ω·Im Z and ω^2; S.D. - Standard Deviation; P - differences between sitting and supine postures by paired t test; NS - not significant (P>0.05).

In the water immersion R was less in one subject and greater in another than in the supine and sitting positions in air. However C was minimal in water immersion in both subjects. The mean value of C (mean±SD in a total number of 8 measurements in each position) was respectively 3.01±0.40 in water immersion and 1.63±0.35 in the sitting position and 1.01±0.24 ml/hPa in the supine position.

DISCUSSION

Oscillatory mechanical parameters of upper airways in the group of four subjects are close to parameters found with a head plethysmograph [3]. R, E and Re Z increase and C and Im Z decrease in the supine position. Congestion and fluid filtration in tissues of a head may be the cause for these changes. We suppose that there are postural changes in rheological properties of upper airway tissues due to blood congestion. Another reason for the increase of R and E may be an increase in stress of the muscles of upper airways which is demonstrated by a decrease in the pharynx and the glottis area in the supine position [4]. In the water immersion the amount of data is too small to make definite conclusions. Only one significant increase of C in comparison with supine and sitting positions may be attributed to a decreased congestion and relaxation of muscles of upper airways.

REFERENCES

1. D'yachenko, A. (1993) Effect of dimensions of airways and posture on respiratory impedance. XIVth Congress of International Society of Biomechanics, Paris, 4-8 July, 1993. Abstracts, v. 1, 304-305.
2. Nacke, H.G., H. Haase, J. Konig, A.I. D'yachenko, V.M. Baranov (1990) A device for measurement a respiratory impedance under space conditions. In Proc. 41st Congr. Int. Astr. Fed., IAF/IAA-90-549, Dresden, Germany, October 1990.
3. Peslin, R., C. Duvivier, C. Gallina, and P. Servantes (1985) Upper airway artifact in respiratory impedance measurements. Amer. Rev. Resp. Dis., 132, 712-714.
4. Shen, H., J. Huang, S. Kitagawa, K. Yamanouchi, S. Samurai, H. Toga, T. Fukunaga, Y. Nagasaka, and N. Ohya (1991) Measurements of the pharyngeal area in patients with obstructive sleep apnea (OSA) during sleep using acoustic reflection technique. Adv. Biosc. 79: 207-209.

COMPARISON OF INDIVIDUAL TRANSFER FUNCTIONS BETWEEN GROUND REAKTION FORCE AND TIBIAL SKIN ACCELERATION

E. Eils, J. Natrup, K. Nicol

Institut für Bewegungswissenschaften, Universität Münster, Germany

INTRODUCTION

To quantify shock waves that are generated at the foot/ground contact in walking and running, bone-mounted and skin-mounted accelerometers were attached to the tibia.

A statistical approach to relate peak rates of tibial bone acceleration (TBA) and ground reaction force (GRF) resulted in high correlation values of r=0.99 (Hennig & Lafortune 1991). A correlation value of r=0.97 follows from relating tibial skin acceleration (TSA) and GRF by using a statistical approach, too (Hennig et al. 1993). Another attempt to capture the relationship between GRF and tibial acceleration was made by calculating transfer functions (Voloshin et al. 1985; Lafortune & Hennig 1993). In contrast to single peak acceleration values, transfer functions provide information about shock transmissibility for the entire foot/ground impact phase. Lafortune and Hennig set up a general tranfer function between GRF and TBA that was relatively free of individual bias and stated that this transfer function could be transmitted to other attempts under similar conditions (Lafortune & Hennig 1993). Own investigations under similar conditions showed that the use of a general transfer function was not suitable for all individuals of our sample. The purpose of the present study is to capture the relationship between GRF and TSA not by a general transfer function but by a comparison of individual transfer functions and different parameters to get more information on the underlying transmission phenomena inside the human body when measuring acceleration on the skin.

METHODS

Six male and six female individuals participated in this study. All subjects performed two heats of rearfoot running across a force platform sized 80 * 80 cm at different velocities (3 m/s and 4.5 m/s). Running speed was controlled by two photocells at equal distance in front and behind of the force platform. Every individual had to reach five good trials at each speed. All trials within a range of 3% of the exact speed were accepted. A small piece of balsa wood was fixed on the skin at the antero-medial aspect of the tibia at half the distance between the medial malleolus and the medial tibial condyle by a double adhesive tape. A six gram accelerometer with its axis parallel to the tibia shaft was glued on the balsa wood and additionally held in place by an elastic bandage that was wrapped around the shank. Ground reaction force and tibial skin acceleration signals were sampled simultaneously at 1000 Hz when the subjects contacted the platform with their right foot. Before calculating mean patterns of GRF and TSA, data were filtered by a 100Hz low pass fourth order digital filter, then the mean of trials 1-4 was calculated. The heelstrike phase (64ms) of that mean signal of both signals were subjected to Fast Fourier Transformation (FFT) to determine the Fourier coefficients F(w) (force) and A(w) (acceleration). An individual transfer function (TF) G(w) was obtained by dividing the Fourier coefficients of the acceleration by the ones of the force ($G(w) = A(w) / F(w)$).

To get an individually calculated acceleration signal the TF was multiplied with the FFT coefficients of the force of the fifth trial of each subjects ($A_5(w) = G(w) * F_5(w)$) and then converted back to time domain. By using time shift, mean of squared differences (MSD) and peak amplitude the quality of fit between measured and calculated TSA was investigated.

RESULTS AND DISCUSSION

Differences between measured and predicted acceleration were found for the individual transfer functions. Only those transfer functions (TFs) were extracted for the comparison

that fulfill the following conditions: i) predicted peak acceleration has to be in a range of 10% of the measured peak acceleration, ii) MSD <1 g^2 and iii) amount of time shift under 1ms. Nine TFs were remaining out of 24 TFs.

The TFs show different characteristics as for the appearing of peaks (Fig.1). In contrast to the results in walking of Voloshin et al. 1985, where the peaks always occur between 15 - 25 Hz and no frequencies over 30 Hz were transmitted by the lower leg, some TFs have a second peak appearing at 46.8 Hz. Lafortune et al. 1993 calculated TFs from a running speed of 4.5m/s that transmits higher frequencies in some cases, too. This discrepancy may suggest that the impact transmissibility of the lower extremity complex is velocity dependent or other factors such as pronation play a role in that part.

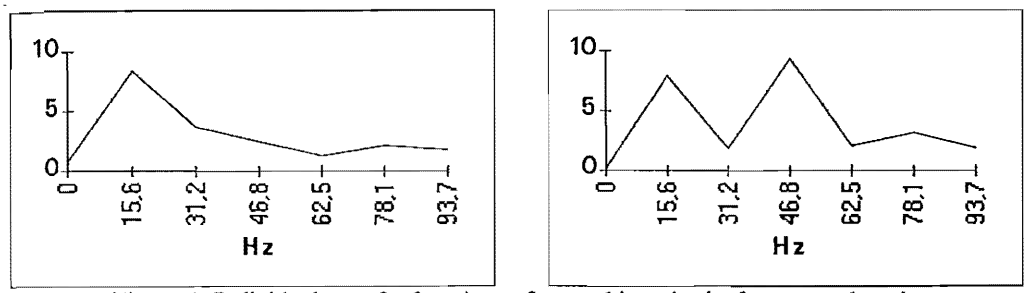

Figure 1: Individual transfer functions of two subjects in the frequency domain

To get more information about the transmission phenomena, the amplitudes of the TFs at all frequencies shown in Fig.1 were statistically compared to running velocity and sex. T-test revealed significant differences ($p<0.05$) between male and female subjects at 15.6 Hz and between running velocities at 31.2 Hz. This means that there is a difference in attenuating these frequencies between the sexes and different running velocities when measuring acceleration on the skin. Another hint of the different attenuation between sexes may be given when comparing the mean values of the frequency contents. The higher frequencies are presented stronger at females than males (Table 1).

	15.6 Hz	31.2 Hz	46.8 Hz	62.5 Hz	78.1 Hz	93.7 Hz
male	7,26	3,01	3,29	0,91	1,9	1,26
female	4,57	3,07	4,2	1,61	2,04	1,95

Table 1: Mean values of the frequency contents

In conclusion, individual TFs in running were statistically compared with different running velocities and sex. Significant differences were found for the frequency of 31.2 Hz between running velocities and for 15.6 Hz between male and female subjects. When trying to generalize the shock transmission of the lower leg when measuring on the skin, care must be taken between sexes and different running velocities.

The irregular appearance of the second peak at 46.8 Hz seems to be unexplainable. Other factors as the ones we investigated could be of importance. To get more inside into this problem further investigations are necessary.

REFERENCES

Hennig, E. and Lafortune, M. (1991) Relationship between ground reaktion force and tibial bone acceleration parameters. Int. J. Sport Biomechanics, 7, 303-309.

Hennig, E., Milani, T. and Lafortune, M. (1993) Use of ground reaktion force parameters in predicting peak tibial accelerations in running. J. Biomechanics, 9, 306-314.

Lafortune, M., Lake, M. and Hennig, E. (1993) Transfer function between tibial acceleration and ground reaktion force. J. Biomechanics, accepted for publication.

Voloshin, A., Burger, C., Wosk, J. and Arcan, M. (1985) An in vivo evaluation of the leg's shock absorbing capacity. Biomechanics IX-B, 112-116.

THE INFLUENCE OF FAST BOWLING TECHNIQUE IN CRICKET ON DISC DEGENERATION : A FOLLOW-UP STUDY.

B. ELLIOTT and A. BURNETT (The University of Western Australia, Perth, Australia), M. KHANGURE (Royal Perth Hospital, Perth, Australia), R. MARSHALL (The University of Auckland, Auckland, New Zealand), and P HARDCASTLE (Sir George Bedbrook Spinal Unit, Perth, Australia).

INTRODUCTION

Young athletes are being forced to train longer, harder, and earlier in life to excel in their chosen sport. Young fast bowlers in cricket (where the spine must flex laterally, extend and rotate to assist the generation of a high ball release speed) have been shown to be particularly prone to overuse injuries, as their musculoskeletal systems are still immature (Elliott et al., 1992). One of the most serious overuse problems for any young athlete is the development of abnormal radiological features in the lumbar spine such as pedicle sclerosis, spondylolysis or intervertebral disc degeneration, as they may cause pain and may debilitate the player (Foster et al., 1989; Elliott et al., 1992; Elliott et al., 1993). Although not as severe as pars interarticularis abnormalities, degeneration and/or bulging of the intervertebral disc may compromise the normal functioning of the disc. The aims of this study were to identify if interverteberal disc abnormalities (reduced disc height, degeneration, bulging or herniation) changed over a two and a half year period for a sample of young fast bowlers. Selected fast bowling actions were related to the presence of these disc abnormalities.

METHODS

Twenty-four male bowlers (mean age 13.7 years), who bowled at a school and club level were tested in 1992 (session 1). This session involved assessing lumbar disc status using magnetic resonance imaging (MRI). These subjects then bowled two maximum velocity trials at a wicket so that their front foot landed on a Kistler force platform during the delivery stride. A Photosonics camera operating at 200Hz filmed perpendicular to the plane of motion, while an overhead camera, operating at 100Hz also filmed each trial. Force data were recorded from the platform on a computer at 500Hz.

All bowlers were then counselled as to the possible causes (particularly that of bowling with a "mixed" action (Foster et al., 1989)), of developing abnormal radiological features in the lumbar spine. Approximately two years later 20 of the initial sample, who were still actively engaged in fast bowling, were re-assessed using the same protocol as for session 1. MRI scans from 1994 (session 2) were used to classify the group into normal (group 1) and abnormal disc groups (group 2). Descriptive statistics were used to assess the presence or changes of disc abnormalities between the two sessions and the bowling actions associated with these changes.

RESULTS AND DISCUSSION

The 20% incidence of intervertebral disc abnormalities (T_{12}-L_1 to L_5-S_1) increased to 45% over the two and a half year period. The incidence of abnormalities by session 2 was higher than the 30% reported by Tertti et al. (1991) for children of the same age who complained of low back pain, but approached the 65% and 70% incidence respectively reported by Elliott et al. (1992) for 18-year old high performance fast

bowlers and Annear et al. (1992) for retired, elite level fast bowlers. No bowlers were reported as having a bony abnormality in session 1, however, by session 2 one bowler showed a spondylolysis on a CT scan. Two of the four bowlers who recorded abnormal disc pathology in session 1 had experienced a deteriorated condition, while the remaining two recorded no change over the two sessions.

The counter-rotation of the trunk between back and front foot impact, (a characteristic of the mixed bowling action), has been shown to predispose bowlers to an increased incidence of bony (Foster et al., 1989; Elliott et al., 1992) and disc abnormalities (Elliott et al., 1993 : session 1) in the lumbar region. All bowlers, who counter-rotated their trunk by greater than 40° between back and front foot impacts, recorded disc or bony abnormalities at session 2. Foster et al. (1989) had previously shown that fast bowlers who counter-rotated their trunk by more than 40° from the shoulder alignment at back foot impact to a more side-on position near front foot impact were more likely to sustain back injuries. Eight of the nine bowlers, who recorded disc abnormalities used the mixed action, while the three bowlers in the sample who used a side-on action recorded normal scans of the lumbar discs. Peak vertical ground reaction force was not related to the incidence of disc abnormality as has previously been reported in the literature.

This study therefore clearly shows that the progression in disc degeneration over the period between the testing sessions is a serious problem facing young fast bowlers, particularly those who used the mixed bowling action. A clinic aimed at modifying technique to one that does not predispose the player to injury was found to be unsuccessful. It would seem that a more long term program must be structured to educate bowlers on how to reduce the risk of developing abnormal radiological features in the lumbar region by using an appropriate action and thus allowing young players to participate in a relatively injury free environment.

REFERENCES

ANNEAR, P., CHAKERA, T., FOSTER, D. and HARDCASTLE, P. (1992). Pars interarticularis stress and disc degeneration in crickets' potent strike force - the fast bowler. Aust. N.Z. J. Surg. 62: 768-773.

ELLIOTT, B., HARDCASTLE, P., BURNETT, A. and FOSTER, D. (1992). The influence of fast bowling and physical factors on radiological features in high performance fast bowlers. J. Sports Med. Train. Rehabil., 3: 113-130.

ELLIOTT, B., DAVIS, J., KHANGURE, M., HARDCASTLE, P. and FOSTER, D. (1993). Disc degeneration and the young fast bowler in cricket. Clin. Biom., 8:227-234.

FOSTER, D.H., JOHN, D., ELLIOTT, B., ACKLAND, T. and FITCH, K. (1989). Back injuries to fast bowlers in cricket : a prospective study. Br. J. Sports Med., 23: 150-154.

TERTTI, M., SALMINEN, J., PAAJANEN, H., TERHO, P and KORMANO, M. (1991). Low-back pain and disk degeneration in children : a case-control MR imagery study. Radiol., 180: 503-507.

Developmental Aspect of Overarm Throwing in Children

H. Enami, S. Yamagami[1]
Research student of Kagawa University, JAPAN
[1]Physical Education, Kagawa University, JAPAN

INTRODUCTION

Many studies on motor development in children have been done with the quantitative data. To understanding child's motor development, the development of the actual motor pattern producing the performance should be investigated. Besides, there have been many qualitative analysis of the kinematics of the thrower's body, while relatively small numbers of quantitative studies have been done on the kinematics of the throwing upper extremity and trunk. In paticular, very little quantative data concerning the upper arm and trunk action during throwing have been reported because a standard method of analysis has yet to be established.

The purpose of this study were to investigate the development of throwing pattern, and to make clear the kinematics of the throwing on the upper arm and trunk in children.

METHODS

The subjects were 119 boys children from 3 to 9 years of age, and were asked to throw a tennis ball for distance with maximum effort. In this study, we have done to classify their throwing motion by the observational evaluation method using 6 throwing pattern (the development of throwing pattarn by Miyamaru, M. 1978). Furthermore, Three dimentional (3-D) high-speed cinematography was used to record their throwing motion. The direct linear transformation (DLT) method was used for 3-D space reconstruction from 2-D images filmed by two phase-locked cameras (100 frames/s). Figure 1 indicates the definition and sign of the torso twist.

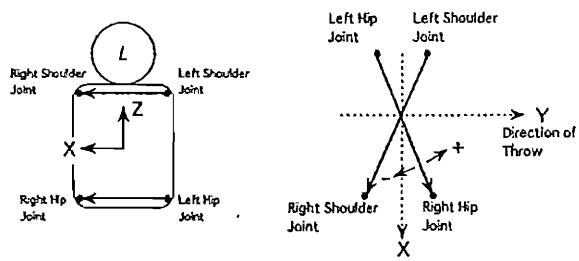

Figure 1 Definition and sign of the torso twist

RESULTS AND DISCUSSION

Table 1 shows the classification of the throwing pattern of boys children. The results of motor development revealed that the throwing pattern developed along with age from the immature pattern 1 to more mature pattern 6 progressively. After the age of four, pattern-4 of throwing was not to be had in children.

Figure 2 shows the torso and upper arm angle for the skilled (pattern-6) and unskilled (pattern-2) boys. At the beginnig of external rotation, these angles showed very similar kinematic pattern. But, at the instant of maximum external rotation, the torso and upper arm was in torso twist angle (skilled boy:4.9° , unskilled boy:-28.8°) and an external rotation angle (skilled boy:-82.5° , unskilled boy:-45.8°). This throwing motion of skilled boy indicates that rotate the hips, the

trunk, and the shoulders to the left while retracting the throwing arm to the final position before starting the forward arm action. Further, in this skilled boy, at the instant of ball release, the angles of abduction and horizontal adduction of the upper arm were both positive. The upper arm, while rapidly internally rotating at the instant of release, was still in an externally rotated position at this instant.

The changes of angles of the joints (abduction/adduction angle at the shoulder joint, internal rotation/external rotation angle at the shoulder joint, horizontal abduction/horizontal adduction angle at the shoulder joint, flexion/extension angle at the elbow joint, and trunk angle of the torso twist) showed different patterns dependent on the skill levels of throwing in the children.

These results suggested the effectiveness of 3-D film motion analysis technique in investigation of the throwing motion and throwing teaching.

TABLE-1 Classification of the throwing pattern of children (Boys)

	3-year-old	4-year-old	5-year-old	6-year-old	7-year-old	8-year-old	9-year-old	Total(%)
Pattern-1	1(16.6)							1 (0.9)
Pattern-2	3(50.0)	3(21.4)	2(11.0)					8 (6.9)
Pattern-3	1(16.6)	9(64.3)	8(44.5)	7(41.2)	5(25.0)	6(30.0)	2 (9.5)	38(32.7)
Pattern-4	1(16.6)							1 (0.9)
Pattern-5		2(14.3)	8(44.5)	8(47.1)	12(48.0)	13(65.0)	17(81.0)	60(51.7)
Pattern-6				2(11.7)	3(12.0)	1 (5.0)	2 (9.5)	8 (6.9)
Total(%)	6 (100)	14 (100)	18 (100)	17 (100)	20 (100)	20 (100)	21 (100)	116 (100)

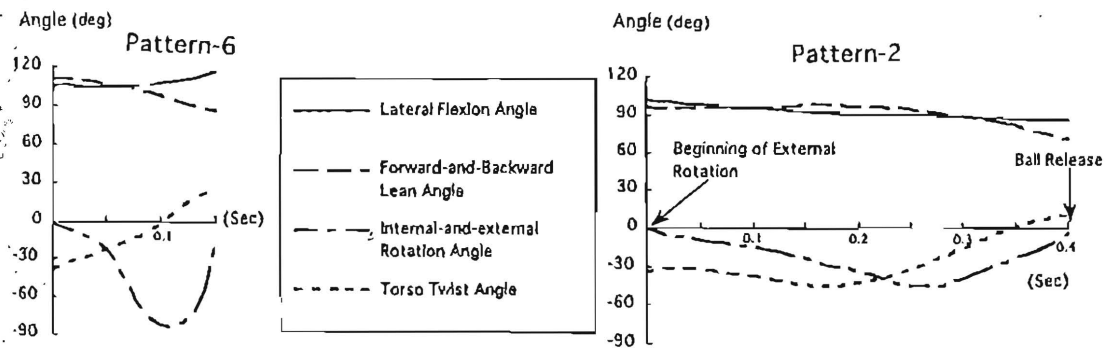

Figure 2 The torso and shoulder angle for the skilled(Pattern-6) and unskilled(Pattern-2) boys

REFERENCES

1)Feltner, M. & Depena, J. :Dynamics of the shoulder and elbow joint of the throwing arm during a baseball pitch. Int. J. Sport Biomech. 2:235-259, 1986.
2)Fukashiro, S. et al:Development of throwing pattern in children. Jap. J. Sport Sci. 1(3):231-236, 1982.
3)Miyamaru, M. :Development of overarm throwing patterns in preschool boys. Transactions of Tokyo women's college in physical education 3:3-16, 1978.
4)Wickstrom, R. L. :Fundamental motor patterns. LEA & FEBIGER. :82-93, 1970.
5)Wild, M. R. :The behavior pattern of throwing and some observations concerning its course of developmental in children. Res. Quart. 9(3):20-24, 1938.

LOWER EXTREMITY JOINT RANGE OF MOTION AS A MEASURE OF EFFICACY FOR SELECTIVE DORSAL RHIZOTOMY SURGERY

J.R. Engsberg, K.S. Olree, T.S. Park

Motion Analysis Laboratory, Department of Neurosurgery, St. Louis Children's Hospital and Washington University Medical School, St. Louis, Missouri, U.S.A.

INTRODUCTION

Pre- and post-surgery gait analyses of children undergoing selective dorsal rhizotomy (SDR) (1) have generally indicated improvement (2). The time and complexity associated with a gait analysis however, often prevent widespread utilization of the procedure as a means of determining SDR efficacy. Physical therapy evaluations such as passive joint range of motion tests performed on these children are less time consuming, less costly and simpler, but lack the objectivity associated with comprehensive gait analysis. The purpose of this investigation was to quantify lower extremity joint range of motion as a means for evaluating the efficacy of SDR surgery.

METHODS

Forty-two children (mean age, 5 years, range 2-16) with cerebral palsy (CP) scheduled for a SDR the following day and 9 children (mean age, 7 years, range 3-17) with able bodies were recruited. Reflective surface markers were placed on both sides of the body at: 1) rostral aspect of proximal head of fifth metatarsal, 2) posterior aspect of calcaneus, 3) lateral malleolus, 4) lateral condyle of tibia, 5) greater trochanter of femur, and 6) iliac crest. A video camera in conjunction with a PEAK motion analysis system was used to record the locations of the markers (60 Hz) during the tests.

For the tests the children were seated on a table in an upright sitting posture with feet not touching the ground. The children were instructed to actively perform at least 3 repetitions of complete knee extension. Two to three practice trials preceded data collection. Verbal instructions, tactile cues, demonstrations and other techniques were used to help the children understand and execute the task. No physical assistance was given during actual collection of the data. The speed of the movement was self-selected but any kicking technique was not accepted. Maximum knee flexion was determined following the same procedure. A second test was conducted with the subject's leg supported at approximately a 45° angle from the vertical. As with the preceding tests, the children performed at least 3 repetitions of maximum dorsiflexion and plantarflexion. The entire procedure usually required less than 15 minutes of patient time.

Video data were tracked to produce 2D locations for the surface markers as a function of time. End range positions for each movement, trial, and subject were determined and averaged for the knee and ankle joints, respectively. Values were then averaged for the respective groups. An unpaired t-test was used to test for significant differences between groups ($p<0.05$). A paired t-test was used to test for significance for 5 children that have thus fall been tested pre- and post-surgery (7 months) ($p<0.05$). Data processing generally required less than 1.5 hours per patient visit.

RESULTS

Results indicated that the children with CP (pre- and post-surgery) had significantly less knee extension and ankle dorsiflexion when compared to similar results

for the children with able bodies (Figures 1 & 2). Significant differences existed between the children with able bodies and the full cohort of children with CP prior to surgery for knee flexion and ankle plantarflexion. Results also indicated a significant level of improvement post-surgery for knee extension and ankle dorsiflexion.

DISCUSSION

The results for the active range of motion at the knee and ankle illustrate the limited motion of the children with CP when compared to results from those with able bodies. This was particularly true for dorsiflexion where the children with CP (84 limbs) could not attain a dorsiflexed position, achieving only 20° of plantarflexion pre-surgery while the children with able bodies achieved 19° of dorsiflexion. Significant improvements post-surgery (10 limbs) for active dorsiflexion and knee extension were 13° and 12°, respectively. This method provides a simple objective evaluation of knee and ankle impairment. It is less time consumming and complex than gait analysis and more objective than physical therapy measurements. Future work evaluating the three methods with the same group of children seem warranted.

REFERENCES

1. Park, TS, Owens JH 1992 New England Journal of Medicine. 318,13:803-808.
2. Vaughan CL et al 1991 J Neurosurgery. 74:178-184.

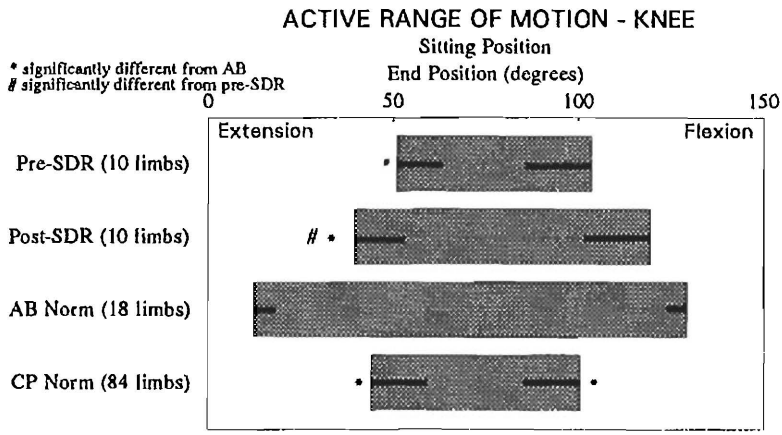

Figure 1. Means and SD for motion at the knees for 42 children with CP and 9 with able bodies. Five children were tested pre- and post- SDR (7 months).

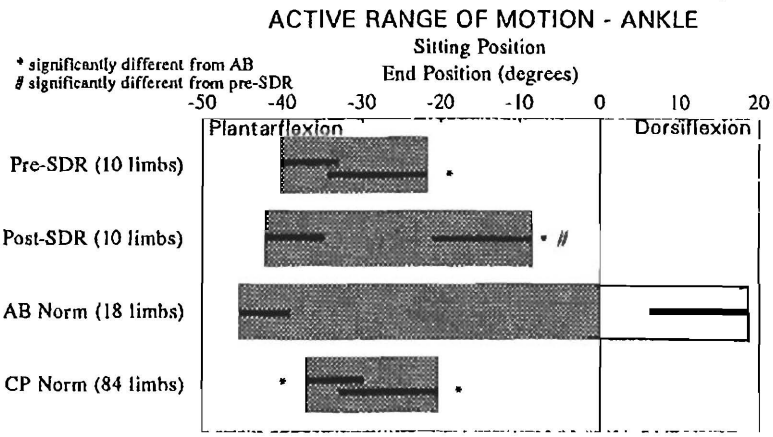

Figure 2. Means and SD for motion at the ankles for 42 children with CP and 9 with able bodies. Five children were tested pre- and post- SDR (7 months).

QUANTIFICATION OF HAMSTRING SPASTICITY IN CHILDREN WITH CEREBRAL PALSY

J.R. Engsberg, K.S. Olree, S.A. Ross, T.S. Park

Motion Analysis Laboratory, Department of Neurosurgery, St. Louis Children's Hospital and Washington University Medical School, St. Louis, Missouri, U.S.A.

INTRODUCTION

A major impairment in cerebral palsy is spasticity. It has been characterized as a velocity dependent resistance to stretch (2). Many surgical, pharmaceutical and therapeutic procedures are performed on children with cerebral palsy to minimize or eliminate the influence of spasticity. To assess the efficacy of these procedures objective measures describing changes in spasticity are required. Investigators have reported measures to quantify spasticity yet a simple objective mechanically based method incorporating speed, resistance, and range of motion for its quantification does not seem to exist (3). The efficacy and possibly the necessity of many procedures to alter the influence of spasticity remains unclear. The purpose of this pilot investigation was to develop a method to quantify spasticity in the hamstrings.

METHODS

Ten children (mean age, 11 years) diagnosed with spastic diplegic cerebral palsy and 6 children with able bodies (mean age, 9 years) volunteered. All subjects were tested on a KinCom isokinetic machine capable of moving the passive leg through a range of motion and measuring the resistive torque. Each child sat upright on the chair of the KinCom machine with stabilization straps placed across the pelvis and thigh. The axis of the KinCom lever arm was aligned with the knee axis of the child. A laboratory coordinate system was set to 0° by moving the lever arm to the horizontal. The leg of the child was attached to the lever arm with Velcro straps. The test starting position was about 60° below the horizontal. The final extension position was determined by utilizing a feature which stopped the machine when a preset torque was reached. The preset torque for the children was determined for each subject and varied between 6 and 20 Nm. Children were instructed to remain as relaxed as possible as the leg rotated from a flexed position to an extended one. Tests for knee extension were conducted at speeds of 10, 30, 60, and 90 °/s and the resistive torque was continuously monitored during the trials. Torque-angle data were processed to eliminate the influence of gravity and other factors which disrupted the signal (e.g., acceleration, machine dynamics). The areas within the torque-angle curves were determined for each speed for each child to yield the work done by the machine on the child. Linear regression was used to determine the slope of the line of best fit for the work-velocity data for each child. The work-velocity slopes for each group of children were averaged and a t-test was used to determine if a significant difference existed between the slopes for each group ($p<0.05$).

RESULTS

Torque-angle data for a typical child with an able body indicated very little change in torque as a function of speed (Figure 1). In contrast, similar data for a typical child with cerebral palsy indicated larger torques with an increase in speed (Figure 2). The work done by the machine on the knees of the children with able bodies (6 legs) remained relatively constant for the 4 speeds (7% increase from slow to fast) while the work done on the children with cerebral palsy (14 legs) increased as the velocity

increased (69% increase from slow to fast) (Table 1). The slope (Joules/(°/s)) of the linear regression line for work as a function of velocity for the children with able bodies was very close to zero (0.0031, SD=0.009) while the corresponding slope for the children cerebral palsy was approximately 10 times greater (0.033, SD=0.019) (Figure 3). These slopes were significantly different from one another.

DISCUSSION

The slope of the work-velocity data incorporates the three major components characterizing spasticity (i.e, speed, resistance, range of motion). While only a small cohort of subjects have thus far been tested, significant differences existed between the groups. Previous investigators have conducted tests similar to the ones carried out in the present investigation (1,3,4). They have not however, processed the data to produce a simple mechanically based variable to characterize all components of spasticity. This method may prove to be a valuable objective measure for quantifying spasticity thus permitting more effective assessment of treatments designed to alter spasticity.

REFERENCES

1. Dahlin, M., Knutsson, E., Nergardh, A. 1993. "Treatment of Spasticity in Children with Low Dose Benzodiazepine." J Neurol Sci. 117:p54-60.

2. Dimitrijevic,M.R.1985 "Spasticity." In Swash, M., Kennard, C. (Eds.) Scientific Basis of Clinical Neurology. Edinburgh: Churchill Livingstone.

3. Rhymer, WZ, Powers, R.K. 1989. "Pathophysiology of Muscular Hypertonia in Spasticity." In Neurosurgery: State of the Art Reviews. 4(2)p291-301.

4. Vandervoort, A.A., et al. 1992. "An Outcome Measure to Quantify Passive Stiffness of the Ankle." Canadian Journal of Public Health - Supplement 2:pS19-S23.

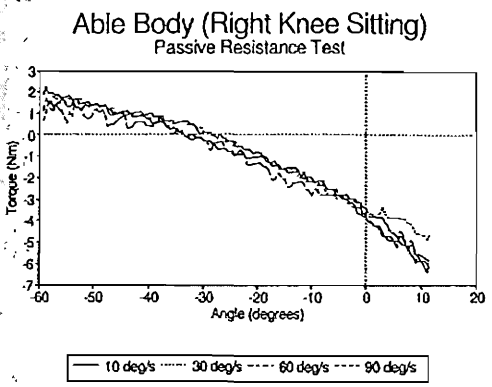

Fig 1. Passive resistance test for AB child.

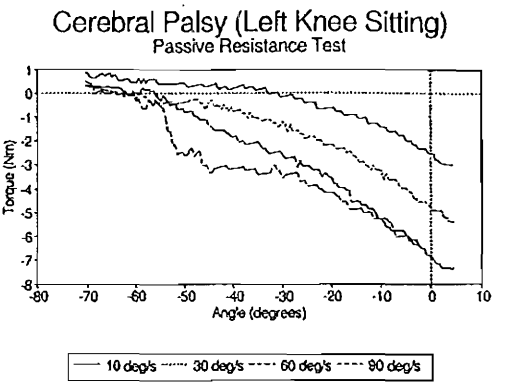

Fig 2. Passive resistance test for CP child.

Table 1. Work done (Joules) by machine on knees of 2 groups of children at 4 speeds.

Group	10°/s	30°/s	60°/s	90°/s
Able Bodied	2.84	2.78	2.91	3.04
(SD)	2.48	2.35	2.12	2.11
Cerebral Palsy	3.40	3.89	4.71	5.75
(SD)	1.51	1.95	1.81	2.58

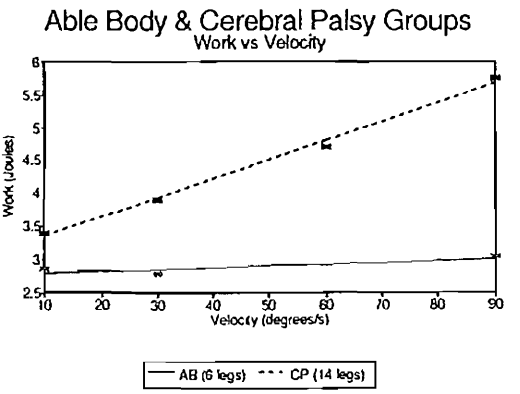

Fig 3. Lines of best fit for 2 groups.

POSTURAL STABILITY IN GOOD AND POOR TRIALS IN RIFLE SHOOTING - A STUDY ON TOP-LEVEL AND NAIVE SHOOTERS

P. Era*, N. Konttinen‡, P. Mehto*, P. Saarela§ and H. Lyytinen‡

*Department of Health Sciences, University of Jyväskylä, Jyväskylä, Finland
‡Department of Psychology, University of Jyväskylä, Jyväskylä, Finland
§Department of Kinesiology, University of Maryland, U.S.A.

INTRODUCTION

In many sports events the role of posture control is central. Shooting may be an extreme example of the role of stability in a sport event: even small changes in posture may lead to significant changes in performance. In normal standing, the oscillations of the body are considerably smaller in experienced shooters than in untrained controls even when tested without supportive clothing (Aalto et al., 1990). Also in conditions corresponding normal competitive shooting the stability of the posture may be much better in top-level shooters than in less experienced shooters during the last seconds preceding the trigger pull (Era et al., submitted, a). The purpose of this study was to analyze if there are differences in stability during the last seconds preceding the shot between good trials and poor trials and if these differences are similar in well trained top-level shooters and less experienced shooters.

METHODS

The subjects were right-handed volunteers (n=24) who represented three different ability levels. Six male and three female subjects were internationally ranked rifle shooters. Eight male shooters were representative of national levels of competition in three-position rifle. The remaining seven males were inexperienced novice subjects, who had basic knowledge about aiming, holding and triggering, but whose experience in shooting was limited.

Testing was conducted indoors using a laser-rifle system (Noptel Co., Finland). The shooting distance was 18 m. During shooting the subject stood on a force platform (Kistler 9861A, area 600 mm * 1200 mm, placed parallel with the shooting track). Each subject chose foot locations freely according to their individual style. Signals were amplified and converted into digits using a micro computer. Using an algorithm developed earlier (Era et al., submitted, b), the horizontal location of the center of pressure (COP) was calculated. On the basis of the coordinates for the COP, the mean moment of velocity of COP movement was calculated. These analyses were carried out in 5 successive windows, 1.5 seconds each, preceding the trigger pull. The quality of performance was described the movement of the aiming mark and the position of the aiming mark at the very moment of the trigger pull (hit point).

RESULTS

In trained top-level or national level shooters no significant difference was observed between the least and most successful trials, whereas among the amateurs the value of the moment of velocity was higher in the less successful shots (Fig. 1).

DISCUSSION

This study indicated that a good performance in the actual shooting (the score and the quality of the aiming as reflected by the movement of the barrel) was associated with the variables describing the stability of the posture only among the unexperienced controls. Among them, a better shooting performance was associated with more stable posture. This could partly be due to the fact that 'poor trials' had clearly different meaning among the highly experienced shooters than among the controls. A difference in performance when hitting 8.5 instead of 10 was something so small that it could not be observed systematically in the force platform data, and a poor result in these highly trained shooters was probably seldom if ever due to a problem in the whole body stabilization. In contrast, in the novise shooters significant differences in the balance parameters between good and poor trials could be observed already 4 - 6 seconds prior to the shot and these differences remained also during the last seconds preceding the shot.

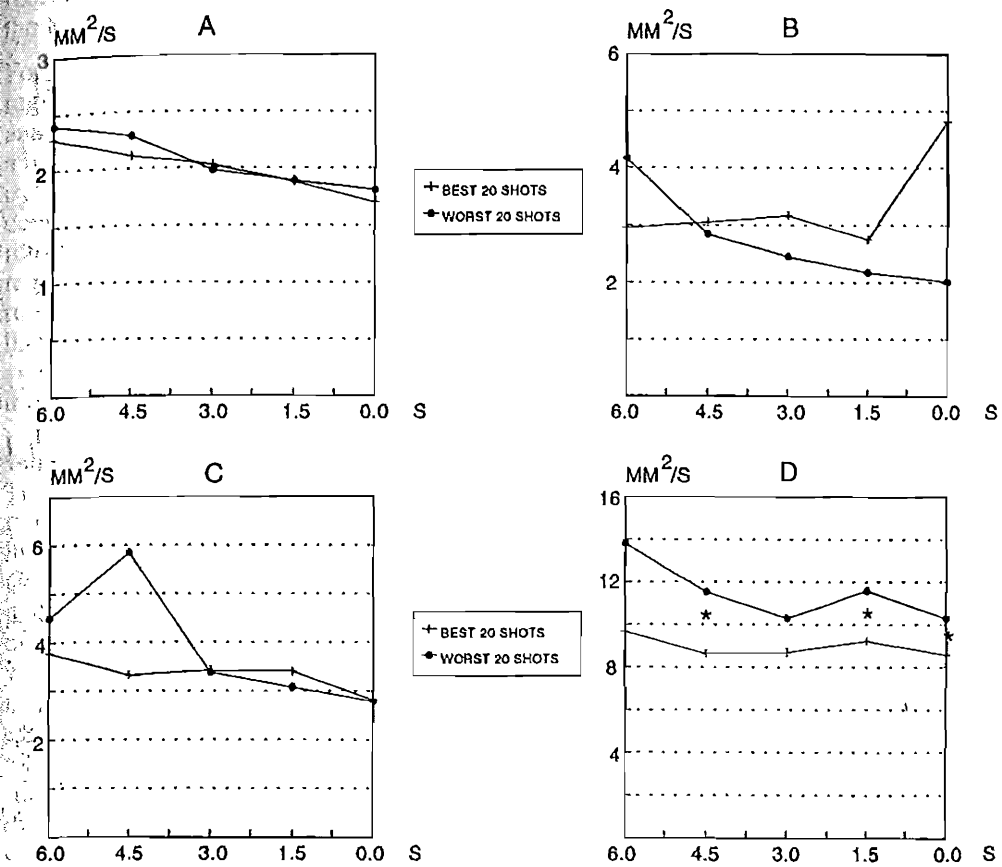

Fig.1. Movement of the center of pressure as indicated by the mean moment of velocity during the last 7.5 seconds preceding the shot in the best and poorest trials of the top-level male (A) and female (B) and national level male shooters (C) and unexperienced controls (D). Means in each window lasting 1.5 sec. in each group and the statistical significance for the differences between the best and worst trials (paired t-test) are shown.
* $p<.05$ ** $p<.01$

REFERENCES

Aalto, H., Pyykkö, I., Ilmarinen, R., Kähkönen, E. and Starck, J. (1990) Postural stability in shooters. Otol. Rhinol. Laryngol. **52**, 232-238.

Era, P., Konttinen, N., Mehto, P., Saarela, P. & Lyytinen, H. Postural stability and skilled performance - a study on top-level and naive rifle shooters. Submitted (a).

Era, P., Schroll, M., Ytting, H., Gause-Nilsson, I., Heikkinen, E. and Steen, B.Postural balance and its sensory-motor correlates in 75-year-old men and women - a cross-national comparative study. Submitted (b).

CONTROL OF MOTOR UNITS IN THE GENERATION OF MUSCLE FORCE

Zeynep Erim*, Carlo J. De Luca*†, and Kiyoshi Mineo‡

*NeuroMuscular Research Center and †Departments of Biomedical Engineering and Neurology, Boston University, Boston, MA USA, ‡ Department of Rehabilitation Medicine, Keio University School of Medicine, Keio, Japan

Introduction:

Previous studies (De Luca *et al*, 1982, De Luca *et al*, 1987) have lead to the concept of *common drive* which proposes that in performing a given task, motor units of a motoneuron pool receive a shared command signal that controls them collectively, as opposed to an arrangement whereby motor units are monitored and controlled individually. Other studies (De Luca and Erim, 1994, Erim *et al*, 1994) have aimed to delineate the rank-ordered aspects of inherent motor unit properties that define their responses to command signals and make the harmonious operation of the system under the *common drive* scenario possible. The goal of this investigation was to obtain a better understanding of the system as well as the characteristics of the driving signal by studying the system in contractions where different force levels were targeted.

Methods:

Myoelectric signals were detected from the Tibialis Anterior muscle of six subjects with a special quadrifilar needle electrode while the subjects generated isometric forces that increased linearly with time (10% of maximal voluntary contraction / s) up to a target level that ranged from 20 to 100 % of the maximal voluntary level. The target levels of 20, 50, 80 and 100% of maximal voluntary contraction (MVC) were maintained for 18, 12, 6 and 2 s, respectively and then force was brought down to 0 at rate of 10% MVC/s. These signals were decomposed into the constituent motor unit action potential trains and an accurate record of the interfiring intervals was obtained using the previously described method of Precision Decomposition.

Results:

The recruitment threshold was calculated for each motor unit that was observed to fire in a stable manner. In all the contractions, including those that reached 100% MVC, the highest recruitment threshold noted was 71.3% MVC. In other words, no recruitment was observed beyond approximately 70% MVC.

For each target force level, the standard deviation and the coefficient of variation of the interspike intervals (computed in the constant force region) were investigated as a function of recruitment threshold. At submaximal force levels, there was no dependency ($p>0.05$) of coefficient of variation on recruitment threshold, while standard deviation increased significantly ($p<0.001$)with increasing recruitment threshold. This could imply that the coefficient of variation of the interpulse intervals is the parameter which the system controls and maintains constant. The dependency of the standard deviation was probably due to the positive correlation between average interpulse interval (IPI) and recruitment threshold (see below) since the standard deviation (σ) and the coefficient of variation are related by $\sigma = CV^* IPI$. At the maximal force level of 100% MVC, the coefficient of variation decreased with increasing recruitment threshold, while standard deviation displayed no dependency on recruitment threshold. This behavior could be related to the fact that at maximal levels, firing rates of all motor units converge to the same value. It was observed that the coefficient of variation increased with increasing target levels.

The joint behavior of pairs of motor units were investigated by cross correlating the continuous mean firing rate signals estimated for each motor unit (by filtering the impulse trains corresponding to the firing times of that unit) in the constant force region. The peaks of the cross correlation functions were located approximately at zero latency in all cases, irrespective of the targeted force level, or the difference in the recruitment thresholds of the motor units analyzed. However, the standard deviation of the peak locations were observed to increase with increasing force, possibly due to the shorter

observation window available. No significant correlation was observed ($p>0.05$) between the peak value of the cross correlation function and the difference in the recruitment thresholds of the units. On the other hand, a weak tendency was observed in the level of cross correlation to increase with increasing target force levels.

For each submaximal force level, average firing rates computed for the constant force region were plotted against the recruitment threshold of the motor unit. Regression analysis revealed a significant correlation ($p<0.001$) between the recruitment threshold of a motor unit and its average firing rate at a given force level. This finding confirmed earlier reports regarding the *onion skin* phenomenon which states that in a given contraction, earlier recruited motor units maintain higher firing rates than their later recruited counterparts. As would be expected from increasing firing rates with force, the regression intercepts showed an increase with increasing target levels. Furthermore the regression slopes showed a tendency to approach zero, which agreed with earlier reports that firing rates of motor units with different recruitment thresholds converge to the same value at maximal force levels. The initial firing rate (calculated as the inverse of the first three interpulse intervals) was found to increase with increasing recruitment threshold.

Discussion:

The results of this study confirmed two previously reported observations regarding the rank-ordered control of motor units: 1)*Common drive* phenomenon was reflected in the high cross correlation peak values centered around zero latency at all force levels. *Common drive* phenomenon refers specifically to the organization of the motoneuron pool. According to this arrangement, the firing activity of individual motor units are effected, not through separate command inputs, but through inherent differences in the way individual motor units respond to a common drive. Such an organization would relieve the central nervous system from the burden of keeping track of and controlling each motor unit separately, and provide a strategy whereby a single command could be employed to regulate the activity of all the motor units in a given motoneuron pool. 2) The inherent properties of motor units that determine their responses to varying input signals are not randomly distributed but closely linked to their recruitment rank. As in the dependency of average firing rates and initial firing rates of motor units, the recruitment rank or recruitment threshold of a motor unit determines its response characteristics. This highly ordered arrangement of motor unit properties makes it possible for a common drive to effect the harmonious operation of the system in an efficient manner.

In addition to providing further confirmation that these notions, which relate to the architecture of the motoneuron pool and the inherent characteristics of individual motor units, hold true at all force levels, the present study provides insight regarding the input signals that drive the motor units. If the inputs received by a motor unit are modeled as a common drive shared by all the other units in the motoneuron pool and a "noise" input specific to that unit, the higher cross correlation values for higher target levels would indicate that common drive increases faster relative to the unshared "noise" component of the inputs seen by the motoneuron as the targeted force level is increased.

References:

De Luca, C.J., LeFever, R.S., McCue, M.P. and Xenakis, A.P. Control scheme governing concurrently active human motor units during voluntary contractions. *Journal of Physiology,* 329: 129-142, 1982.

De Luca, C.J. Control properties of motor units. *Journal of Experimental Biology,* 115: 125-136, 1985.

De Luca, C.J. and Erim, Z. The common drive of motor units in regulating muscle force *Trends in Neurosciences,* Vol.17, No.7, 1994.

Erim, Z., De Luca, C.J. and Mineo,K. Rank-Ordered Regulation of Motor Units. *Proceedings of the Tenth Congress of the International Society of Electrophysiology and Kinesiology*, June 1994.

THE EFFECTS OF RUNNING TRAINING ON THE COLLAGEN FIBER SPATIAL ORIENTATION IN THE REPAIR TISSUE OF FULL-THICKNESS ARTICULAR CARTILAGE DEFECTS

Margarida Espanha[1], Mika Hyttinen[2] and Armando Moreno[1]
[1] Lab. of Anatomophysiology, Faculty of Human Kinetics, Lisboa, Portugal
[2] Dept. of Anatomy, Univ. of Kuopio, Kuopio, Finland

INTRODUCTION.

Articular cartilage (AC) once injured possesses limited capacity for repair. The repair of full-thickness defects which violate subchondral bone is influenced by several factors, namely, the maturity of the AC, the position of the defect, the size and the type of articular function after defect occurrence. These type of defects have access to inflammatory and marrow stem cells, heal transiently but imperfectly, and degenerate. Early motion has been reported to produce a better cartilage repair. More recently, continuous passive motion (CPM) has been introduced as a procedure for improving this limited repair ability in full-thickness defects. Also postoperative exercise was found not detrimental to the AC response in horses (French, 1989). The purpose of this study was to investigate if mild running exercise results in improved repair of AC materialized by a better collagen fiber arrangment in osteochondral defects.

METHODS.

Thirty male Wistar mature rats were anaesthetized and through a medial parapatellar incision full-thickness AC defects (0.85 mm ø) were drilled into the medial condyle until bleeding was observed. One week post-operatively, the animals were divided in the folowing groups: cage activity for 4 weeks (n=4) and 8 weeks (n=5) providing intermittent active motion (IAM) and running training (RT) for 4 weeks (n=10) and 8 weeks (n=12). Animals were euthanized and distal femur samples were fixed in 4% paraformadehyde in 0.1 M sodium phosphate buffer, pH 7.4, decalcified with 7.5% EDTA and processed for paraffin embedding. Histological sections were cut (5 µm) through the center of the lesion perpendicularly to the surface, dewaxed and treated with bovine testicular hyaluronidase. Polarization analyses were performed on unstained (cover-slip mounted with DPX) sections using a polarized light microscope equipped with a lambda/4 compensator plate and monochromatic plate (lambda=591.4 nm) connected to a cCCD camera system. A Macintosh II computer eqquiped with a 256 grey-level monitor and an image analysis software (IP Lab Spectrum) were also used. Optical retardation values (ORVs) of birefringence were determined in central and junctional areas of the repair tissue using defined regions of interest (ROIs) (Figure 1) and at two different positions [parallel to the scar surface (45° position) and at 0° position (extinction position)]. For statistical analysis t-test for unrelated samples was used.

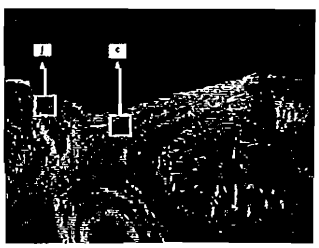

Figure 1 - Examples of ROIs at junction (j) and central (c) areas of the scar tissue

RESULTS.

Qualitative PLM observations indicated a great variability in the organization of the repair tissue from defect to defect. Both groups showed different patterns of collagen fiber orientation, except in the superficial zone where fibers with the same orientation as in the superficial zone of normal AC were observed. These observations also showed a lack of fibril continuity between the repair tissue and the adjacent AC, even when light microscopy demonstrated an apparent continuity of the tissue.
With respect to the quantitative analysis at 4 weeks the ORVs of birefringence were significantly higher in IAM group except in the junctional area at 45°position (Figure 2A) but on the contrary at 8 weeks RT group showed ORVs higher than IAM group at both positions and in central and junctional areas, being these differences more significant at 45° position (Figure 2B). The results of IAM groups (4 and 8 weeks) were very variable at both positions (Figure 2C). On the other hand the RT groups showed a significative increase in the ORVs from 4 to 8 weeks in central and junctional areas at both positions (Figure 2D).

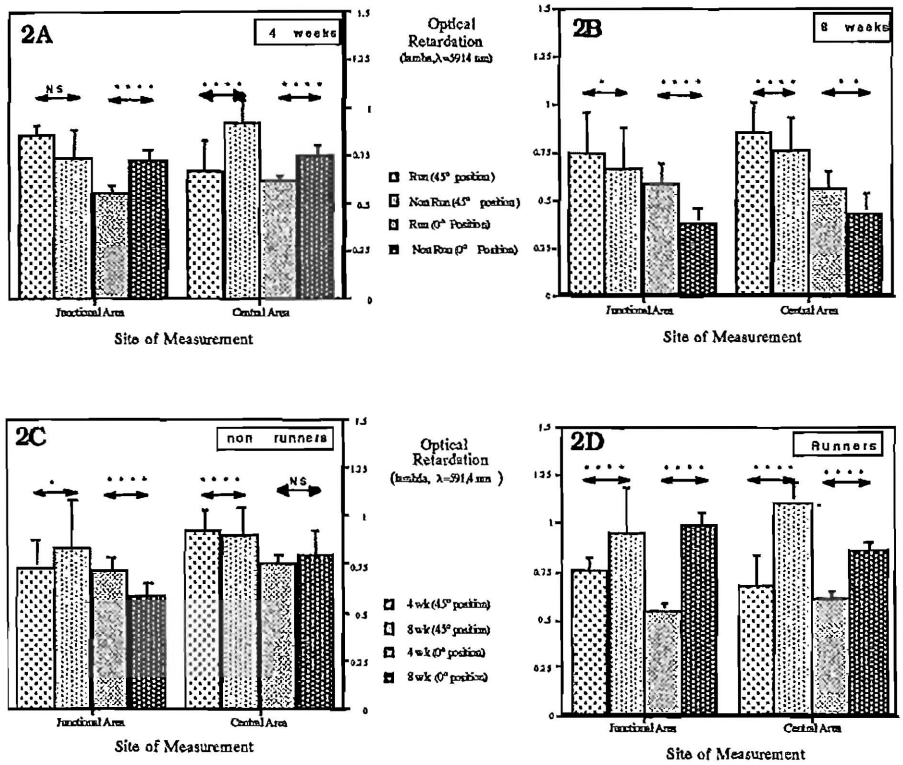

Figure 2. Optical retardation values (ORVs) of runners (run) and non runners (non run) animals at 4 weeks (4 wk) and 8 weeks (8 wk) and at 45° and 0° positions. * $p<0.05$; ** $p<0.01$; *** $p<0.001$; **** $p<0.0001$; NS - non significative

DISCUSSION.

This study allowed quantitative characterization of the collagen network of repair tissue of defects in AC. The higher ORVs of IAM group at 4 weeks can indicate that the running training probably is responsible for the collagen fiber spatial orientation at random during the early stage of the repair. No major alterations with time were seen in the IAM group suggesting that these arrangment remained almost the same. Running exercise influenced the outcome of the repair tissue as shown by the higher retardation values of RT animals at 8 weeks. CPM treatment improved the repair tissue of osteochondral defects (Salter et al., 1980). Large osteochondral defects treated with periosteal grafts also improve after several weeks of CPM showing higher % of collagen type II (O´Driscoll et al., 1986). Todhunter et al. (1993) also found higher % of collagen in exercised ponies. At 8 weeks the differences between IAM and RT groups were more significatant in the central area and, since at 4 weeks the RT group demonstrated lower values it seems that the most evident modification from 4 to 8 weeks was in the central area of the scar tissue suggesting formation of highly oriented collagen network. Post-operatively mild running training might enhance the quality of the scar tissue by improving the nutritional supply to it and providing mechanical stimulation which can be responsible for the closed packed collagen fibers in the runners animals at 8 weeks indicating either improved collagen organization or increased amount of collagen.

REFERENCES.

French, D.A., Barber, S.M., Leach, D.H. and Doige (1989) Vet Surg 18:312-321

O´Driscoll, S.W., Keely, F.W. and Salter, R.B. (1986) J Bone Joint Surg 68A(7):1017-35

Salter R.B., Simmonds, D.F., Malcolm, B.W., Rumble, E.J., MacMichael, D. and Clements, N.D. (1980) J Bone Joint Surg 62A:1237-1251.

Todhunter, R.J., Minor, R.R., Wootton, J.A.M., Krook, L., Burton-Wurster, N. and Lust, G.(1993) J Orthop Res 11(6):782-795

Acknowledgements: This study was supported in part by Helsinn Produtos Farmacêuticos, S.A..

A COMPARISON OF MEDIAL ARCH ANGLE AND CALCANEAL INCLINATION WITH THREE DIMENSIONAL REARFOOT MOVEMENT DURING THE STANCE PHASE OF WALKING.

A. Fahey, R. Smith and A.E. Hunt.
Faculty of Health Sciences, The University of Sydney, Sydney, Australia.

INTRODUCTION

Foot shape has been suggested as a factor which may predispose an individual to lower limb injuries (Subotnick, 1981). Abnormally shaped feet (for example flat or overpronated feet) are thought to move excessively during walking and running and thus cause lower limb injuries. Measures of foot shape may be clinically important because they are believed to identify the individuals who display this excessive foot movement and are at risk of injury. Recent experimental research suggests that some clinical measures of foot shape do not identify people with abnormal foot movement. Measures such as the height of the navicular, arch index and other footprint measures have been shown to be unable to identify people with excessive foot movement during the stance phase of walking and running (Nigg, et al, 1993; Hamill, et al, 1989). However, other measures of foot shape exist and further research is needed to determine if any these measurements can be used clinically to the identify the individuals who display excessive foot movement.

The purpose of the present study was to determine if either medial arch angle or calcaneal inclination (two measures of foot shape) can be used to identify those people who display excessive rearfoot eversion or abduction (leg internal rotation) during the stance phase of walking.

METHODS.

Nineteen males aged between 18 and 26 volunteered to participate in the present study. Calcaneal inclination and medial arch angle were measured while the subjects stood; calcaneal inclination was measured with a protractor and medial arch angle was measured with a small goniometer. Calcaneal inclination was defined as the number of degrees the midline of the calcaneus deviated from being perpendicular to the floor and medial arch angle was defined as the angle formed by the medial malleolus, the navicular and the head of the first metatarsal. The three dimensional kinematics of the right rearfoot were recorded with the Motion Analysis System™. Hyper-reflective markers were attached to bony landmarks on the foot and shank. The positions of these markers were recorded while the foot was in a standardised reference position (Gant, 1993), which was used as the baseline for the kinematic measurements. Foot movement was recorded with four cameras as the subjects walked along a flat walkway. Five stance phases were recorded for each subject, then averaged. The maximum amounts of foot eversion and abduction were determined for each subject from the average curves. Correlations were performed to determine if either calcaneal inclination or medial arch angle were related to the maximum amount of foot eversion or abduction during the stance phase of walking.

RESULTS

The scatter plots for the four correlations performed in the present study are presented in Figures 1-4. The only significant correlation was between calcaneal inclination and the maximum amount of eversion during the stance phase of walking ($r = 0.46$; $p = 0.48$). Subjects with a more everted calcaneus in standing displayed more rearfoot eversion during the stance phase of walking. While significant this relationship only explained 21% of the variation in maximum eversion. There were no other significant correlations.

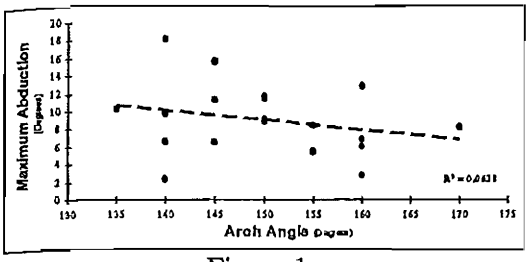

Figure 1

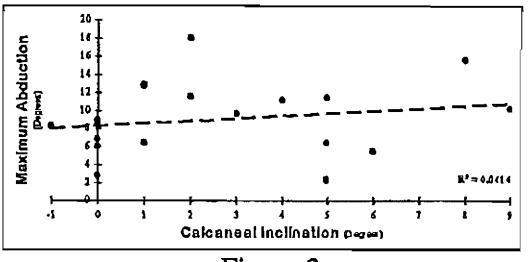

Figure 2

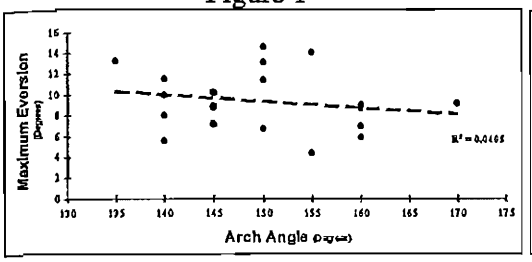

Figure 3

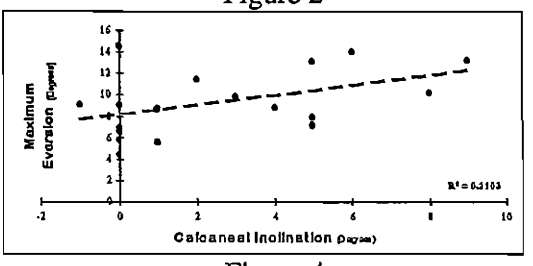

Figure 4

Figures 1, 2, 3, and 4 show the four correlations which were performed in the present study. Each dot represents one subject and the dashed lines represent the least squares regression line. The only significant correlation is in figure 4.

DISCUSSION

The comparison of absolute kinematic measurements used in the present study assumes that the baseline of each subject is identical. Great care was taken to ensure that each subject was placed in the same reference position (which was used as the baseline), thus the correlations performed in present study are valid.

In the present study the only significant correlation was between calcaneal inclination and maximum eversion, however, this correlation is not strong enough to suggest that calcaneal inclination can be used clinically to identify people with excessive foot eversion. In fact, the subject who displayed the most eversion during walking had a calcaneal inclination of 0°, which is considered normal. Thus, using calcaneal inclination alone to prescribe treatment may result in this treatment going to the inappropriate people.

There was no relationship between medial arch angle and either the maximum amount of eversion or abduction, thus people with flatter arches do not display excessive foot eversion or abduction (leg internal rotation). This finding contradicts the currently held hypothesis that clinically measured flat (or overpronated) feet move excessively during walking. In conclusion, neither calcaneal inclination or medial arch angle should not be used clinically to identify people with excessive foot eversion or abduction during the stance phase of walking.

REFERENCE LIST

Gant R. (1993). The accuracy and reliability of a method of measuring three-dimensional kinematics of the foot during the stance phase of walking, and its application to patients with osteoarthritis of the knee. Unpublished Masters' Thesis, Faculty of Health Sciences, The University of Sydney, Australia.

Hamill J., Bates B.T., Knutzen K.M. and Kirkpatrick G.M. (1989). Relationship between selected static and dynamic lower extremity measures. Clin. Biomechanics, 4(4), 217-225.

Nigg B.M., Cole G.K. and Nachbauer W. (1993). Effects of arch height of the foot on angular motion of the lower extremities in running. J. Biomechanics, 26(8), 909-916.

Subotnick S.I. (1981). Flat foot. Physician and Sportsmedicine, 9(8), 85-91

THE EVALUATION OF VERTICAL FORCE LOAD RATE FOR LOCOMOTOR STUDIES

N. Fell and A. Lees.
Centre for Sport and Exercise Sciences, School of Human Sciences, Liverpool John Moores University, Liverpool, L3 3AF, UK.

INTRODUCTION

Load rate is a characteristic measurement variable of the vertical ground reaction force, and it has been widely used to assess the shock absorbing characteristics of individuals, styles of locomotion and footwear. During normal heel-toe running the greatest load rate is associated with the initial or impact force peak. It has been defined as the magnitude of the force peak above the base line force value divided by the time from the onset of the force to the time at which the peak force is achieved (Lees and McCullagh, 1984). This may be termed the *average load rate*. However, in order to overcome the 'end effects' some authors (e.g. Miller, 1990) have used the central portion of the impact slope. The load rate quantified in such a way may be termed the *effective load rate*. A further difficulty is apparent when estimating load rates where data over the region of interest are clearly not linear (e.g. the drive off peak for heel-toe running or the vertical GRF data for fore-foot running). An alternative method would be to use the *dynamic load rate*, defined as the continuous first differential of the force curve (Nigg, 1986). The dynamic load rate is therefore characterised by a graphical profile rather than just by a numerical value. The aim of this study was therefore to quantify the dynamic load rate for heel-toe and fore-foot running, and to compare the peak dynamic load rate estimates with the conventionally computed average and effective load rates.

METHOD

Two subjects were required to run bare-foot over a Kistler force platform (Type 9281). They were required to complete two series of ten runs (heel-toe and fore-foot), each at a speed of 4 $m.s^{-1}$. The force signals were sampled at 1000 Hz and were used to compute the average, effective and maximum dynamic load rates. The average load rate was calculated as defined by Lees and McCullagh (1984) between the points A and B in Figure 1. The effective load rate was computed over the visually linear portion of the impact force peak (from points C to D in Figure 1). For each method of calculation, the load rate was computed from each trial and the mean value (n=10) determined.

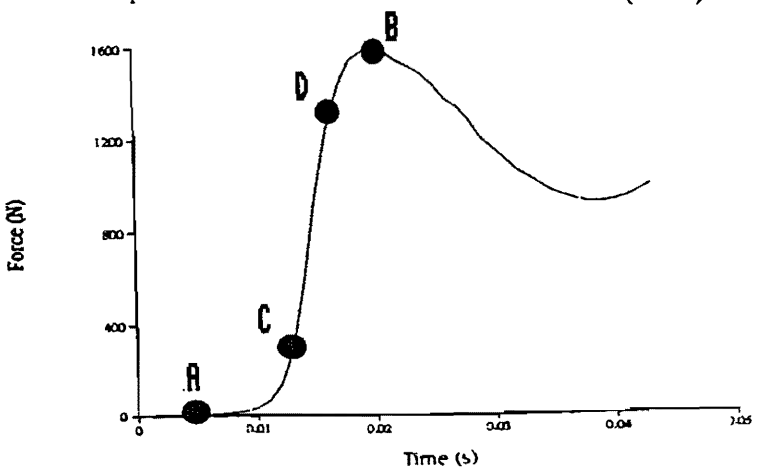

Figure 1. The impact peak in heel-toe running amplified in time. Points A to B and C to D indicate the points between which the average and effective load rates may be computed.

RESULTS AND DISCUSSION

A one-way ANOVA with repeated measures established that there were significant differences ($p<0.001$) between each of the three estimates of load rate for heel-toe and fore-foot running for both subjects. As an estimate of the load rate applied to the body during running, the peak dynamic load rate gave a significantly higher value than the average or effective load rate. It is therefore more likely to be a truer representation of the actual load rate or shock experienced by the body after the compression of the calcaneal fat pad. A further comparison of these estimates of load rate has shown that the load rate can be underestimated in heel-toe running by some 20% or more using the effective load rate, and by over 60% using the average load rate. In fore-foot running the discrepancies are so large between each approach that it is doubtful if anything other than the dynamic load rate could be meaningfully used.

TABLE 1. A comparison of load rates for heel-toe and fore-foot running (kN^{-1}).

		Subject A		Subject B	
		mean	SD	mean	SD
Heel-toe running	average	166.7	42.0	231.3	54.6
	effective	269.2	54.1	471.3	73.0
	peak dynamic	396.2	65.8	607.9	82.4
Fore-foot running	average	17.3	1.2	21.8	1.6
	effective	19.3	2.1	23.7	1.7
	peak dynamic	144.5	35.9	318.3	106.8

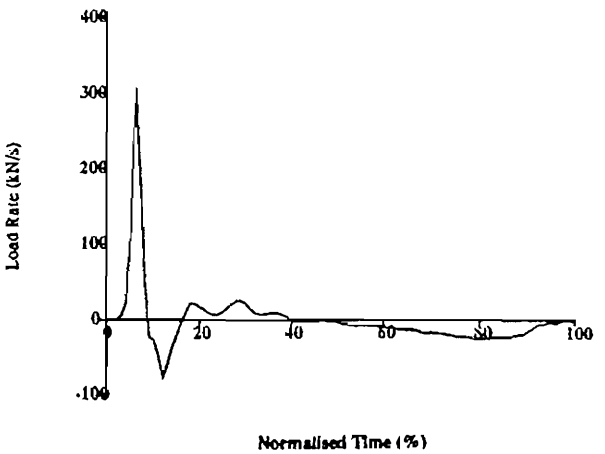

Figure 2. Dynamic load rate for heel-toe running.

It was also apparent that at as well as the initial peak in the dynamic load rate, there were at least two and possibly three additional peaks (Figure 2). It is therefore suggested that the dynamic load rate gives a more detailed picture of the absorption of force than the average or effective load rates. The peaks in the dynamic load rate data are thought to reflect some underlying structural mechanisms which are important as part of a sequence of progressive shock absorption.

REFERENCES

Lees, A. and McCullagh, P. (1984) A preliminary investigation into the shock absorbency characteristics of footwear and foot inserts. J. Hum. Mvmt Stud. 10, 95-106.

Miller, D. I. (1990) Ground reaction forces in distance running. In Cavanagh, P. R. (ed) Biomechanics of Distance Running. Champaign, Ill.: Human Kinetics.

Nigg, B. M. (1986) Biomechanics of running shoes. Champaign, Ill.: Human Kinetics.

EFFECTS OF ARM SUPPORT OR SUSPENSION ON SHOULDER AND ARM MUSCLE ACTIVITY DURING SEDENTARY WORK

Yi Feng, Wim Grooten and Ulf P. Arborelius.
Kinesiology Research Group, Department of Neuroscience,
Karolinska Institutet, Stockholm, Sweden

INTRODUCTION

Occupations with static sitting posture are known to cause problems in the shoulder region, even if the mechanical load is low (Hagberg & Wegman 1987). One way to assess the load on the muscles is to use electromyography - EMG - (Hagberg 1981). The aim of this study is to evaluate the activation of shoulder and arm muscles during various work tasks, with the lower arm supported by different types of arm supports. This is a continuation of our previous work, concerning e.g. evaluation of balancers as an aid in industry (Arborelius & Harms-Ringdahl 1986).

METHODS

The subjects were asked to perform four tasks: typing, simulated assembly work in two different positions, and simulated pipetting. The supports used were: no support, fixed arm support, horizontal movable arm, "flexible arm" support which could move in vertical and horizontal direction, and lower arm suspension with balancer (10N force).

EMG was used to measure muscle activity. The signals were recorded with surface electrodes, low pass filtered, A/D converted and turned to amplitude distributions. To make comparisons possible between the levels of activity in different muscles and subjects, a normalization was performed, with activity during isometric maximum (95 percentile of EMG recording) as a reference.

EMG from the following muscles was registered: Deltoideus pars ant., Deltoideus pars lat., Trapezius upper part and dorsal wrist extensors (Extensor carpi rad. long. & brev.). 20 seconds of EMG was analyzed for each action. Movement and force data were recorded, and are under processing and will be discussed in another paper.

RESULT

Table I shows the over all mean (and SD) from individual median activity with and without supports. Activity is expressed as % of reference (IMVC) contraction.

	No support		Support	
Delt.ant.	6.2	(5.3)	2.4	(3.0)
Delt.lat.	4.5	(3.7)	2.1	(2.1)
Trap.up.	11.5	(7.3)	7.0	(7.0)
Wrist ext.	12.0	(6.8)	11.3	(6.3)

An example of mean cumulative EMG curves from nine subjects, trapezius muscle and low assembly work, is presented in Figure 1. Cumulative relative distribution on Y-axis and % of reference amplitude on X-axis. The use of supports give a shift to the left, corresponding to lower EMG amplitude. Filled circle: No arm support, Open circle: Balancer (K-Block), Filled square: "Flex." support, Open square: Horizontal movable, Open triangle: Fix support.

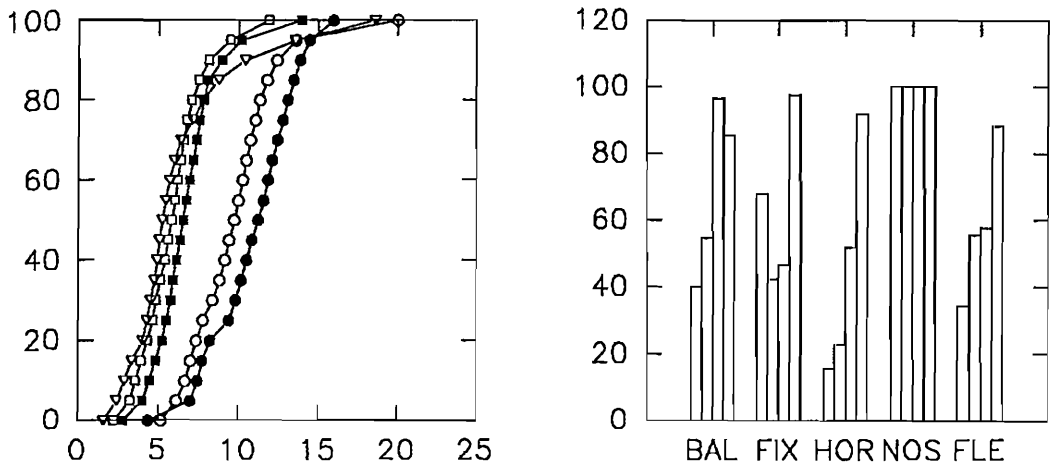

In Fig. 2. the mean for muscles (in the same order as table above) of individual medians for activity during low assembly work are shown, with activity without support (NOS) set to 100%. A statistical analysis (Kruskal-Wallis one-way analysis of variance by ranks) showed that the (except for wrist extensor) there was a significant difference (p=0.05) for each muscle between supports, both with "no support" included or excluded.

To show which support that was best for a specific task, ranks were used. In Table II ranks for the different tasks and all muscles are shown to the right. To the left is the total ranks (all tasks and muscles) and the sum of all individual ranks for the same device. Lowest rank = lowest EMG.

	Total rank	Sum	Typing	Pipet.	Assembly Low	Assembly High
Horizontal	1	278	1	1	1	2
Fix	2	332	4	2	3	1
Flex arm	3	336	2	4	2	2
Balancer	4	387	3	3	4	3
No support	5	512	5	5	5	4

DISCUSSION

The muscular activity in shoulder muscles can be reduced by the use of arm supports. Our investigation gives no information about the effect of fatigue, but possibly the effect could be more prominent over longer time. In our study the over all best effect, on muscle activity, was provided by the horizontal movable support. This support, however, can not easily be used for work which requires more vertical movement. We plan to investigate this further.

References:

Arborelius, U.P., Harms-Ringdahl, K. The results from a full scale field test of an arm suspension balancer. Extended abstr. In proceedings "Work With Display Units", Stockholm, May 1986, 329-332.

Hagberg, M. On evaluation of local muscular load and fatigue by electromyography. Arbete och Hälsa. 1981, 24.

Hagberg, M., Wegman, D.H. Prevalence rates and odds ratios of shoulder neck diseases in different occupational groups. Brit. J. Ind. Med. 1987, 44, 602-610.

CALCULATION OF AREA OF STABILOMETRIC SIGNALS USING PRINCIPAL COMPONENT ANALYSIS

Liliam Fernandes de Oliveira[1,2], David Martin Simpson[1], Jurandir Nadal[1]
[1] Biomedical Engineering Program, COPPE/UFRJ, and [2] School of Physical Education and Sports - Federal University of Rio de Janeiro(UFRJ), Rio de Janeiro, Brasil.
E-mail: DAVID@SERV.PEB.UFRJ.BR

INTRODUCTION

The stabilometric signal describes body sway by measuring the excursion of the centre of pressure in the frontal and sagital planes from signals recorded by a force platform on which the patient stands. Various parameters have been extracted from these signals to quantitatively study equilibrium and posture control. One is the area covered by the centre of pressure (CP) in the x (lateral) - y (anterior posterior) plane during an interval of time. A conventional method for area calculation is based on an ellipse, whose major axis is determined from the standard deviation along the regression line fitted to the stabilogram in the x-y plane. The minor axis is found correspondingly in the orthogonal direction. This study proposes the use of principal component analysis as an alternative to regression, which from theory, simulation and the analysis of 112 stabilograms is shown to be more reliable.

METHODS

Supposing the data to follow approximately a 2-Dimensional Gaussian distribution, an ellipse is defined with radii 1.96 times the standard deviations along the major axes, thus covering 95% of the samples. The orientation of the principal axis is usually defined by linear regression applied to the data (Odenrick et al., 1987, Hasan et al., 1990). In regression analysis, the residual distance between the data samples and the regression line in the direction of the dependent variable is minimized, requiring that one of the axes (x or y) be defined as the dependent, the other being the independent variable (regression y vs. x or x vs. y). The resulting estimate of the inclination of the principal axis is biased, an effect known in statistics as regression to the mean. The estimated angle can differ quite widely depending on which axis is chosen as dependent, a choice which in stabilometry seems arbitrary. The accuracy also depends on the angle and therefore the experimental conditions of the test.

Principal component analysis (PCA) minimizes the deviation in a direction orthogonal to the line fitted to the data, which intuitively is more suitable for the present problem. There is no need to define x or y as dependent, as the technique determines the direction of maximum (and minimal) variance of the scatter plot. The slope of the major axis is the first eigenvector of the covariance matrix, and the variance along this axis is the corresponding (larger) eigenvalue. The second eigenvector and value define the direction of the minor axis (orthogonal to the first) and its variance. For the x, y data, the calculation is very simple:

$$s_{pc}^2 = \frac{s_x^2 + s_y^2 \pm \sqrt{(s_x^2 - s_y^2)^2 + 4(s_{xy}^2)^2}}{2} \quad (1)$$

where s_x^2, s_y^2 are the estimated variances in the x and y directions respectively, and s_{xy}^2 is the covariance between x and y. The two solutions for s_{pc}^2 correspond to variances along the two axes, respectively. The angles can also readily be calculated:

$$\alpha_{pc} = \tan^{-1}\frac{s_{pc}^2 - s_x^2}{s_{xy}^2} = \tan^{-1}\frac{s_{xy}^2}{s_{pc}^2 - s_y^2}. \quad (2)$$

The two solutions of equation (1) give the inclination of the major and minor axis, respectively.

SIMULATION

To test the differences between regression and PCA, simulations were carried out. Two independent normal distributions (1500 samples each in the x and y directions) were generated (with variances of 2 and 1 respectively) and rotated in the range of 0 to 90°. The area of the ellipse and the slope of the principal axis were calculated for each angle by linear regression of x vs. y and y vs. x, and principal components. The area and the slope of the major axis calculated by PCA gave only a small estimation error throughout the rotation. Regression y vs. x gave areas and slopes near the correct value for angles close to zero degrees, while regression x vs. y was best for angles near 90°.

APPLICATION TO STABILOMETRIC DATA

Twenty eight normal young female (22 ± 2 years old) were tested by means of stabilometry with 4 test protocols (eyes open and eyes close with feet apart and feet together), 30 seconds each. Subjects were instructed to look forwards and maintain an upright position on a three point vertical force platform. The sampling rate for the signals from the cells was 50 Hz. The areas and inclinations of the ellipses were then calculated using linear regression and PCA for each subject and each experimental condition.

RESULTS AND DISCUSSION

With feet apart and eyes open or closed, the angles calculated by principal components and regression x vs. y tend to agree. Regression y vs. x frequently gave differing angle estimates. With feet together this picture tends to reverse and regression x vs. y becomes the 'odd-one-out'. With feet apart, the displacement of the CP tends to be more anterior posterior with angles near 90°, which would indicate greater reliability of the regression x vs. y, considering the simulation results. With the feet together, the displacement pattern seems to be more disperse, sometimes with a strong lateral tendency. The inclination of the ellipse is near zero degrees and regression y vs. x becomes more reliable. For both cases, feet apart or together, the differences in angle estimates can be very large, but PCA almost always agrees with either one or the other of the regression estimates.

The results for the area estimates show a similar pattern, though the differences in estimates are less pronounced. As expected, when two methods gave similar angle estimates, the areas calculated tend also to agree.

CONCLUSION

The angles and areas calculated by linear regression depends on the inclination of the ellipse. The results of regression y vs. x and x vs. y can differ greatly; principal component analysis, which we have suggested as an alternative, improved the estimate of angle and area, and appeared reliable in all tests. Additionally, the calculations necessary are no more difficult than those for regression.

REFERENCES

Hassan, S., Goldner, D., Lichestein, M.J., Wood, A. and Shiavi, R.A. (1990) Selecting a suitable biomechanics platform measure of sway. *Ann. Int. Conf. IEEE Eng in Med & Biol. Soc.* **12**(5), 2105-2106.

Odenrick, P., Tropp, H. and Örtengren, R. (1987) A method for measurement of postural control in upright stance. In: *Biomechanics* **X-A**, B.Jonsson (Ed.), Human Kinetics, Champaign, IL, 443-449.

A PILOT STUDY ON THE IMPROVEMENT PROVIDED BY HIP HORIZONTAL ROTATION ON RECIPROCATING ORTHOSIS FOR PARAPLEGICS

M. Ferrarin[1,2], M. Rabuffetti[2], M. Lusvardi[3] and A. Pedotti [1,2]
[1] Dipartimento di Bioingegneria, Politecnico di Milano, Milano, Italy
[2] Centro di Bioingegneria, Fond Pro Juventute IRCCS - Politecnico di Milano, Italy
[3] Officine Ortopediche Rizzoli, Bologna, Italy

INTRODUCTION

Since late 1960's several orthotic systems (ParaWalker, RGO, ARGO) have been developed in order to allow paraplegic patient with thoracic level lesions to walk again. While the success of these systems was high for myelomeningocele children, their application to adult traumatic paraplegics was shown to be more problematic, for the higher mechanical stress provided to the orthosis and for the increase of efforts needed by the upper limbs. For these reasons the high energy consumption associated with such locomotion remains one of the main problems to be solved in adult patients.

Various attempts have been proposed to reduce the cost of locomotion, both modifying the structural design of the orthosis (to minimise deformations) and adding Functional Electrical Stimulation of lower leg muscles in order better to distribute the effort between lower and upper limbs. A crucial point in this optimisation process is the possibility to use quantitative evaluation procedure to guide the modifications and to assess the real improvement during the functional use. The mostly reported approach is to evaluate the energy consumption during walking by means of oxygen consumption measurements [1,2], the main drawbacks being the low accuracy of such a method and the difficulty to find direct correlation with design parameters. In our opinion multifactorial biomechanical analysis of gait seems better to face to these problems.

In previous works we have developed biomechanical procedure both to analyse the deformation occurring in the orthosis during walking [3] and to quantify the modification induced by FES [4] on walking pattern. In this pilot study the results coming from the analysis of a new hip joint for reciprocating orthosis are presented.

METHODS

The new hip joint (R^2GO, [5]) is characterised by the simultaneous horizontal and sagittal rotation with a 1.8 ratio between the two movements: each 1.8 degrees of flexion/extension is associated with 1 degree of external/internal leg rotation. A pair of bowden cables links the hip joint of both sides, as in the standard RGO [2], in order to guarantee a reciprocal movement. The goal of the new joint is to allow a pelvic rotation as in healthy walking, not permitted by the classical RGO joints unless orthotic deformations. In fig.1 feet, legs, pelvis and head of a patient during a left step are schematised in a top view: the possibility to rotate pelvis at each step is clearly shown.

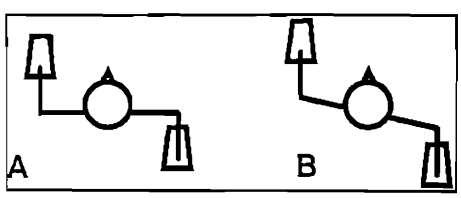

Fig.1 - Top view of the patient during the double support phase (left leg in forward position) with normal RGO (A) and R^2GO (B).

A paraplegic patient (male, 22 years, 164 cm height, 50 Kg weight) with a complete injury at T5 level was selected and analysed during walking with his LSU-RGO orthosis both with the standard hip joint and with the new one. To collect kinematic data an ELITE system (BTS, Milano) was used with a 4 TV cameras configuration (a couple for each side) in order to allow a 3D analysis of the total body. The acquisition protocol and the considered landmarks were reported in a previous work [2].

RESULTS

Time course of pelvic rotation angle, measured respect a transversal laboratory axis, and right hip sagittal angle are presented in fig.2A and B for RGO and R^{2}GO respectively. Time is expressed as percentage of the gait cycle from one right heel strike to the next one; bar diagram represent walking phases of lower limbs and walking frame. Each graph shows average values ± one standard deviation on five different trials.

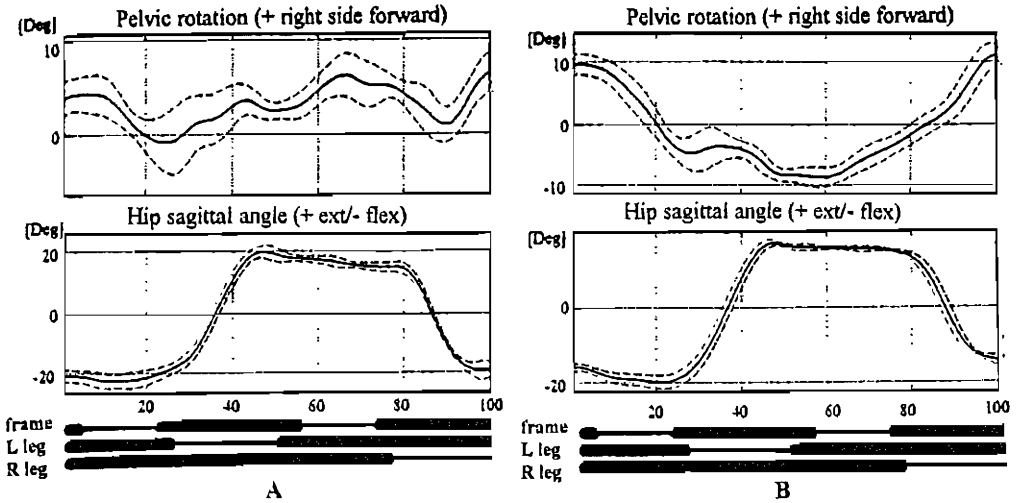

Fig.2 - Pelvic rotation and hip sagittal angle (average value ± std) during the gait cycle with RGO (A) and R^{2}GO (B). Positive values mean forward rotation of right side of pelvis and hip extension. Bold line: stance phase, thin line: swing phase.

DISCUSSION

As shown in fig.2 the sagittal hip angle are similar in both orthoses while the pelvic rotation has a different range (7 deg in A versus 18 deg in B) and a different pattern. With R^{2}GO during walking the pelvis is rotating in accordance with the forward leg: at right heel strike (0%), when hip is maximally flexed, the right side of pelvis is in forward position; vice versa at left heel strike (50%) the left side of pelvis is in forward position. With the classical RGO the pelvic rotation is lower and uncorrelated with the different phases of gait cycle, because it is related to deformations occurring to the orthosis that tends to force the pelvis into a fixed position in the horizontal plane.

The presented method appears to be able to quantify the improvement induced in walking pattern by hip joint modifications. We believe that this technique will be a useful tool for further improvement in hip joint design, particularly in the choice of the best ratio between horizontal and sagittal rotation not yet optimised.

REFERENCES

[1] Nene, A.V., Patrick, J.H. (1990). Energy cost of locomotion using the ParaWalker-Electrical Stimulation "Hybrid" Orthosis. *Arch Phys Med Rehabil*, 71:116-120

[2] Hirokawa, S. et al. (1990). Energy consumption in paraplegic ambulation using the Reciprocating Gait Orthosis and Electric stimulation of the thigh muscles. *Arch Phys Med Rehabil*, 71:687-694

[3] Ferrarin, M., Stallard, J., Palmieri, R., Pedotti, A. (1993). Estimation of deformation in a walking orthosis for paraplegic patients. *Clin Biomech*, 8: 255-261

[4] Ferrarin, M., Rabuffetti, M., Pedotti, A. (1994).Biomechanical analysis of paraplegic gait assisted by hybrid orthosis. In Proc. of World Cong on Medical Physics & Biomedical Engineering, 21-26 august 1994, Rio de Janeiro, p.867

[5] Lusvardi, M., Varroni, P., Ferrari A. (1995). The R^{2}GO: a reciprocating orthosis with 2 degrees of freedom hip joint. In: Proc. of 8th World Congress of the International Society for Prosthetics and Orthotics, Melbourne, april 2-7, 1995 (submitted to)

REPEATABILITY OF FOOTBALL OFFENSIVE SCHEMES. A STATISTICAL EVALUATION BY THE MORPHOLOGICAL VARIATION ANALYSIS.

V.F. Ferrario, C. Sforza, S. Dugnani, G. Michielon, F. Mauro.

Laboratorio di Anatomia Funzionale dell'Apparato Locomotore,
I.S.E.F. Lombardia, Università degli Studi di Milano, Italy.

INTRODUCTION

The Morphological Variation Analysis (MVA) has recently been developed to quantify shape differences in the arrangement of body segments during the execution of sports movements (Ferrario et al., 1994a). Any sport movement can be divided into single frames or moments, each characterized by a peculiar body shape, i.e. a particular arrangement of body segments, which can be described by a set of landmarks. Correspondingly, any action of a football team can be described by series of reciprocal positions of the players, who will correspond to the body landmarks of the classic application (Ferrario et al., 1994b). In this report MVA has been applied to analyze the within-team morphological variability of two offensive schemes in the football. Indeed, in a well functioning team, the offensive schemes in a significant moment of the action, a part from the defensive response, should be the same, i.e. the players should have the same reciprocal positions.

MATERIALS AND METHODS

Two juniores (players aged 15 to 17) football teams of different level (one quasi-professional, one amateur) were analyzed. A TV-camera was positioned 16 m above one half of the field, and the reciprocal positions of the players during two different offensive schemes were filmed (Fig. 1). Each scheme was repeated 20 (quasi-professionals) or 10 (amateurs) times. For each scheme, the single frame corresponding to the cross by player #1 was evaluated, and the position of the eight players (close circles in Fig. 1) was digitized using a semiautomated instrument (LAFAL Videoanalyzer, CUBE srl, Italy). The position of the goalkeeper was not evaluated. Each player thus corresponded to a body landmark in the classic MVA applications, and his coordinates were analyzed by MVA (Ferrario et al., 1994a, b). The player position was calculated from the most posterior image of the heels: both left and right heels were digitized, and mean coordinates computed. This position should correspond to an approximate "centre of gravity" of the player on the ground. An algorithm developed on purpose allowed for the correction of parallax. The analysis was performed separately for the two teams and for the two schemes.

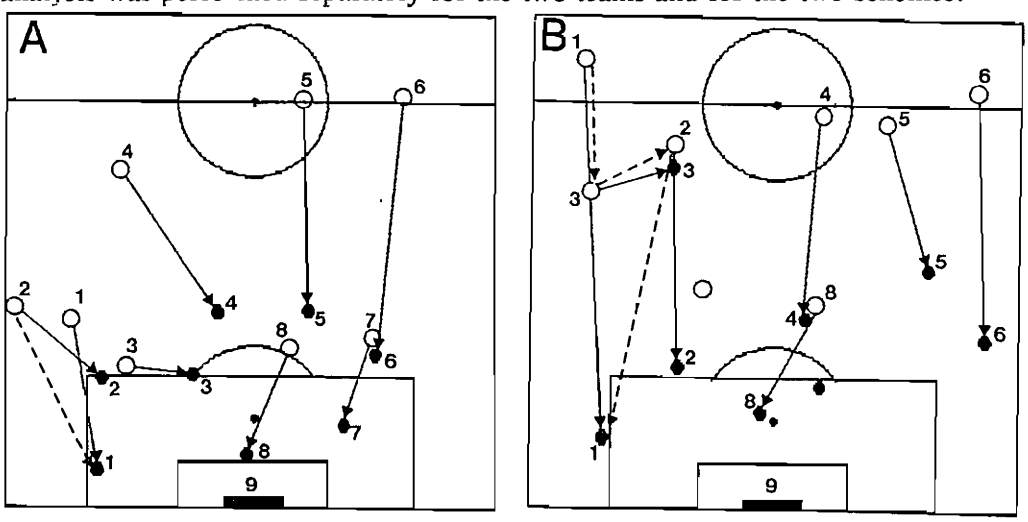

Fig. 1. The two offensive schemes: A, trow-in; B, wing attack with interchanging positions. The players' positions at the beginning of the scheme (open circles), their movements (solid arrows), the positions they should have at the end of the scheme (close circles), and the ball movement (broken arrow) are indicated. The position of the closed circles corresponds to the analyzed frame (cross by player #1). Player #9: goalkeeper. The numbers refer to the position of players not to their identity.

RESULTS

The schemes were performed during a standard training session: the coach first explained the scheme, then the players trained for about two weeks before the TV session. The schemes were also performed at the normal play speed, but without opponent (defensive) players: the following considerations thus pertain to the repeatability of the offensive scheme *in se*. A first qualitative inspection evaluated the films: in all the repetitions of the two offensive schemes the eight players moved in the field with an adequate precision, and the frame corresponding to the cross by the player #1 was always well defined. Only this frame was further analyzed with the quantitative MVA.

Both teams showed a higher reproducibility (i.e. lower MVF) of the reciprocal positions of the players in the trow-in scheme (Table 1); the reproducibility was lower in the amateur team. In the trow-in of the best team, players #5 and 6 had the highest variability; conversely, in the same scheme of the amateur team the variability was more distributed among the players. In the wing attack of the best team, the position of player #2 relative to the two attacks had the highest variability.

In order to evaluate the effect of fatigue, MVA calculations were repeated for the first 15 repetitions of both actions performed by the quasi-professional team. No differences were found for the trow-in scheme, while in the wing attack the first 15 repetitions had a lower variability (lower MVF in Table 1).

Table 1. Morphological variation factors MVF computed in the offensive schemes, and most variable distances (less repeatable reciprocal positions of the eight players) during the analyzed frame of movement (cross by the player #1).

	Trow-in		Wing attack	
Team (repetitions)	MVF	distances	MVF	distances
Quasi-professional (20)	12.77	5-6, 5-7, 4-5	11.90	2-7, 2-8, 1-2
Quasi-professional (15)	14.22	5-7, 5-6, 5-8	7.90	2-8, 1-2, 4-7
Amateur (10)	18.40	2-3, 4-5, 7-8	21.50	6-7, 3-8, 3-8

DISCUSSION

Our findings confirm that the quasi-professional team had higher training level and players' coordination than the amateur team: the offensive schemes resulted more reproducible. Moreover, the more or less repeatable positions of the players were well correlated to the "technical maturity" of each player: for example, the most variable positions of players #5 and 6 of the best team could be explained by a relative distraction during the play because they were not directly interested in the trow-in scheme.

The highest differences between teams were demonstrated for the wing attack, which was also highly influenced by the effect of fatigue. Indeed, the trow-in scheme was easier to understand and perform even for the less expert players, and implied smaller movements in the field. Obviously, the presence of opponent players would have modified the same offensive schemes: further investigations would analyze the repeatability of more complex schemes.

To the best of our knowledge, this is the first report that analyzed the repeatability of a team play using a consistent number of players, a high speed play, and a large outdoor field. A part from the technical football considerations, the protocol employed in this study could be proposed for further quantitative investigations on the play schemes: evaluation of the training, play tactics, correction of errors, in most of the team plays (football, handball, volleyball, basketball).

Ferrario VF, Sforza C, Alberti G, Mauro F. Quantitative assessment of body shape during the standing long jump test. Proposal of a new method. J. Biomechanics, 27: 663, 1994a.

Ferrario VF, Sforza C, Bazan E, Mauro L, Michielon G. The repeatability of the defensive formation in the volleyball evaluated by the Morphological Variation Analysis. Proc. Int. Congr. Appl. Res. Sports, Helsinki, 1994b, p 10.

APPLICATION OF THE MORPHOLOGICAL VARIATION ANALYSIS TO THE BASKETBALL: REPEATABILITY OF ATTACK SCHEMES.

V.F. Ferrario, C. Sforza, E. Casiraghi, F. Mauro, A. Miani.

Laboratorio di Anatomia Funzionale dell'Apparato Locomotore,
I.S.E.F. Lombardia, Università degli Studi di Milano, Italy.

INTRODUCTION

Most of the attacks performed in the basketball follow a patterned play. The evaluation of the offensive movements is usually qualitative: indeed, quantitative analyses of these movements, of the time necessary for their perfect repeatability, and of the players' ability to follow them have never been performed. One of the motives could be the lack of adequate statistical tools. A recently developed method for the quantification of shape differences in the arrangement of body segments during the execution of sports movements (Morphological Variation Analysis, MVA, Ferrario et al., 1994a) seems suitable also for the analysis of the within-team morphological variability during the execution of offensive schemes. Any basketball scheme can be described by series of reciprocal positions of the players, who will correspond to the body landmarks of the classic MVA application (Ferrario et al., 1994b). Indeed, in a well functioning team, the offensive movements in a significant moment of the action, a part from the defensive response, should be the same, i.e. the players should have the same reciprocal positions.

MATERIALS AND METHODS

Three basketball teams of three players each were analyzed: 1. juniores male players aged 16 (national championship); 2. high school male players aged 11-12 (regional championship); 3. amateur female players aged 19. A TV-camera was positioned 6.3 m above the center of the floor, and the reciprocal positions of the players during two offensive schemes were filmed (Fig. 1). Each movement was repeated 20 times by each team. For each movement, the single frame where player #1 (give-and-go) or #2 (distorting defense option) received the ball for the lay-up was evaluated, and the position of the three players (close circles in Fig. 1) was digitized using a semiautomated instrument (LAFAL Videoanalyzer, CUBE srl, Italy). Each player thus corresponded to a body landmark in the classic MVA applications, and his/her coordinates were analyzed by MVA (Ferrario et al., 1994a, b). The player position was calculated from the most posterior image of the heels: both left and right heels were digitized, and mean coordinates computed. This position should correspond to an approximate "centre of gravity" of the player on the floor. Parallax was corrected using an algorithm developed on purpose. The analysis was performed separately for the three teams and for the two moves.

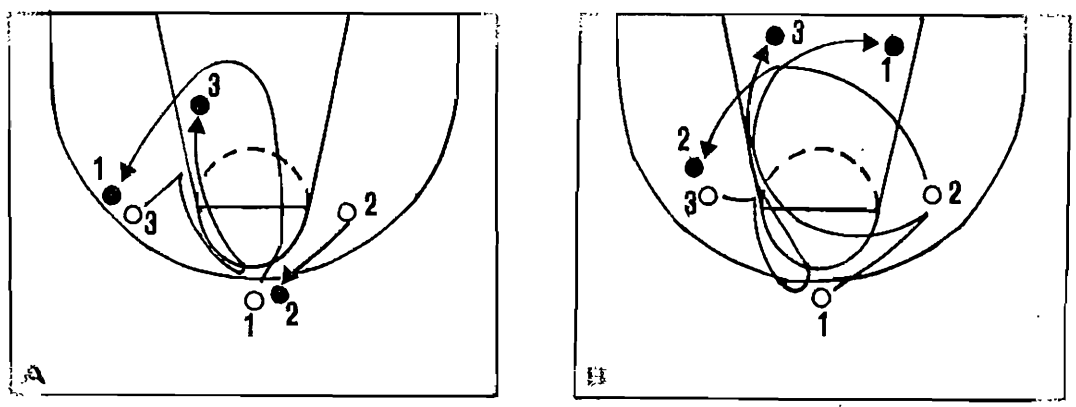

Fig. 1. The two offensive movements: A, give-and-go; B, distorting defense option. The players' positions at the beginning of the scheme (open circles), their movements, and the positions they should have at the end of the scheme (close circles) are indicated. The position of the closed circles corresponds to the analyzed frame (player #1 in A, #2 in B, receiving the ball for the lay-up).

Both offensive plays were performed at the normal play speed, but without opponent (defensive) players: the following considerations thus pertain to the repeatability of the attacks *in se*. A first qualitative inspection evaluated the films: in all the repetitions of the two offensive schemes the three players moved in the court with an adequate precision, and the frame where player #1 (give-and-go) or #2 (distorting defense) received the ball for the lay-up was always well defined. Only this frame was further analyzed with the quantitative MVA.

In both the high school and amateur teams the repeatability of the reciprocal positions of the players was higher in the give-and-go scheme (lower MVFs in Table 1) than in the distorting defense option of give-and-go. Conversely, the juniores team had a poor reproducibility of the give-and-go scheme: the MVF was higher than the values scored by the low level teams in the same scheme, and it was also higher than the MVF scored by the same team during the repetitions of the other scheme.

Table 1. Morphological variation factors MVF computed in the offensive schemes during the analyzed frame of attack (close circles in fig. 1).

Team	Give-and-go	Distorting defense
1. Juniores	12.983	8.327
2. High school	8.748	13.513
3. Amateur	8.293	14.633

DISCUSSION

This investigation analyzed the repeatability of two offensive scheme of different technical difficulty. Indeed, the give-and-go scheme was easier to understand and perform even for the less expert players, and implied a lower number of ball passes and players' movements. Surprisingly, the repeatability of this option was lower in the best team, while the other two teams well reproduced the coacher's instructions. This first scheme was unfamiliar to the juniores players: it is usually learned at the beginning of the basketball training, but it is no more used in high-level championships. The scheme thus resulted banal to them. These players diversified the scheme during the 20 repetitions, probably imagining the presence of defensive players. Obviously, opponent players would have modified the same offensive move in all three teams: further investigations would analyze the repeatability of more complex schemes. On the contrary, the high school players were used to the give-and-go that is part of their routine training.

The other offensive option (distorting defense) was more complex, and the situation reversed: the high-school and amateur teams did not reproduce it with the same reciprocal positions of the three players because the scheme was new to them, and the movements involved were relatively too complex to be learned without a precedent practice opportunity. Conversely, the juniores team well reproduced a common offensive way to play.

Our findings confirm that the players' coordination depend on the difficulty of the task to be performed. MVA could be used to quantify the team coordination during the execution of new patterned plays: this could be a measure of the ability to understand and apply new play situations. A part from the technical basketball considerations, the protocol employed in this study could be proposed for further quantitative investigations on the play schemes: evaluation of the training, play tactics, correction of errors, in most of the team plays (football, handball, volleyball, basketball).

Ferrario VF, Sforza C, Alberti G, Mauro F. Quantitative assessment of body shape during the standing long jump test. Proposal of a new method. J. Biomechanics, 27: 663, 1994a.

Ferrario VF, Sforza C, Bazan E, Mauro L, Michielon G. The repeatability of the defensive formation in the volleyball evaluated by the Morphological Variation Analysis. Proc. Int. Congr. Appl. Res. Sports, Helsinki, 1994b, p 10.

ANALYSIS OF THE PERFORMANCE OF ABOVE-KNEE AMPUTEES IN CLIMBING STAIRS

C. R. Ferreira, Faculty of Human Kinetics, Lisbon, Portugal
M. A. Barúna, Federal University of Uberlândia, Brasil
K. Correia da Silva, Gulbenkian Institute of Science, Oeiras, Portugal

INTRODUCTION

Although a large investment has been already made in the study of the walking performance of amputees (Skinner & Effeney,1985), a greater understanding of the capacities of these subjects is still needed. In this context we undertook the present study in order to analyse the performance of above-knee amputees (AKA) in tasks related to locomotion. Usually the evaluation of the functionality and adaptation to the prosthesis is done through the performance of walking tasks on level surfaces. We studied two groups of individuals, one of able bodied (AB) subjects and a AKA group, performing two different tasks , namely, level ground (LG) walking and climbing stairs (CS).

METHODS

For each individual and for each task three trials were recorded. The CS task corresponded to the climbing of a staircase of three 16 cm in height steps (fig.1). The performances were normalised by comparing a complete LG walking cycle and the climbing CS from the first to the second step. These performances were filmed at a rate of 25 frames per second by two video cameras, one located at the side and another at the back of the track and the three-dimensional data reconstruction is done according to a procedure similar to that of Gervais and Mariano (1983). Twenty reflective marks were located on convenient anatomic points and their co-ordinates were collected using a software program we developed (Ferreira & Correia da Silva, 1994).

Fig .1

A thirteen segments body model is used to calculate the center of mass (CM). The percent values of the CM co-ordinates relative to the subject's height is calculated along the vertical (Z axis), the horizontal antero-posterior (Y axis) and the axis X normal to the previous ones using a method developed by Enseberg *et al.* (1992). The sagittal and lateral inclinations of the trunk and the sagittal rotation of the knee are also computed..

RESULTS AND DISCUSSIONS

Of this study we only present the results which were obtained with regards to the location of the CM . Table 1 presents the average values of CM relative co-ordinates along the three axes for the two groups of subjects and for the performance of the two tasks. The CM for the AKA group performing the LG and CS tasks is located at a lower level (Z), further to the back (Y) and, generally, on the side of the prosthesis (X) as compared with its location for the AB

Table 1

Axis	Z		Y		X	
Group	AB	AKA	AB	AKA	AB	AKA
Walk (LG)	56.081	53.404	0.988	-0.196	0.300	-0.733
Climbing (CS)	49.263	45.792	1.887	0.977	-0.097	-0.698

group performing the same tasks. These results agree with those obtained Engsberg *et al.* (1992) for the LG task. The CM location along the Z axis is determined fundamentally by the forward flexion of the trunk (fig.2) and, for both groups of subjects, is lower for the CS task than for the LG tasks as a result of the need to place this center on the vertical of the propulsive limb.

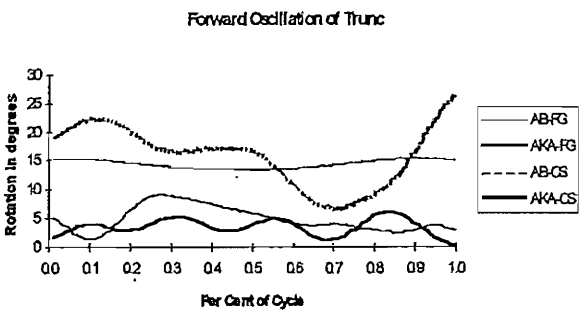

Fig. 2

For both tasks, the CM location along the Y axis (figs. 3 and 4) is similar for the two groups and only slightly more posterior for the AKA group in result of the larger backwards rotation of the arm opposite to the prosthesis.

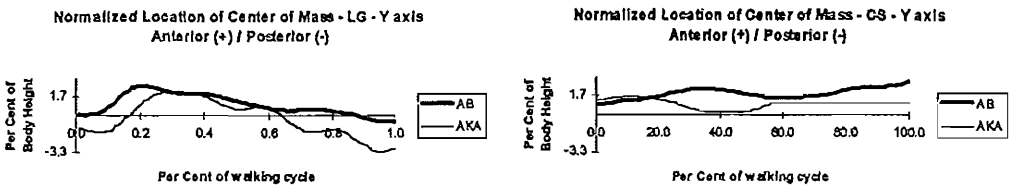

Fig. 3 e 4

The CM location along the X axis (figs. 5 and 6) is, for the AKA group, always opposite to the prosthetic side as a result of the trunk compensating inclination in that direction. For the AB group, the CM oscillates naturally from side to side of the body sagittal plane.

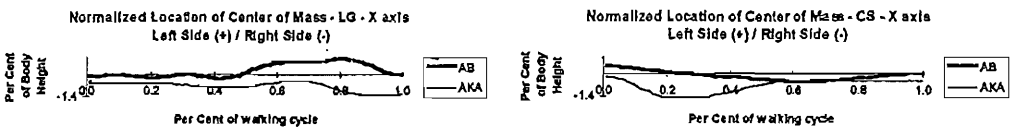

Fig. 5 e 6

CONCLUSIONS

We may conclude from these results that the two tasks correspond to significantly different performances and that the differences are more profound for the AKA group.

The use of a staircase to test the performance of AKA subjects is clinically relevant as it brings up some of the most serious problems associated with the quality of adaptation of the prosthesis to the patient.

REFERENCES

Engsberg, J., K. Tedford & J. Harder (1992). Center of mass location and segment angular orientation of below-knee-amputee and able-bodied children during walking. *Arch. Phys. Med. Reahabili*, 73, 1163-1168.

Ferreira, C. & K. Correia da Silva (1994). A low cost package for analysis of the human body kinematics. *Abstract of XII International Symposium in Sports (ISBS'94).* Budapest Hungary.

Gervais, P. & G.W. Mariano (1983). A procedure for determining angular positional data relative to the principal axes of the human body. *J. Biomechanics*, 2, 109-113.

Skinner H.B. & D.J. Effeney (1985). Gait Analysis in Amputees. *American Journal of Physical Medicine*, 64,82-89.

DEVELOPMENT OF A TREADMILL FOR MEASURING VERTICAL GROUND REACTION FORCES AND CENTER OF PRESSURE DURING GAIT

J. B. Fewster and G. A. Smith
Oregon State University
Corvallis, Oregon USA

INTRODUCTION

Floor-mounted force plates have enabled researchers to measure and understand the forces in human gait. However, this equipment limits the study to one or two foot strikes and necessitates carefully controlled, time-consuming procedures to obtain desired gait velocities. If the researcher wishes to measure more than two successive foot strikes or measure forces during changes of velocity or gait, such as during the walk-run transition, such methods prove inadequate. A tool is needed which can measure vertical ground reaction forces (vGRF's) and center of pressure (COP) over multiple cycles while providing control of locomotion speed.

Ground-reaction force measuring treadmills have been built for individual research projects (E. Hennig, personal communication; Johnson, et al., 1993; Kram & Powell, 1989; Newman & Alexander, 1993) and recently one has become available commercially (Fuglewicz & Klavoon, 1994). Hennig and Johnson et al. encountered problems with excessive noise, believed to be due to the drive motor, and higher than expected vGRF's, possibly from the treadmill bed flexing with each foot strike. Some projects have involved building a dedicated treadmill (Fuglewicz & Klavoon, 1994; Kram & Powell, 1989; Newman & Alexander, 1993) or using expensive hardware (Hennig). The goal of this project was to build a treadmill capable of measuring vGRF's and COP using an existing treadmill and low-cost, non-dedicated hardware with the resulting device having a high natural frequency, minimal flexion with each foot strike and low noise to prevent degradation of the force data.

METHODS

An existing treadmill (Quinton Q55) was modified to meet the stated goals. The motor unit was disconnected from the treadmill bed and vibrationally isolated save for a single drive belt connecting the two. The bed was set on six rigid supports with a uniaxial piezoelectric transducer (PCB Piezotronics 208A03 or 208A02) at each point of loading. Alignment pins prevented the bed from moving in the horizontal plane.

Each transducer was powered by its own signal conditioning unit (PCB Piezotronics 484B or 484B02) which sent unity gain signals to an A/D board and microcomputer for data collection. A Visual Basic (v. 3.0) program collected data from all six channels, summed across channels to yield total vGRF and calculated the COP during stance.

RESULTS

The resulting device may be seen in Figure 1. Signal conditioning is positioned next to the treadmill. Note the three rigid supports visible below the bed.

Figure 2 illustrates unfiltered data collected from a subject running at 10 km/hour. The top graph shows the six individual signals which make up the total vGRF plotted below. The third graph represents anterior-posterior COP, measured from the front support of the treadmill.

DISCUSSION

The six-support structure further stiffened a relatively rigid bed. In combination with the loss of motor-unit weight, the natural frequency of the treadmill bed was raised to approximately 275 Hz. Standard filtering techniques can readily reduce noise at such frequencies.

Force measurements were done by small, inexpensive transducers. Each transducer-signal conditioning unit produced a long time-constant resulting in a stable zero-point during successive impacts. The front four supports had larger force-range transducers than the two rear supports, corresponding to the higher forces involved in heel strike and a subject's normal positioning on the treadmill.

Data collected from a subject running at 10 km/hour demonstrates great similarity to expected vGRF curves. Flexing of the bed did not occur with heel-strike, providing

force values within the expected range. The mounting of the treadmill bed in the manner illustrated resulted in little vibration from the motor as demonstrated by minimal noise in the transducer outputs during each flight phase. After summing forces across channels, the unfiltered signal (~1800N--peak vGRF during running) to vibrational noise (±8N--during flight phase) ratio was approximately 225:1. During flight a slight downward drift was noticed which amounted to ~35N, believed to be due to the hardware used. The resulting signal to drift ratio was ~50:1.

By summing the moments about the front supports, the A-P COP was calculated for stance. While landing and toe-off values were somewhat noisy, the midstance section illustrates the constant velocity rearward motion of the foot on the belt. Filtering of the raw signals before calculating COP should alleviate much of the noise.

This device successfully measures the vGRF's while a subject runs on the treadmill. Successive foot strikes may be recorded and the speed controlled by the researcher, greatly facilitating kinetic gait research. The ability to calculate the COP during repeated stance phases provides additional kinetic information. These results were achieved using an existing treadmill which may be easily removed from this setup and returned to its normal use. Transducers and signal conditioning were neither dedicated nor expensive. The problems of higher than normal vGRF's and excessive noise (Hennig; Johnson, et al., 1993) were minimized.

REFERENCES

Fuglewicz, D., & Klavoon, W. (1994) A ground-reaction-force measuring treadmill. In *Proceedings of the 18th Annual Meeting of the American Society of Biomechanics*. Ohio State University, Columbus, Ohio.

Johnson, L.W., Calder, C.A., & Smith, G.A. (1993). Instrumenting an exercise treadmill for evaluation of vertical ground reaction forces. In *Proceedings of the 1993 SEM Spring Conference*. Dearborn, MI.

Kram, R., & Powell, A.J. (1989) A treadmill-mounted force platform. *J. Appl. Physiol.* **67**, 1692-1698.

Newman, D., & Alexander, H.L. (1993). Human locomotion and workload for simulated lunar and Martian environments. *Acta Astronautica* **29**, 613-620.

ACKNOWLEDGMENTS

This research was supported by a Reebok Graduate Student Research Grant on Human Performance and Injury Prevention from the American College of Sports Medicine Foundation and by equipment donations from PCB Piezotronics, Inc.

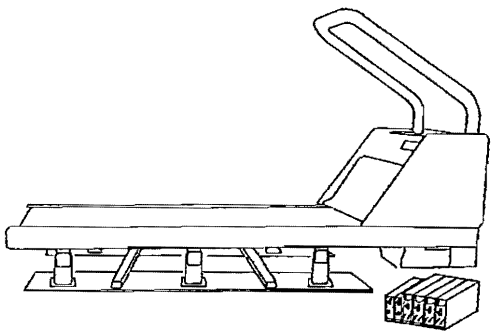

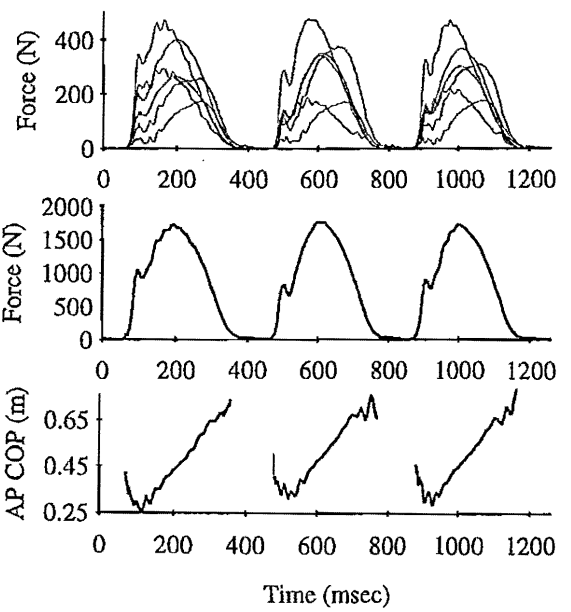

Figure 1 (above): The treadmill apparatus with supporting structure. **Figure 2** (right): Unfiltered running data. The top graph plots the six transducer outputs while the middle graph represents the summed forces. The bottom graph illustrates A-P COP during stance.

ESTIMATION OF LOWER EXTREMITIES MUSCLE ENDURANCE, BASED ON POWER CHANGE IN THE TIME FUNCTION

K. Fidelus, Cz.Urbanik, Academy of Physical Education, Warsaw, Poland

The purpose of this research was to estime the lower extremities endurance on the basis on the decrease of power developed during a take-off series. The slope of a simple regression line was adopted as a measure of endurance.
The hypothesis was: that competitors basing their training process on low-energy sources will achieve higher endurance.

MATERIALS AND METHODS

A group of 15 Warsaw Academy of Physical Education students (mean age 23±2 years, mean body mass 77±6 kg, mean height 181±8cm) training in different disciplines and possessing at least sport category II, took part in the research.
Measurements were taken on an incline plain (K.Fidelus, C.Urbanik 1993, K.Fidelus et al. 1994). Lying on the carriage, the examined performed a series of take-offs against the platform with maximum power. The trolley reached its maximum height from the platform, and rolled down because of gravity. The task given to the examined was to brake against the gained momentum (passive action) and to a perform following take-off (active action). A thin line, fixed to the carriage, passed through a revolution meter, and a device for recording the displacement of the carriage, both interfaced to the computer. Special software was designed for data processing (work, power, time).

RESULTS

To estimate the maximum value of power each examined person performed 2 series of 6 take-off with a 3 minute break in between. Then, after a following 3 minutes he performed a series of 70 take-offs, tending to develop maximum power at each movement. If initial power proved, the test was interrupted. The course of power in time is described both by the straight-line equation and simple regression equation. In both cases a significant correlation ($p<0,001$) of power decrease in function of time was proved. It was adopted, that in the simple regression equation ($P=a-bt$), factor b informs about endurance. Approximation based on equation of simple regression of power value (P) in time function (t), is shown on figure1. Presented factors of equations of power decrease simple regression in time function clearly divide the examined into the following:
P_1- those who developed low initial power, and have low power decrease in time (long-distance racers, cyclists).
P_2- in the group of sprinters the highest average initial power and its lowest decrease was observed.
P3- analysing results of team-games representatives large diversification of power and its decrease factor was noticed. Volleyball players and soccer player develop high power, while handball players and basketball players significantly lower.
In all cases the factor of power decrease in time was significant at the level of $p<0,001$. Representatives of group P_1, likewise soccer and handball players registered the smallest decrease of this factor after a 180-second effort. The ones to achieve maximum power were sprinters and basketball players. Fast decrease of power occurs in group P_2. After about 90 seconds the power they developed was a half of maximum power value, and after 180 seconds it dropped to 40% of Pmax.

THE DISCUSSION

Evaluation of physical features level usually involves doubts and different opinions. This refers in particular to endurance estimation, which is usually identified with amount of oxygen consumed per minute in comparison to outstanding competitors' achievements (P.O.Astrand 1978). However, such a relation was not proved with reference to lower-categories competitors, or those not training (D.L.Costil 1970). It follows from practical observations and energy conversion zones(S.Kozlowski et al 1983, N.I.Wolkow 1989) that higher endurance level occurs at in competitors taking part in sport events, in which sport achievements are determined by lower

power value developed in a long-time period (long distance racers, cyclists, oarsmen). In cases where maximum power is needed (sprint, jumps, acrobatics etc.) the endurance is lower, and in team- games representatives it is established on medium level. Evaluating the decrease of power in time function, the proof was achieved ,that more efficient slope of simple regression line (b)occurred in long-distance racers and cyclists cases. The immediate drop of power occurred in the sprinters group. In team games players, the endurance level is diverse. The lowest endurance characterises volleyball players, which is probably determined by game specifics, where based on high general endurance, short, intense technical actions are performed. On the other hand, in bandy players, who performed a cykloergometer exercises, a significant decrease in anaerobic power of about 47% over a time interval from 0-15 to 45-60s. (K.Hakkinen et al. 1991). In 20% of rugby players and 15% of cross-country runners, who performed a 30 s treadmill exercise, a power decrease (reflected by running speed) was observed (M.E.Cheetam et al. 1985).

The research proved the hypothesis, that a slope of simple regression of power decrease in time is an appropriate measure of lower extremities muscles endurance. Hypothetically, this relation will occur in other muscle groups. The endurance can be estimated not only by measurement of internal power variation in time. This method is very general, because it evaluates endurance in efforts of 10-20 s as well as 100-200 s duration.

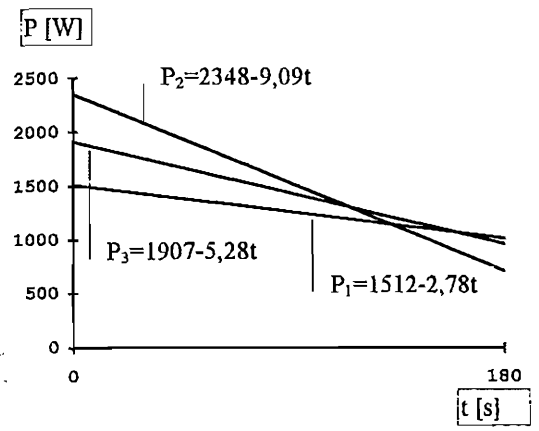

Fig.1. Regression line for the decrease in power (P) in time (t).
P_1- Long -distance racers,
P_2- Sprinters,
P_3- Game players

REFERENCES

1. Astrand P.O. (1978) Health and Fitness. Univeraltrych, Stockholm

2. Cheetham M.E., C.Williams, H.K.Lakomy (1985) A laboratory running test: Metabolic responses of sprint and endurance trained athletes. Br.J.Sports Med.19:81-84

3. Costill D.L. (1970) Metabolic responses during distance running. J.Appl.Physiol. 28:251-255

4. Fidelus K., Cz.Urbanik (1993) Relationship between the training power, work, rest period and the increase of the muscular torque. International Society of Biomechanics XIVth Congress. Paris, 4-8 July:414-415

5. Fidelus K., Cz.Urbanik, K.Grudniak (1994) Time changes of power output as an endurance index of lower limb muscles. Biology of Sport.Vol.11. 2:115-121

6. Hakkinen K., P.Sinnemaki (1991) Changes in physical fitness profile during the competitive season in elite bandy players. J.Sports Med.Phys.Fitn. 31:37-43

7. Kozłowski S., K.Nazar (1983) Beztlenowe i tlenowe procesy metaboliczne w pracujących mięśniach - koncepcja progu beztlenowego. Sport Wyczynowy. 8-9:3-11

8. Wołkow N.I. (1989) Bioenergetyczne podstawy i oceny wytrzymałości. Sport Wyczynowy. 7-8:3-15

HIP JOINT LOADING DURING ACTIVITIES OF DAILY LIVING

A.M. Fitzsimmons, A.C. Nicol, J. Lane and I.G.Kelly

Bioengineering Unit, University of Strathclyde, Glasgow, Scotland

INTRODUCTION

With recent advances in materials characteristics and surgical techniques, the long term success rate of total hip replacements should have continued to improve at a rapid pace. However, the high number of revisions currently carried out indicate that this is not the case.

Design calculations for hip prostheses and recent mechanical testing have so far been based on hip joint forces determined for level walking. During activities that involve larger ranges of 3D joint motion, the resultant hip joint force and its components may significantly differ from those of level walking. The intersegmental moments produced by such activities will be altered and require appropriate alterations in the forces produced by muscles which cross the hip joint. It is possible that the loading on the hip joint that results from such activities may be responsible for the loosening and failure of implants.

Hence the aim of this project was to calculate the magnitude of the hip force vector produced during various activities of daily living.

METHOD

The activities investigated were car entry/exit, bath entry/exit, walking with a turn, stair ascent/descent, sit/stand and level walking. The car and bath activities were included since hip replacement patients regularly comment on the difficulty which these activities impose.

16 post-operative hip replacement patients and 10 age-matched non-arthritic subjects have undergone tests in the biomechanics laboratory at Strathclyde University. The patients were analysed between 12 and 24 months after their operation. Specially constructed frames were used to represent the car and bath and a 5 step staircase was used for stair negotiation tests. Whilst the subjects performed the activities, a 6 camera Vicon motion analysis system provided the 3D position and orientation of the hip joint and limb segments and 2 Kistler force platforms provided ground reaction forces.

A 3D model based on a rigid body mechanics approach was developed to calculate muscle and then hip joint forces using input data which included the following:

- Vicon and force platform outputs
- Anatomical muscle data
- Subject specific anthropometric data

38 muscles elements have been included in the model. Where muscles do not act in straight lines but wrap around underlying structures, algorithms to correct for the curved path have been included. A linear optimisation procedure has been used to calculate the muscle forces in this indeterminant system. The procedure chooses the combination of muscle forces which acts to minimize the maximum muscle stress.

RESULTS AND DISCUSSION

A sample of the results for non-arthritic subjects is presented in table 1. The values shown are resultant hip joint forces in terms of body weight in a selection of the activities performed. For the majority of activities, the results are for 5 subjects . The average peak value is given for each activity along with the range of peak values incurred.

Table 1 - Preliminary results

Activity	Ave peak resultant hip joint force x body weight	Range of peak resultant hip joint force x body weight
Gait	4.97	3.23 - 6.26
Standing up	3.45	2.56 - 5.01
Stair ascent	4.67	3.38 - 6.03
Car entry	6.45	5.25 - 8.21
Car exit	5.94	4.51 - 8.08
Bath entry	5.63	4.65 - 6.60

The average peak value of 4.97 times body weight for gait lies within the range of values observed in the past. Such values have varied greatly. At a speed of 1.1m/s, Rydell (1966) recorded 2.95 times body weight from the telemeterised prosthesis implanted in his second more active subject. Paul and Poulson (1974) calculated values up to 10 times body weight in fast walking at approximately 2m/s.

In stair climbing Rydell measured 3.38 times body weight in his second subject whilst Crowninshield et al (1978) recorded over 7 times body weight. The average value of 4.67 times body weight calculated in this study lies within this range.

Similarly, the average peak value of 3.45 times body weight calculated for rising from a chair in this study compares with that of Crowninshield et al which was over 3 times body weight.

The values of resultant hip joint force reported in table 1 for car entry and exit are those for the left hip when getting into and out of the front left passenger seat. Those for bath entry correspond to the side of the first foot to be put into the bath. The test period was started when the subject's foot touched the bath floor and ended when the subject was sitting in the bath on the bath stool provided for safety in all bath tests.

Interestingly, the average peak resultant values for the bath and car activities in table 1 are greater than those for walking, stair ascent and rising from a chair. Although preliminary, these results have implications for the loading on hip joint prostheses. However, it is recognised and has been observed that patients with hip replacements sometimes perform activities in a different manner to non-arthritic subjects. Firmer conclusions with regard to prosthetic hip joint loading will be drawn once more results have been generated.

REFERENCES

Rydell, N.W. (1966) Forces acting on the femoral head-prosthesis. *Acta orthop. scand. Suppl.* **88**.

Paul, J.P. and Poulson, J. (1974) The analysis of forces transmitted by joints in the human body. *Proc. 5th Int. Conf. Stress Analysis*, 3.34-3.42.

Crowninshield et al. (1978) A biomechanical investigation of the human hip. *J.Biomechanics* **11**, 75-85.

CYCLIC DEFORMATION BEHAVIOUR AND MICRODAMAGE ACCUMULATION OF CORTICAL BONE

C. Fleck, D. Eifler, Department of Materials Science, University of Kaiserslautern

Kaiserslautern, Germany

INTRODUCTION

Permanent implants have gained growing importance in orthopaedics during the last decades. Despite improvements concerning materials and design they still fail after 10 to 20 years due to biomechanical and/or biological incompatibilities. In order to increase the life time of these implants it is necessary to understand the cyclic deformation behaviour and the remodeling processes of the bone itself and at the bone implant interface. It is widely accepted nowadays that fatigue damage occurs in bone under physiological loading conditions. This damage is assumed to be one stimulus for the permanent remodeling of bone (Frost, 1994). Fatigue fractures are avoided as long as, on one hand, damage formation and repair and, on the other hand, bone resorption and formation as a response to the loading conditions are in balance. Despite its clinical and physiological relevance the fatigue behaviour of bone has not been thoroughly examined. Former work focused on aspects concerning fatigue life and its dependence on microstructure, porosity or density (see e.g. Carter & Caler, 1981). During cyclic loading, bone shows increasingly non-linear behaviour with an increase in the area of the hysteresis loop and a decrease in stiffness (see e.g. Pattin, 1990). In the present work the cyclic deformation behaviour of cortical bone under uniaxial loading conditions is characterised by the development of the plastic strain amplitude, the stiffness and the plastic mean strain as functions of number of cycles and correlated with the results of light and scanning electron microscopic observations.

METHODS

Flat fatigue specimens with a gauge length of 10 mm and a reduced cross-section of 5 by 6 mm were machined in longitudinal direction from the mid-diaphysis of horse tibiae. Strain was measured by an extensometer attached to the gauge length. Uniaxial, stress-controlled constant amplitude tests were performed on a servohydraulic testing system with a sinusoidal waveform and a frequency of 5 Hz. Specimens were loaded with stress amplitudes between 30 and 75 N/mm^2 without or with various tensile or compressive mean stresses. Microstructural investigations were performed after predetermined numbers of cycles. Crack initiation and growth were examined on the surfaces and in the bulk of the specimens by light and scanning electron microscopy. The specimens were stored in Ringer's solution at 4 °C and kept wet during machining and testing.

RESULTS

The cyclic deformation behaviour of cortical bone is characterised by cyclic softening. In the first cycle, a characteristic plastic strain amplitude develops, the value of which depends on stress amplitude respectively mean stress. Subsequently, the plastic strain amplitude increases continuously as a function of the number of cycles. This increase is more pronounced just before final failure. Increasing stress amplitudes under loading without mean stress lead to characteristic higher plastic strain amplitudes with a linear relationship between stress amplitude and average plastic strain amplitude. At constant stress amplitude, decreasing compressive and increasing tensile mean stresses result in higher plastic strain amplitudes. Caused by the accumulation of microstructural damage the stiffness of the specimens decreases with increasing number of cycles. Under loading without mean stress, this decrease is generally pronounced towards final failure and still more pronounced with increasing stress amplitudes. As a function of fatigue life ratio, under loading with compressive mean stresses hardly any change in stiffness can be observed for the greatest part of fatigue life followed by a sharp decrease before final failure. Tensile and zero mean stresses lead to a gradual decrease in stiffness as a function of fatigue life ratio. Under cyclic loading without mean stress cyclic creep occurs. Due to non-symmetrical deformation during tensile and compressive loading the plastic mean strain increases continuously as a function of number of cycles. Higher stress amplitudes lead to higher plastic mean strains, which

again is described by a linear relationship between stress amplitude and average plastic mean strain. Increasing compressive mean stresses prevent cyclic creep besides a small decrease in plastic mean strain before final failure. Increasing tensile mean stresses result in more pronounced cyclic creep effects.
Lightmicroscopic investigations revealed crack initiation on the surfaces and in the bulk of the specimens. First surface cracks could be observed after the first cycles for loading without mean stress or with compressive mean stresses. Under loading with tensile mean stresses first cracks are initiated after 5 % of fatigue life. The majority of surface cracks originates at sites of high stress intensity at Haversian or Volkmann canals. This observation is in good agreement with results from cyclic bending tests after a defined number of cycles (Carter & Hayes, 1977). The surface cracks usually propagate along the lamellae and cement lines of the Haversian systems or the interstitial bone. As a function of the loading conditions, more cracks are orientated rather parallel (0° - 30°) or rather orthogonally (60° - 90°) with respect to the loading direction. Under loading without mean stress, lower stress amplitudes result in a majority of cracks propagating in a longitudinal direction, i.e. rather parallel to the loading direction. With increasing stress amplitudes, the majority of cracks is orientated rather orthogonally to the loading direction. Compressive mean stresses promote crack propagation in a longitudinal direction whereas tensile mean stresses in average lead to a higher proportion of cracks with a rather orthogonal orientation. Some cracks initiate in the bulk of the specimens, which was also observed after axial strain-controlled loading (Schaffler et al., 1989). The observed behaviour of crack propagation in dependence of crack length and loading conditions is reflected by the appearance of the fracture surfaces. Generally, the area caused by fatigue crack growth has a rough appearance. Loading without mean stress leads to an orientation of this area under a more acute angle towards the loading direction for lower stress amplitudes and under an increasingly plane angle for higher stress amplitudes. Increasing tensile mean stresses also result in planer angles towards the loading direction. With increasing crack length, the fracture surface appears smoother. The area of final fracture is generally orientated orthogonally to the loading direction.

DISCUSSION

The cyclic deformation behaviour of cortical bone is characterised by cyclic softening. Light and scanning electron microscopic investigations revealed the main damage mechanism to be crack initiation and growth along the lamellae and cement lines. The non-elastic deformation due to the opening of cracks leads to an increase of the plastic strain amplitudes. Presumably viscoelastic and creep deformation are also included in the plastic strain amplitudes. "Fictive plastic strain amplitude" therefore is the more correct term. Loading with zero or tensile mean stresses results in cyclic creep. The crack propagation behaviour is strongly influenced by the loading conditions as well as by the microstructure. With increasing stress amplitudes and tensile mean stresses as well as with increasing crack length the microstructure becomes less important for the crack growth behaviour. It is then more and more determined by the loading conditions, i.e. the influence of normal stress on crack growth is promoted.

REFERENCES

Carter, D.R., Caler, W.E. (1981), Uniaxial fatigue of human cortical bone - The influence of tissue physical characteristics, J. Biomechanics **14**, 461-470

Carter, D. R., Hayes, W. C. (1977), Compact bone fatigue damage - A microscopic examination, Clin. Orthop. Rel. Res. **127**, 265-274

Frost, H.M. (1994), Some biologic features involved in Wolff's law, pers. comm., 2nd World Congress of Biomechanics, Amsterdam

Pattin, C. A. G. (1990), Cyclic mechanical property degradation in bone during fatigue loading, PhD-Dissertation, Stanford University, USA

Schaffler, M. B., Radin, E. L., Burr, D. B.(1989), Mechanical and morphological effects of strain rate on fatigue of compact bone, Bone **10**, 207-214

ACKNOWLEDGEMENTS

This work was performed at the Department of Materials Science, University of Essen, Germany and supported by a grant of the "Graduiertenkolleg Biomaterialien: Verbundwerkstoffe im Anwendungsbereich Medizin" (Nordrhein-Westfalen, Germany)

BIOMECHANICS OF THE GLENOHUMERAL JOINT AS RELATED TO ANTHROPOMETRIC FACTORS DERIVED FROM FRESH CADAVER SPECIMENS

P. Franklin, H.A.C. Jacob, A. Imhoff and A.C. Nicol
Bioengineering Unit, University of Strathclyde, Glasgow, Scotland and Biomechanics Unit, Balgrist, University of Zürich, Switzerland

INTRODUCTION

Biomechanical studies of the shoulder have had a long and varied history from the EMG studies of Duchenne (1867), the works of Fick and Weber (1877) and the works of Cleland (1881) to the important study of Inman et al. (1944), using Comparative anatomy, x-ray analysis and EMG study and the modern methods of Van der Helm et al. (1992) using finite element techniques to model the shoulder. An area where research is lacking is that of accurate anthropometric data of structures pertaining to the action of the glenohumeral joint which is necessary to form any theoretical model dealing with the forces crossing this joint. Published data has failed to reveal such information and thus an investigation, using fresh (unembalmed) shoulder specimens, was carried out to meet these requirements.

METHODS AND MATERIALS

The topography of the glenohumeral articular surfaces was recorded using the moiré fringe technique which assigns a polynomial equation to the articular surfaces. These equations can be used to produce a number of two-dimensional profiles, or contours, of the articulating surfaces of the glenohumeral joint. The equations can also be used to find the radius of curvature of the surfaces at any point on the contour.

The moment arms of muscles crossing the glenohumeral joint were calculated as a ratio of tendon travel to joint angulation. The moment arms are thus defined for a given motion and with respect to an average centre of rotation of the joint during this motion. Furthermore a factor is used in order to estimate the muscle force distribution amongst these muscles during the given motion. This factor is the normalised cross-sectional area (NCSA) of the muscles of the shoulder as determined by Karlsson and Järvholm (1988).

The mechanical advantage of those muscles crossing the glenohumeral joint were found with respect to the tendon displacement which occurred as the glenohumeral joint was dislocated. The investigation was performed under circumstances in which the glenohumeral joint was seen to be vulnerable to anterior dislocation or subluxation. The effect of the depth of the glenoid was investigated by performing the experiment with a normal glenoid fossa and with a spacer inserted between the glenoid fossa and the humeral head which effectively flattened the surface of the glenoid fossa.

RESULTS AND DISCUSSION

Analysis of the contours of the glenohumeral articulating joint surfaces found through the moiré technique revealed that surface contact is not maintained over the whole glenoidal area. The glenoid fossa has a generally larger radius of curvature than the humeral head, implying that there is little contact area between the two surfaces and hence there is little inherent stability in the joint and stability comes from the surrounding musculature.

The method used to find the moment arms of those muscles crossing the glenohumeral joint did not need the prior knowledge of the centre of rotation of the joint whilst the moment arms are given only in the plane of rotation. Consequently the investigation found the moment arms of the muscles crossing the glenohumeral joint during different stages of abduction, adduction, flexion, external and internal rotation. At

the initiation of abduction the moment arm of the supraspinatus was similar to that of the anterior and middle deltoid which shows that these three muscles all initiate abduction of the humerus in approximately equal proportions. As the humerus is raised the moment arm of the supraspinatus does decrease to zero (figure 1). Figure 2 shows the changing moment arms of the different parts of the subscapularis as the humerus is internally rotated at different degrees of abduction.

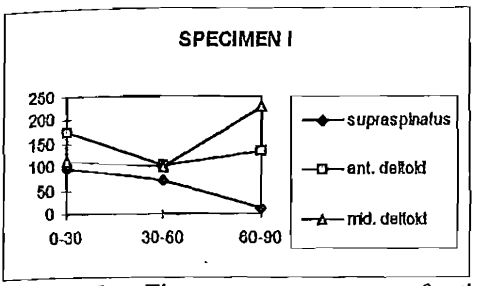

Figure 1. The moment arms of the supraspinatus, anterior and middle deltoid from 0°-30°, 30°-60° and 60°-90° abduction.

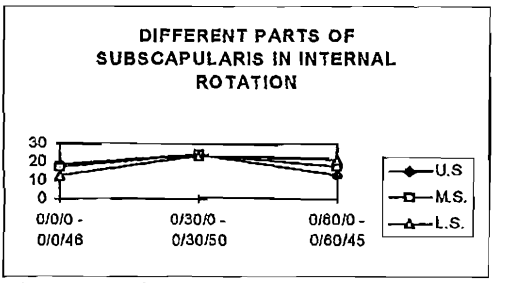

Figure 2. The moment arms of the upper subscapularis (U.S.), middle subscapularis (M.S.) and the lower subscapularis (L.S) during internal rotation from 0° to maximum internal rotation at 0°, 30° and 60° abduction.

The glenohumeral joint was seen to be prone to anterior dislocation when the humerus was elevated 60° in a plane 45° posteriorly to the plane of the scapula. When a force was applied to the humerus anteriorly the mechanical advantage of all parts of the deltoid were negative implying that the shearing component of the muscle brought about translation of the humeral head on the glenoid in the direction of the force. When a force was applied to the humeral head antero-posteriorly the mechanical advantage of all parts of the deltoid were positive implying that the shearing component of the muscle worked against the destabilising force. Thus the direction of the destabilising force is a significant factor in anterior dislocation or subluxation and under the conditions where the glenohumeral joint is prone to dislocation the shearing component of the deltoid works to bring about anterior translation of the humeral head on the glenoid. The subscapularis had no mechanical advantage at all in the position where the glenohumeral joint was seen to be vulnerable to dislocation whatever the direction of the destabilising force. This implies that the muscle does not act as a dynamic constraint to anterior translation. The supraspinatus and infraspinatus were seen to have the greatest positive mechanical advantage under the conditions previously described. This implies that these two muscles are the greatest dynamic constraints to anterior translation of the humeral head on the glenoid and that any damage to these two muscles will lead to subluxation or dislocation of the glenohumeral joint.

REFERENCES

1. Cleland J. (1881) Shoulder girdle and its movements. Lancet 1:283-284.
2. Duchenne G.B. (1867) Physiologie des mouvements. Translated and edited by E.B. Kaplan. Philadelphia, J.B. Lippincott Company, 1949.
3. Fick A.E., and Weber E. (1877) Anatomisch-Mechanische studie ueber die schultermuskeln. Proceedings of the Physical.-Medicin. Gesellschaft, Würzburg.
4. Inman V.T., Saunders J.B. and Abbot L.C.(1944) Observation on the function of the shoulder joint. J.Bone Jt Surg 26:1-30.
5. Karlsson D., and Järvholm U. (1988) Force-producing ability in all shoulder muscles, as determined by cross-sectional areas. Preprints 1988:2 Centre for Biomechanics, C.T.H.
6. Van der Helm F.C.T., Veeger H.E.J., Pronk G.M., Van der Woude L.H.V. and Rozendal R.H. (1992) Geometry parameters for musculoskeletal modelling of the shoulder system J Biomech 25:129-144.

EMG TO MUSCLE FORCE CALIBRATION IN DYNAMIC MOVEMENTS

Frazer, M.B, Norman, R.W. and McGill, S.M.

Occupational Biomechanics Laboratory, Department of Kinesiology, University of Waterloo, Waterloo, Canada

INTRODUCTION

Lumbar spine tissue force time histories have been estimated via EMG assisted models (Granata and Marras, 1993; McGill, 1992). In these models scaling factors for the conversion of the EMG to force requires maximal voluntary contractions (MVCs) in flexion and extension of the trunk. The need for MVCs eliminates application of these models to people who are unable to produce a "true" MVC because of pain. This paper describes a method that does not require MVCs and makes the use of calibrated EMG applicable to injured populations.

METHODS

A three dimensional, twelve channel, EMG assisted model of the lumbar spine was utilized (McGill, 1992). The maximal effort EMG scaling factors required for Equation 1 were obtained for a subject who performed a standard set of static flexion and extension contractions. The EMG_{max} and P_O terms in Equation 1 were replaced by an EMG-to-Force factor (EF) (Equation 2), obtained from a pair of isometric flexion and extension efforts (Equation 3).

$$F_m(t) = G(t) * \left[(EMG(t) / EMG_{max}) * P_O * \delta(t) * \Omega(t) + F_{pec}(t)\right]_m \quad (1)$$

$$F_m(t) = G(t) * \left[EMG(t) * EF * \delta(t) * \Omega(t) + F_{pec}(t)\right]_m \quad (2)$$

$$EF_m = \left[(AMF_{HI} - AMF_{LO}) / (AEMG_{HI} - AEMG_{LO})\right]_m \quad (3)$$

Where:

$F_m(t)$ = Muscle Force (N/Unit Area)
EMG(t) = EMG Amplitude
P_O = Muscle Force/Unit Area
$\Omega(t)$ = Velocity Factor
m = muscle fascicle
$AEMG_{HI, LO}$ = Ave $EMG_{70\%, 60\% MVC}$
G(t) = Gain Factor
EMG_{max} = Max EMG Amplitude
$\delta(t)$ = Length Factor
$F_{pec}(t)$ = Passive Elastic Component
EF = EMG-to-Force Factor (N/Unit EMG)
$AMF_{HI, LO}$ = Ave $Muscle\ Force_{70\%, 60\% MVC}$

To compare the two techniques, Equations 1 and 2 were used in the dynamic model, applied to three repetitions of full range trunk flexion and extension.

RESULTS

The two methods of determining the scaling factors are illustrated in Figure 1. The MVC approach assumes that the subject is producing true maximal effort (100% MVC) and incorporates an experimentally based non-linear EMG to force equation. The EF approach assumes a linear EMG-to-Force curve (produced in Equation 3). This accommodates a small range of biological variability in the approach without substantial error.

For the simple flexion-extension task, the two methods produce similar extensor muscle force time histories with the EF method producing a smaller net extensor

muscle force (Figure 2). The average RMS difference in L4/L5 compressions between the two methods was 200 N (12% MVC). The average gain required by the MVC approach was 1.2 and the EF method was 1.13 (RMS difference = 0.15).

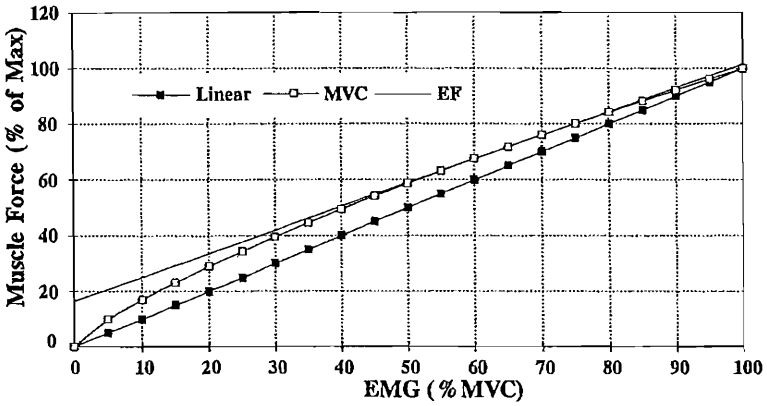

Figure 1 Muscle force produced by EMG activation. **Linear** (linear from 0 to 100% MVC), **MVC** (the model approach based on experimental data (non-linear), and **EF** (linear relationship extrapolated from HI (70%) and LO (60%) efforts).

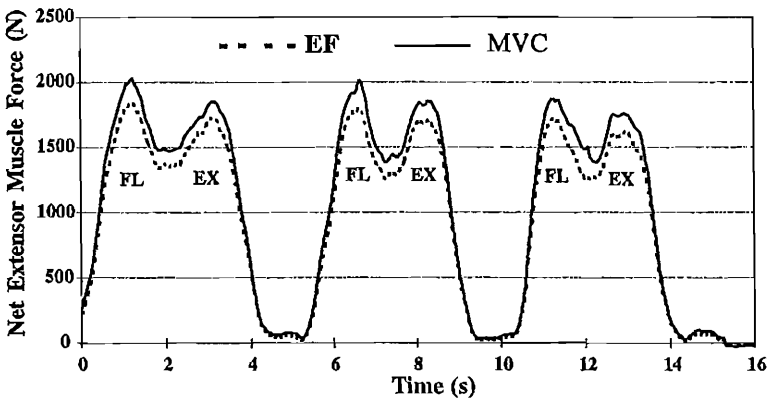

Figure 2 Trunk extensor muscle force (sum of 20 thoracic and lumbar muscle fascicles) during the performance of three cycles of flexion (FL) and extension (EX) as determined by the **EF** and **MVC** scaling factor methods.

DISCUSSION

The similarity of the net extensor force and L4/L5 compressive force between the two methods is encouraging. This development allows the model to be applied to individuals unable to produce a "true" MVC. The differences in muscle force distribution between the two methods (not presented here) reflects the sensitivity of the EMG-to-Force processing technique to the calibration procedure.

REFERENCES

Granata, K.P. and Marras W.S. (1993) An EMG assisted model of loads on the lumbar spine during asymmetric trunk extensions, J. Biomechanics, 26, 1429-1438.

McGill, S.M. (1992) A myoelectrically based dynamic three-dimensional model to predict loads on lumbar spine tissues during lateral bending, J. Biomechanics, 25, 395-414.

This work is supported by the Canadian Memorial Chiropractic College.

MUSCLE ACTIVATION DURING ACCELERATION-PHASE IN SPRINT RUNNING WITH SPECIAL REFERENCE TO STARTING POSTURE

Ulrich Frick, Dietmar Schmidtbleicher, Roland Stutz
Institute of Sport Sciences, Johann Wolfgang Goethe-University, Frankfurt, Germany

INTRODUCTION

Studies on muscle activation in sprint running concentrate on sprint push off (1), phase of peak-velocity (3) or artificial running velocities (2). To our knowledge, no studies are published, describing muscle activation throughout the acceleration-phase. This is of interest, because during the acceleration-phase body-posture and joint-movements are changing considerable and therefore the relative contribution of certain muscles to the generation of performance may change, too. This could be of importance concerning recommendations for training (strength training of certain muscle groups; coordination-exercises), because present conclusions on training regimens for sprinters reflect muscle activation during peak-velocity, only (4,5).
Therefore the purpose of the study[1] was to analyse the activation of leg and hip extensor and flexor muscles and their relative changes during acceleration-phase in sprint running, with special reference to starting posture.

METHODS

After warm-up and preparation exercises 12 male subjects executed eight 30m-dashs. They were performed from a starting-block (crouch start) or from a contact-platform (standing start) in an alternating order.
Intermediate times of 5m-intervalls were taken via 6 (double) light gates. Duration of ground contact (contact time) was registrated using a pressure-transducer inside the shoe. Angle-time-characteristics of ankle-, knee- and hip-joint were measured with electro-goniometers. Muscle activation of mm.soleus (SO), gastrocnemius (GA), vastus lateralis (VL), rectus femoris (RF), biceps femoris (BF) and glutaeus maximus (GM) was determined via surface-EMG. To estimate the relative contribution of each measured muscle to the total activation of all measured muscles, we determined the total activation of each muscle during the functional phases of each step cycle and then calculated the percentage of the respective muscle. For better understanding we combined data of muscles according to their main function during a step cycle (SO + GA = plantar flexors; VL + RF during ground contact = knee extensors; BF + GM = hip extensors; RF during swing phase = hip flexor).
For description of data means and standard deviations were calculated. Differences were tested for significance ($p<0.05$) via students or paired t-test or multiple factorial repeated measures analysis of variance using SPSSPC-program.

RESULTS

During acceleration phase of sprint running muscle activation is changing considerable (fig.1). In the beginning knee extensors contribute most to the total activation of all measured muscles (TAMM). This is significantly more pronounced in crouch start (CS) condition compared to standing start (SS) condition (fig.1&2). During the following steps the relative contribution of knee extensors is declining significantly. In contrast to these muscles the hip extensors enhance their relative contribution to TAMM significantly (fig.1&2). This is significantly more distinct in CS compared to SS (fig.1&2). While hip flexor increases its relative contribution to TAMM significantly during acceleration-phase in both conditions plantar flexors don't vary this parameter in a significant manner (fig.1&2).

[1]this study was supported by a grant of the Bundesinstitut für Sportwissenschaften (VF0407/05/12/93)

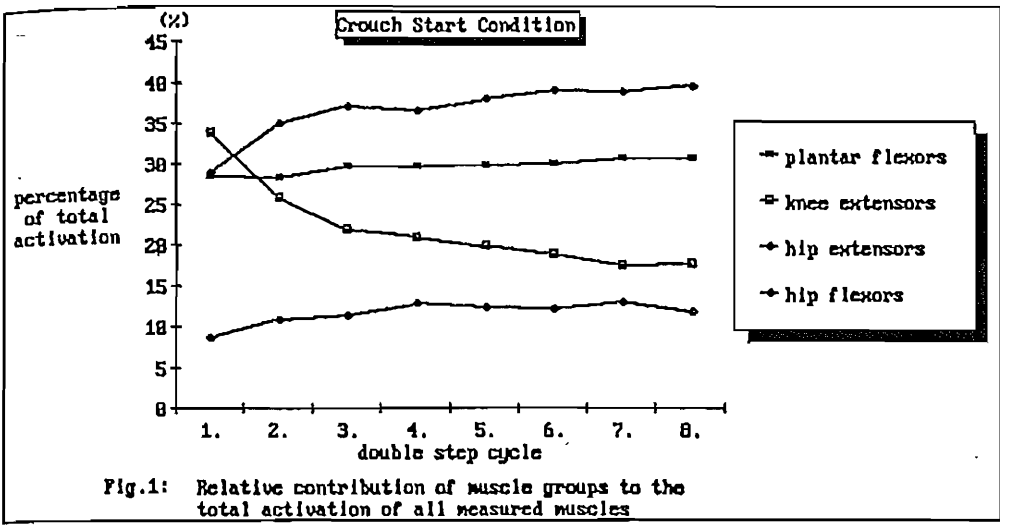

Fig.1: Relative contribution of muscle groups to the total activation of all measured muscles

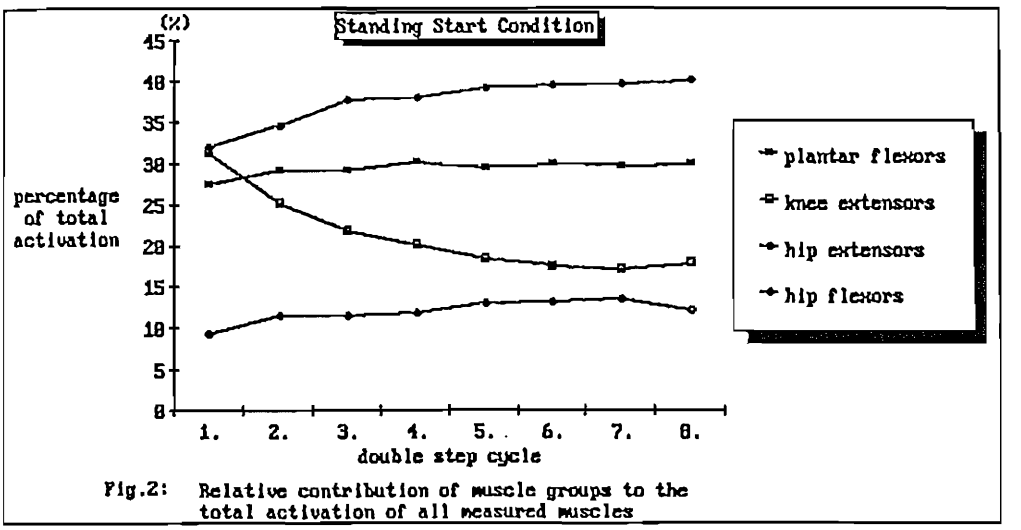

Fig.2: Relative contribution of muscle groups to the total activation of all measured muscles

DISCUSSION

Obviously the relative contribution of the investigated muscles to the total activation of all of them is changing during acceleration-phase of sprint running significantly and the effects are more pronounced in crouch start compared to standing start. Therefore the importance of the respective muscles to the generation of performance should vary during acceleration-phase. During the initial phase (0 m to 5 m) knee extensors and plantar flexors are more dominant. Whereas in the later phase of acceleration (20 m to 30 m) activation of hip extensors and plantar flexors is more distinct. For that reason a well-balanced training of all muscle groups involved should be preferred to training regimens concentrating on one aspect only (4,5).

REFERENCES

1. Jacobs R, van Ingen Schenau GJ (1992) Intermuscular coordination in a sprint push-off.. J. Biomechanics 25, p.953-965.
2. Mero A, Komi PV (1987) Electromyographic activity in sprinting at speeds ranging from submaximal to supramaximal. Med Sci Sports Exercise 19, p.266-274.
3. Wiemann K (1986) Die Muskelaktivität beim Laufen. Leistungssport 17, p.27-31.
4. Wiemann K (1989) Die ischiocruralen Muskeln beim Sprint. LdLa 28, p.763-786, 816-818.
5. Wiemann K, Tidow G (1994) Die Adduktoren beim Sprint - bisher vernachlässigt? LdLa 33, 7 p.15-18, 8 p.15-18.

CHANGES IN SPRINT KINEMATICS THROUGH THE CONSCIOUS EMPHASES ON THE LEG MOTION

N. FUJII, M. AE, K. MIYASHITA, Y. MORIOKA, and Y. MIYASHITA
Institute of Health and Sport Sciences, University of TSUKUBA, TSUKUBA, JAPAN

INTRODUCTION

It is well known that some characteristics of the leg movement in sprint are related to running velocity (Ito et al. (1993)). Although some instructions for the improvement of the leg movement are based on these relationships, it is not always possible to improve the leg movement of the young sprinters. One of the reasons of the differences between coach's expectations and the actual motions of the sprinter would be that the change in leg movement of a given segment and/or phase influences the movements of other segments and phases, because the body segments and movement phases closely relate each other. The purpose of this study was to investigate the changes of the leg motions in sprint running, which were induced by different emphases on the leg motion, and to obtain some suggestions to the sprint training.

METHOD

Five male sprinters served as subjects (height: 1.76 ± 0.06 m, weight: 704 ± 75 N). Two dimensional leg movements were recorded with a high-speed video camera operating 250 fps, which was panned in order to take large images of the subjects. Subjects were asked to emphasize the leg motions consciously and to sprint as fast as possible. Motions emphasized were (a) quick recovery of the leg after the toe-off (TO), (b) quick knee flexion after TO, (c) quick swinging back of the leg before the touchdown (TD), and (d) high knees. Their own sprint motions were studied as control. Sixteen kinematic parameters of the hip and knee joints were selected and analyzed: angles at TO and TD of the hip and knee, maximum flexion and extension angles of the hip and knee, angular velocities at TO and TD of the hip and knee, and maximum angular velocities of flexion and extension of the hip and knee. These parameters were normalized by mean values and standard deviations to each subject and parameter. Principal factors of the leg motions were analyzed on the normalized parameters.

Eighteen male sprinters (height: 1.74 ± 0.06 m, weight: 655 ± 60 N) including five subjects of the first experiment served as subjects. Two dimensional leg motions were recorded with a high-speed video camera in the same manner as above. Sprinting speed was measured as the average speed of 30 m interval where the leg motions were recorded. The relationships between the sprinting speed and the leg motions were analyzed without normalization of parameters.

RESULTS AND DISCUSSIONS

Six principal factors were derived from the analysis of the data of the first experiment. Figure 1 shows the kinematic parameters of three principal factors out of six factors. In Figure 1 (a) of the principle factor 1, the change in the angular velocity of the hip at TD was related to the change in both the angular velocity of the knee at TD and the minimum angle of the hip in the late recovery phase. The coefficients of correlation between parameters also means that the increase in the angular velocity of extension of the

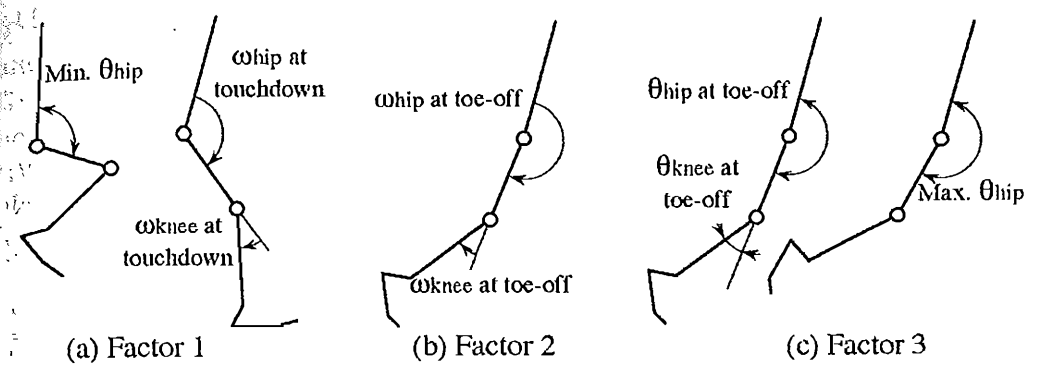

Figure 1 Principal factors of sprint. It was difficult to independently change the kinematic parameters in each factor.

hip at TD caused the decrease in the velocity of flexion of the knee at TD (r=0.542) and related to the minimum angle of the hip (r=0.586). These relationships are explained by the kinetics of the leg motion. The large angular velocity of extension of the hip at TD is due to the large angular acceleration of the hip, which causes the large joint force at the knee in the direction of the knee extension. Therefore the angular velocity of flexion of the knee at TD decreases. The hip flexion before TD also causes the large range of motion of the hip for acceleration. In the similar manner, it is explained that the large angular velocity of extension of the hip at TO related to the small angular velocity of flexion of the knee at TO in the principal factor 2, as shown in Figure 1 (b).

Figure 2 shows the relationships between the sprinting speed and the kinematic parameters collected in the second experiment. The large angular velocity of extension of the hip and the large flexion angle of the knee at TD related to the sprinting speed. Although the large knee angle at TD was caused by the large angular velocity of the knee joint before TD, it was difficult to increase both the angular velocity of extension of the hip and the angular velocity of flexion of the knee in the same time only through the conscious emphases without preparations, e.g. strength training specific to sprint.

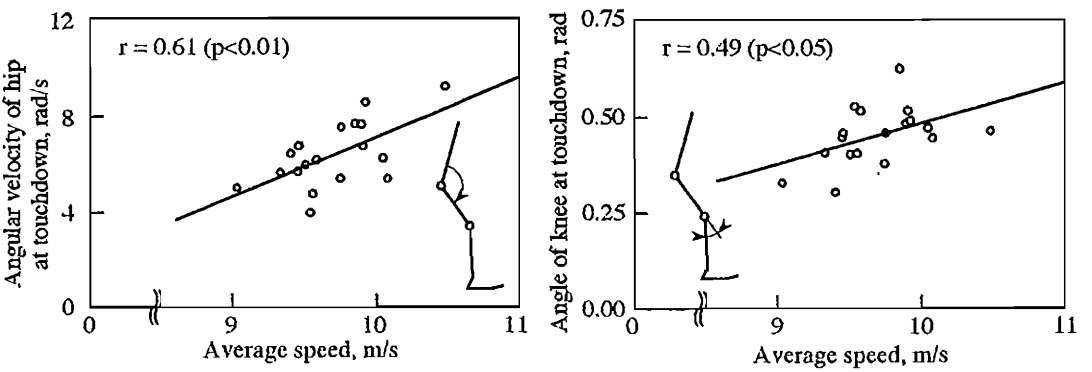

(a) Angular velocity of the hip at touchdown (b) Angle of the knee at touchdown

Figure 2 Relationships between sprinting speed and parameters of the leg motion.

REFERENCE

Ito A. et al. (1993) Leg movement analysis of gold and silver medalists in men's 100m at the III World Championships in Athletics. Proceedings of XIV International Congress of Biomechanics, Vol.I, 624-625.

ACTIVATION PATTERNS OF ANTAGONISTIC PAIRS OF MONO- AND BI-ARTICULAR MUSCLES DURING ARM PUSH MOVEMENTS

T. Fujikawa, T. Oshima, M. Kumamoto and T. Yamamoto
Faculty of Engineering, Toyama Prefectural University
Kosugi, Toyama 939-03, JAPAN

INTRODUCTION

Kumamoto et al. (1994) revealed that the existence of antagonistic pair of bi-articular muscles greatly contributed to the hybrid position/force control and compliance control of the end point of the upper and lower limbs, and resulted in smooth and precise movements of the limbs. However, activation patterns of the mono-articular muscles were not clearly described in the previous paper (1). Now in the present experiments, activation patterns of antagonistic pairs of mono-articular muscles as well as bi-articular muscles during arm push movements were examined in terms of electromyographic kinesiology.

METHODS

Subjects employed were 9 healthy young male adults, and muscles tested were deltoid anterior (Da) and posterior (Ds) portions, brachialis (Br), biceps brachii long head (Blo), and triceps brachii lateral (Tla) and long (Tlo) heads. EMGs, utilizing conventional surface electrodes, and the maximum force (F_{max}) exerted at the wrist joint were simultaneously recorded during isometric arm push movements. An experimental posture is shown in Fig.1. Selected joint angles of $\theta 1$, $\theta 2$ and $\theta 3$ were, 40°, 90° and 50°, and 50°, 60° and 30°, respectively. Line S-W was set around minus 10°. Experiment A; all subjects were requested to perform arm push movements in wider range of directions than in their most common daily movements, from -90° to +100°. Experiment B; only a few subjects were requested to perform arm push and pull movements in all round directions (360°), and EMG recordings, without force recordings, were attempted.

RESULTS AND DISCUSSION

The maximum forces (F_{max}) developed at the wrist joint with changes in the force direction (θf) were shown in Fig. 2. In Fig. 2, the curves of F_{max} well correspond to the stiffness curves obtained from the mechanical two-joints link model (1). However, the directions (θf) of the highest F_{max} were between 5° and 10°, whereas they were 0° in the mechanical model. This directional shift of the highest F_{max} might be due to more complex muscular alignment than in the simplified mechanical model.

In experiment A, a representative pattern, where integrated EMGs (IEMGs) of the muscles tested were plotted with changes in force directions, was shown in Fig. 3. The Blo and the Tlo reversed

their activity levels around 25°, and the Da and the Ds, around -20°, and the Br and the Tla, around 100°. The results obtained here and from the other joint angular conditions suggested that crossing points of activity levels of the pairs of antagonistic muscles of the Blo and Tlo, the Da and Ds, and the Br and Tla, were in-between directions 0° and *a* shown in Fig.1, directions *e* and 0°, and directions *a* and *b*, respectively.

In experiment B, a pattern of IEMGs of each pair of the antagonistic mono- and bi-articular muscles was not typical as shown in the mechanical model (1), but was enough to suggest that each crossing point of the activation levels of the pair is in-between adjacent directions. Therefore, if a two-joints link model has simplified muscular alignments, such as one pair of antagonistic mono-articular muscles on each joint S and joint E, and one pair of antagonistic bi-articular muscles on both joints S and E, a schematic diagram shown in Fig. 5 will be lead naturally. Reliability of the schematic diagram will be discussed in terms of mechanical control engineering later on by our colleague.

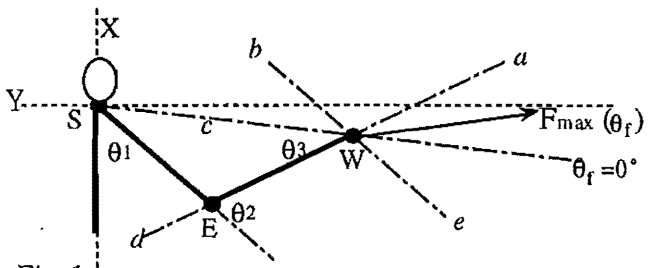

Fig.1

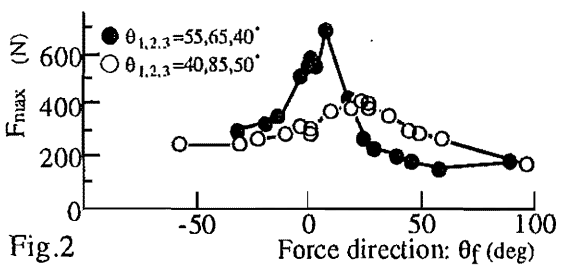

Fig.2

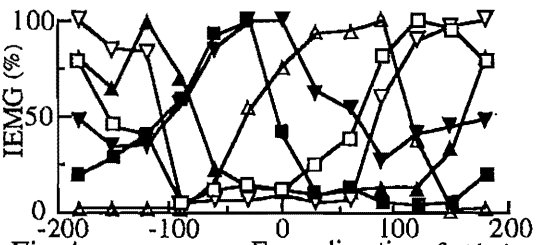

Fig.4 $\theta_{1,2,3}$=35,85,45° △ Da, ▲ Ds, ▽Br, ▼ Tla, □Blo, ■ Tlo

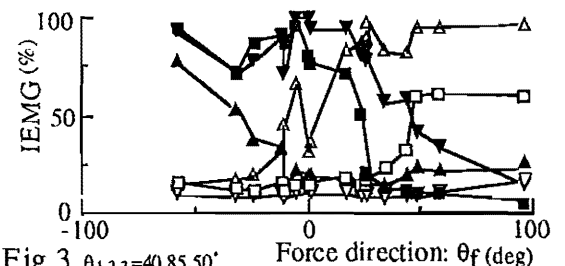

Fig.3 $\theta_{1,2,3}$=40,85,50° △ Da, ▲ Ds, ▽Br, ▼ Tla, □Blo, ■ Tlo

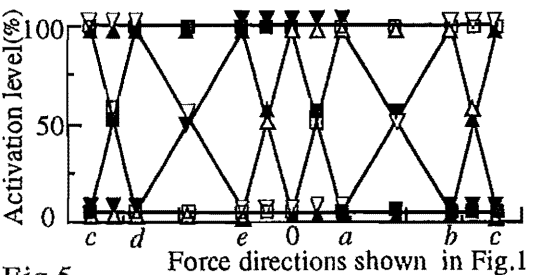

Fig.5 △ Da, ▲ Ds, ▽Br, ▼ Tla, □Blo, ■ Tlo

REFERENCES

(1) Kumamoto, M., Oshima, T. and Yamamoto, T. (1994) Control properties induced by the existence of antagonistic pairs of bi-articular muscles - mechanical engineering model analyses. Human Movement Science. **13,** 1-25.

Contribution of Series Elastic Component in Elbow Flexion using Stretch-Shortening Cycle

Senshi FUKASHIRO, Jun'ichi OKADA and Tetsuo FUKUNAGA
Dept. of Life Sci., The Univ. of Tokyo, Komaba 3-8-1, Meguro, Tokyo 153, Japan

INTRODUCTION

The skeletal muscle-tendon complex demonstrates elastic behavior especially when the muscle is activated and simultaneously stretched prior to concentric action. Although this complex consists of contractile and series elastic components (CC and SEC), the potentiation by elasticity is considered due to the contribution of SEC. The purpose of this study was to examine the contribution of SEC in human elbow flexion using stretch-shortening cycle (SSC) exercise in comparison with pure concentric action (CA).

METHODS

The subject was asked to perform the following two tasks using the ergometer shown in Fig.1. 1: maximal elbow flexion from 120deg as CA, 2: maximal elbow SSC exercise in which the elbow was flexed as fast as possible after extension from 90 to 120deg. Quick counter movement was emphasized in the SSC. Six weights (i.e. 2,3,5,7,9 and 13kgw) were loaded in these two tasks respectively.

The biceps brachii is defined as the equivalent elbow flexor. The force and displacement data were directly measured (Fig.1) and were recalculated to those in distal end of m.biceps brachii, considering moment arm. The power in whole muscle (P_{Total}) was obtained from the force and the velocity between origin and insertion of m.biceps brachii. On the other hand, the force(F)-length(l) relation of SEC in elbow flexors was estimated by the Quick Release method, referring to Poussen et al. (1990). The stiffness constant 'k' of SEC was calculated assuming a quadratic characteristics of SEC, i.e. $F=kl^2$. Then, the power by SEC (P_{SEC})was calculated in $P_{SEC}= F \cdot l$ /sec. Also, the positive work of whole muscle (W_{Total}) and SEC (W_{SEC}) was respectively calculated from the power curve integrated by time, i.e. Work= $\int P(d)t$. The power and work by CC (P_{CC} and W_{CC}) were obtained from the difference between Total and SEC.

RESULTS AND DISCUSSION

Figure 2 showed the typical curves of P_{Total}, P_{SEC} and P_{CC} in CA and SSC. Because the SEC is stretched in the first phase of CA, the onset of the P_{Total} can be observed subsequent to the increment of P_{CC}. A little W_{SEC} was recognized in the subsequent phase. On the other hand, the different pattern was found in SSC. Since the SEC is stretched considerably in elbow extension phase, the CC has to perform positive work during that phase in SSC. Although the P_{CC} decreased slightly in the counter phase of SSC, the P_{CC} increased again in the subsequent elbow flexion phase. In this positive phase, the W_{SEC} contributed greatly to the W_{Total} in SSC.

Figure 3 showed the W_{CC} and W_{SEC} in the different loads of CA and SSC. Although

the W_{Total} was almost same in each load, the contribution of W_{SEC} was extremely different. The percent of the W_{SEC} to the W_{Total} showed 8.6 ±1.1% in CA and 20.1 ±3.8% in SSC, respectively. It can be said that the W_{SEC} was found to perform about 2 times contribution in SSC in comparison with that in CA. As the major part of SEC is located in the tendinous tissues of muscle, this contribution is considered to be done by tendon.

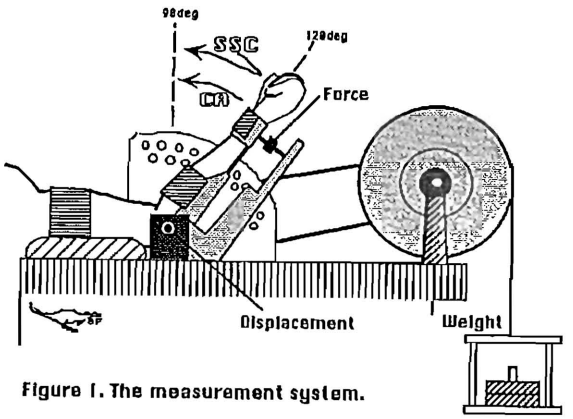

Figure 1. The measurement system.

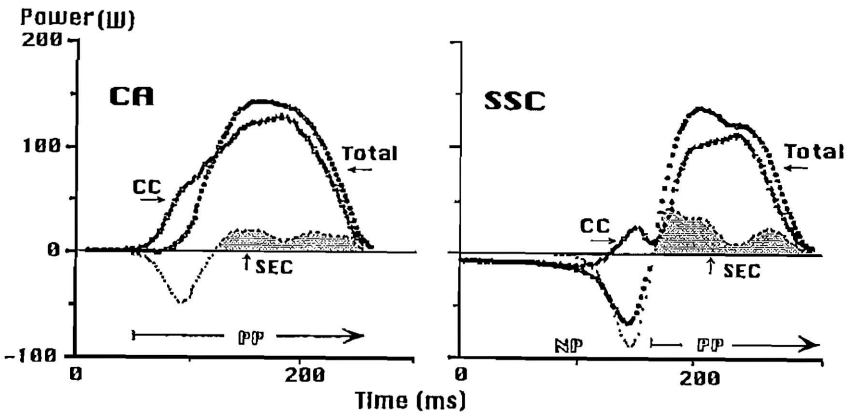

Figure 2. The typical power curves in CA and SSC (load: 3kgw).
*Total, SEC and CC: see text (CC= Total - SEC). NP/PP: Negative/Positive phases.

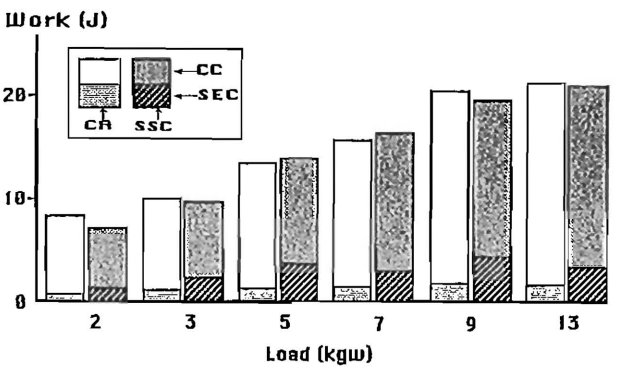

Figure 3. The contribution of W_{SEC} and W_{CC} to the W_{Total} in different loads.

Reference Pousson,M., et al.: Changes in elastic characteristics of human muscle induced by eccentric exercise. J.Biomech. 23(4):343-348,1990.

FORCE-VELOCITY CHARACTERISTICS BETWEEN WEIGHTLIFTERS AND BODYBUILDERS IN MONO- AND MULTI-ARTICULAR MOVEMENTS

K. Funato, A. Matsuo, S.Ikegawa and T. Fukunaga
Department of Sports Sciences, College of Arts and Sciences, University of Tokyo, Komaba 3-8-1, Meguro-ku, Tokyo 153, Japan

INTRODUCTION

Training for weightlifters(WL) is aimed to increase the muscle power i.e., improve the higher speed production under the heavier loaded condition, on the other hand bodybuilder's(BB) training is focused just on muscle hypertrophy. Those difference might result muscle morphological and functional changes between WL and BB. This study was undertaken to examine the characteristics of resistance training between WL and BB from the force - velocity relations developed during mono- and multi-articular movements and anatomical cross-sectional area of the muscle.

METHODS

Joint torque and movement power : For the single isolated joint torque measurements, isokinetic dynamometer (Dynamic Tension Meter, Sakai Medical Co., Japan) was used for concentric and eccentric actions for extension and flexion of elbow and knee joint. Movement speeds selected were 0, 5 and 15rpm.

A "Power Processor" dynamometer was manufactured for the measurement of specific movement power especially for the multi-articular movement. The body of the Power Processor was composed of a electrical rotary encoder to measure the axis revolving time and a load cell to measure the tension of the wire. The loads were provided by electrically controlled pawder brake system. Data for the time of revolution and wire tension were sampled every 5 ms and recorded digitally on personal computer. Instantaneous power was obtained by multiplying the instantaneous velocity and force values for every 5 ms. Peak values obtained from respective curves (PP: peak power, PV: peak velocity and PF: peak force) were taken for the analysis. Movements selected were high clean (HIC) and bench press (BPR) as shown in the figure.

Morphological measurements: Lean body mass (LBM) and %fat were determined by underwater weighing technique. Anatomical cross-sectional area (ACSA) of the muscle of extensor and flexor of knee and elbow were determined by using ultrasound techniques. The measured site was 60% distal from acromion for right upper arm and 50% distal from trochanterion for right thigh, respectively.

Subjects: 30 bodybuilders those who trained for more than five years including the winners of world and national body building competition and 25 national Olympic weightlifters were selected as the subjects of this study. Additionally 27 sedentary healthy males were tested for the comparison to the athletes.

RESULTS AND DISCUSSION

Lean body mass for BB (68.6 kg in average) were significantly ($p < .05$) larger than that for WL (62.8kg) and ACSAs for both extensors and flexors in elbow joint were larger in BB than in WL.

Static torque developed for isolated single joint movement have tendency to be larger in BB than WL in both absolute and relative to LBM values (Table 1). Static torque for knee flexor on the other hand, showed larger value in WL than that in BB. Maximum

static torque per ACSA in elbow flexor and extensor showed statistically larger in WL and sedentary control group than in BB. This might be suggested that the training method for BB might not be accompanied the functional increase of the muscle force with the muscle hypertrophy. One of the reason of the small value in absolute strength for BB was interpreted as the inefficient transportation of muscle tension of the muscle fiber to tendon due to the enlargement in muscle fiber pennation angle.

For power developed during multi-articular movement, BPR showed statistically larger in BB (9.1W/kgLBM) than WL (8.1W/kgLBM) on the other hand, WL (28.0W/kgLBM) demonstrated statistically larger value than BB (20.8W/kgLBM) in the movement of HIC (Table 1). It is suggested that dominance in the mono-articular torque does not necessary demonstrate the increase in the power developed by multi-articular movement. The difference in power shown between WL and BB was interpreted as the characteristics of movement speed of resistance training which each athletes usually performed, i.e., fast lift and slow lift.

Force - velocity relations obtained from HIC movement in WL shifted rightward compared to that of BB, indicating the WL developed the maximum power under lighter load and higher speed condition.

The results of the present study suggest that respective resistance training for WL and BB might cause unique changes in muscle hypertrophy and torque or power output for isolated and multi-articular movement.

Table 1. Static torque for elbow and knee joint and power developed in bench press and high clean movement.

Static Torque		Body Builders		Weightlifters
Elbow Flexion	(Nm)	76.0 ± 14.7	NS	69.2 ± 17.0
	(Nm/KgLBM)	1.2 ± 0.1	>	1.1 ± 0.2
Elbow Extension	(Nm)	97.9 ± 25.5	>	81.0 ± 23.5
	(Nm/KgLBM)	1.5 ± 0.3	>>	1.3 ± 0.2
Knee Flexion	(Nm)	157.2 ± 31.5	NS	167.9 ± 40.2
	(Nm/KgLBM)	2.3 ± 0.3	<<	2.7 ± 0.5
Knee Extension	(Nm)	304.3 ± 68.9	>>>	240.8 ± 56.8
	(Nm/KgLBM)	4.5 ± 0.8	>	3.9 ± 0.8
Power				
Bench Press	(W)	623.3 ± 143.2	>	533.9 ± 141.5
	(W/KgLBM)	9.1 ± 1.8	NS	8.4 ± 1.3
High Clean	(W)	1423.7 ± 361.7	<	1766.0 ± 575.6
	(W/KgLBM)	20.8 ± 4.8	<<<	28.0 ± 6.1

< : $p<0.05$, << : $P<0.01$, <<< : $p<0.001$

THE MODULATION OF SOLEUS H-REFLEX BY AUDITORY STIMULATION DURING HOMONYMOUS MUSCLE CONTRACTION.

Toshiaki FURUBAYASHI and Tomoyoshi KOMIYAMA
Department of Sports and Health Science, Faculty of Education, Chiba University, Chiba (JAPAN)

PURPOSE

It has been known that proprioceptive and teleceptive mechanisms play an important role in human motor control. Extensive studies with vision have been conducted in the teleceptive mechanisms. However, it has not been known how auditory stimulation affect the motor control system. Therefore, we examined the effects of auditory stimulation on intraspinal motor neuron as an index of H-reflex in the soleus muscle (Sol).

METHODS

The experiments were performed on 10 normal subjects aged 20-34 years. All subjects gave informed consent to the experimental procedures.

In these experiments, the posture and motor task used were as follows; (A) Sitting at rest, (B) Standing at rest, (C) Forward support standing and (D) Isometric plantar flexion while sitting. In cases (A) and (D), the subjects were comfortably seated in an armchair, with knee and ankle joint at 170 and 110 degrees, respectively. the right foot was fixed into place on a foot plate transducer. In case of (C), the subjects held a bar which was set in front of them to relax the Sol. In case of (D), amount of voluntary contraction was as same as the background EMG obtained standing at rest. Auditory stimulation of 100ms duration (1ms pulse, 10ms interval, 11train), 0.5Khz and 110dB (sensation level) intensity was presented to both ears through headphones (conditioning stimulation; C). EMG responses were recorded with bipolar surface electrodes placed on the skin overlying the right Sol. Sol H-reflex rectangular pulse of electrical simulation (test stimulation; T). Stimulus intensity was set to about 40% of the maximum M-response.

RESULTS

Fig. 1 shows the time course of the auditory effects on Sol H-reflex. Facilitatory effects were observed at 40-50ms after auditory stimulation. Maximum facilitation was attained about 100ms. Fig. 2 shows a summary of the results obtained from seven subjects. In cases (B) and (D), a statistically significant depression in the facilitatory effect relative to that for sitting at rest (A) could be seen. This effect was not significant while in the forward supporting case (C).

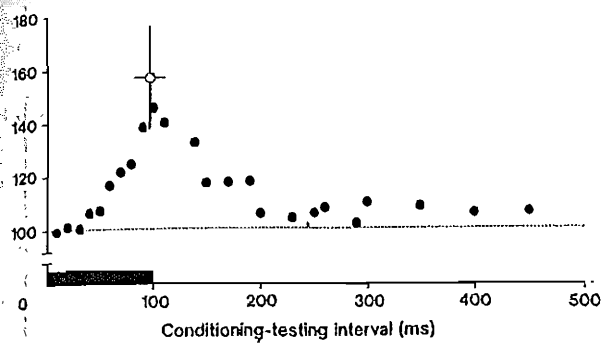

Fig-1. Time course of facilitatory effects by auditory stimulation. Open circle with horizontal and vertical bars show the mean and standard deviation of the c-t interval and the amount of the H-reflex facilitation in which maximum facilitatory effects were obtained respectively.

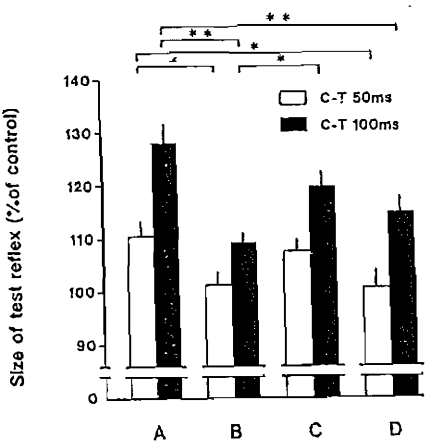

Fig-2. Facilitatory effects between 4 tasks by auditory stimulation. A: sitting at rest. :Standing. C: Forward support standing. D: isometric planter flexion while sitting.

DISCUSSION

In the previous studies in acute cats, it has been reported that auditory stimulation elicits facilitation alone, inhibition alone or a combination of both effects (Wright and Barnes, 1972). In human experiment, EMG activity can be elicited with the startle reflex in Sol and forearm flexor (Rossigno, 1975, Brown et al., 1991). In the present study, we observed the facilitatory effects of H-reflex of Sol. Therefore we strongly suggest that auditory startle reflex is not only flexor reflex, but also reflex that occurs as a purposeful combined action. Brown et al. (1991) have observed that in ankle plantar flexion tasks and during crouching tasks, the amount of EMG increase in Sol and biceps brachii, respectively. However in the present study, the facilitatory effect decreased in the H-reflex. Therefore it is more likely that there exist some descending pathways which depress Ia afferent input during auditory stimulation.

REFERENCE

Brown, O., Rothwell, J.C. et al. (1991): Brain ., 114, 1891-1902.
Rorrignol, S. (1975): Electroenceph. Clin. Neurophysiol., 39, 389-397.
Wrigh, C.G. and barnes, C.d. (1972): Brain Res. 36, 307-331.

HELICAL TRANSLATION IN JOINTS
A CLASSIFICATION CONCEPT

Franz K. Fuss, Angelika H. Fuss

Institute of Anatomy 1, Division of Biomechanics, Univ. of Vienna, Vienna, Austria

INTRODUCTION

Within the group of "hinge joints", so called "screw joints" with distorted joint surfaces are distinguished (e.g., tarsal joint of hoofed animals and kangaroos; Barnett et al., 1961) which perform a translation during motion. Even the human humeroulnar joint has been lively debated whether a screw thread exists or not (Fick, 1911). The human knee has been clearly identified as a screw joint with a translation of up to 4 mm (Blankevoort et al , 1990). The aim of this paper is to analyze the helical translation in various joints and to propose a classification concept.

PRINCIPLE

The common principle of 3-D-kinematics is that a moved rigid body performs a rotation about an axis (finite helical axis) combined with a (helical) translation (HT) along the axis. It should be noted, that, if the axis changes its direction during motion, the HT does that too.

METHOD

The Tarsós$^{\beta}$ examination system consisting of a Macintosh workstation (Macintosh IIci 80/5), an electromagnetic digitizer/tracker (Polhemus 3Space® Isotrak® M100, McDonnell Douglas, Colchester, Vermont, USA) and a specialized software package (Tarsós$^{\beta}$ 2.0, Inst. Anat. Vienna, calculating the helical axis parameters, helical translation and pitch [translation per rotation]) was used (Fuss, 1993, 1994). Concerning the HT, the accuracy of the system was tested using a technical hinge and a screw. Care was taken of metallic fixation devices which might impair the magnetic field of the digitizer. Each analysis was carried out at least three times to test the reproducibility.

JOINTS ANALYZED

Man (*Homo sapiens*): humeroulnar joint (4 specimens), knee - femorotibial joint (5), knee - femoropatellar joint (5), talocrural joint (3), talocalcaneonavicular joint (3), various joints within the wrist joints (extension/flexion, 2), radioulnar joints (2), shoulder system (humerus vs. trunk, abduction; 47), atlantoaxial joint (rotation, 2), atlantooccipital joint (rotation, 2); animals: tarsal joints (horse - *Equus caballus*, camel - *Camelus dromedarius*), hoof joints (horse), knee - femorotibial joint (crocodile - *Crocodilus niloticus*, ostrich - *Struthio camelus*, wallaby - *Macropus agilis*, baboon - *Papio ursinus*, lion - *Panthera leo*, elephant - *Loxodonta africana*, hippo - *Hippopotamus amphibius*, camel, horse), knee - femoropatellar joint (pig - *Sus scrofa domestica*), tibiofibular joint (crocodile,ostrich). The human joints were cadaver specimens analyzed within three days after death (partially deep-frozen). The human shoulder system was analyzed in test persons (Fuss, 1994) The human tibiofemoral joint, all patellofemoral joints and the human shoulder system were analyzed under unloaded and stressed conditions. The animal joints were partially fresh and partially fixed with carbol.

CLASSIFICATION

The following coordinate system was used: x-axis pointing anteriorly (cranially in quadrupeds), y-axis pointing cranially (dorsally) and z-axis to the right. The helical translation was always depicted for a right joint (if symmetric), when the distal element of the joint is moved according to the thumb rule (clockwise motion when looking in the direction of the respective axis). A positive HT is hence an anterior (cranial), cranial (dorsal) or lateral shift.

RESULTS

Concerning the accuracy of the system, the standard deviation from the ideal line (no helical translation in the hinge, constant helical translation in the screw) was 0.07 mm. All examined joints showed more or less screw motions. Joints with an increasing HT and with a HT changing direction during motion could be distinguished. The amounts of HT where found between 1 mm and 1 cm. The HT did not always change during stress situations (knee, shoulder). All HTs were reproducible within the single joints and rather unchanged (with some individual variability) comparing identical joints. Examples of the

human humeroulnar joint (Fig.1) and of the ostrich knee joint (Fig.2) are depicted below.

Figure 1: translation of the human humeroulnar joint

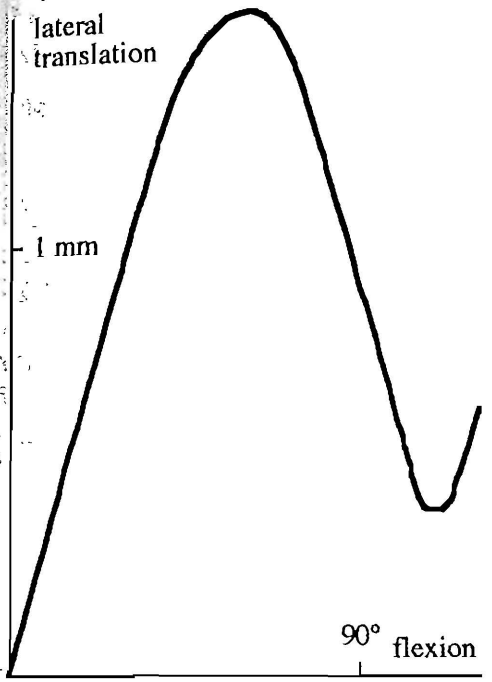

Figure 2: translation of the femoro-tibial (knee) joint of the ostrich

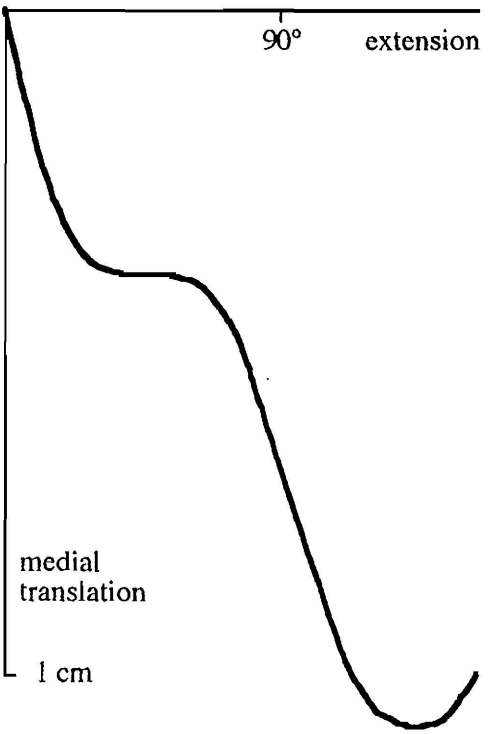

DISCUSSION

Joint surfaces are designed to transmit forces (muscle, ligament and external forces [gravitation, inertia and reaction forces]) between the elements and to perform a guided motion. These forces influence the shape of the articular surfaces. As forces occur in three main directions, the exceptional case of a pure rotation (without translation) is excluded. HT must hence be regarded a common case. The shape of joint surfaces guarantees a reproducible HT. If the joint is stressed, viscoelastic behavior of ligaments and articular cartilage can change the HT. HTs of more than 1 cm were found. In this connection it should be noted that, comparing 2 identical joints, the joint size influences the amount of HT.

References:

Barnett C.H., Davies D.V., and MacConaill M.A. (1961) Synovial joints. London: Longmans.

Blankevoort L., Huiskes R., and De Lange A. (1990) Helical axes of passive knee joint motions. J. Biomech. 23:1219-1229.

Fick R. (1911) Handbuch der Anatomie und Mechanik der Gelenke. Vol.3. Jena: Fischer.

Fuss F.K. (1993) Helical axis surface of the knee joint. XIVth Congress of the International Society of Biomechanics, Paris, 4.-8. 7. 1993 (Abstract).

Fuss F.K., and Wurzl G.H. (1994) Clinical assessment of shoulder kinematics by means of helical axes parameters. 2nd World Congress of Biomechanics, Amsterdam 10.-15.7.1994 (Abstract).

THE EFFECT OF FOUR ASYMMETRY FACTORS ON TRIAXIAL NET MUSCULAR MOMENTS AT THE L5/S1 JOINT DURING LIFTING

Denis Gagnon, Michel Mercier & Christian Larivière
Laboratoire de biomécanique occupationnelle, Faculté d'éducation physique et sportive, Université de Sherbrooke, Sherbrooke, Québec, Canada

INTRODUCTION

It is generally assumed that the L5/S1 joint net muscular moments that are out of the plane of motion could be neglected if the trunk moves in the sagittal plane when lifting a load. However, common workplace factors like diagonal handgrip, non parallel feet position and uneven load distribution may contribute to the generation of non negligible asymmetrical loading at L5/S1. The purpose of this study was to determine the effect of four asymmetry factors (trunk motion, handgrip, feet position and load distribution) on triaxial net muscular moments at L5/S1. It was hypothesized that relative to standard symmetric lifting (1) the trunk asymmetry factor would generate more axial rotation and lateral bending at L5/S1 and (2) asymmetry of handgrip or feet position or load distribution combined with symmetric trunk motion would generate more axial rotation and lateral bending at L5/S1.

METHODS

Subjects & tasks. Ten university male students (age: 21.8 ± 1.2 yr; mass: 72.7 ± 9.5 kg; height: 176.0 ± 5.3 cm) participated to the study. They were physically active and had no recent history of low back problems. Eight lifting tasks (Table 1) were randomly performed 3 times with a 131 N load for a total of 24 trials by subject. For each task, the origin and end positions of the external load were standardized as well as handgrip, feet and load center of mass positions.

Table 1. Asymmetry factors for the eight lifting tasks

Task	Trunk vs Sagittal Plane	Hand Grip L/R	Feet Position L/R	External Load		
				Center of Mass Position	Level at Origin of Task	Level/Side at End of Task
T1	Symmetric	8/8	Parallel	Center	Floor	Shoulder/C
T2	Symmetric	7/3	Parallel	Center	Floor	Shoulder/C
T3	Symmetric	8/8	Rear/Front	Center	Floor	Shoulder/C
T4	Symmetric	8/8	Parallel	Left	Floor	Shoulder/C
T5	Asymmetric	7/3	Rear/Front	Left	Floor	Shoulder/L
T6	Asymmetric	7/3	Rear/Front	Center	Floor	Floor/L
T7	Asymmetric	7/3	Rear/Front	Center	Floor	Shoulder/L
T8	Asymmetric	7/3	Rear/Front	Center	Shoulder	Shoulder/L

Data acquisition & analysis. Four synchronized video cameras and two force platforms were used to collect data. After digitization, 3D reconstruction via DLT[2], digital filtering[3] and 3D kinematics determination, a dynamic 3D multisegment model[1] was used to compute the net joint loading. The net moments at the L5/S1 joint were computed about the three anatomic axes of the trunk (Axial Rotation: M_{AR} about longitudinal axis; Lateral Bending: M_{LB} about sagittal axis; Flexion & Extension: M_{FE} about transverse axis; Resultant moment: M_R).

RESULTS

Table 2. Maximum (avg(S.D.)) triaxial net muscular moments (N·m) at L5/S1

Net Moment		Lifting Task (N=235; n_4=28; n_5=27; others=30)							
		T1	T2	T3	T4	T5	T6	T7	T8
M_{AR}	L	17(7)	24(9)	23(12)	30(13)	44(15)	52(13)	37(12)	34(11)
	R	-11(10)	-10(8)	-6(8)	-6(5)	-34(10)	0(0)	-40(10)	-39(12)
M_{LB}	L	23(11)	48(15)	18(13)	13(6)	30(12)	0(0)	36(11)	48(13)
	R	-16(15)	-48(25)	-31(25)	-42(18)	-85(30)	-115(24)	-63(26)	-12(19)
M_{FE}	F	0(0)	0(0)	0(0)	0(0)	0(0)	0(0)	0(0)	0(0)
	E	-254(38)	-243(32)	-247(32)	-245(42)	-218(28)	-173(14)	-236(26)	-169(20)
M_R		255(38)	249(33)	250(33)	248(42)	235(30)	223(25)	246(29)	175(19)

Positive values for left axial rotation (M_{AR} L), left lateral bending (M_{LB} L) and flexion (M_{FE} F)

DISCUSSION

Effect of trunk asymmetry. Descriptive statistics seem to support the first hypothesis of this study for axial rotation but not for lateral bending. Left lateral bending moments for symmetrical task T2 (7/3 diagonal handgrip) were greater or equal to those generated during all the tasks involving trunk asymmetry (T5-T8). Right lateral bending moments for T2 and T4 (load center of mass to the left) were greater than those generated during T8 (load moved at shoulder level) but lower than those of the other asymmetrical tasks (T5-T7). These results emphasize the effect of other factors than trunk asymmetry to generate significant lateral bending moments at L5/S1 during symmetrical lifting.

Effect of the other asymmetry factors for symmetric lifting. The second hypothesis of this study is partly supported. Left (T2) and right (T2-T4) lateral bending moments were larger than those generated during a standard symmetric lift (T1). Left axial rotation moments were greater for T4 than T1 for symmetrical lifting. For the symmetrical tasks T2-T4, the results show that an analysis limited to the extension moment would have ignored significant loading, mainly in lateral bending. Even standard symmetric lifting (T1) generated left axial rotation and lateral bending values greater than those previously obtained through a sensitivity analysis[1].

In conclusion, common workplace factors like diagonal handgrip and uneven load distribution could generate non negligible loading on the lumbar spine. The effect of these factors on the asymmetrical distribution of net lumbar spine loading could be as important as those of dynamic factors.

REFERENCES

1. Gagnon, D., & Gagnon, M. (1992) The influence of dynamic factors on triaxial net muscular moments at the L5/S1 joint during asymmetrical lifting and lowering. *J. Biomechanics*, **25**, 891-901.
2. Walton, J.S. (1981) Close-range cine-photogrammetry: a technique for quantifying human gross motion. Unpublished doctoral dissertation, Pennsylvania State University (UMI #8120471).
3. Winter, D.A. (1990) *Biomechanics and Motor Control of Human Movement.* Wiley-Interscience.

ACKNOWLEDGMENTS

Project supported by Fonds FCAR of Québec.

EFFECTS OF FEET POSITIONING ON THE BIOMECHANICS OF KNEE JOINTS IN HANDLING TASKS

M. Gagnon[1], A. Plamondon[2] and D. Gravel[1]
[1] Université de Montréal, Montréal, Québec, Canada
[2] Université Laurentienne, Sudbury, Ontario, Canada

INTRODUCTION

In the first part of this study already published (1), it had been shown that, when asymmetric lifting is performed by pivoting the feet, asymmetries of trunk posture and trunk efforts are considerably reduced; the opposite was found when lifting involved a torsion about the longitudinal axis of the trunk (full twist and half twist techniques), with the feet maintained in a fixed position. As it had already been demonstrated, in specific contexts of symmetric sagittal plane lifts, that an inverse relationship existed between loadings on the spinal joints and loadings on the knees (2), further analyses of the data were thus performed to assess the performance of these asymmetric lifting techniques with regards to knee joint loadings. It was then hypothesized in the present study, that foot pivoting would be more stressful for the knee joints and that the full twist technique would be less stressful for these joints.

METHODOLOGY

Nine students in physical education with limited experience in manual materials handling were used as subjects; their mean age was 23.2 yr (range: 19-30 yr). The task consisted of lifting a 16 kg load from a shelf placed at the subject's left, at a height of 68 cm from the force platform level and to bring it through a 90° position to the right on a shelf at a height of 80 cm. Three modes of lifting were used: 1) where the trunk was flexed forwards and twisted fully to grasp the load, with the feet in a fixed position and facing the shelf of deposit to the right, 2) with half twist and the feet in a fixed position midway between the shelves and 3) where the subject pivoted simultaneously on both feet, consequently facing the load at all times. The load was handled with an asymmetric and diagonal hand position. The subjects were free to select their feet spacing.

The 3D data were collected using two AMTI force platforms and two 16 mm Locam cameras which were synchronized at 100 Hz and coupled with two large mirrors. The 3D locations of the markers were obtained by direct linear transformation procedures. A dynamic 3D multi-segment model was constructed; the analysis was performed on each segment, starting at the feet and ending at the trunk, to produce the net reaction forces and moments at each joint. The net moments were reported about the three orthogonal axes on the segments. Analyses of variance with repeated measures were applied to test the differences between the techniques; linear contrasts were applied to located the differences; a probability level of 0.05 was chosen.

RESULTS

With foot pivoting, knee efforts were generally larger than for the other techniques, about the three axes and for the resultant; knee flexion at the moment of maximal efforts and the maximal lateral distance between the feet were also larger for the pivoting technique (Table 1). Oppositely, there was a tendency for reduced knee moments with the full twist technique (with one exception for the moment in right lateral bending for the right knee). Intermediary results were observed for the half twist technique.

DISCUSSION

The results confirmed that there is an inverse relationship between loadings on the spinal joints and loadings on the knee joints, for asymmetrical lifting. Previous

results on trunk posture and efforts had shown the potential advantage of the pivoting technique and the disadvantage of the techniques with trunk twisting (1); the opposite was found when analysing knee efforts. Foot pivoting was associated with relatively large moments, specially in lateral bending. Moreover, the larger knee flexion and the larger base of support (lateral distance between the feet) suggests that the control of balance may be an important factor involved in this strategy; however, the increased knee flexion may well be an adaptation to facilitate knee torsion efforts. At the light of the combined results concerning the spinal joint (1) and the knee joints, one cannot conclude that foot pivoting is an optimal strategy; modifications of this strategy by pivoting alternately on each foot may produce different conclusions worth investigating. In this global context, the half twist technique with the feet in an intermediary position between the shelves may appear optimal; as a matter of fact, this technique produced intermediary loadings for the back (1) and knee joints. Other patterns of footwork as well as different grips and load manoeuvers should be investigated on the basis of comparative observations of expert and novice workers.

Table 1. Means and standard deviations (in parentheses) for selected variables of the tasks

Variables	Lifting techniques			Significance levels			
	Full twist (1)	Half twist (2)	Pivoting (3)	Global	(1)vs(2)	(1)vs(3)	(2)vs(3)
•Max resulting moment: left knee (Nm)	71 (28)	76 (28)	90 (28)	0.03	NS	0.03	NS
•Max lateral distance between feet (m)	0.38 (0.01)	0.40 (0.04)	0.43 (0.04)	0.00	NS	0.01	0.03
•Max extension moment: right knee (Nm)	12 (8)	18 (15)	30 (17)	0.00	NS	0.01	0.01
•Max left twist moment: left knee (Nm)	-12 (4)	-20 (5)	-23 (8)	0.00	0.00	0.00	NS
•Knee flexion for max. left twist moment (°)	29 (8)	33 (9)	44 (11)	0.00	NS	0.00	0.05
•Max left bending moment: left knee (Nm)	12 (11)	38 (19)	65 (21)	0.00	0.01	0.00	0.00
•Max right bending moment: right knee (Nm)	-19 (12)	-7 (7)	-39 (21)	0.00	0.02	0.01	0.00

REFERENCES

1. Gagnon, M., Plamondon, A. and Gravel, D. (1993). Pivoting with the load. An alternative for protecting the back in asymmetrical lifting. Spine 18, 1515-1524.
2. Bejjani, F.J., Gross, C.M. and Pugh, J.W. (1984). Model for static lifting: relationship of loads on the spine and the knee. J. Biomechanics 17, 281-286.

ACKNOWLEDGEMENTS

This study was supported with grants from IRSST and NSERC.

FATIGUE INDUCED CHANGES IN TREMOR AMPLITUDE DURING AND AFTER AN ISOKINETIC EXERCISE SESSION

J.Gajewski*, A.Wit**, J.T.Viitasalo***

* Academy of Physical Education, Warsaw, Poland
** Institute of Sport, Warsaw, Poland
*** Research Institute for Olympic Sports, Jyväskylä, Finland

INTRODUCTION

An increase in tremor amplitude caused by heavy muscular work was reported in several studies (Lippold, 1981; Arblaster et al., 1989)has been shown to be of a central nervous system origin (Furness et al., 1977). This suggests that changes in tremor caused by physical effort reflect a local state of fatigue in the nervous system. The stretch reflex is thought to be involved (Stiles, 1980; Prochazka and Trend, 1988). Results given by Furness et al.(1977) as well as results of our previous studies (Viitasalo and Gajewski, 1994) indicate that tremor measurements can be utilized for quantitative estimation of fatigue. Such a fast and non-invasive method would certainly be interesting from the point of view of sport and occupational physiology.

Arblaster et al. (1989) has shown that a single, strong, brief effort causes an immediate decrease and then, after few minutes, a significant increase in tremor amplitude. Also, Lippold (1981) has demonstrated that the increase in tremor amplitude is delayed with respect to the end of performed work.

The aim of this study was to determine a time course (pattern) of changes in tremor amplitude characteristics during and after an isokinetic training session.

METHODS

Nineteen untrained males served as subjects in the study. The subjects took part in a controlled isokinetic training session on the Computerized Exercise System ARIEL. Each training session consisted of a standardized warming-up followed by 7 sets of bench press (with three minutes intervals in between). Each set consisted of ten repetitions done at a bar angular velocity of 25 deg/s. The subject were asked to use their maximal strength during the exercise.

Forearm tremor was measured with an accelerometer after warming-up, one minute after the end of each set and then five times (five minutes in between) starting at fifth minute after the last set. During the measurement the subject, while sitting on a dynamometer chair, flexed his left forearm isometrically against a spring. The actual force value was shown to the subject as a feed-back to maintain the desired force level and forearm's position.

The power spectrum density function (PSD) was estimated for each acceleration signal. Due to the proposition given in our previous study (Viitasalo and Gajewski, 1994) the logarithmic amplitude index (LAI) was calculated as the lnPSD's average in 9 to 20 Hz frequency band (found as the most sensitive to fatigue).

RESULTS

The averaged course of LAI's increase (with respect to initial value) is shown in Fig.1. The statistical analysis (the two-way ANOVA) revealed that the log-amplitude index was statistically significantly ($p<0.05$) different for subsequent measurements ($F=17.48$, d.f.=10, 180). Rather great differences in LAI were found between subjects ($F=163.31$, d.f.=18, 180). Statistically significant decrease in LAI was found when comparing results after the fourth and the fifth set. The greatest values of LAI were registered about ten minutes after the last set of the training session.

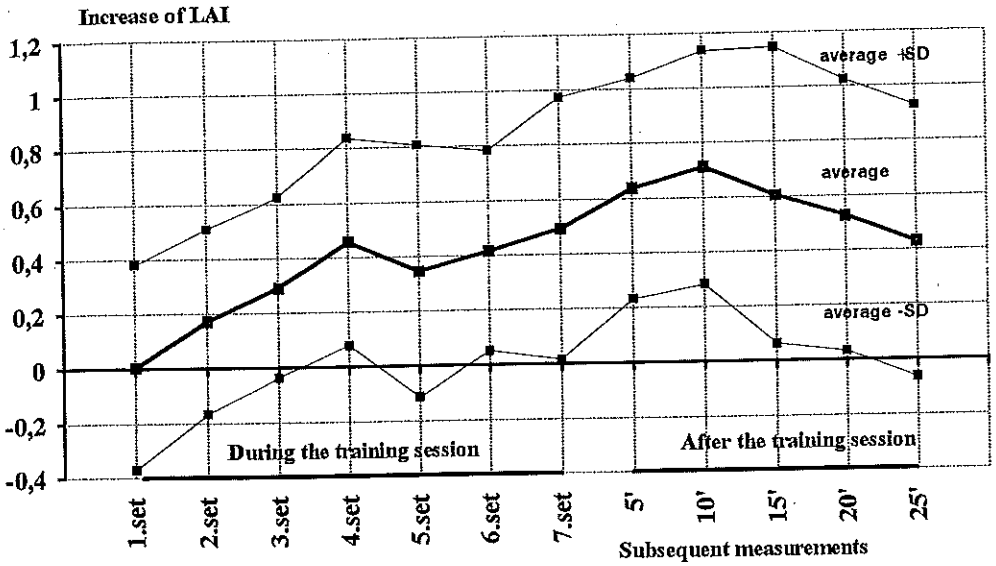

Fig. 1. The averaged (±SD) increase of the tremor log-amplitude indicator (with respect to its initial value) after subsequent exercise sets and after the whole training session.

DISCUSSION

The isokinetic work increased tremor amplitude during and after the training session, however, this type of work was not expected to influence the stretch reflex properties. The tremor response on physical effort was delayed what is in line with the previous findings (Furness et al., 1977; Lippold, 1981). On the other hand, the greatest values of amplitude were found quicker then reported by Furness et al. (1977). The effect of short term decrease in amplitude (described by Arblaster et al., 1989) caused that tremor amplitude measured between exercise sets was lower then the same measured after the training session. The cumulative effect of the performed work was then seen during recovery. Although the values of tremor log-amplitude index (LAI) differed much between subjects, a similar pattern of the LAI changes was observed in the whole group.

REFERENCES

1. Arblaster, L.A., Lakie, M., Walsh, E.G. 1989. Does brief isometric effort always increase physiological tremor in humans? *Journal of Physiology*, 409, 5P
2. Furness, P., Jessop, J., Lippold, O.C.J. 1977. Long-lasting increases in the tremor of human hand muscles following brief, strong effort. *Journal of Physiology* 265, 821-831.
3. Lippold, O.C.J. 1981. The tremor in fatigue. In: Human muscle fatigue: physiological mechanisms. London CIBA Foundation symposium 82, Pitman Medical, 234-248.
4. Prochazka, A., Trend, P.S.J. 1988. Instability in human forearm movements studied with feed-back-controlled muscle vibration. *Journal of Physiology*, 402, 421-442.
5. Stiles, R.N. 1980. Mechanical and neural feedback factors in postural hand tremor of normal subjects. *Journal of Neurophysiology*, 44, 40-59.
6. Viitasalo, J.T., Gajewski, J. 1994. Effects of strength training - induced fatigue on tremor spectrum in elbow flexion. *Human Movement Science* 13, 129-141

REAL-TIME DISPLAY OF THE PRESSURE FIELD UNDER THE FOOT IN THE STANDING POSITION

*Galliot, P., **O'Driscoll, S., ***Pierre G., and *** Vauge C.
* SEMEV, Laboratoire de Biomécanique, 10 rue E. d'Orves, 94230 Cachan - France; ** Trainee from CORK Technical College (Ireland); *** Laboratoire d'Instrumentation Physique - Université Paris XII-Val de Marne - 94010 Créteil - France

INTRODUCTION

Using piezo-resistive sensors of the FSR type [Force Sensing Resistor/TM], we have built a prototype of a system for retrieving and processing values - taken at 16 points - of the under-foot pressure of a person standing immobile. This first project was intended to test new components, which are more convenient to use than the piezo-electric sensors previously used, and to develop multiplexing circuits and the data display algorithms. The results obtained were satisfactory and suggest that sole plates can be made for measuring the under-foot pressure field at, typically, 256 points under each foot of a moving subject, at appreciably less cost than with systems using piezo-electric sensors.

METHODS

The measuring rig is a square platform measuring 40 X 40 cm with sixteen measuring points arranged on a (4 X 4) rectangular mesh with a spacing of about 3 X 6 cm positioned under one foot of the subject standing immobile on the platform.The active component at each measurement point is an FSR sensor (made by INTERLINK, distributed in France by ALCYON) inserted between two sheets of synthetic rubber 1.5 mm thick and fitted with a thin, rigid cylindrical washer designed to convert the downward force into a pressure that is substantially uniform over the entire surface of the FSR which is circular and of the same diameter as the washer (approximately 15 mm).

The FSR sensors consist of two bonded sheets of polymer material, one carrying two arrays of interlinked electrodes, the other coated with a semiconducting polymer whose electrical resistivity is a decreasing function of the pressure exerted. Thus when no force is applied, the resistance measured between the electrodes is high (typically above 1 megohm). As the force increases, the resistance falls according to a polynomial law, which is reversible and observed over more than three decades. By connecting a fixed value resistance in series with each sensor, a divide circuit is produced for the potential difference (continuous, for example) applied to the electrodes, the output voltage from which can easily be used to indicate the force acting on the sensor, through a load-bearing device used to render the pressure uniform. The FSR sensors have a response time of about 2 ms and are insensitive to vibration and acoustic noise, unlike piezo-electric sensors.

In our system, the voltages supplied by the 16 voltage dividers are fed in turn to an analogue/digital conversion card through a multiplexer using CMOS circuits (HC 4051 of type 1 X 8), controlled by 3 logical variables provided by the card. The existing system can immediately be extended to 64

channels by suitable progamming, and ultimately to 256 channels simply by adding a second multiplexer.

The data acquisition card (a EUROSMART type PC-MES2) has 8 analogue inputs, 8 TTL logic inputs, 2 analogue outputs, 8 logic outputs and 3 counters. This is largely sufficient for our application , which uses only 2 analogue inputs (measurement signal and power reference) and 3 logic outputs (to control the multiplexer).

The FSR sensors operate at 10 V DC produced from the 220 V mains supply by a power pack mounted in the platform. The connecting leads to the sensors are all combined in a ribbon cable connected to the acquisition card, installed in a compatible 386 DX 33 PC. This initial version can only be used for making measurements on an immobile subject, but in principle there is no difficulty in adapting it to a moving subject by using a miniaturised microcomputer or an HF link between the subject and the computer.

RESULTS

Pressure data acquisition and processing software:

We have developed a computer program which makes it possible for the voltage values taken from each of the 16 sensors to be fed in turn to an A/D input of the acquisition card.The signals are routed in this way by the analogue multiplexer described above, controlled by a 3-letter logic word formulated by the program.

The card takes at least 25ms to convert one value. To process the data in real time as they are measured, while displaying the values on the computer screen, the program utilises two 2-dimensional tables, one of which loads, at time t, the values measured on the 16 sensors, and then transfers them at time (t+ 55ms) approximately into a second table serving the display program, the display persisting throughout the next sequence of data acquisition.

The data are stored continuously in a zone of the hard disk. When this is full, the program initiates data transfer to a diskette previously inserted in the external drive and thus frees the hard disk for a new cycle.

The under-foot pressures were shown on a 2-dimensional histogram assumed to be seen in perspective from the subject's point of view (an axial view looking down at about 60°). This representation seemed to us to be very vivid, but it can easily be modified.

CONCLUSION

We have built a complete prototype of a system which can measure, using FSR sensors, and display the pressure field at 16 points under the foot of a standing immobile subject.

A mass production version of this system could have applications in routine foot inspection, in view of its low cost. In a mobile version, for example with 256 measurement points per foot, it could constitute a simple tool for the functional investigation of walking or running, for orthopaedic use or for training on foot or mounted on a horse.

ANTERIOR TRANSLATION OF THE HUMERAL HEAD DURING ANTEFLEXION AGAINST RESISTANCE OF THE UPPER LIMB

*Galliot, P., *Lécuyer, Ph., *Dantin, F., **Benzaïd, M.N.
* SEMEV, Laboratoire de Biomécanique, 10 rue E. d'Orves, 94230 Cachan, France; ** Hôpital de Lagny, Service de Radiologie, Lagny, France

INTRODUCTION

Different authors have studied the humeral head excursion towards the glenoid cavity with the use of roentgenoraphic technics. Howell et Al. worked on the humeral excursion within the horizontal plane of the movement, whereas Poppen and Walker did it within the scapular plane.
We chose to observe the humeral head excursion during the initial phase of anterior elevation against resistance. During nearly all the usual movements, the arm is located ahead of the frontal plane, in aim to direct the hands in the visual field. And so, the humeral head is submitted to muscular forces of anterior traction.
This preliminary study points out that during this initial phase of anteflexion, the humeral head describes a physiological anterior translation on a 2 mm distance within the horizontal plane of analysis.

METHODS

The measurement of the translations was done on roentgenograms. Two points were determined to identify the humeral head and two points for the glenoid cavity. Then the gap between the two sequences was assessed, from the initial relaxed position to the second acting position.

Roentgenographic Technique:

The anterior translation of the humeral head on the glenoid cavity is well readable in the horizontal plane: the horizontal plane allows to outline at the same time the glenoid cavity, the joint space and the humeral head.
A review of radiological literature could not find out an appropriate view.
The realisation of an acute roentgenogram has to consider constraints brought by radiological technics to avoid superimposition of different structures; the direction of the incident x-ray beam must lead to a deformation of anatomical shapes as small as possible. So the incident beam has been chosen to be directed caudad to cephalad and the x-ray source was located under the axillar fossa.
The film cassette was horizontally fixed up, on top of the x-rayed shoulder.

Data collection and analysis:

Ten subjects were volontary for this experiment, with no prior history of shoulder pain or acute trauma.
The x-rayed subject was sitting with arm placed in 30° abduction; the fore-arm was laying on a table, the hand holding a vertical fixed rod.
The first plate was taken while the subject was completely motionless, and the upper limb muscles were relaxed.
The second roentgenogram was taken in the same conditions, with the subject pushing on the fixed rod and so realizing an anteflexion against resistance; the trunk must stay motionless.

RESULTS

The first roentgenogram gived the reference frame for the glenoid cavity and the humeral head. The second roentgenogram gived the measure of the humeral head excursion during the anteflexion opposite to resistance, that recruits the pectoralis major muscle. The average anterior translation was 2 mm .

These translations are allowed by the small concavity of the glenoid cavity, by the organization of the fiber bundles in the glenohumeral capsulo-ligamentous apparatus and by the binding muscles relaxed state for the position of the subject during the experiment.

DISCUSSION

This experiment maked possible the study of the cinematics of the glenohumeral joint in vivo. In spite of the limits given by the radiological process that we used, it gived an approach to physiological conditions of the glenohumeral joint working.

Our own process has to be validated by using it on most important series.

It can contribute to improve the analysis of the glenohumeral anterior instability by defining the standard situation and therefore by calculating the pathological anterior translations that could indicate damages to the shoulder anterior system of stabilization.

By this way, it may complete the Leclerc sequence that is useful to estimate the efficiency of the superior system of stabilization.

CONCLUSION

The elaboration of a new radiological view in the horizontal plane and its use in a dynamic way show the possibility for translations to occur during the anterior elevation for the healthy glenohumeral head in vivo.

The further study will permit to extend this pilot experiment to more subjects without prior trauma or shoulder pain and then to define average values for physiological anterior translations. This could serve as a basis for evaluation of dynamic anterior instabilities of the glenohumeral joint.

REFERENCES

1. Howell, S. M., Galinat, B. J., Renzi, A. J., and Marone P. J.: Normal and Abnormal Mechanics of the Glenohumeral Joint in the Horizontal Plane. J. Bone Joint Surg., 1988, 70-A, N°2, 227-232.
2. Matsen, F., Lippitt S., Iserin A.: Mécanismes patho-anatomiques de l'instabilité gléno-humérale. In "Instabilité chronique de l'épaule", SOFCOT p7-13, ESF, 1994.
3. Poppen N. K. and Walker P. S.: Forces at the Glenohumeral Joint in Abduction. Clinical Orthopaedics and Related Research, 1978, N°135,165-170.
4. Poppen N. K. and Walker P. S.: Normal and Abnormal Motion of the Shoulder. J. Bone Joint Surg., 1976, 58-A, N°2, 195-201.
5. Sintzoff, S.: Imagerie de l'épaule. Masson, 1992.
6. Turkel, S.J., Panio, M.W., Marshall, J.L., Girgis, F.G.: Stabilizing mechanisms preventing anterior dislocation of the glenohumeral joint. J. Bone Joint Surg., 1981, 63-A, 1208.

DISTRIBUTION PROBLEMS AT LUMBAR JOINT L_5/S_1 - AN OPTIMIZATION METHOD COMBINED WITH EMG-BASED SWITCH TECHNIQUE

Jie Gao, Gert-Peter Brüggemann
German Sport University Cologne, Germany

INTRODUCTION

Considerable work has been directed towards an understanding of low back pain and spine injuries. The understanding of the injury mechanism is a prerequisite to reduce individual risk and improve the load induced by work. To estimate the mechanical load on the lumbar spine and specifically on vertebra and disc biomechanical models have been used. To solve the indeterminate problem distributing the external forces and moments to the biological structures, two basic approaches can be differentiated: optimization techniques (e.g. Schultz et al., 1983) and EMG assisted models (e.g. McGill and Norman, 1986).

The purpose of this study is to develop and apply a model of the lumbar spine in order to estimate the spinal load at the joint L_5/S_1 using an optimization method combined with EMG-based switch techniques.

MODELS AND METHODS

To reduce the complexity of the problem, a simplified model of the spine is used. It is assumed that the trunk consists of three rigid segments, the pelvis segment, the lumbar segment L_1-L_5 and the thoraco and cervical segment C_1-Th_{12}. The three rotational angles of each segment are chosen as generalized coordinates.

In a first step the resultant force and moment at L_5/S_1 were determined using inverse dynamics of a multibody system. In a second step this resultant force and moment must be distributed to the internal structures. Generally, the forces in the muscles and ligaments and on the articular surfaces related to the intersegmental resultant force and moment are given by the following equations:

$$\boldsymbol{F} = \Sigma \boldsymbol{f}_i^m + \Sigma \boldsymbol{f}_i^l + \Sigma \boldsymbol{f}_i^c,$$
$$\boldsymbol{M} = \Sigma \boldsymbol{r}_i^m \times \boldsymbol{f}_i^m + \Sigma \boldsymbol{r}_i^l \times \boldsymbol{f}_i^l + \Sigma \boldsymbol{r}_i^c \times \boldsymbol{f}_i^c, \quad (1)$$

where the vectors $\boldsymbol{F}$, $\boldsymbol{M}$ are the intersegmental resultant force and moment, respectively, defined at the joint center J (any arbitrary location within the joint); the vectors $\boldsymbol{f}_i^m$, $\boldsymbol{f}_i^l$, $\boldsymbol{f}_i^c$ are the forces in the ith muscle and ligament and on the articular surface contact region, respectively, with their lever vectors $\boldsymbol{r}_i^m$, $\boldsymbol{r}_i^l$, $\boldsymbol{r}_i^c$, $\times$ denotes the vector (cross) product.

For such a system there is an infinite number of possible solutions for the unknowns. To solve this problem, the number of the unknown forces in the equations (1) must be reduced. It is assumed that: (a) the influence of ligaments is neglected; (b) minor muscles are omitted; (c) the contact forces are summed up to one resultant force; the action line of this contact force is further assumed to go through the disc center. Thus, the equations (1) can be presented in the form:

$$\boldsymbol{F} = \Sigma \boldsymbol{f}_i^m + \boldsymbol{f}^c,$$
$$\boldsymbol{M} = \Sigma \boldsymbol{r}_i^m \times \boldsymbol{f}_i^m. \quad (2)$$

In order to get a reasonable reduction of muscle forces, EMG data were used to reduce the number of unknowns. EMG signals (rectus abdominus, oblique externus, erector spinae and latissimus dorsi) were applied to determine muscle activities. A muscle activity below a given threshold indicated that for this period of time the muscle was assumed to be inactive and therefore was switched off in the mathematical model.

If the number of the unknown forces after this simplification process is still greater than the number of the equations, the system is an indeterminate system with a reduced order. One method to solve this problem is to find an optimum solution. The optimization criterion is the minimization of quadratic summation of all muscle stresses which are defined as individual muscle forces divided by their physiological cross-sectional area.

APPLICATIONS

Several experiments were carried out under laboratory conditions. Six video cameras were used to measure the movement of the subject (height: 1.78 m, weight: 74 kg). The movements were analyzed with the Motion Analysis System operating at 60 Hz. EMG was collected simultaneously at a frequency of 2000 Hz.

The subject carried out the following movements: (1) flexion forwards about 90°; (2) extension backwards; (3) lifting a weight of 6 kg from the front with straight knees; (4) lifting a weight of 6 kg from the front with bent knees.

RESULTS AND CONCLUSIONS

The experimental results showed a very good correlation of EMG signals with calculated muscle forces. EMG signals of different muscle groups, the muscle and artificial contact forces calculated using this method are given in Fig. 1 and 2 for the movement (2). The muscle activities were divided into three intervals according to the EMG signals. Using this method we also analyzed two simple lifting techniques. From the results we may conclude: keeping the trunk as erect as possible, bending the knees could be the better lifting technique. It can reduce some back muscle force to lift the similar weight without increasing the compressive load on the articular contact surface. In other words, using the same muscle forces we can lift heavier objects with the second technique (movement (4)) than with the first technique (movement (3)).

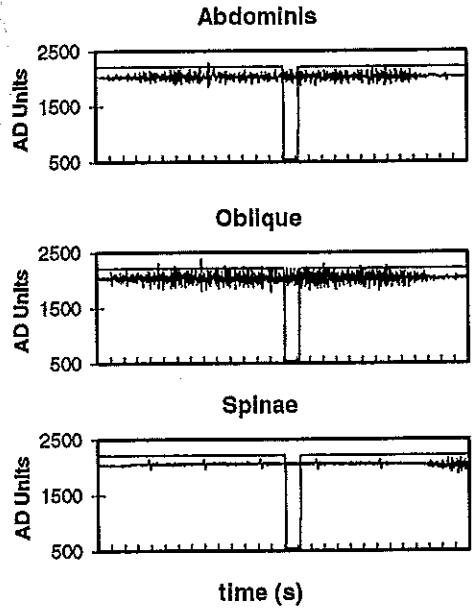

Fig. 1 EMG data for different muscles

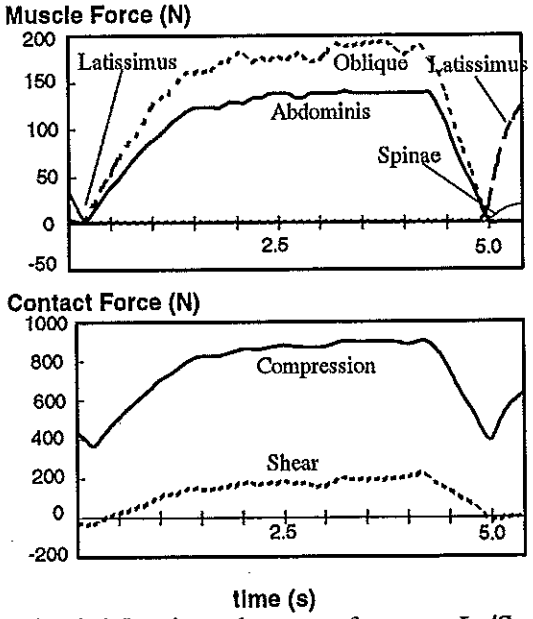

Fig. 2 Muscle and contact forces at L_5/S_1

LITERATURE

Crowninshield, R.D. and Brand, R.A. (1981): The Prediction of Forces in Joint Structures: Distribution of Intersegmental Resultants. *Exercise and Sport Sciences Reviews,* Vol. 9, 159-181.

McGill, S.M. and Norman, R.W. (1986): Partitioning of the L_4/L_5 dynamic moment into disc, ligamentous and muscular components during lifting. *Spine* 11, 666-678.

Pope, M.H. and Novotny, J.E. (1993): Spinal Biomechanics. *Journal of Biomechanical Engineering,* 115, Nov, 569-574.

Schultz, A. B., Haderspeck, K., Warwick, D. and Portillo, D. (1983): Use of lumbar trunk muscles in isometric performance of mechanically complex standing tasks. *J. orthop. Res.* 1, 77-91..

COMPARISON OF TORQUE AND ELECTROMYOGRAPHY OF ELBOW FLEXORS OBTAINED AT 9:00 A.M AND 6:00 P.M.

A. GAUTHIER, D. DAVENNE, A. MARTIN, G.COMETTI and J. VAN HOECKE
Groupe Analyse du Mouvement, Université de Bourgogne, Dijon, France.

INTRODUCTION

It is commonly accepted that, with sports and athletics, performance undergoes circadian rhythms. Such variations clearly result from established alterations of the basic elements of performance : heart rate, level of arousal and bioenergetics (for review, see Winget et al., 1985). A circadian rhythm in muscular strength during isometric contractions of short duration has been shown but was not very well documented. It is assumed that the trough and the peak were measured at the early the morning and the end of the afternoon.

For futher informations, at this extremes of the circadian rhythm (i.e 9:00 a.m and 18:00 p.m), electromyographic signal of elbow flexors were recorded during isometric contractions performed at 90°elbow flexion angle on an isokinetic dynamometer.

METHODS

Subjects : Twelve physical education students, 6 males and 6 females (mean ±SE ; age : 22.1 years ±0.4 ; height : 174.8 cm ±2.7 ; weight : 67.5 kg ±2), volunteered to take part in the study.

The subjects were classified as "moderately morning types" (n=4), "moderately evening types (n=1) or "neither type" (n=7), based on their responses to the self-assessment questionnaire of Horne and Östberg (1976) to determine morningness-eveningness. They had to cut their physical activity during the day of experiment.

Experimental procedures : 2 test sessions were obtained at 9:00 a.m and 6:00 p.m. The interval of 9 hours was fixed to allow full recovering between the 2 test sessions. The order of the 2 test sessions was randomly assigned for each pair of subjects. Each these sessions started by a rest period during which the subject was kept lying down for 30 min and oral temperature was assessed. Then, the electromyography activity and the isometric torque of the elbow flexor measured. During the whole experiment, the laboratory temperature was kept to 19 ±0.5°C.

Biomechanical tets were carried out using an isokinetic dynamometer (Biodex : Biodex Shirley corporation, NY, USA). The subject carried out 3 maximal isometric voluntary contractions (MVC) of 6 sec at 90° elbow flexion angle (0° corresponding to full elbow extension). A rest of 2 min was allowed between each trial.

Electromyography (EMG) recordings of the non-dominant arm were made using two pairs of silver silver-chloride surface electrodes. They were positionned on the belly of the biceps muscle. The surface electrodes remained applied during the 24 hr. The myoelectrical signal was amplified with a bandwidth frequency ranging from 1.5 Hz to 2 kHz. The amplitude activity as Root Mean Square (RMS) was calculated under isometric conditions over a 1 sec period when the torque was constant. Torque, angular position and EMG signals were digitized on line (sampling frequency 1000 Hz) using a digital computer (AT 386).

Statistics : Morning and afternoon results were compared using a repeated-measures analysis of variance (ANOVA). A significance level of 0.05 was used in all analysis. All results are provided as mean ±SE

RESULTS AND DISCUSSION

Results of the test sessions are presented in Table 1. Statistical analysis revealed significant differences between the morning and afternoon mean scores for oral temperature and for the torque of the efbow flexors in isometric condition. However, ANOVA did not reveal differences between the morning and afternoon mean scores for the RMS values. The torque of the elbow flexors was 8,3% greater ($p<0.05$) for the afternoon test session compared to the morning one. Oral temperature was also greater during the afternoon test session compared to the morning one.

	Morning (9:00 a.m)		Afternoon (6:00 p.m)		9:00 a.m v.s 6:00 p.m
	Mean	SE	Mean	SE	
Temperature (°C)	36,33	0,09	36,52	0,07	p = 0,035
Torque (%)	90,13	1,98	97,63	1,09	p = 0,0005
RMS (%)	86,40	4,15	79,34	4,04	p = 0,19

Table 1 : Results of morning (9:00 a.m) and afternoon (6:00 p.m) of oral temperature, torque and RMS.

Temperature is an excellent chronobiological marker (Horne and Östberg, 1976). Coldwells et al. (1994) ascribe the differences of the torque to temperature changes because temperature is minimal when the torque is minimal and maximal when the torque is maximal. Similarly, we observe that in our recordings, temperature and torque vary concomitantly and the question arise, if there are a direct causal link between the two parameters. Different authors (Bergh et al.1979, Petrofsky and Lind 1980) studied the maximal strength at different muscle temperatures varying from 28°C to 39°C. Their results prove that the isometric strength is not affected or very slightly by these variations. So that it seems very unlikely that, in the course of our experiment, the torque could be modified because of observed range of temperature changes.

The torque developed at 9:00 a.m might be lower than the one developed at 6:00 p.m because the coactivation of the antagonists might be more important at 6:00 p.m, so that the torque obtained after contracting the agonists is greater. Another possible way to explain the variations of the torque can be found at muscle command level. On the one hand, analysis of variance, when applied to the RMS recorded did not show significant differences, so during our experiment, the muscular control remained unchanged for the 2 test sessions. On the other hand, the maximal torque developed by the elbow flexors at 6:00 p.m was significantly higher than the 9:00 a.m values. Thus, after these results, we can conclude that the neuromuscular efficiency is consequently higher at 6:00 p.m. Factors which might be involved in this variations are : enzymatic activities, ATP and calcium supply, as much they are the main limited factors of the muscular contractions.

REFERENCES

Winget, C.M., DeRoshia, C. W. and Holley, D. C., (1985). Circadian rhythms and athletic performance. *Med. Sci. Sports Exerc.*, **17**, 498-516.

Horne, J.A. and Östberg, O. (1976). A self-assessment questionnaire to determine morningness-eveningness in human circadian rhythms. *Inter J Chronobiol*, **4**, 97-110.

Coldwells, A., Atkinson, G. and Reilly T. (1994). Source of variation in back and leg dynamometry. *Ergonomics* **37**, 79-86.

Bergh, U. and Ekblom, B. (1979). Influence of muscle temperature on maximal muscle strength and power output in human skeletal muscles. *Acta Physiol Scand*, **107**, 33-37.

Petrofsky, J.S. and Lind, A.R. (1980). The influence of temperature on the amplitude and frequency components of the EMG during brief and sustained isometric contractions. *Eur J Appl Physiol*, **44**, 189-200.

FATIGUE-INDUCED KINEMATICS STRIDE MODIFICATION DURING ALL-OUT TEST AT 100 % SPEED AT VO_2 MAX IN 12 ELITE RUNNERS.

F. Gazeau*, V. Billat** et J.P. Blanchi*
* EA 597, Uni. J. Fourier, BP 53X - 38041 Grenoble Cedex - FRANCE
** Unité 296 INSERM Paris XII, 61 avenue Général de Gaulle 94100 Créteil FRANCE

I) INTRODUCTION :

A recent paper (Billat et al., 1994a) had showed the reproductibility but the great variability between subelite long-distance runners of their time to exhaustion at the velocity which elicits VO2 max and called the maximal aerobic speed (MAS). The present study wanted to go deeper in the reason of this large difference between runners having the same VO2 max. The question was to know if the kinematics modifications registred the all-out test was more or less important for athletes having the longest time to exhaustion at MAS. This study focused on the difference between the right and left side of the stride.

II) METHODS :

The study was conducted on 12 elite male distance runners : their age, body mass, height, VO2 max and MAS were : 25 ± 3 years, 69 ± 8 kg, 177 ± 6 cm, 75.5 ± 4.9 $ml.min^{-1}.kg^{-1}$, 22,4 ± 0,9 $km.h^{-1}$ (mean ± SD). The VO2 max and MAS were measured in a preliminary test session using a progressive exercice protocol on treadmill. Tlim was then measured on treadmill at one week's of interval. Following a 15-min warm-up period at 60 % of MAS the speed was quickly increased (less than 20 s) up to the MAS, the runners beeing verbaly encouraged to run untill exhaustion. Runners were filmed during the tlim test at MAS with a 200 HZ frequency (NAC HSV 400).

Kinematics stride variables : support and recovery phase (RP) time and amplitude were compared at the first 30 s of the tlim test and the last 8 s before the runner's surrender (ANOVA test for repeated measure).

III) RESULTS :

The time limit mean value was equal to 5:42 ± 1:08 (min:sec). It could be observed significant increases of amplitude and support time during the all-out test at MAS (table I, + 2.14 and 3.19 % respectively). This results are in accordance with Williams and al. (1988) who have reported a significant increase of the stride amplitude at the end of a race performed at a constant speed (the % of MAS is not specified) However kinematics variables variations during the tlim test were not significantly correlated with tlim (r=0,44; p>0,05).

Subj. n°	Evolution of amplitude with fatigue (%)			Evolution of contact time with fatigue (%)			Evolution of RP time with fatigue (%)		
	LEFT side	RIGHT side	BOTH side	LEFT side	RIGHT side	BOTH side	LEFT side	RIGHT side	BOTH side
1	-0,8 N.S.	3,75 S.	**1,47 N.S.**	10,15 S.	8,52 S.	**9,34 S**	-1,66 N.S.	-0,55 N.S.	**-1,11 N.S.**
2	0 N.S	0 N.S.	**0 N.S**	8,45 S.	9,16 S.	**8,8 S.**	-3,23 S.	-3,92 S.	**-3,57 S.**
3	5,44 S.	7,05 S.	**6,24 S.**	7,87 S.	3,94 T.	**5,9 S.**	5,6 S.	7,08 S.	**6,34 S.**
4	2,83 N.S.	5,86 S.	**4,34 S.**	1,41 N.S.	4,38 T.	**2,89 N.S.**	5,52 S.	3,13 S	**4,33 S.**
5	3,07 S.	-3,44 N.S.	**-0,18 N.S.**	7,58 S.	2,1 N.S.	**4,84 S.**	-3,19 S.	-1,05 N.S.	**-2,12 S.**
6	0,6 N.S.	0,41 N.S.	**0,5 N.S.**	4,58 S.	4,9 S.	**4,74 S.**	-0,96 N.S.	-1,24 N.S.	**-1,1 N.S.**

7	3,29 S.	3,61 S.	**3,45 S.**	0,92 N.S.	1,65 N.S.	**1,29 N.S.**	4,63 S.	3,21 S.	**3,92 S.**
8	1,23 N.S.	4,06 S.	**2,64 S.**	-1,03 N.S.	2,59 N.S.	**0,78 N.S.**	4,2 S.	2,48 S.	**3,34 S.**
9	2,57 S.	5,3 S.	**3,94 S.**	3,1 S.	2,53 N.S.	**2,82 S.**	4,26 S.	4,76 S.	**4,51 S.**
10	3,92 S.	4,8 S.	**4,36 S.**	2,13 N.S.	4,83 S.	**3,48 S.**	5,22 S.	4,45 S.	**4,84 S.**
11	-3,18 S.	1,88 N.S.	**-0,64 N.S.**	-5,3 S.	1,44 N.S.	**-1,93 N.S.**	1,00 N.S.	-1,22 N.S.	**-0,11 N.S.**
12	-3,6 N.S.	2,79 N.S.	**-0,4 N.S.**	-8,68 S.	-0,66 N.S.	**-4,67 S.**	2,81 S.	-0,75 N.S.	**1,03 N.S.**
Total	1,28 N.S.	3,00 S.	**2,14 S.**	2,60 N.S.	3,78 S.	**3,19 S.**	2,01 N.S.	1,36 N.S.	**1,69 N.S.**

Table 1 : S : $p<0.05$, NS : $p>0.1$, T : $0.1<p<0.05$

IV) DISCUSSION :

Individual adaptations have to be considered, eventhough more of the runners increase their support and decrease their RP durations with fatigue (Table 1). Further studies are necessary to understand the physiological background of modification with an electromyographic study of the lower limb extensors and hip flexors and extensors during this time limit test.

V) REFERENCES :

Billat, V., Pinoteau J., Petit B., Renoux J.C., Koralsztein J.P. (1994 a).Reproductibility of running time to exhaustion at VO2 max in sub-elite runners. Med. Sci. Sports and Exercice., **26**, 254-257

Williams, K.R., Snow, R., Agruss, C. (1988). Changes in distance running kinematics with fatigue. Med. and Sci. in Sports and Exerc., **20**, 138-162

THE TACTICAL BATON

P.L. Gervais and J.P. Baudin

Faculty of Physical Education and Recreation, University of Alberta

Edmonton, Canada

INTRODUCTION

It has been proposed that the Tactical or extendable Baton could be an attractive functional alternative to the duty baton that is currently being used by the majority of law enforcement officials. A primary justification for the adoption of the Tactical Baton is that this less conspicuous intermediate weapon will be carried more frequently by the law enforcement professions thus providing greater protection to the professional and potentially less risk to the law breaking individual(s) and the public by reducing the possible use of a firearm. It has also been suggested by the manufactures and members of the local law enforcement agencies that the Tactical Baton, being lighter and better balanced than traditional batons is, a more manageable device to yield thus making it more suitable perhaps to smaller, less physically robust officers. Given that the traditional duty baton is the most accepted impact weapon used by law enforcement agencies, the purpose of this study was to compare the movement patterns and impact characteristics between the traditional duty baton and various tactical batons.

To effectively control or stop an assailant's hostilities the impacting device, the baton, must be swung to strike with a large force achieved through a fast delivery. In karate, Walker (1975) proposed that the objective of a strike was to maximize the deformation damage at the area of contact. Mechanically this relates to 1) the amount of energy lost to deformation (or the work done) during the impact, and to 2) the impact forces and stresses imposed. As described by Walker, the work done during the impact is dependent on the coefficient of restitution (where the strike occurs), the contacting masses, and the velocity of the colliding objects. From the perceived objective of defense and disabling an attacker, how the baton is swung (speed), where an individual is struck and with how much force and pressure will determine the overall effectiveness of a strike or series of strikes with a baton.

METHODS

Three ASP (Armament Systems and Procedures, Inc) tactical batons (40.6cm[16"], 53.3cm[24"], 66cm[26"]) made of aerospace grade steel alloy, a 61cm aluminum side handle baton and a traditional 66cm wooden baton were compared to the standard issue traditional duty baton (made of PVC material , 66cm in length). Four skilled subjects (2 males, 2 females) from the Edmonton Police Service and University of Alberta's Campus Security volunteered to participate in this study. An impact swing and two practice/training movement sequences were analyzed for this study. For the impact swing subjects were asked to swing and strike a force measuring device, consisting of a contact surface welded to a plunger which contacted a piezoelectric force transducer. Two trials, at maximum voluntary impact swing, for each baton were sampled at 5000 Hz. The Forehand and Forehand/Backhand swings were video taped using 2 SVHS recorders. The video data were subsequently digitized at 60 Hz and the 3 dimensional spatial location of the upper body joint centres and the baton were found using the DLT. Data were smoothed using a quintic spline.

RESULTS AND DISCUSSION

The three APS Tactical batons, the side handle baton and wood duty baton all

produced smaller impact forces when compared to what was achieved with the PVC duty ba' on (Figure 1). For the purposes of illustration and comparison we modelled the

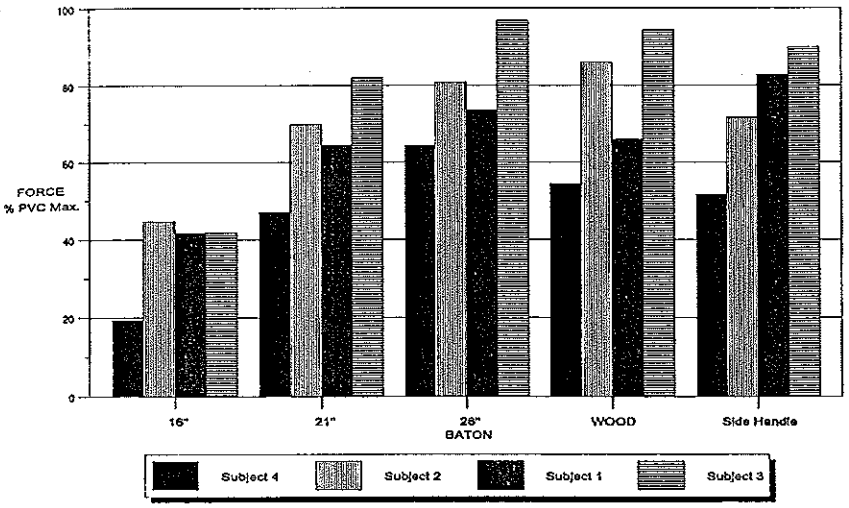

Fig. 1 AVERAGE PEAK IMPACT FORCES. Values expressed as a percent of the subject's maximum impact force with the PVC baton.

impact pressure by suggesting a contact area in which the baton could compress soft tissue to ½ it's diameter over a contact length of 6 cm. This would result in the following expression for pressure: **Peak Pressure** = Peak Impact Force X Contact Area

where: Contact Area = 6 cm x ½ (2π x radius of the baton at contact).

The extendable batons produced on average higher impact peak pressures than those produced with the PVC baton. The impact pressures ranged from approximately 50% to 135%, 110% to 230%, and 125% to 275% of the PVC maximum for the 40.6cm, 53.3cm and 66cm extendable tactical batons respectively. The recorded impact forces and pressure values, would in most likelihood far exceed the impact loads that could be generated in the field during an actual confrontation with an assailant. In addition to these considerations the amount of mechanical work done on the assailant, which dictates the resulting stresses, is dependent on the material or tissue struck. A large muscle group which is fully contracted will experience far less trauma than if the same blow were delivered to an area with little muscle or adipose tissue over the bone.

The physical characteristics of the tactical batons are different from those of the standard issue PVC duty baton. The movement patterns for two baton training skills were also investigated to determine the possible influence these physical differences may have on the use of the batons. The officers in this study tended to swing all the other batons faster than the PVC baton for forehand strikes. The officers also had greater strike frequencies when swinging the 40.6cm tactical baton. Another factor that may also influence the officer's safety is their proximity to the opponent in order to deliver a maximal blow or a series of blows. The 66cm extendable baton afforded the greatest reach and the 40.6cm extendable baton the least. The 53.3cm extendable, PVC and Wooden baton differed between 1 cm and 5 cm with respect to reach.

In summary, a large number of interdependent factors which relate to the effective and appropriate use of these intermediate weapons must be considered in their evaluation. In light of their intended use, no single factor can conclusively dictate a baton's superiority over another with respect to the inherent risks or effectiveness.

REFERENCES

Walker, J.D. (1975). Karate strikes. *Am J Physics.* Vol. 43. Oct. p. 845.

CORRELATIONS, ASYMMETRIES AND NORMALIZING FACTORS FOR SPATIAL-TEMPORAL MEASUREMENTS OF GAIT

C. Giacomozzi, V. Macellari, R. Saggini*

Biomedical Engineering Laboratory, Istituto Superiore di Sanità, Rome, Italy
*Dipartimento di Medicina dello Sport, University G. D'Annunzio, Chieti, Italy

INTRODUCTION

Human gait can be investigated by means of a variety of instruments, from simple foot switches to sophisticated optoelectronic systems. A great amount of parameters of gait, spatial and temporal, can be measured and used as basic information for the functional assessment of the locomotor system.

A large pressure platform developed at the authors' laboratory (A. Lo Verde et al., 1991) has been used to collect data from about 600 healthy subjects aged 3-80 (C. Giacomozzi, V. Macellari, R. Saggini, 1993). Software procedures were implemented which: i) reduce, as much as possible, artifacts and errors resulting from the natural variability of gait and from the technical characteristics of the instrument; ii) find correlations among the measured parameters so as to reduce redundant measurements, and emphasize the most relevant ones; iii) detect normalizing factors in order to standardise the parameters of the gait, and make them independent from the physical characteristics of each subject, an essential factor when comparing data from subjects of different age, sex, etc; iv) reveal the asymmetries between the left side and the right side of the human body, typical of gait even in healthy subjects.The final aim was to obtain normative data to which make reference for the assessment of pathologies of gait.

METHODS

The large size of the pressure platform allows the simultaneous acquisition of at least three complete steps. Each subject was asked to walk on the platform forward and backward three times at his/her natural speed and thus at least eighteen steps were acquired (C. Giacomozzi, V. Macellari, R. Saggini, 1993). For each subject the protocol was applied twice, first with the subject barefoot and then shod.

Spatial and temporal parameters were arithmetically averaged in order to minimize two contributions to the standard deviation: the natural variability of gait, and the quantization error of the instrument. Quantization for spatial and temporal measurements is 0.5 cm and 15 ms, respectively. Normal distribution of data related to the single subject was verified by means of the chi-square test.

Mean values were collected into four groups: females (n. 266): a) barefoot, b) shod; males (n. 330): c) barefoot, d) shod.

The parameters of Grieve's equations were calculated iteratively for each group. The equations were applied according to the formulation reported in S. Hirokawa, 1989.

Correlations among the measured parameters were investigated by evaluating Pearson's coefficient related to each couple of parameters. Linear and squared regression models were applied to correctly normalize the parameters of gait with respect to the physical characteristics of each subject.

Asymmetries were investigated by means of the paired Student's t-test, Pearson's coefficient of correlation, and by evaluating symmetry indexes as reported in literature (S. Hirokawa, 1989; E.Y. Chao et al., 1983). Two different criteria were followed: i) evaluation of asymmetries between the left side and the right side of the human body, in which case the groups of samples to be compared were the sum of the values for the left and for the right; ii) evaluation of side dominance where, for each subject, the ratio between the smaller and the larger value is calculated. In this way, there is no compensation due to the different behaviours of the subjects. The symmetry index for each parameter consists in the mean value of all the ratios.

RESULTS

Grieve's equations of gait.

The 1st Grieve's equation was applied to the four groups in the form $f = a*(V')\text{^}b$, where f is the cadence, expressed in stride/min, and V' is the ratio between the mean velocity and the subject's height, expressed in s^{-1}.The iterative method converged within maximum 8 iterations; values for a ranged from 64.910 to 70.876, while values for b ranged from 0.553 to 0.772.

The 2nd Grieve's equation was applied in the form $t_s = a * T + b$, where t_s is the stance phase, expressed in s, and T is the cycle time expressed in s. The iterative method converged within maximum 8 iterations; values for a ranged from 0.668 to 0.699, while values for b ranged from -0.080 to -0.55.

Correlation indexes.

Absolute values of Pearson's coefficient greater than 0.950 have been found - both for males and females walking barefoot - for the following couples of parameters: height - leg length; footprint length - foot length; stride - step; gait cycle - stance phase. The correlation is weaker between footprint length and foot length for shod females. A high correlation between footprint length and leg length has been found only for shod males.

Linear and squared regression models.

Linear regression models with respect to height fit most spatial parameters well - except for toe-out angle, contact area, footprint width and stride breadth - and partially fit the stance phase and the swing phase. The stance, swing, and double support phases showed slight linear trends when referred to velocity. Squared relations were found between body mass and stride, and between body mass and the body segment lengths considered. Linear regression models fit the contact area well, and the stance phase partially.

Asymmetries.

Comparison between the left side and the right side. The symmetry index was never significantly different from 1.000, mainly due to the compensation among subjects. The paired Student's t-test revealed significant differences ($p < 0.05$) between the mean values of the left and right toe-out angle, both for males and females, barefoot and shod. Significant differences were also found with respect to: footprint width only for barefoot females; stride breadth only for barefoot males; stance phase only for shod females.

Comparison between the smaller and the greater value of each parameter.

Particularly interesting, in this case, are the values obtained for the symmetry indexes. The following example refers to females walking barefoot.

symmetry indexes

footprint length	footprint width	contact area	toe-out angle	step	stride breadth	stance phase	swing phase	double support phase
0.985	0.963	0.926	0.670	0.973	0.969	0.981	0.970	0.919

DISCUSSION

Of all spatial parameters, only toe-out angle and stride breadth did not correlate to the other parameters of gait. Toe-out angle showed a great asymmetry that must be taken into account when investigating the pathologies of gait. The remaining spatial parameters were correlated to the physical characteristics of the subject, according to coefficients which vary with respect to sex and to subject condition (barefoot or shod). A good standardisation for the step can be obtained by normalizing it with respect to stride.

Among the temporal parameters, the stance and swing phases can be satisfactorily standardised by normalizing them with respect to the gait cycle. The double support phase turned out to be a parameter of interest because of its greater independence from the other characteristics of gait.

Great attention must be paid to the effect of shoes on gait. As an example, all the symmetry indexes but for toe-out angle improved when walking with shoes, and the standard deviations of most parameters diminished.

REFERENCES

Lo Verde A., Macellari M. (1991) Footprint averaging in a detecting platform system. *Proceedings of the XIIIth International Congress on Biomechanics, 444-446.*

Giacomozzi C., Macellari V. and Saggini R. (1993) Normative data of distance-temporal parameters of gait. *Biomechanics - XIV ISB Congress - Paris, July 4-8.*

Hirokawa S. (1989) Normal gait characteristics under temporal and distance constraints. *J. Biomed. Eng., Vol.11, November, 449-456.*

Chao E.Y., Laughman R.K., Schneider E. and Stauffer R.N. (1983) Normative data of knee joint motion and ground reaction forces in adult level walking. *J. Biomechanics, Vol.16, No.3, 219-233.*

COMPARISON OF GROUND REACTION FORCE MEASUREMENTS BETWEEN NORMAL AND SCOLIOTIC GAIT USING TIME AND FREQUENCY DOMAIN ANALYSIS.

Giakas G., and Baltzopoulos V.

Department of Movement Science, University of Liverpool, Liverpool, UK

INTRODUCTION

Gait is an important factor for the aetiology of idiopathic scoliosis (Sutherland *et al.*, 1980), but there is only a limited number of gait studies in idiopathic scoliosis. The purpose of this study was therefore to examine time and frequency domain ground reaction force (GRF) parameters in scoliotic children, control children and adults. The inter- and intra- subject coefficient of variation (CV) (Parker *et al.*, 1993), and bilateral symmetry using a symmetry index, were also examined.

METHODS

Twenty male adults and 20 female adolescents without any known injury or disease affecting their gait, and 20 adolescent females with idiopathic scoliosis, participated as the control children (CC), control adults (CA) and scoliotic (SC) groups respectively. An AMTI multi component force platform system, sampling at 500Hz, was used to record the vertical (Z), anterior-posterior (Y) and medial-lateral (X) force axis data.

Ten successful trials with the left and right side were collected and their mean was calculated in order to reduce variability problems according to (Hamill and McNiven, 1990). Seven force parameters were used to examine GRF in the time domain. The highest frequency contained in the 95% of signal power was chosen as the criterion to represent frequency content.

RESULTS

Statistical analysis showed no significant differences ($p>0.05$) in all GRF force parameters between all groups. Equivalent results were calculated for the intra-subject CV and bilateral asymmetry. The inter-subject CV of the SC group was significantly higher ($p<0.05$) than the CC group and this was significantly higher than the CA group in all force parameters (Figure 1).

The frequency content and the associated inter-subject variability and asymmetry of the CA and CC groups were similar. The only difference ($p<0.05$) was the inter- and intra-subject CV in the Y and inter-subject CV in the Z components. These parameters were significantly higher in the CC compared to CA group (Figure 2).

The SC group exhibited significantly higher ($p<0.05$) frequency content (Table 1), inter- and intra-subject CV and asymmetry in the X; inter- and intra-subject CV in the Y; and inter-subject CV in the Z components compared to the other two groups (see also Figure 2).

Group	X		Y		Z	
	L	R	L	R	L	R
CA	24,53	24,57	17,35	16,31	18,61	19,49
CC	24,42	22,96	15,53	15,83	15,65	15,95
SC	49,04	51,26	15,22	15,47	16,76	17,01

Table 1. Mean frequency content in the X, Y and Z components with the left (L) and right (R) sides from the three groups.

DISCUSSION

Although there were not any significant differences between the time domain parameters of the CA, CC and SC groups, the inter-subject CV of the SC group was substantially higher ($p<0.05$) than the other two groups. In addition, the inter-subject variability of the CA was significantly lower than the other two groups indicating general consistency of gait in adults as opposed to adolescents. Scoliotic children did not exhibit significantly different asymmetry in time domain

parameters compared to CA and CC groups. This is an important finding which indicates that normal asymmetry of time domain variables during gait is not altered in scoliotic children.

Frequency content, inter- and intra-subject frequency content CV, and asymmetry were significantly higher in the SC group. This was observed mainly in the X component, whereas small (not significant) differences existed in the other two components. The high frequency magnitude in X, indicates substantial instability in this direction, which is probably due to the medial-lateral deformity of the spine. The substantial inter- and intra- subject variability reflects the difficulty of scoliotic children to perform consistent gait trials.

There were considerable frequency content differences between individuals in the SC group. It can therefore be concluded that scoliotic children show different patterns of frequency content. However, the level of the deformity (off-set angle) was poorly correlated with all GRF time and frequency domain parameters (maximum r=0.56). Therefore it is more appropriate to consider the results individually rather than to make generalizations concerning scoliotic gait. The high frequency content in the X direction may affect the development of the deformity and therefore further investigation of gait mechanics is required.

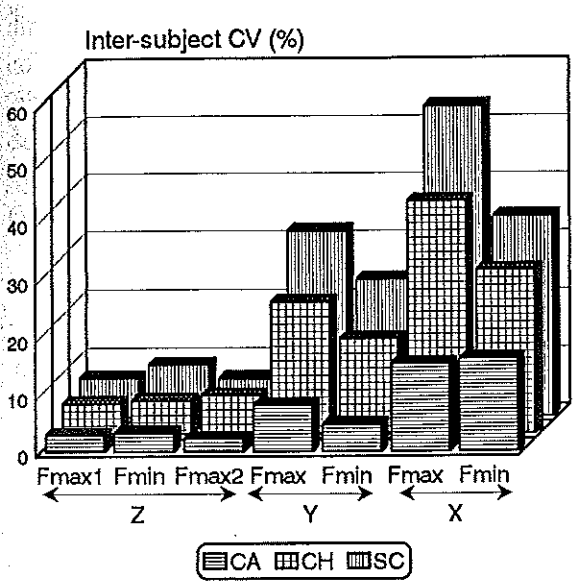

Figure 1. Mean (left-right) inter-subject CV of force time domain parameters performed from all groups. (max: maximum force; min: minimum force)

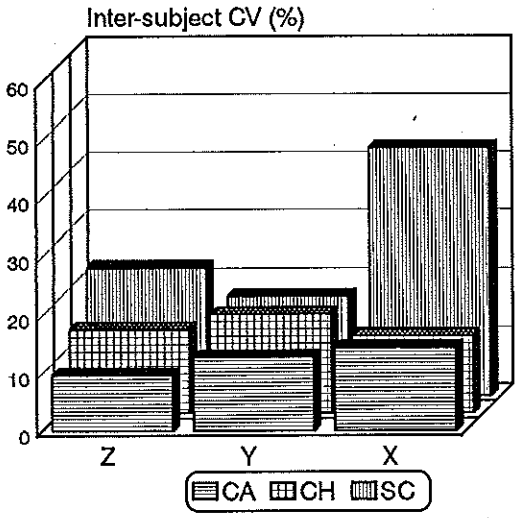

Figure 2. Mean (left-right) inter-subject CV of frequency content from all groups.

REFERENCES

Hamill, J. and S. McNiven (1990). Reliability of selected ground reaction force parameters during walking. *Human Movement Science*, 9, 117-131.

Parker, H., D. Larkin and T. Ackland (1993). Stability and change in children's skill. *Psychological Research*, 55, 182-189.

Sutherland, D., R. Olshen, L. Cooper and S. Woo (1980). The development of mature gait. *J. Bone Jt Surg.*, 62, 336-353.

A THREE-DIMENSIONAL BIOMECHANICAL ANALYSIS OF THE HUMAN KINETIC CHAIN MOTOR PATTERNS DURING THE AIMING IN AIR-RIFLE SHOOTING.

Gianikellis, K.; Dura, J.V.; Hoyos, J.V.
Instituto Valenciano de Educación Física. Universidad de Valencia.
Instituto de Biomecánica de Valencia. Universidad Politécnica de Valencia. (España).

INTRODUCTION

In contrast to all sport activities the most important characteristic in target sports (shooting or archery) is to eliminate any movements that could perturb the shooter-gun system stability. The capacity of the shooters to develop and control the quasi-static motor patterns during the aiming has been proved to be fundamental to obtain good results. From the mechanical point of view, the shooter-gun system is oscillating around a static position during the aiming. According to an important principle of general systems theory, the behaviour of the system emerges from the dynamic interaction of its parts. The purpose of this study is to describe and evaluate the small amplitude multijoint movements as a first step to obtain information about the principles that underlie the generation of the postural adjustments. Nickel, 1981; Iskra et al., 1988; Larue et al., 1989; Mason et al., 1990; Zatsiorsky and Aktov, 1990 are refered as some of the main contributors in the biomechanics of shooting sports.

METHODS

An experienced shooter requested that he should wear a special designed suit to perform 60 shots (7.81 $\pm$ 1.38) with an air-rifle, so that the kinematic and stabilometric data were collected. A measurement chain, including a Sonic Digitizer (GP8-3D) and a strain-gauge Force Platform (Dinascan) described elsewere (Gianikellis et al. 1994) (Fig.1), has been developed in order to measure the three-dimensional coordinates of the superficial landmarks, defining three segments (upper trunk-lower trunk-rifle), and the postural sway. The sample rate of the sonic digitizer is 66.6 Hz and the calculated standard deviation 0.1 mm. The sample rate of the Force Platform was 100 Hz and the precision of the Centre of Pressure (CP) coordinates is 2 mm. An analysis of error was carried out to validate the precision of the measurement system. A multifactorial balanced model, with five factors (two levels each) and 32 repetitions, has been designed to validate the effects of these factors and their interactions on the precision. The considered factors were: a) the emitters to be used, b) their distance to the microphones, c) their height, d) their orientation to the microphones and e) the sampling rate. The results obtained after the ANOVA analysis validated the configuration of the measurement system. The treatment of the data aimed to smoothing and differentiation was carried out using the subroutine package based on the natural B-spline functions according to the true predicted mean-squared error (Woltring, 1986). Then the aiming time (last 5 s) was divided into ten intervals (500 ms) and some parameters were calculated, as some criterion of the stability of the shooter-rifle system. This procedure was repeated out for every emitter (marker) and for the derived geometrical centers of every segment (defined by three markers). Besides the evolution of the azimuthal and

elevation angles of the rifle, upper trunk and lower trunk, as well as the Euler angles of these segments referred to the global system of reference were computed.

RESULTS AND DISCUSSION

The above mentioned stability parameters of the estimated kinematic magnitudes are: a) the standard deviations of the three-dimensional coordinates of the body landmarks and of the geometrical centers of every segment, b) the range of their movement, c) the total displacement of the markers respect to an averaged position, d) the length of the trajectory of every marker and e) the absolute velocity of every marker. The statistical analysis of the data has shown significant ($p<0.0004$ - $p<0.005$) linear correlations ($r=-.45$ - $r=-.35$) between the obtained target score and the stability parameters of the lower trunk during the seventh interval (2-1.5 s before the shot). The results seem to corroborate the shooters' opinion. According to them in this interval they start pressing gradually the trigger and any involuntary movement could affect negatively the score. Besides, it seems to be very important and very difficult to control the small oscillations of the lower trunk (pelvis) before any correction of the aiming point during this process ($r=-.42$, $p<0.0009$). Up to now, it has been considered only the kinematics of the gun (bow) in the biomechanics of shooting sports. The here presented findings support the opinion that the behaviour of the system emerges from the dynamic interaction of its parts and stimulate a different approximation in the study of these sports, which are important (13 medals) in the Olympic program.

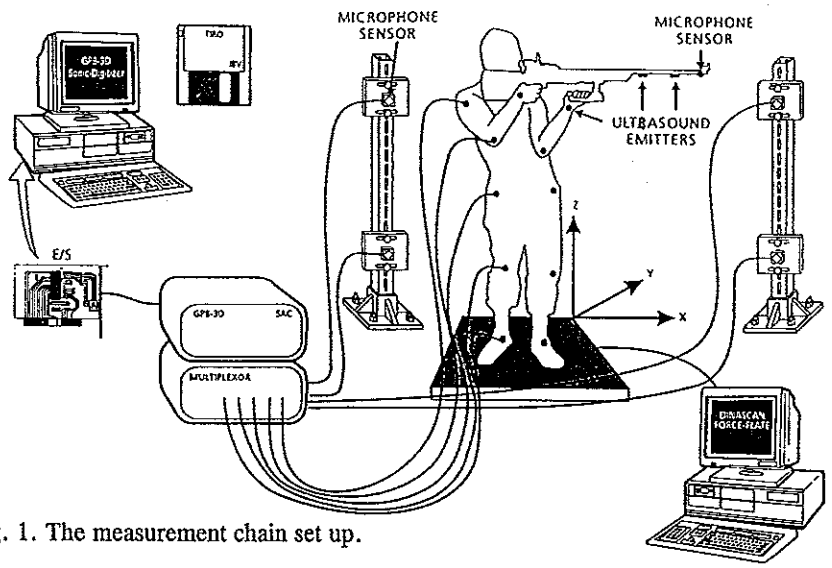

Fig. 1. The measurement chain set up.

REFERENCES

Gianikellis et al. (1992). Sonic digitizing: a new method for kinematic analysis of highly precise sports and movements - air rifle and pistol shooting. Proceedings X I.S.B.S. Symposium. Milano.

Gianikellis et al. (1994). A measurement chain applicable in the biomechanics of shooting sports. Proceedings XII I.S.B.S. Symposium. Budapest.

Zatsiorsky, V.M.; Aktov, A.V. (1990). Biomechanics of highly precise movements: the aiming process in air rifle shooting. J. Biom. 23, Suppl.(I), 35-41.

SIMULATION OF SWING AND GROUND IMPACT PHASES OF GAIT

H.S Gill & J.J. O'Connor

Oxford Orthopaedic Engineering Centre, University of Oxford, Oxford, England

INTRODUCTION

There is interest in studying the swing and early ground impact phases of gait in order to identify the gait determinants responsible for producing the large impulsive loads observed during the heelstrike of some subjects. This loading is termed the *heelstrike impulsive loading* or *hil.*

Repeated impulsive loading has been demonstrated to produce degenerative changes in the articular cartilage of rabbits [1]. A large *hil*, exhibited by a significant proportion of the population [2], is thought to be one of the mechanical factors responsible for degenerative changes in human knee cartilage, possibly leading to osteoarthrosis [1,3].

This study is concerned with investigating the foot contact phase of gait, both through experiment and simulation. The impulsive loads experienced by the lower limb at the instant of ground contact are dependent upon the kinematics of the limb at the end of swing phase. In order to study this event a sagittal plane three degree of freedom model of the lower limb has been developed to simulate the swing and early foot/ground contact phase of gait. Data for the simulation has been gathered from gait trials

METHOD

The two-dimensional model represents the lower limb as a three-body linkage, connected by ideal frictionless pin joints. The three angles formed by the limb segments to the vertical were chosen as the general co-ordinates and the states of the system. The equations of motion were generated using a Lagrangian formulation. The simulation was implemented in Matlab (The MathsWorks Inc., Mass., USA). The control inputs to the simulation (in the first instant) were the torques about the hip, knee and ankle joints and the vertical and horizontal accelerations at the hip. The joint moments were calculated from gait data, using inverse dynamics, as were the hip accelerations and velocities. The swing phase of gait was simulated, using the measured gait data to provide the initial conditions. A Runga-Kutta integration scheme was used. Gait data was measured using a Vicon 370 (Oxford Metrics Ltd., Oxford, UK) gait analysis system.

The simulation was terminated when contact with the ground was imminent and the final conditions were used as input to the impulsive equations. Three of these equations were generated from the extension of Lagrange's equations to impulsive motion. Since there are five unknowns, the three angular velocities after impact and the two components of the impulse, another two equations were required. These were formulated from considering the post impact condition of the foot segment remaining in contact with the ground and rolling without slip. The hip velocities were assumed to be constant during the time of the impulse.

RESULTS

The predicted state trajectories for a typical simulation are shown in Figure 1, they are compared to the measured trajectories for the same cycle. It is seen from Figure 1 that the simulation predicted the measured cycle well. The impulse equations provide an estimate of the impulsive loading at the moment of ground contact. The estimation of the position of the ground is highly dependent upon the measurement resolution of the gait analysis system and a few millimetres difference in the position of the ground produces large changes in the calculated impulsive forces. Gait trials are currently being conducted using foot switches to determine the instant of ground contact which will

allow the estimate of the ground position to be improved. Values of peak forces of the order of five to ten times body weight have been calculated for some subjects, these agree with the measurements made by accelerometers placed on the ankles of subjects.

DISCUSSION

The simulation allows a prediction of impulsive loading, due to the conditions found at the termination of swing phase. Currently the errors in measurement of the raw gait data is effecting the estimated values, but the use of temporal measurements with foot switches should alleviate this problem. The simulation model will be developed to provide control inputs with muscle forces. It is hypothesised that the effects of antagonistic quadriceps/hamstrings activity during late swing or heelstrike will greatly effect the impulsive loading at ground contact.

Gait studies with symptomatic pre-osteoarthritic subjects are also under way. Using the data from this group in comparison with normals, it may be possible to identify those features of the gait pattern which predispose a large hil.

REFERENCES

[1] Radin, E.L., Martin, B.M., Burr, D.B., Caterson, B., Boyd, R.D. and Goodwin, C. (1984) Effects of mechanical loading on the tissues of the rabbit knee. *J Orthop Res.* **2**, 221-234.

[2] Radin, E.L., Yang, K.H., Riegger, C., Kish V.L. and O'Connor, J.J. (1991) Relationship between lower limb dynamics and knee joint pain. *J. Orthop. Res.* **9**, 398-405.

[3] Radin, E.L., Swann, D.A., Paul, I.L. and McGrath, P.J. (1982) Factors influencing cartilage wear *in vitro*. *Arthr. Rheum.* **25**, 974-980.

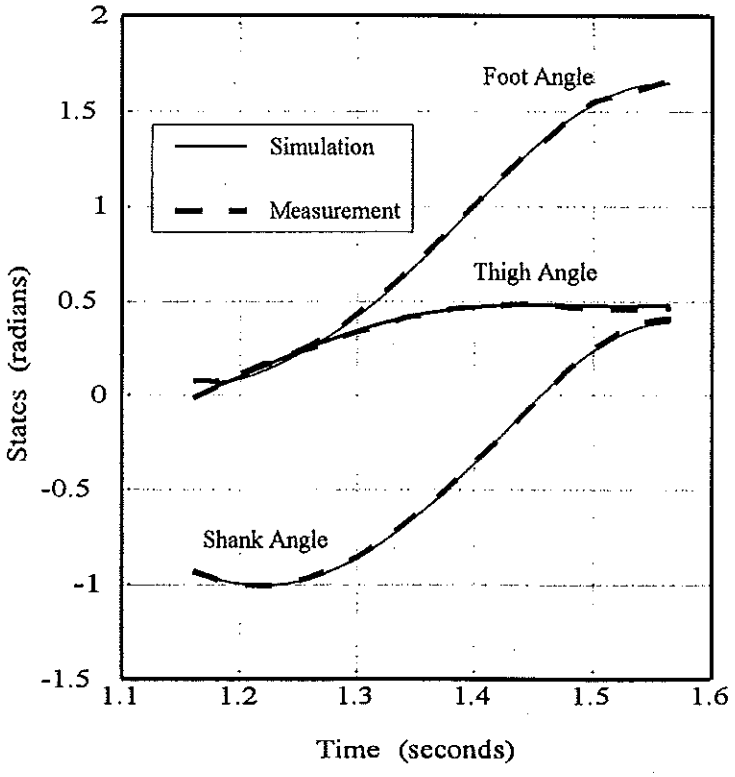

Figure 1. Measured and predicted states (limb segment angles) for the swing phase of a typical gait cycle.

THE REPRESENTATION OF JOINT DYNAMICS WITHIN THE CALCULATION OF INTERNAL LOADS

U. Glitsch
Institute of Biomechanics, German Sport University Cologne, Germany

INTRODUCTION

In recent years a great number of studies related to the calculation of internal loads in human beings have been carried out. There has been considerable controvercy concerning the handling of the redundancy problem of the musculo-skeletal system. Primarily, the choice of the optimization criterion on muscle recruitment caused a lot of dissent. Compared to this, the discussion on appropriate joint models was rare. In the past most joint models were mainly based on geometry or were only 2-dimensional, and therefore, not very suitable within a 3-dimensional inverse dynamics approach. The present study focuses on methods of a 3-dimensional joint representation and their influence on internal load calculations.

METHODS

Basically, there are several different methods available for dealing with redundant mechanical systems. In this study, the joint models are embedded in an inverse dynamics approach of the lower limb containing mass and inertia properties of the foot, shank and thigh, further, the lines of action of 47 muscles according to BRAND et al (1982). The inverse dynamics approach delivers the intersegmental moments of the ankle, knee and hip joints from coupled kinematic and dynamic motion analysis data. Applying mathematical optimization methods, the load distribution among the biological structures is calculated with respect to some optimization criterion. Usually, the optimization procedures control only the muscle activation, and the joint mechanics is defined static by the degrees of freedom of the relevant joint. The incorporation of additional constraint equations and additional terms in the cost function offers the opportunity to analyze any arbitrary joint type. At this point, it should be noticed that the geometrical gear mechanism is of less importance than the dynamic load carrying capabilities of the joint surfaces and associated ligaments. The optimization problem can be described as

$$\text{Min} \sum_{m=1}^{q} (g_m \cdot f_m)^k + \underbrace{\sum_{i=q+1}^{q+n} (g_i \cdot f_i)^k}_{(*)}$$

constraints:

$$\sum_{l=1}^{q+n} f_l (\vec{r}_{lj} \times \vec{F}_l) + \vec{M}_{Gj} = 0, \qquad j = 1,\ldots,3$$

$$f_m \geq 0, \qquad m = 1,\ldots,q$$

$$\left\| \vec{F}_l \right\| = 1, \qquad l = 1,\ldots,n,$$

where f_m $(m = 1,\ldots,q)$ are the magnitudes of the muscle forces with the associated weighting functions $g_m \geq 0$, f_i $(i = q+1,\ldots,q+n)$ are the constraint forces of the joints with the associated weighting coefficients $g_i \geq 0$, $\vec{F}_l (l = 1,\ldots,n)$ are the unit vectors of the internal forces with the correspondent lever arms $\vec{r}_{lj}$ and $\vec{M}_{Gj}$ $(j = 1,\ldots,3)$ are the intersegmental moments of the three joints. The term (*) is the penalty function for the representation of the joint dynamics. A geometric interpretation of the joints' constraint forces can be obtained from the example Fig. 1 with 4 constraint forces. Different joint types are modeled by setting the weights $g_i \geq 0$ $(i = q+1,\ldots,q+n)$. For example a value of $g_i = 0$ eliminates the correspondent degree of freedom of the relevant joint, or

in contrast, a value of $g_i = 10^5$ ($>> g_i$) adds one degree of freedom of the joint. Besides hinge joints and spherical joints, each intermediate type may be represented. At this moment, the definition of the penalty function is somewhat arbitrary. If individual anatomic data are available, the joint's constraint forces can be defined according to articular contact points, ligaments, etc. The assumptions about the lines of action of these forces are absolutely necessary because otherwise the dynamic equations are indeterminate (see CHENG et al 1990).

RESULTS

The tests of hinge and spherical joint types at the knee and the ankle joint (the hip joint being consistently spherical) revealed that hinge joints tend to keep the muscle forces low but increase dramatically the internal joints' stresses (see Tab.1). For a running data set, the torsional load caused by the transversal joint's constraint forces at the knee reached about 7.5 times the correspondent transversal component of the intersegmental moment at maximum. On the other hand, of course spherical joints do not have to bear torsional loads, but the muscles themselves have to balance the entire intersegmental moments. This may result in inconceivable muscle forces (see Tab.1). Adjusting the joints' constraints to a compromise between hinge and spherical joints yield results with moderate internal joint stresses and moderate muscle forces.

Tab.1: Internal load parameters of a quadratic muscle stress minimization with hinge, spherical and intermediate ($g_{48\text{-}51}$ = (.085,0.0,.155) joint types at knee and ankle joint of a running trial (v=5m/s).

joint type	max. torsional knee joint load*	max. muscle force [kN]	max. muscle stress [MPa]
hinge	7.5	3.96	2.55
spherical	0.0	14.03	12.37
intermediate	1.9	3.99	2.58

*in multiples of the max. transversal intersegmental moment

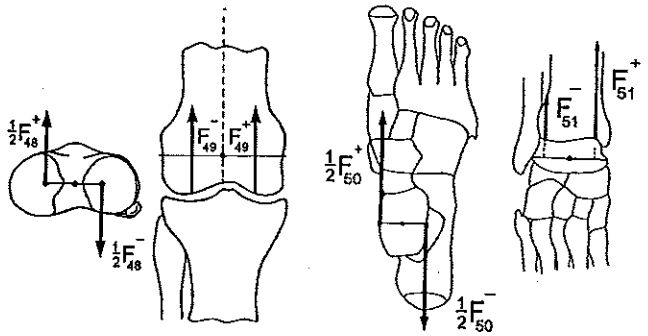

Fig.1: Constraint forces at knee (left) and ankle (right) joint.

CONCLUSION

The study revealed the importance of the joint's modeling in the analysis of internal loads. Usually, the joint reconstruction affects the results much more than the decision for a certain optimization criterion of muscle activation. However, the shortcoming of all internal load calculations is the lack of an objective external evaluation criterion. Direct in-vivo force measurements in human beings are problematic for many reasons and limited to a very few situations at present. Therefore, it is necessary to improve the dynamic models of the musculo-skeletal system.

REFERENCE

Cheng, R.C.-K., Brown, T.D. and Andrews, J.G. (1990) Non-uniqueness of the bicompartmental contact force solution in a lumped-parameter mathematical model of the knee. *J. Biomech.* **23**, 353-355.

MAXIMUM LOAD TEST ON THE AFFECTED AND UNAFFECTED LEGS IN STANDING FOLLOWING STROKE

Goldie, P. A., Evans, O. M., Matyas, T. M.
Faculty of Health Sciences, La Trobe University, Carlton, Victoria 3053, Australia.

INTRODUCTION

The ability to perturb the standing posture by voluntary movements of the body above the base of support is often compromised following stroke. In particular a deficit has been found in transferring body weight to the affected leg. Using a challenging task in which stroke patients were required to transfer from double stance to single stance, Pai et al (1994) found that 14 stroke patients failed in 80% of trials to the affected leg. Interestingly, they also failed in 52% of trials to the unaffected leg. Dettman et al. (1987) found a deficit in displacing the centre of pressure to the affected leg and, to a lesser extent, to the unaffected leg in a group of 15 chronic stroke patients. No data were available from patients in the rehabilitation phase. As noted by Pai et al. (1994) treatment protocols focus on improving weight transference at this early stage. Therefore, this study aimed to quantify the deficit in loading onto each leg by comparing stroke patients in the rehabilitation phase with healthy control subjects matched by age and gender. The testing protocol required that subjects load the leg maximally whilst still keeping the unloaded leg in contact with the floor. This made it possible to obtain a score for all subjects, regardless of performance level, and to avoid the problems of loss of balance for those who could adopt the single leg stance posture (Hasan et al., 1990). We addressed previous methodological problems in using the stability limits test with stroke patients by testing each leg separately on a single force platform. Maximum loading was quantified in the lateral direction in parallel two-legged stance and also in the forward direction in step stance, which is functionally relevant to the task of walking. Anecdotal clinical observations suggested that loading in the forward direction may be more challenging than in the lateral direction. The following specific hypotheses were tested: i) stroke patients would load less weight on both legs in either direction than control subjects; ii) stroke patients would load less weight onto the affected leg than the unaffected leg in both directions; iii) stroke patients would load less weight in the forward direction than the lateral direction on both legs.

METHOD

Twelve stroke patients with a first unilateral stroke of cortical or sub-cortical type were referred from three inpatient rehabilitation centres provided they could stand for 30 seconds. The median age was 64 years and the median time between stroke and testing was 37 days (IQR=31 to 56). Standardized stance positions were used for parallel and step stance with 10 centimetres between the shoes. The vertical force signal was sampled at 100Hz from a Kistler force platform for 15 seconds during three consecutive five second trials in which the patients transferred as much weight as possible onto the loading leg which was on the force platform. The other leg remained lightly in contact with the floor surrounding the force platform. The order of testing for direction (forward/lateral) and leg (affected/unaffected) was counterbalanced. An identical testing protocol was applied to 12 healthy control subjects who were matched by gender and age to the stroke patients. The "affected leg" of the control subjects was assigned to correspond to the affected leg of the age-matched stroke patients. Mann-Whitney U test was used to compare the two groups of subjects for each task and Wilcoxon signed-rank test was used to make within subject comparisons.

RESULTS

The Figure shows boxplots for both groups of subjects for loading on the affected and unaffected legs in both directions. The stroke patients loaded less body weight onto each leg in the forward and lateral directions when compared to the corresponding performance score for the control subjects ($p < 0.01$).. The stroke patients loaded less weight onto the affected leg than the unaffected leg in the forward direction (Z_W=-2.98, $p < 0.01$) and in the lateral direction (Z_W=-2.2, $p < 0.05$). The stroke patients loaded less weight in the forward direction than the lateral direction on the affected leg (Z_W=-2.98, $p < 0.01$). No such difference was found for the unaffected leg (Z_W=-0.55, $p > 0.05$).

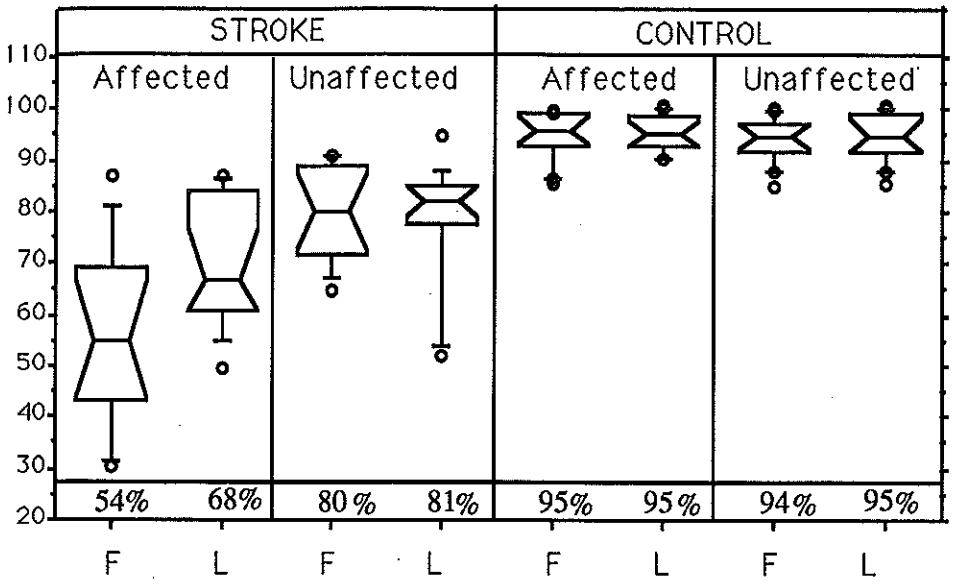

The Figure shows distributions of performance scores for each group on each leg in two directions. Each boxplot shows the median (value shown), 25th & 75th percentiles (box limits), the 10th and 90th percentiles (whiskers) and individual values which lie outside these limits. F=Forward; L=Lateral

DISCUSSION

By comparison to control subjects the stroke patients had a deficit on both legs for weight-shifting in the lateral and forward directions, thus confirming in patients at an early stage post-stroke similar findings to the more chronic stroke population. The deficit in weight shifting to either leg could be due to difficulty in executing the transfer of body weight or inability to provide the support moment on the loaded leg. Patients may have reduced strategies for recovering from such challenging and potentially unstable postures and may be appropriately apprehensive about performing the task. Therefore, cognitive factors may also influence the performance. The deficit was not confined to the affected side, indicating the need for treatment strategies to improve weight-shifting on both legs. The decrease in performance on the unaffected leg indicates that treatment goals should not be set at simply improving performance on the affected leg to the same level as the unaffected leg. Although performance on the unaffected leg was superior to the affected leg, it still does not provide a normal standard. Using the same testing protocol control subjects were able to load approximately 95% of body weight on both legs in either direction. The findings of this study, although based on a relatively small group, provide empirical evidence from healthy subjects which can be used for setting treatment goals.

Loading was more challenging in the forward direction than the lateral direction for the stroke patients on the affected leg. Maximum loading in the forward direction is likely to require a larger displacement of the centre of pressure because of the differences in the position of the feet. Whereas control subjects lifted the rear heel when the hips and shoulders were displaced forward over the loading leg to obtain maximal loading, the stroke patients kept both feet in contact with the floor. High performance scores in the lateral direction could be achieved without any alteration of the base of support. The reluctance of stroke patients to raise the heel and thus decrease the base of support may explain why the performance scores were less in the forward direction than the lateral direction. Alternatively, stroke patients may be more apprehensive to transfer weight in the forward direction because recovery srategies from this position are more difficult and may require a stepping response. Regardless of the cause, the findings indicate that performance in loading on the affected leg was worse in the forward direction than the lateral direction for stroke patients.

Dettman, M., et al. (1994) Am. J. Phys. Med. 66, 77-91.
Hasan, S., et al. (1990) J. Biomech. 23, 783-789.
Pai, Y., et al. (1994) Phys. Ther. 74, 647-659.

MECHANICAL CONTRIBUTION OF ISOLATED STRETCH EVOKED EMG-RESPONSES

A. Gollhofer*, P.V. Komi**, M. Voigt***, C. Nicol****

* Institut für Sportwissenschaft, University of Stuttgart, Stuttgart, Germany
**Department of Biology of Physical Activity, University of Jyväskylä, Jyväskylä, Finland
*** Center for Sensory-Motor Interaction, Aalborg University, Aalborg, Denmark
**** Department of Sport Sciences, University of Méditerrannée, Marseille, France

INTRODUCTION

The mechanical contribution of stretch reflex activation has received considerable attention. Based on the classical paper of Nichols (5) stretch reflex activation is assumed to enhance the range of short range elastic stiffness during active lengthening. Hoffer and Andreassen (2) presented experimental evidence that the hysteresis behavior of the neuromuscular system depends on the influence of the reflex contribution. In man, the stretch reflex contribution may also be important in the efficient transfer from the lengthening to shortening phase of the stretch-shortening cycle (SSC) (1,3). During passive dorsiflexion stretch, the force alterations following reflex activation in human has been recently reported using in-vivo Achilles tendon force (ATF) measurements (6). The present study examines further these responses resulting from the mechanical stimulation of the triceps surae tendomuscular complex.

METHODS

Rapid mechanical dorsiflexion stimuli on the right ankle joint were caused by a feedback controlled torque ergometer. The subjects (n=5) were sitting with both feet on the ergometer pedals. The stretch reflexes from the soleus and gastrocnemius muscles were picked up during a series of 36 mechanical stimuli, delivered randomly. Both single and double stimuli were used. In two subjects ATF was registered directly from the buckle transducer applied surgically around the Achilles tendon (4), and the analysis was performed in a manner similar to that of Nicol et al. (6).

RESULTS

The responses following the mechanical disturbance can be divided into a first response that is exclusively determined by the mechanical displacement and a second response lasting for 400 ms. This second response was in close connection with the amplitude and/or the integral of stretch reflex response occurring 40-45 ms after the mechanical stimulation (fig. 1). However, in situations where the reached stretched position was maintained constant (fig. 2), the recorded force did not return to zero, but instead demonstrated additional reflexly induced enhancement.

DISCUSSION

The present results agree with those of Nicol et al. (6) that the reflexly induced ATF contribution is substantial even in single passively induced dorsiflexion stretches. The magnitude of this enhancement seems to be related to the velocity of stretch as well as to the concomitantly changing EMG amplitudes. In maintained stretch situations, the observed force potentiation may have considerable relevance to real SSC motor function emphasizing the mechanical importance of an active stretch reflex system in a manner described so well in isolated models by Hoffer & Andreassen (2).

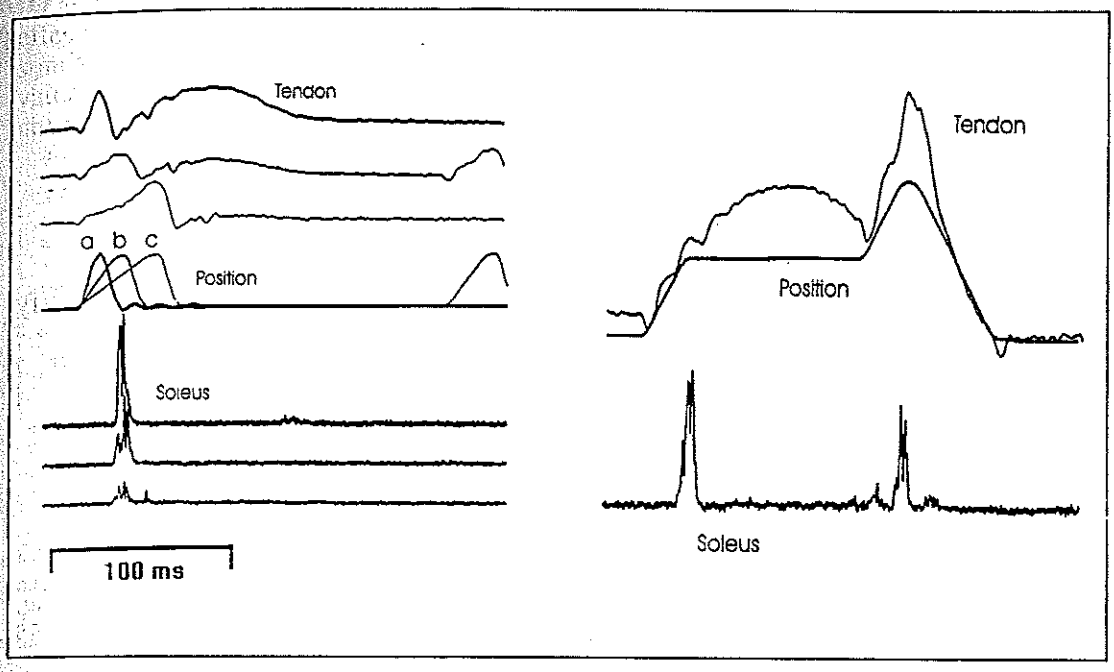

Fig. 1: Achilles tendon force, position signal and EMG-response of the m. soleus from three lengthening velocities (a,b,c)

Fig. 2: Achilles tendon force, position signal and EMG-response of m. soleus in the condition with two successive mechanical stimuli

REFERENCES

1. Gollhofer, A. and Schmidtbleicher, D. (1989) Stretch reflex responses of the human m. triceps surae following mechanical stimulation. In. Gregor, R.J., Zernicke, R.F. & Whiting, W.C. (eds.): Proc. XII ISB, Los Angeles, 219-220
2. Hoffer, J.A. and Andreassen. S. (1981) Regulation of soleus muscle stiffness in premammilary cats intrinsic and reflex components. J. Neurophysiol. 45, 267-285
3. Komi, P.V. (1984) Physiological and biomechanical correlates of muscle function. Effects of muscle structure and stretch-shortening cycle on force and speed. Exerc. Sport Sci. Rev. 12, 81-121
4. Komi, P.V., Salonen, M., Järvinen, M. and Kokko, O. (1987) In vivo registration of Achilles tendon forces in man. I. Methodological development. Int. J. Sports Med. 8, 3-8
5. Nichols, T.R. (1974) Soleus muscle stiffness and its reflex control, Cambridge, Harward Uni.
6. Nicol, C., Komi, P.V., Gollhofer, A. and Järvinen, M. (1994) Reflex contribution to Achilles tendon force during controlled stretches. Med. Sci. Sports Exerc. 26(5) (Suppl.): s 21

SPONTANEOUS SENSORIMOTOR ACTIVITY ON UNSTABLE PLATFORM : EFFECT OF EQUILIBRIUM TRAINING ACCORDING TO GENDER AND VISION

E.GOLOMER *, P.DUPUI **, H.MONOD *.

* Laboratoire de Physiologie du Travail et du Sport, Université Paris VI; ** Laboratoire de Physiologie, URA CNRS 649 Université Paul Sabatier Toulouse

INTRODUCTION

Servocontrolled platforms usually allowed studies about sudden external disturbance and sport (Perrin Ph. et al.1993). Cremieux and Mesure (1992) specify how factors related to the sex of subjects or to the practice of sports could influence the role of the different characteristics of vision in upright posture with accelerometers, but spontaneous dynamic equilibrium has rarely been examined. The purpose of the present study is to determine the effect of sport equilibrium training on spontaneous equilibrium quality according to gender and vision.

METHODS

Dynamic balance conditions were realized by asking trained equilibrium feminine and masculine gender subjects, comparatively to untrained subjects, to stand on an unstable and minimal area (stabilometer). The stabilometer is a seesaw consisting of a platform (square of 50 cm) with a cylindrical curved base (radius 55 cm), height of system (6 cm). The recordings (stabilograms) were monitored by means of an accelerometer placed under the platform.

The check sample is chosen in order to distinguish the role of age from the role of training. The 44 subjects are divided in two categories : prepubertal subjects and adult subjects who have a sedentary occupation and a good health. The trained equilibrium subjects are 37 sport acrobats : prepubertal with two years training of international level and adult professionnal and 31 Paris Opera classical ballet dancers in good health.

The balance parameters are recorded for 4 experimental conditions, in two positions : frontal sway (FS) and anteroposterior sway (APS) with two visual conditions : eyes open (EO) and eyes closed (EC). For each of 112 subjects, the stabilogram is recorded and its power spectra was obtained by a Fast Fourier Transform process. According to Dupui et al.(1990), we have chosen to cut the frequency spectrum at 3 band boundaries : below 0.5 Hz, from 0.5 to 2 Hz and from 2 to 20 Hz.

Statistic study for stabilogram parameter and power spectra parameters is realized by analysis of variance (ANOVA) for two factors : gender and training. Following these analysis, Student't test or Mann and Whitney test are used.

RESULTS

For gender study, ANOVA tests show that stabilogram values for all conditions (FS and APS $p < 0.01$ with EO and $p < 0.001$ with EC) and all categories are dependent on gender factor. For this parameter, girls and women values are lower than for boys and men.

Power spectra values, for total energy, excepted with EO in FS and APS, and all bands of frequency depend on gender ($p < 0.001$). Feminine values are lower than masculine one except for adult sport acrobats. In this category, masculine values are not statistically different from feminine values whatever the position or visual conditions. In addition, in FS, masculine adult untrained subjects would have similar values to feminine values of 18 years old category. The reason is that it is presently very difficult to obtain truly sedentary healthy subjects. For instance, they ride a bicycle once or twice a month, which represents a reduced equilibrium training.

For training study, stabilogram values are dependent on training factor ($p<0.01$) except for EO in FS, the equilibrium trained subjects values are lower than for untrained subjects. This result is significant only for feminine values and for APS with EC (dancers $p<0.05$, sport acrobats $p<0.001$). In power spectra, effects of equilibrium training are more obvious. For acrobat category, girl are similar to adult values and girl acrobat values are similar to feminine dancer values. For masculine values, it is different : in FS boy acrobats are lower than untrained ($p<0.05$) but higher than adult acrobats ($p<0.02$).

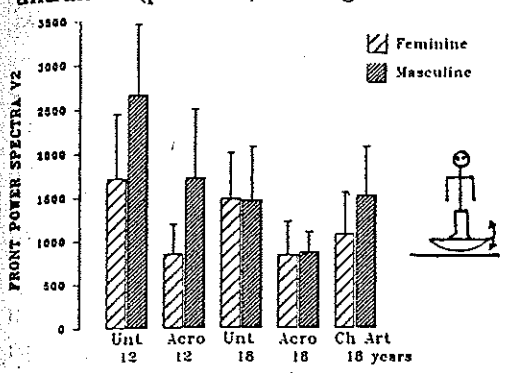

Fig 1

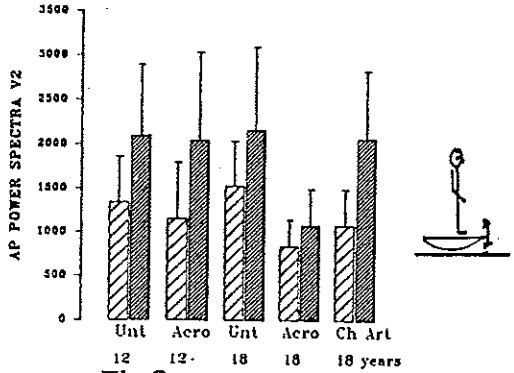

Fig 2

Example of gender and performance differences during eyes-closed spontaneous dynamic equilibrium test for total power spectra parameter: figure 1 in frontal position (Front power spectra volt2), comparative study between untrained subjects (Unt) : prepubertal (10 boys and 12 girls, twelve years old) and adult subjects (10 men and 12 women, eighteen years old) and trained subjects: sport acrobats (Acro) (6 boys, 16 girls and 7 men, 8 women); choreographical artists (Ch Art) (15 men, 16 women); figure 2 in anteroposterior position (AP power spectra)

DISCUSSION

Gender difference exists in dynamic spontaneous equilibrium, these results match those found in static conditions (Cremieux, 1992) with novices and experts in judo. More than visual conditions, we think that morphological differences may be a biomechanical factor which explains a poorer stability in men than in women. Study is being realized in order to verify this hypothesis.

On the other hand, with a sport equilibrium training, gender differences could be suppressed. The equilibrium learning is a means to improve natural quality equilibrium and could prevent falls for instance in older people.

It exists an early modification of equilibrium quality for girls in LS and APS, for boys modification occurs only in LS and is similar to the adult untrained subjects having a reduced practice. Exploration in FS is interesting to obtain early result about the beginning and APS about confirmed learning. Indeed, it is more difficult to control body destabilization in APS than in FS (Day et al., 1993). In this study, most angular movement occured between the trunk and upper leg for all stance width, in APS, while in FS angular motion about the ankle dominated when the feet were closer together.

REFERENCES

Cremieux J., Mesure S. (1992) Differential sensitivity to static visual cues in the control of postural equilibrium. vol1 in Posture and Gait: Control Mechanism. p.159-62.

Day B.L., Steiger M.J., Thompson P.D., Marsden C.D. (1993). Effect of vision and stance width on human body motion when standing: implications for afferent control of lateral sway. J. Physiol. 439, 479-499.

Dupui Ph., Costes Salon M.C., Montoya R., Séverac A., Lazerges M., Pagès B., Bessou P. (1990) Intérêt de l'analyse fréquentielle des oscillations posturales lors de l'équilibre dynamique. Soc. Et. Rech. Mult. Locom. Paris, Collège de France.

Perrin Ph., Perrin C., Courant Ph., Bené M.C. (1993) Hip and ankle strategies assessed with posturographic records. ISB XIV Congress.

WALKING DIFFERENCES BETWEEN NORMAL AND KNEE OSTEOARTHRITIC PATIENTS AT DIFFERENT SPEEDS OF GAIT.

AUTHORS: Gómez Pellico,L., García Martín,J., Rodríguez Torres,R., Rodríguez Rodríguez,L.P.

Department of Morphological Sciences and Surgery. University of Alcalá de Henares. Alcalá de Henares. (Madrid). Spain.

INTRODUCTION

Several authors (Grote, 1991; Laughman et al., 1984; Messier et al., 1992; Stauffer et al., 1977) have described the meaningful gait parameters of the knee osteoarthritic patients, but they only have studied one range of gait velocity in these patients. Our purpose was to study at slow, free and fast speeds of gait the differences in some kinetic and kinematic parameters between a normal group of people and knee osteoarthritic patients age-matched with them and relating these differences to their clinical implications, looking for a discriminant technique to distinguish between both groups easily.

REVIEW OF RELATED LITERATURE

Some authors have reported different ways to evaluate the biomechanics of the knee. Among the first were Stauffer et al., (1977) who explained some gait characteristics of knee osteoarthritic patients, studied with force platforms at free speed. In the same way, Laughman et al., (1984) published a Performance Index obtained from the most significant parameters in the biomechanics of the knee. Grote (1991) followed a similar methodology and also studied six centres of pressure but only in unilateral osteoarthritis of the knee and at free speed. Messier et al., (1992) studied different degrees of severity of knee osteoarthritis at fast speed of gait only with one force plattform.

METHODS

A group of 28 bilateral knee osteoarthritic patients has been compared in their way of walking with a control group of 19 normal people studying some kinetic (vertical, fore-aft and lateral components of ground reaction forces) and kinematic (step length, single and double support times) parameters and some temporal indices.

The diagnosis of osteoarthritis was made on the basis of clinical, X-ray and laboratory findings, following the American Rheumatism Association criteria of 1986 and mostly all of the patients suffered from moderate degree of osteoarthritis. They were assessed about their pain, articular ROM and muscular strength clinically.

Data were recorded from two force platforms aligned in a walkway when the subjects walked at their selfselected slow, free and fast speeds of gait, following the methodology of (Kirtley et al., 1985). A one way ANOVA was made as statistical study for the parameters and the different indices included.

RESULTS

We have observed only one parameter different (left flat foot force) between the normal and the knee osteoarthritic patients groups in the slow gait. In contrast all the kinematic and most of the kinetic parameters showed significant differences at free speed of gait between both groups. At fast speed of gait we have observed more differences in number of parameters and significant level of them than in the previous speeds of walking between normal and patient groups in both the kinetic and the kinematic parameters.

Finally we have not found any difference between both groups in the temporal indices (single and double support times / total support time) in any of the different speeds of gait studied.

DISCUSSION AND CONCLUSIONS

The absence of differences in the slow gait, drove us to say that this gait is not interesting for discriminant purposes. The flatten of the vertical components of ground reaction forces has been noted as a manifestation of reluctance by the affected limbs to accept body weight (Grote 1991).

The existance of numerous differences in most of the kinetic and kinematic parameters studied in the free and fast speeds of walking allowed us to say that they are useful to discriminate between both groups, being more different the way of walking of the osteoarthritic patients when they increase their speed of gait.

The observance of higher level of significance in the kinematic (0,001) than in the kinetic parameters (0,01) in the fast speed, permitted us to afirm that the knee osteoarthritic gait is more different in its temporo-spatial organization than in the forces exerted by these patients, compared with normal people.

In contrast at different speeds of walking it does not exit a desestructuration in the gait of knee osteoarthritic patiens, compared with a normal population, since they had no differences in the temporal gait indices studied.

REFERENCES

Grote,R.H. (1991) Wave parameters in stance of osteoarthritic knee patients. In Proccedings of the XIII Congress of the International Society of Biomechanics. Australia.

Kirtley,C., Whittle,M.W., Jefferson,R.J. (1985) Influence of walking speed on gait parameters. J. Biomed. Eng. 7,282-288.

Laughman,R.K., Stauffer,R.N., Ilstrup,D.M., Chao,E.Y.S. (1984) Functional evaluation of total knee replacement. J. Orthop. Res. 2,307-313.

Messier,S.P., Loeser,R.P., Hoover,J.L., Semble,E.L., Wise,C.M. (1992) Osteoarthritis of the knee: Effects on gait, strength and flexibility. Arch. Phys. Med. Rehabil. 73,29-36.

Stauffer,R.N., Chao,E.Y.S., Györy,A.N. (1977) Biomechanical gait analysis of the diseased knee joint. Clin. Orthop. Rel. Res. 126,246-255.

EFFECTS OF ENDOTOXINS ON MUSCLE FATIGUE AND RECOVERY

F.Goubel[1],C.Vanhoutte[1],O.Allaf[1],M.Verleye[2],J.M.Gillardin[2]

1-Département Génie Biologique, Université de Technologie, Compiègne, France
2-Laboratoires Biocodex, Compiègne, France

INTRODUCTION

It is not uncommon that patients suffering from bacterial infection complain of musculo-skeletal pain and of impaired performance capacity. However the mechanisms behind these symptoms are not well defined (Friman et al.,1991). Since loss of muscle function during fatigue induced by electrical stimulation is an important determinant of exercise performance, the aim of the present study was to demonstrate that bacterial infection can act directly on skeletal muscle to modify its fatigue characteristics. For this purpose in vitro experiments were performed on rat muscles after injection of lipopolysaccharides (LPS).Endotoxins as LPS - which are components of the cell wall of gram-negative bacteria -are known to induce physiological and behavioral changes in rodents similar to those observed in humans suffering from fatigue induced by infection.

METHODS

Eighteen male Wistar rats initially weighing about 300 g were assigned randomly to two groups. The first group (n = 9) was treated with LPS. For this purpose, LPS from Klebsiella pneumoniae(Sigma Chemical, St Louis, Mo) was dissolved in physiological saline and injected intraperitoneally at 3 mg/kg body weight at times zero and 24 hours. Muscle analyses were performed 48 hours after the first injection of LPS. The second group (n = 9) receiving physiological saline served as control (CON).As in a previous study (Allaf et al.,1993) experiments were performed on whole epitrochlearis muscles.The muscle was excised from an anesthetized rat and mounted horizontally in a chamber for mechanical analyses. The chamber was perfused with a buffered physiological salt solution maintained at 25° C. The physiological solution was continuously gassed with 95 % O_2 and 5 % CO_2. The tendons were connected to the transducers of an ergometer as previously described (Lensel-Corbeil and Goubel 1989). Stimulation was delivered to two parallel silver electrodes located on either side of the muscle and connected as alternate anode and cathode. Muscle was adjusted to a reference length (L_0) defined as the length at which maximum isometric twitch tension was elicited. 3 - 5 twitches were recorded. Maximal twitch tension (Pt_0) and associated contraction time (CT) were measured. Then, a fatigue test was performed using a procedure similar to that first described by Burke et al. (1973) for motor units and applied to isolated whole muscle by other investigators. For this purpose, 330-ms trains of 40 Hz were delivered once per second for 2 min. Then a 30-min recovery period was observed. Muscle recovery was followed by eliciting twitches every 5 min.(Pt_1 to Pt_6) Resistance to fatigue was quantified by calculating a fatigue index (FI) , ratio between tension production at 2 min. and maximum tension (P_{40} max). Twitch amplitudes were used as indexes of recovery.Differences between the two groups of rats were tested using Cochran's test. For each group of rats (i.e. 18 muscles), each parameter was expressed as mean ± SD .

RESULTS

For the CON group, initial isometric twitches had an amplitude of 13.8 ± 2.7 g whereas their CT was 29.6 ± 2.9 ms. P_{40} max was 46.0 ± 10.7 g. FI was 19.2 ± 7.1% During recovery twitch amplitude (relative to Pt_0) increased from 0.39±0.01 to 0.55±0.19.For the LPS group, maximal isometric twitches had an amplitude of 15.9 ± 6.0 g whereas their CT was 33.2 ± 3.1 ms. P_{40} max was 45.8 ± 17.9 g. All these mechanical parameters did not differ from controls. On the contrary,FI (9.7 ± 4.3 %)was significantly lower than for controls ($p < 0.01$) and, as attested by Pt_1 to Pt_6 values, recovery was more pronounced in the CON group (Fig.1).

DISCUSSION

Results reported here confirm that the epitrochlearis muscle of the rat is mechanically a fast muscle . This is consistent with the fact that this muscle consists predominantly of type II fibres (Allaf et al.,1993). Furthermore, fatigue indexes indicate an important sensitivity to fatigue since FI at 2 min lower than 40% are usually reported for fast muscles of the rat .

It cannot be argued that problems with regard to the diffusion of substrates and oxygen are responsible for the observed fall in tension during fatigue tests. The epitrochlearis muscle of the rat is sufficiently thin to avoid this kind of artifact. Moreover

such a preparation is currently used as an in vitro model for metabolic studies (Wallberg-Henriksson ,1987) since it allows adequate diffusion of substrates to the entire muscle. Thus, it can be asserted that FI values reported here reflect a genuine physiological property.

LPS treatment did not modify the mechanism of force generation in absence of fatigue since twitches and initial P_{40} were similar in both populations. A modification in these mechanical characteristics would involve changes in rate of activation of actin-myosin interactions and modifications in contractile proteins. Such an adaptation is impossible within 48 hours. Nevertheless LPS induced an increase in fatigability of the epitrochlearis muscle and a deficit in force production during recovery. It is well known that LPS injection in rats brings on a state of fatigue with reduced physical performance (Hart 1988). Present results demonstrate that bacterial infection can act on skeletal muscle to decrease its resistance to fatigue during repetitive stimulation and to alter the subsequent recovery phase.In conclusion, the in vitro preparation of the epitrochlearis muscle of the rat appears to be a suitable model for studying muscle fatigue induced by infection. Such a preparation would be useful for testing, in terms of muscle mechanical response, the efficacy of drugs proposed for antifatigue therapy in humans.

REFERENCES

Allaf, O.,Okiemy, G. & Goubel, F. 1993. The epitrochlearis muscle of the rat : a useful model for muscle mechanics. *XIVth ISB Congress ,Paris* **1** ,80-81.

Burke, R.E., Levine, D.N., Tsairis, P. & Zajac, F.E. 1973. Physiological types and histochemical profiles in motor units of the cat gastrocnemius. *J Physiol (Lond)* **234** , 723-748.

Friman, G., Ilbäck ,N.G., Crawford, D.J. & Neufeld, H.A. 1991. Metabolic responses to swimming exercise in Streptococcus pneumoniae infected rats. *Med Sci Sport Exerc* **23** , 415-421.

Hart,B.L. 1988. Biological basis of the behavior of sick animals. *Neurosci. Biobehav. Rev.* **12**,123-137.

Lensel-Corbeil, G. & Goubel, F. 1989. Series elasticity in frog sartorius muscle during release and stretch. *Arch Int Physiol Biochim* **97** , 499-509.

Wallberg-Henriksson, H. 1987. Glucose transport into skeletal muscle. *Acta Physiol Scand* **131**, Suppl. 564.

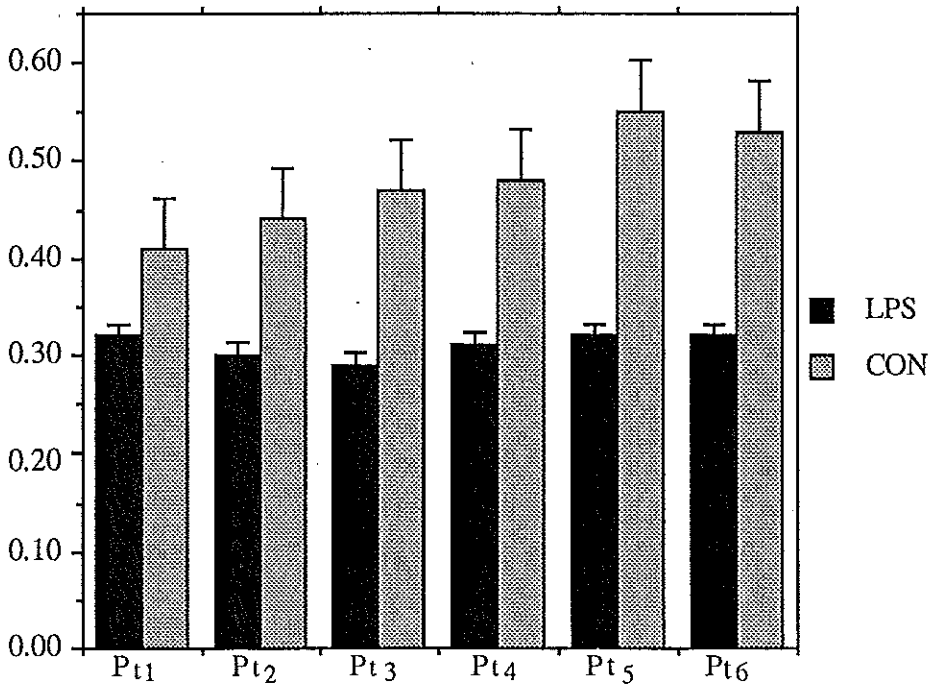

Fig 1. Relative amplitude of twitches during recovery

ECCENTRIC CONTRACTIONS ARE SPECIFIED *A PRIORI* BY THE CNS

Grabiner, Mark D., Owings, Tammy M., George, Michele R., Enoka, Roger M.
Department of Biomedical Engineering, The Cleveland Clinic Foundation
Cleveland, Ohio, USA

INTRODUCTION

Compared to concentric contractions, voluntary eccentric contractions of skeletal muscle are associated with lesser levels of muscle activation (surface EMG) at similar submaximum forces, and lesser levels of muscle activation but greater forces during maximum voluntary contractions (Tesch et al., 1990). Furthermore, subjects appear unable to maximally activate a muscle during an eccentric contraction compared with isometric and concentric contractions (Westing et al., 1990). At the motor unit level, eccentric contractions may involve lower initial discharge rates (Tax et al., 1990) and may differ in recruitment order (Nardone et al., 1989). It is unclear whether these differences have a central or peripheral origin. The aim of the study was to compare activation levels of a knee extensor muscle for intended and unexpected eccentric contractions to assess the origin of these differences.

METHODS

Fourteen subjects participated in the study. Maximum isokinetic knee extensions of the right leg were performed on a KIN-COM isokinetic dynamometer at a speed of 60 deg/s. EMG of the right vastus lateralis (VL) and hamstrings were collected using bipolar surface electrodes. The detected EMG signals were amplified, bandpass filtered, digitized at 1 kHz (along with the the signals from the KIN-COM), and stored for offline processing.

Three trials each of maximum concentric and eccentric contractions of the knee extensors were performed through a 30 degree range of motion from an initial knee flexion angle of 50 degrees. The order of administration was randomized across subjects. For the final trial, the subject's knee was positioned at 50 degrees of knee flexion and the subject instructed to perform a maximum concentric knee extension contraction. However, the Kin-Com was programmed to unexpectedly (to the subject) induce an eccentric contraction. Only one trial of this condition was performed.

The smoothed digitized force data was used to calculate the knee extension moment. The dependent variables were the peak knee-extension moment and the full-wave rectified and integrated EMG signal for 100 ms following the onset of activation. Because the EMG was analyzed for the intial 100 ms of the contraction, it is not likely that the signal could have been modified by either reflexive or voluntary processes. The EMG of the VL was normalized to that obtained during a maximum voluntary concentric contraction. The EMG of the hamstrings was normalized to that observed during a maximum voluntary knee flexion contraction.

RESULTS

The experimental protocol was effective in causing an unexpected eccentric contraction. The subjects expressed reactions ranging from surprise to confusion. However, there were no qualitative observations of diminished performance during these trials. Generally, the shapes of the initial force-time curves of the intended and expected eccentric contractions were similar. The shape of the force-time curve during the latter part of the range of motion was affected qualitatively, in some subjects, during the unexpected

eccentric contraction. However, as the statistics indicate, these effects did not influence the peak knee-extension moments.

The peak knee-extension moments generated during the concentric and eccentric contractions were 127.1±34.50 and 245.8±52.40 N·m, respectively ($p<0.001$). For the unexpected eccentric contraction the peak knee-extension force was 245.8±38.4 N·m, which was significantly greater than the concentric contraction ($p<0.001$) but not different from the intended eccentric contraction ($p=0.995$).

The activation level of the VL during the maximum voluntary eccentric contraction was 0.84±0.41% of the maximum voluntary concentric condition. For the unexpected eccentric contraction, the level of VL activation was 1.04±0.40% of the maximum concentric contraction EMG. The activation levels of the intended and unexpected eccentric contractions were not significantly different ($p=0.083$).

The activation level of the hamstrings muscles was not significantly different across conditions ($p=0.098$). Coactivation of the hamstrings during the maximum voluntary concentric and eccentric contractions were 10.6±0.06% and 12.6±0.07% of the maximum voluntary knee-flexion contraction, respectively. The hamstrings activation level during the unexpected eccentric contraction was 11.2±0.07% of the maximum voluntary knee flexion contraction.

DISCUSSION:

Not surprisingly, the maximum eccentric knee extensor moment was significantly greater, and the surface EMG of the vastus lateralis muscle substantially less than the maximum concentric contraction. When the subjects intended to perform a maximum isokinetic concentric contraction but were unexpectedly forced into an eccentric contraction, the knee extensor moment was similar to that of the intended eccentric contraction but the muscle activation was similar to that of the concentric contraction. This observation suggests that the difference in muscle activation between the concentric and eccentric contractions was of suprasegmental origin.

Behm and Sale (1993) had subjects train with rapid unilateral contractions performed isokinetically or isometrically. Training produced similar velocity-specific increases in peak moment for both legs, indicating that the intended rather than the actual movement velocity was critical for the specificity effect. Taken together, these results suggest that the descending signal includes information that distinguishes between eccentric, concentric, and isometric contractions.

REFERENCES

Behm and Sale (1993): Intended rather than actual movement velocity determines velocity-specific training response. *J Appl Physiol*, 74:359-368.

Nardone et al (1989) Selective recruitment of high-threshold human motor units during voluntary isotonic lengthening of active muscles. *J Physiol*, 409:451-471.

Tax et al (1990). Differences in coordination of elbow flexors in force tasks and in movement. *Exp Brain Res*, 81:567-572.

Tesch et al. Force and EMG signal patterns during repeated bouts of concentric and eccentric muscle actions (1990). *Acta Physiol Scand*, 138:263-271.

Westing et al (1990). Effects of electrical stimulation on eccentric and concentric torque-velocity relationships during knee extension in man. *Acta Physiol Scand*, 140:17-22.

THEORETICAL METHOD OF IMPACT PROTECTION DESIGNING FOR MAN-OPERATOR.

E.V.Grafeev and V.P.Tregoubov, St. Petersburg State University

St. Petersburg, Russia

INTRODUCTION.

The purpose of this work is to establish some grounding in theory for designing of optimal impact protection of human body. Such a problem is solved usually by numerical methods (by computer simulation). At present work the analytical dependence is established between the human body dynamic characteristics and the impact parameters for protection characteristic .

METHODS.

The diagram for model of "human-protection system" is showed in Fig. 1, where $\mathbf{m}$, $\mathbf{b}$, $\mathbf{c}$ are the mass, the stiffness and damping coefficients of human body accordingly; $\mathbf{m_p}$ is the mass and $\mathbf{F}$ is the force characteristic of protection system. The known P.Payne's "DRI model" (Dynamic Response Index) is the example of such human body model.

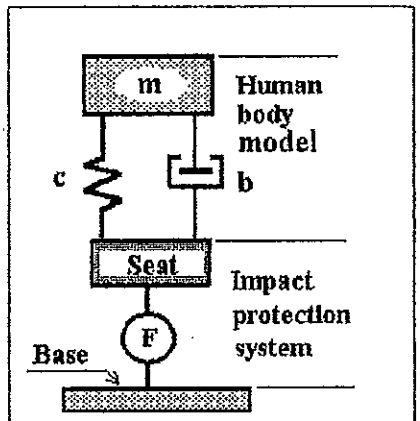

Fig.1. The diagram for model of "human - protection system".

The external action $\mathbf{s(t)}$ has the kinematic excitation character with the given maximum duration $\mathbf{T}$ and limited final velocity $\mathbf{V}$, i.e.

$$\int_0^T |\dot{s}(t)|dt \le V \qquad (1)$$

Thus the specific law of base motion $\mathbf{s(t)}$ is not given in advance.

The following performance indexes were selected for the protection system: the peak values $(\mathbf{I_w})$ of seat acceleration $(\mathbf{W_p})$ and the maximum displacement $(\mathbf{I_p})$ of seat relative to the base $(\mathbf{x})$.

It is necessary to find such the force characteristic of protection system that:

1) $\mathbf{I_w}$ is less than the maximum tolerable value of the seat acceleration $\mathbf{W_{tol}}$;

2) $\mathbf{W_p}$ is the least of other protection system. The seat trajectory satisfying these conditions is called the optimally trajectory.

RESULTS.

The following method for designing of for optimally impact protection system is proposed. On the basis of the graph-analytical method it is established that the seat must move with the maximum tolerable acceleration $\mathbf{W_{tol}}$ to provide the seat trajectory to be optimum. It can be prove that the impact is maximum adverse if the velocity of base is changed from $\mathbf{0}$ to $\mathbf{V}$. In this case the relative displacement of seat is maximum in comparison with any other form of the kinematic excitation. This maximum value is equal:

$$\max(I_p) = \left| T\left(V - \frac{1}{2} W_{tol} T \right) \right| \qquad (2)$$

Then we can determine the human body reaction on the seat as a function of time $F(t)$. The a one-to-one correspondence under the conditions formulated above exist between relative seat displacement and time:

$$x = \left(\frac{1}{2}W_{tol}t - V\right)t \qquad \text{and} \qquad t = \varphi(x) = \frac{V}{W_{tol}} - \sqrt{2\frac{x}{W_{tol}} + \left(\frac{V}{W_{tol}}\right)^2} \qquad (3)$$

So $t = \varphi(x)$, we can find the nonlinear relation between F and x in an explicit form $F=F(t)$, i.e. to present the force characteristic in an analytical form. This relation has an awkward form therefore it is not presented here and the general form is:

$$F = F(x; T, V, W_{tol}; m, c, b, m_p)$$

DISCUSSION.

In Fig.2 two force characteristics are showed. The curve 1 corresponds the model satisfying to condition $b^2 \le 4mc$. Its parameters are $m = 57$, $c = 159500$, $b = 1350$. The curve 2 corresponds the model satisfying to the condition $b^2 \ge 4mc$ and it parameters are $m = 57$, $c = 52700$, $b = 5700$. The mass of seat selected $m_p = 1,6$. The parameters of the kinematic excitation are $V = 1,96$ and $T = 0,04$. The maximum tolerable acceleration of seat is $W_{tol} = 49$. On the basis of this comparison, it is concluded that model presentation of human body is a primary importance in protection system designing. That is why we are to take proper account of human body dynamics and proposed method makes it possible.

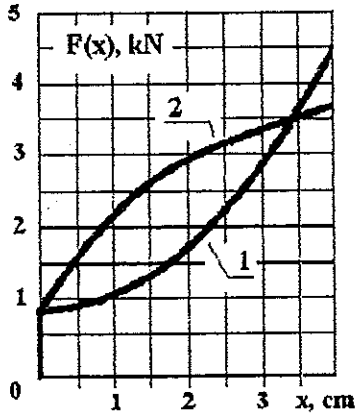

Fig.2. The force characteristics of the proctection system.

The work was supported by Russian Foundation of Fundamental Researches.

A THREE DIMENSIONAL ANALYSIS OF THE LONG JUMP TAKE-OFF.

P. Graham-Smith, A. Lees and S. Townend.
Centre For Sport And Exercise Sciences, Liverpool John Moores University, Liverpool, L3 3AF, UK.

INTRODUCTION

Kinematic analyses of the long jump have traditionally concentrated on the sagittal plane and especially on the projectile parameters at take-off (TO). In addition, the height and speed of the centre of mass (CM) and the extension of the touch-down (TD) leg at the instant of TD have been well documented. However, recent studies have outlined the need for three dimensional analyses. Fukashiro et al.(1993) identified trunk rotation and in particular hip rotation as important factors influencing the world record jump of Mike Powell. Lees et al.(1993) and Lees et al.(1994) stated that a 'pivoting' action of the TO leg during the compression phase of the TO was responsible for approximately 66% of the total vertical velocity (Vy) gain. The effectiveness of this 'lift' mechanism is influenced by the resistance of the leg to flex at the knee and the hip. Whilst changes in the knee joint angle can be successfully measured using a two dimensional analysis, the hip joint angle cannot. The aim of this study was to quantify the three dimensional activity of the hip and knee joint angles of the TO leg. The relationships between changes in these angles and the amount of Vy gained from TD to maximum knee flexion (MKF), denoting the end of the compression phase, was also examined.

METHOD

The eight finalists in the 1994 UK National Championships were filmed using two high speed 16mm cine-cameras (Locam and Photosonics). The cameras were positioned approximately 90 degrees apart and both recorded at a frequency of 100 Hz. Digitising equipment included a NAC cine projector and a TDS digitising tablet. Eighteen jumps ranging from 7.02m to 7.58m were digitised three times each to assess errors. The film was analysed using a 14 segment model defined by 18 points and incorporated segmental data proposed by Dempster (1955). The three-dimensional coordinates were obtained using the DLT method. The data was smoothed using a Butterworth 2nd order filter with padded end points and a cut-off frequency of 8 Hz. The three dimensional angles were calculated using the scalar product. The average angles taken from the three trials were used to reduce errors. Relationships were tested using the Pearson Product Moment Correlation Coefficient.

RESULTS

The average 3D hip and knee joint angles and Vy at the instants of TD, MKF and TO are presented in Table 1. The 3D hip joint angle was measured in the plane defined by both hip joints and the knee joint centre. This angle can be described as a complex of hip abduction / adduction, flexion / extension and pelvic rotation and tilt. The 3D knee joint angle essentially describes flexion / extension. Using 3 repeated measures the error of the 3D angular measurements, estimated from the average standard error, was less than 1.65 degrees for the hip and 0.75 degrees for the knee.

Table 1. 3D Hip and knee joint angles at TD, MKF and TO. (n=18)

	3D Hip angle (deg)		3D Knee angle (deg)		Vertical Velocity (m/s)	
	Mean	SD	Mean	SD	Mean	SD
TD	100.2	2.8	165.5	4.1	-0.083	0.202
MKF	91.0	4.9	139.7	5.7	2.339	0.314
TO	99.1	3.5	169.0	3.1	3.412	0.286
Min	89.6	4.8				

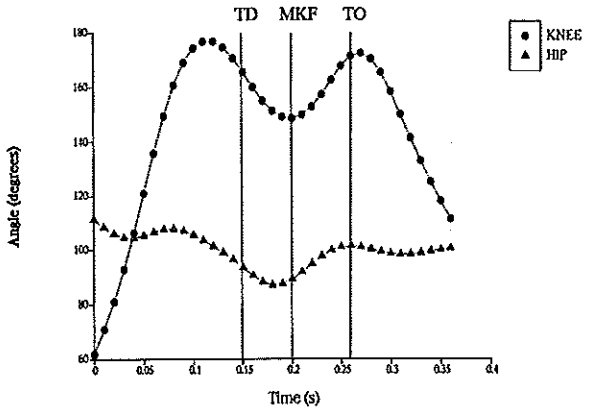

Figure 1. Changes in hip and knee joint angles in the TO phase of the long jump.

DISCUSSION

The average change in the knee angle during the compression phase was approximately 26 degrees. The profile of the hip joint angle was similar to that of the knee, but the range was less, averaging 10 degrees,(see figure 1). A correlation coefficient value of -0.693 ($p<0.01$) between the minimum hip joint angle and the maximum knee flexion angle revealed a significant negative relationship. This information provided strong evidence to confirm that the effectiveness of the 'pivot' mechanism is influenced by actions of both the hip and knee joints. A correlation coefficient value of -0.485 ($p<0.05$) between the minimum hip joint angle and the amount of Vy gained from TD to MKF was found to be significant. In contrast the maximum knee flexion angle did not correlate with Vy gained from TD to MKF. The implication of this finding is for athletes to develop the eccentric mechanisms of the hip joint. This could be done by incorporating one-legged plyometric drills into training regimens.

REFERENCES

Lees, A., Fowler, N. and Derby, D. (1993). A biomechanical analysis of the last stride, touch-down and take-off characteristics of the women's long jump. *Journal of Sports Sciences*, **11**, 303-314.

Lees, A., Graham-Smith, P. and Fowler, N. (1994). A biomechanical analysis of the last stride, touch-down and take-off characteristics of the men's long jump. *Journal of Applied Biomechanics*, **10**(1), 61-78.

Fukashiro, S., Wakayama, A., Kojima, T., Arai, T., Itoh, N., Ae, M., Kobayashi, K. and Matsui, H. (1993). World record long jump: three dimensional analysis of take-off motion of Powell and Lewis. In, Abstracts of the International Society of Biomechanics, XIVth Congress, Paris,4-8 July, 1993, vol I, 434-435.

DEFORMATION OF BRAIN TISSUE

Frieder A. Grieshaber and Uwe Faust

Institut für Biomedizinische Technik, Universität Stuttgart, Stuttgart, Deutschland

INTRODUCTION

More and more the minimal invasive methods are applied in brain surgery. The following steps may be distinguished: diagnosis, planning of surgical intervetion. Basis of planning are CT- resp. MR-Images. After a three dimensional reconstruction the most favourable path of guiding instruments will be determinated. Deformations and displacements of brain structure occur because of the different direction of the vector of gravity during diagnostic procedure and surgical intervention, the discharge of liquor cerebrospinalis and the mechanical forces by instruments used for the intervention. The surgeon has to take into consideration the deformation and displacement of the region of interest. Characteristic points of anatomy can be helpful to navigate instruments, but it is difficult to find and recognize them.

METHODS

In the underliing work a method to calculate the deformations and displacements of brain structures will be presented. A set of MR-images will be segmented on a SUN station. Classification and three dimensional reconstruction of distinguishable regions of brain will be carried out. This data set is transfered into the preprocessor of the Finite Element Program ANSYS. Material properties as density and elasticity will be assigned to the solid models. Than the boundary conditions and loads will be described and the solver can be started. The best way to guide instruments will be iterativly estimated.

Until now examinations have been done on fresh brains from cows taken immediately after slaughtering. Ultrasonic (US) investigations have yielded the material properties. The influence of three different loads has been estimated on a preliminary model of the brain of a cow: discharge of liquor cerebrospinalis, changing of position and influence of a rod.

Imageprocessing

The MR-images are processed with a method described by Dellepiane (1989). This is a three dimensional tool called Surface-Preserving-Smoothing. The results are put into a segmentation process which works with a region growing module. A Fuzzy-Controller classifies the regions into anatomical structures. The surface of each structure is extracted and converted into a format which can be understood by the FEM program ANSYS.

Mechanical Properties

The elasticity and density of the brain are estimated by ultrsonic (3,5 MHz) measurements in HF-transmission mode. The brain is prepared by putting it into molten agar (39 C) and cut into slices after solidification. From slices of 1 cm thickness the local distribution of velocity c_{11} and reflectivity are measured. After this c_{22} can be recorded from stripes and c_{33} from cubes. With these results the distribution of elasticity in three orthogonal directions can be calculated. These numbers are required for FE-Analysis.

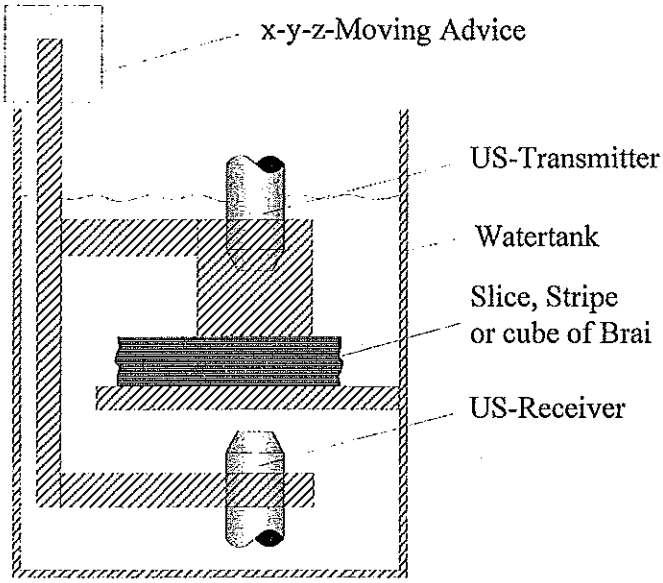

Fig. 1: Setup of US-Measure-Desk

RESULTS

The US-investigation yields differences of density between 1,22 and 1,24 g/cm³. The speed of sound strongly depends on the direction of propagation. The divergence of elasticity in orthotropic directions amounts to 20 %. Therefore brain tissue cannot be considered as isotropic but as an anisotropic material. Figure 2 shows the distribution of speed of sound as one result of an US-investigation of a slice of brain of a cow.

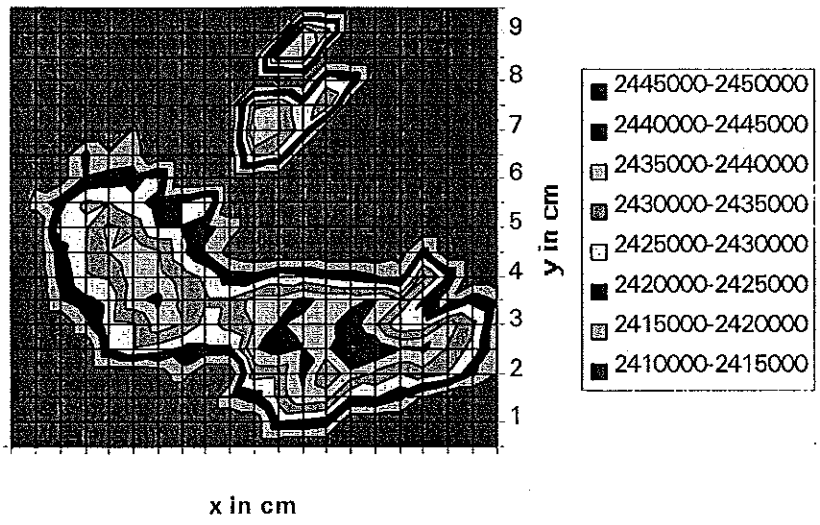

Fig. 2: Distribution of speed of sound of a slice of cow's brain (frontal cut).

REFERENCE

Dellepiane, S., Serpico, S.B. and Vernazza, G. (1989) A framework for processing and interpretation of three-dimensional signal from multislices. In *Signal Processing* **18**, 239-258.

TRAINING EFFECT OF STATIC STRETCHING ON NEURAL AND MECHANICAL PROPERTIES OF THE HUMAN TRICEPS SURAE

GUISSARD N., DUCHATEAU J. and HAINAUT K.

Laboratory of Biology, Université Libre de Bruxelles, Belgium

INTRODUCTION

Muscle stretching appears to be helpful in the prevention of injury (Ekstrand and Gillquist, 1982) and the preparation for sporting activities in that increasing the range of joint motion (Etnyre and Lee, 1988). Recent studies have shown that static stretching for short (30 s) and long (10 min.) durations does not affect the mechanical properties of the muscle (Guissard et al, 1988; Guissard et al, 1991). In fact, while muscle stretching does not change the excitability of the Soleus (Sol) motoneurone pool and the mechanical properties of the Triceps Surae but it does increase the range of ankle motion. This study is designed to test the effects of a six week static stretching training program on the excitability of the Sol motoneurones and the mechanical properties of the Triceps Surae.

METHODOLOGY

The experiments were carried out on 12 healthy subjects of both sexes (aged 21-35 years) who gave their informed consent to participating in these experiments. The training program consisted of 30 daily stretching sessions of 10 min. duration performed 5 times a week. The right-hand side muscles were trained, while the contralateral ones served as control. The electrical and mechanical properties of the Triceps Surae were tested before, during and after the training session, and also 30 days later.

During the experiment the subject lay prone on a table with both legs extended and the foot strapped to a movable support (Guissard et al, 1988). While the maximal voluntary contraction (MVC) torque and the passive tension changes in the muscle-tendon unit were recorded by means of a strain gauge transducer, the maximal angular ankle velocity and range of motion were estimated from the output signal of a linear potentiometer. The electromyographic (EMG) activity was recorded from the Sol by means of two silver surface electrodes fixed over the motor point. The ground electrode was placed over the tibia. The motor point was located by electrical stimulation and during the successive experimental sessions, the electrodes were placed in identical position. The Hoffmann (H) reflex was elicited by electrical stimulation of the tibial nerve (Guissard et al, 1988) and the tendon (T) reflex was induced by mechanical percution to the Achilles tendon by means of a reflex hammer. In both cases, maximal EMG responses were recorded and expressed as percentage of the maximal motor wave (M max) peak-to-peak amplitude. The signals were stored on FM tape prior to computer analysis.

RESULTS

By the day following the last training session the range of ankle motion had been augmented by $7.6 \pm 0.5°$ (mean $\pm$ SE), with 56 % of this gain being reached after only 10 sessions. After training, the relationship between the length and passive tension of the muscle-tendon unit showed an overall decrease in tension for a given length. During training, the means of the Hmax/Mmax and Tmax/Mmax ratios were reduced by 17 and 33 % respectively, without any significant change in the angular velocity and torque produced during 5 sec MVC's (cf Table 1). It should be pointed out that after one month's in the interruption of training, 75 % of the gain in the range of ankle motion was maintained although the Hmax/Mmax returned to the control values (0.52 ± 0.02).

Table 1 : Comparison of the electrophysiological and mechanical characteristics (mean ± SE) of the subjects before and after training.

	Before training	After training
Range of motion (°)	24.6 ± 0.8	32.2 ± 0.8***
Hmax/Mmax	0.53 ± 0.02	0.44 ± 0.03**
T max/Mmax	0.22 ± 0.04	0.14 ± 0.03*
MVC (N)	521 ± 32	549 ± 30
Angular Velocity (°/sec)	534 ± 11	540 ± 20

Statistically significant at : * $p < 0.05$; ** $p < 0.01$; *** $p < 0.001$

DISCUSSION AND CONCLUSION

In a previous study, we show that 10 min of static stretching increases the range of joint motion without causing any changes in motoneurone excitability and muscle power capacity (Guissard et al, 1991). The present results indicate that training by static stretching induces a long lasting gain in the range of ankle joint motion The results show that this gain is associated with a decrease in the Hmax/Mmax and Tmax/Mmax ratios. The larger decrease in the latter ratio suggests that not only the motoneurone excitability changes, but also the spindle sensitivity. However, the finding that the gain in the range of motion is still present at a time when both reflexes have returned to the control values favours the idea that the gain is not closely controlled by the neural changes and thus is mainly related to modifications to mechanical properties.

REFERENCES

- Ekstrand, J. and Gillquist, J. (1982) The frequency of muscle tightness and injury in soccer players. Am. J. Sports Med. 10:75-78.
- Etnyre, B.R. and Lee, E.J. (1988) Chronic and acute flexibility of men and women using three different stretching techniques. Res. Quart. 59:222-228.
- Guissard, N., Duchateau, J. and Hainaut, K. (1988) Muscle stretching and motoneuron excitability. Eur. J. Appl. 58:47-52.
- Guissard, N., Duchateau, J. and Hainaut, K. (1991) Acute effect of static stretching on neural and mechanical properties of the human Triceps Surae. Abstracts 8th International Congress on Biomechanics (Perth), 264-265.

This work was supported by the Université Libre de Bruxelles and NATO (RG n°930261)

SHORT-TERM POTENTIATION OF POWER PERFORMANCE INDUCED BY MAXIMAL VOLUNTARY CONTRACTIONS [1]

Arne Güllich, Dietmar Schmidtbleicher

J. W. Goethe-Universität, Insitut für Sportwissenschaften, Ginnheimer Landstraße 39, 60487 Frankfurt/Main, Germany

INTRODUCTION

The competitive results in many events mainly depend on the athletes' power. Numerous reports from top athletes show that best power performances are obtained directly after carrying out some heavy resistance exercise. The aim of the present study was to compare athletes' power output before and immediately after maximal voluntary contractions (MVCs).

METHODS

28 power event athletes volunteered for the study. In order to estimate the power output of the lower extremities, countermovement-jumps and drop-jumps (CMJs, DJs) were carried out. The calculated retest-reliability coefficient for the mean center of gravity (CG) height of 8 jumps was r_{tt}=.98 (e_sx=0.8 cm). The jumps were recorded before and after unilateral isometric leg extensors MVCs. For the investigation of the power output of the arms' extensors, the athletes were placed dorsally on a table. They were asked to push a light bar vertically (test 'bar push'). A photoelectrical receptor system permitted the measurement of the displacement-time-relation of the bar movement with an accuracy of 4 mm and 1/50000 sec. The retest-reliability coefficients of the measurements were between r_{tt}=.90 (t_{4mm}; e_sx=1.86 ms) and r_{tt}=.99 (t_{40cm}; e_sx=3.81 ms). MVCs were conducted in the same movement.

5 sessions with different treatments (maximal and submaximal contractions with different rest intervals) were carried out.

RESULTS

In the first session, 2 control sets of CMJs were recorded. While the subjects' mean CG height was 0.1 cm less in the second set, they jumped 1.1 cm higher, immediately after 3 MVCs (2.6%, p<.01; see fig. 1). Similar effects were induced by all tested variations of maximal contractions. In the DJs, the contact time was almost constant, but post-MVC, the height of CG was enhanced significantly (3.2%, p<.05).

The movement times in the test 'arm push' were increased by 1.5 to 2.8% in the second control set of session 1. After 3 MVCs, primarily the times of the initial part of the movement were reduced (t_{4mm}: 12.3%, p<.01). All the different treatments of MVCs induced t_{4mm} decreases between 9.3% and 12.9% (p<.05). The improvement of initial movement behaviour revealed a considerable left-shift of the whole velocity-time course. A decrease of only 2.8% at t_{4mm} was found after sub-MVCs (3x90%; p>.05). Consequently, there exists no remarkable left-shift of the velocity-time-curve.

DISCUSSION

The data from the test 'arm push' suggest that the observed short-term power improvements can be ascribed to an enhancement of rate of force development (RFD). Since morphological changes within the contractile proteins are merely unlikely between pre- and post-test (up to 12 min.), it is assumed that the changes are related to enzymatic alterations and/or an increment of the neuromuscular activation. Probably, the presented data have to be interpreted, considering the mechanisms of the posttetanic potentiation

[1] This project has been supported by the Bundesinstitut für Sportwissenschaft, project number VF 0407/05/20/94

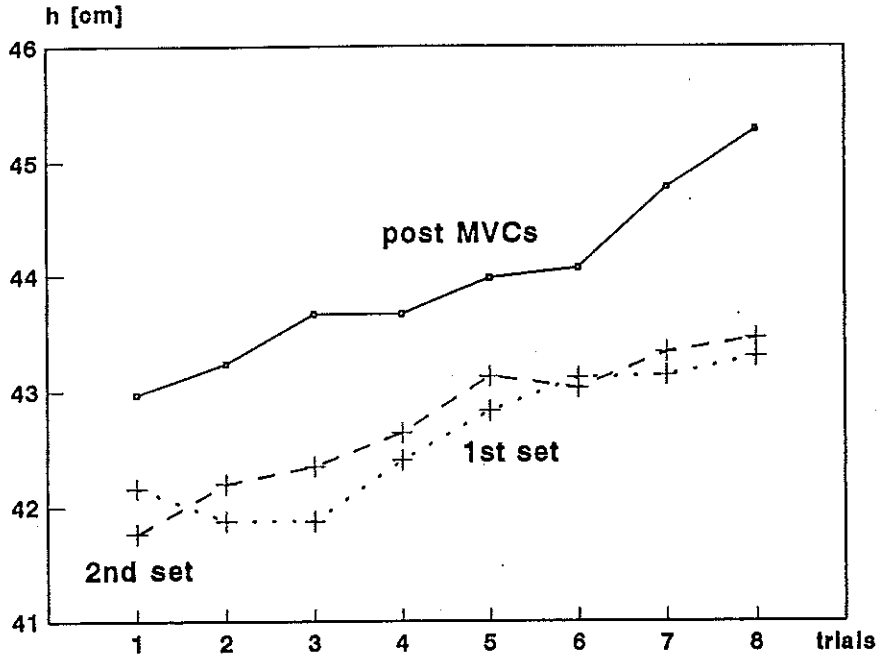

Fig. 1: CMJ height before (sets 1 and 2) and post-MVCs. n = 26. $p < .05$.

(PtP). This consideration obtains support from the results of H-reflex measurements that were carried out with 5 physical education students: Following 5 MVCs of triceps surae, the M- and H-wave amplitudes recorded at m. gastr., were increased (H: 25%; $p<.05$; M: $p>.05$).

After high frequency stimulation of synaptic connections, such as effected during MVCs, the synaptic efficacy is enhanced for a few minutes. These changes can presumably be attributed to an increment of transmitter output, and a remaining postsynaptic membrane potential shift. These factors raise the activation probability of each motoneuron (LÜSCHER et al. 1983, KOERBER/ MENDELL 1991, GOSSARD et al. 1994). Additionally, the actomyosin cycling rate is probably altered due to a higher degree of Myosin-LC-phosphorylation (HOUSTON et al. 1985).

References

GOSSARD, J.-P./ FLOETER, M.K./ KAWAI, Y./ BURKE, R.E./ CHANG, T./ SCHIFF, S.J.: Fluctuations of excitability in the monosynaptic reflex pathway to lumbar motoneurons in the cat. J. Neurophysiol. 72 (1994) 1229-1239

HOUSTON, M.E./ GREEN, H.J./ STULL, J.T.: Myosin light chain phosphorylation and isometric twitch potentiation in intact human muscle. Pflügers Arch. 403 (1985) 348-352

KOERBER, H.R./ MENDELL, L.M.: Modulation of synaptic transmission at Ia-afferent connections on motoneurons during high-frequency afferent stimulaton: Dependence on motor task. J. Neurophysiol. 65 (1991) 1313-1320

LÜSCHER, H.-R./ RUENZEL, P./ HENNEMANN, E.: Composite EPSPs in motoneurons of different sizes before and during PtP: Implications for transmission failure and its relief. J. Neurophysiol. 49 (1983) 169-289

THREE DIMENSIONAL FINITE ELEMENT MODELLING OF HUMAN SCAPULA USING COMPUTER TOMOGRAPHY.

S. Gupta [1,3], F.C.T. Van der Helm [1], C.W. Spoor [1], A.L. Schwab [2], B. L. Kaptein [1]

[1]Laboratory of Measurement & Control, WbMT-MR, [2]Technical Mechanics, WbMT-TM, Delft University of Technology, Mekelweg 2, 2628 CD Delft, The Netherlands.
[3]Dept. of Applied Mechanics, Bengal Engineering College, Howrah 711 103, W.B, India.

Introduction

The finite element method (FEM) has become an indispensable tool in orthopaedics research to estimate stresses and strains in various bones and in endoprostheses. FEM calculations can reveal the stress field within the bone and help in the design and development of total joint replacements. The shoulder is a complex structure in the human body with a large range of motions. The most important joint in the shoulder girdle is the glenohumeral joint connecting the scapula and the humerus. Failure of the glenoid component of a shoulder prosthesis by loosening is a well- known problem. It takes FEM to analyse a possible mechanical cause of the loosening.
Research on glenoid arthoplasty requires reliable data on mechanical properties of scapula trabecular bone. Such properties can be estimated from computer tomography (CT) scans by using relations between the apparent density, elastic modulus and CT grey values. For a long term reliability of a prosthesis, it is also necessary to simulate adaptive bone remodelling.
Objectives of this study are:
(1) to find expressions relating apparent density and elastic modulus to CT grey values
(2) to generate, using these two expressions, a 3D finite element model of irregularly shaped bone like the scapula from CT scans.

Methodology

A cadaveric scapula was treated with hydrogen peroxide to remove soft tissues. CT scans of the dried scapula were made at the Department of Radiology, Academic Hospital Leiden, on a Philip CT scanner of type SR7000. Images had 320 X 320 pixel of size 0.5 X 0.5 mm; the slice thickness was 3 mm. A total number of 66 slices were obtained to cover the whole scapula. The images were transferred to a SUN SPARC10 workstation and with the help of image processing software (SCIL - Image) the position of the pixel were related to the corresponding CT grey values. Bone contours were found in each CT slice with the help of an optimization procedure - the 'minimum cost method'. The coordinates of the points defining a bone contour were stored in a MATLAB file and were converted into ASCII format. Keypoints were generated from contour data for each CT scan slice. Splines through the keypoints approximated the contours and were used to define areas. This procedure was repeated for all CT slices. A skin like area was generated by connecting the approximated contour of two consecutive slices. Volumes between two slices were obtained by connecting the upper, lower, and skin like outer surface area of two adjacent slices.

Element selection and generation

In reality the structure of scapula consists of an outer hard, dense cortical shell and an inner solid cancellous bone region. The main reason for using shell elements is the presence of a very thin bony shell in the nearly flat part of the scapula. Modelling this part by solid elements would either require too many elements, or the elements would be too distorted. Once shell elements are present in the model, it seems only logical to represent also the cortex by shell elements. The combination of solid and shell elements will not only represent a realistic model of scapula but also reduce computational time and complexity. The cortical shell was modelled as 3D eight-node shell elements with bending stiffness. The inner volume was filled with 3D twenty-node solid elements. The shell elements can be overlaid on the solid elements so that they share common nodes.

Assigning material properties

The position of the centroid of each element and the equivalent cubic volume are mapped onto the original CT images. The average CT grey value for the cubic volume is calculated and can be related to material properties.

Characterization of properties and relations

A linear relationship: $\rho = 0.0004\ H + 0.5099$

was used to describe the apparent density ρ ($g.cm^{-3}$), as a function of H (CT grey value in Hounsfield units).This relation was determined by two points. The first point represents the absence of bone (0 $g.cm^{-3}$) for which the CT grey value is -1200. The second point is represented by the density of cortical bone (1.8 $g.cm^{-3}$) having CT grey value 2895. Apparent density and elastic modulus of scapula trabecular bone samples were obtained from Frich (1994). A third order polynomial regression curve:

$$E = 171.4\ \rho - 98.3\ \rho^2 + 2166.4\ \rho^3$$

was calculated to relate the elastic modulus E (MPa) to the apparent density ρ ($g.cm^{-3}$), with correlation coefficient, R= 0.96.

The matrix containing, the CT grey values, for all elements can be read into ANSYS and the values of density and elastic modulus can be obtained using the above relations.

The material properties for each element can be assigned to the finite element model by proper input statements.

Conclusions

This study enables us: (1) to build a good representation of the scapula, (2) the methodology can be applied to other bones in vivo.

In the near future this data will be combined with the musculoskeletal model of the shoulder to obtain realistic estimates of force acting on the scapula.

Reference

(1) Frich.L.H., Glenoidal Knoglestyrke og knoglestruktur; University Hospital Aarhus, Denmark, 1994.

(2) Van der Helm FCT, The Shoulder Mechanism A Dynamic Approach, Ph.D Thesis, Delft University of Technology, 1991.

Arm postural stiffness field variations with external loads

Irina Gurevich and Tamar Flash
Dept. of Appl. Math. and Computer Science, Weizmann Inst. of Science, Rehovot, Israel

INTRODUCTION

Previous studies have demonstrated that the mechanical behavior of a two-joint arm can be described as being *spring-like* [2]. The mechanical interactions between the limb and the environment were characterized by the arm stiffness field. Experimentally measured stiffness matrices were graphically represented as ellipses characterized by their size, shape and orientation. It was found that the postural hand stiffness ellipses are oriented in a polar direction with the major axis pointing along the radial direction [5], [2].

The present study was aimed at characterizing and modeling the arm stiffness field during the maintenance of posture in the presence of external loads. This was part of a more extensive study aimed at investigating motor adaptation to the unexpected introduction of elastic loads. Here, we have analyzed the static stiffness field measured at different arm configurations in the horizontal plane both in the absence and presence of external bias forces.

METHODS

Hand stiffness measurements during posture were performed using a two-degrees-of-freedom planar manipulandum. The data were processed using a similar procedure to the one described in [2]. For each measuring condition the elements of the hand stiffness matrix were computed and geometrically represented by the stiffness ellipse.

RESULTS

We have investigated the effects of bias forces on the characteristics of the arm stiffness field and statistical analysis was applied to assess those effects. The results indicated that the polar orientation of the hand stiffness field observed in the unloaded case is maintained in the presence of external loads while both the size and shape of the stiffness ellipses vary with the loads. To examine the effect of arm configuration $\vec{\Theta}$ and the magnitude and direction of an external force $\vec{F}$ applied at the hand on the joint stiffness matrix R, it was derived from the measured hand stiffness matrix K as follows:

$$R = J^T(\vec{\Theta})KJ(\vec{\Theta}) + \frac{\partial J^T(\vec{\Theta})}{\partial \vec{\Theta}}\vec{F}, \quad (1)$$

(see in [4]), where $J(\vec{\Theta})$ is the arm Jacobian.

MODELLING THE JOINT STIFFNESS FIELD

Based on the experimental results we developed a mathematical model which has successfully accounted for the experimentally observed variations in the elements of joint stiffness matrix as a function of the external loads. The force T generated by a neurally activated muscle was modeled by an exponential torque/angle relationship expressed as follows:

$$T = A(\epsilon^{\alpha r(\theta-\theta_0)} - 1), \quad (2)$$

where r is the muscle moment arm, θ is the joint angle and θ_0 is the joint angle

elbow and two-joint groups of muscles which contribute to different elements of the arm joint stiffness matrix. Based on mathematical analysis we have shown (Gurevich [3]) that given that the static stiffness field has a polar orientation in both the loaded and unloaded cases, and using the above nonlinear muscle force/angle relationship, all four elements of the joint stiffness matrix in the loaded case can be represented by:

$$R_{ij}^{L} = C R_{ij}^{0} + a_{ij} T_1 + b_{ij} T_2, \tag{3}$$

where C is a constant gain factor representing the amount of co-contraction, R_{ij}^{0} is the corresponding joint stiffness element in the unloaded case, a_{ij} and b_{ij} are coefficients whose values depend only on arm configuration and muscle parameters, and T_1 and T_2 are the shoulder and elbow joint torques exerted by the external load. To test the validity of this model (3), the values of the unknown parameters $C, R_{ij}^{0}, a_{ij}, b_{ij}$ were chosen so as to minimize the squared errors between the values of the joint stiffnesses (R_{ij}^{L}) estimated according to (3) and their measured counterparts for all subjects at all the different measuring positions.

DISCUSSION

Our joint stiffness model which was developed based on the assumption that postural control is associated with the setting of the muscle rest lengths, successfully accounted for the observed joint stiffness variations. This model suggests a possible control strategy which the nervous system may use when adapting the motor output to various external conditions. This strategy involves arm stiffness modification while maintaining the polar orientation of the stiffness field. Moreover, the stiffness field in the presence of the loads was found to result from the summation of stiffness components responsible for maintaining posture in the unloaded case and load-related components linearly dependent on the externally applied joint torques.

References

[1] Feldman A.G. Change in the length of the muscle as a consequence of the shift in equilibrium in the muscle-load system. *Biophysics*, 19:544–548, 1974.

[2] Mussa-Ivaldi F.A., Hogan N., and Bizzi E. Neural, mechanical and geometric factors subserving arm posture in humans. *Journal of Neuroscience*, 5:2732–2743, 1985.

[3] Gurevich I. *Strategies of motor adaptation to external loads during planar two-joint arm movement.* PhD thesis, Dept. of Applied Mathematics & Computer Sc., The Weizmann Institute of Science, 1993.

[4] McIntyre J. *Utilizing Elastic System Properties for the control of Posture and Movement.* PhD thesis, Dept. of Brain and cognitive Sc. of MIT, 1990.

[5] Flash T. and Mussa-Ivaldi F. Human arm stiffness characteristics during the maintenance of posture. *Experimental Brain Research*, pages 315–326, 1990.

HUMAN MODELING IN 3-DIMENSIONAL VIRTUAL ENVIRONMENTS

Jari Haijanen, Pirkko-Liisa Rasa, Mikko Hirvonen, Arto Kuusisto, Heikki Laitinen

Finnish Institute of Occupational Health, Department of Safety

Vantaa, Finland

INTRODUCTION

A new generation of computer-aided human modeling systems has been developed during the last decade. These systems offer a large variety of possibilities to analyze and visualize human task behavior in a virtual enviroment, and they provide tools to evaluate workpaces and machinery already early in the design stage. One of the most advanced human modeling packages, called *Jack*™ software, has been developed at the University of Pennsylvania. This system aids in the definition, manipulation, animation, and analysis of human factors performance of human models.

In the *Jack* software, the body of the human model consists of 69 segments, 68 joints and 121 degrees of freedom, including a 17-segment flexible torso and fully articulated hands. This fully jointed dynamic 3-dimensional virtual figure includes both wire frame and solid models. The *Jack* software is controlled interactively by keyboard commands, by a mouse and pop-up menus, or it may be controlled externally through direct sensing of sensors. For example Badler et al. (1993) used the *Jack* software and an electromagnetic measurement system called Flock of Birds (FOB) for the simulation of human body motions.

The objective of the study was to evaluate the usability of the *Jack* software in the field of human factors design and ergonomics for developing a new clinical chemistry analyzer. The main effort was focused on the to realization of reliable human factors analysis with the human model.

METHODS

In the first phase, the main functions of the analyzer and daily working tasks of the users were defined in order to find the most crucial tasks. After that, a simplified 3-dimensional model of the clinical analyzer was made, and some specific work tasks were modelled using the *Jack* software.

The model of the clinical analyser was built by modifying the software's own geometrical objects, such as cylinders, cubes and planes. Three female and male (5, 50 and 95 percentile) figures were created by accessing the Spreadsheet Anthropometric Scaling System (SASS) (Figure 1). In the SASS a statistical population data is organized into segment dimensions, joint limits, centers of mass and strengths.

Various design alternatives, e.g. main dimensions of the analyzer and locations of the analysis equipment, were explored by viewing zone, reach and strength studies.

The *Jack* software was used to determine whether the work task in question meets the given ergonomic requirements, e.g. whether operator should have adequate field-of-vision, whether controls are reachable, and work tasks do not cause too much physical strain to the user.

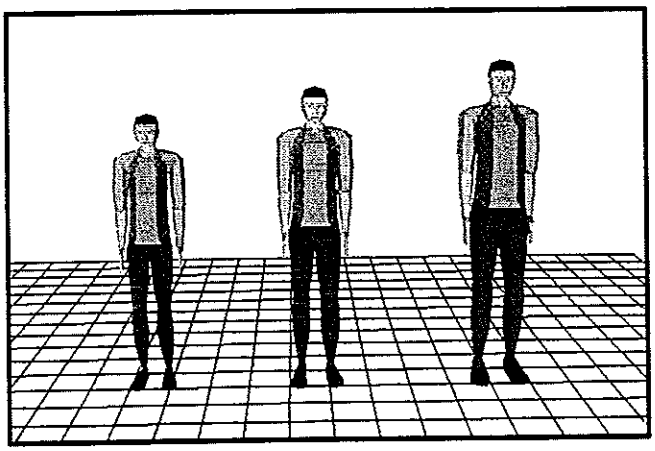

Figure 1. 5, 50 and 95 percentile *Jack* male figures made by the SASS.

RESULTS

In the analysis, the clinical analyzer was found to fulfill the demands of good ergonomics. However, some minor proposals for improvements were made.

The posture positioning of the fully jointed 3-dimensional human model was easy to do with the interactive interface. Illustrative static torque display windows made the strength studies rapid. Also, the visualization capabilities of the *Jack* software were excellent, because of the various additional windows, presenting the model's viewpoin, a 2-dimensional projected and a external camera view. On the other hand, the modeling of the analyzer should be somewhat easier, as well as the use of the SASS.

DISCUSSION

The *Jack* software contains familiar tools, such as the mouse and pop-up menus, which facilitate learning in the beginning. The average designer is able to operate the modeling system after a few days of training. The *Jack* software is very versatile and advanced. Therefore, the hardware requirements, user's expertise in human factors and ergonomics, and the time used by the user will increase in propotion to the opportunities of the software that are used during the design process.

In this study, the *Jack* software was used alone, with no additional modeling software; this caused some difficulties especially in the modeling of the analyzer. These problems could have been avoided, if the design of the analyzer had been done using a seperate CAD system and then transferred and converted to the *Jack* geometry. In general, the preferred method is to use previously made CAD designs, since the *Jack* software is laborious for modeling detailed virtual work environments.

Badler, N.,I., Hollick, M.J. & Granieri, J.P.: Real-time Control of a Virtual Human Using Minimal Sensors. Presence 1993; 2(1):1-5.

EFFECTS OF SCREW TYPE, MATERIAL, TOOL HANDLE SHAPE, AND WORKING LEVEL ON THE LOAD IMPOSED ON THE UPPER LIMB IN DRIVING SCREWS IN ASSEMBLY WORK

Marketta Häkkänen, Eira Viikari-Juntura and Esa-Pekka Takala

Department of Physiology, Finnish Institute of Occupational Health

Helsinki, Finland

INTRODUCTION

Musculoskeletal disorders in the upper limb constitute a major problem among assemblers. In a variety of industries their job characteristics involve frequent use of hand tools, repetitiveness, forcefulness and awkward wrist postures. These are known to be associated with the disorders of the hand and arm (Silverstein et al 1987). However, there is a lack of knowledge of the effect of workplace attributes such as the type of tool, materials and work level on the work load imposed on the upper limb. The aim of the present study was to measure the upper limb exposure in driving screws in assembly work. The study was a part of an intervention study which was designed to reduce musculoskeletal disorders in trailer assembly factory.

METHODS

An experimental set-up was constructed in the factory. It was used to measure both the force and the time needed to drive screws into different materials. The system consisted of a computer connected to a force plate on top of which pieces of materials were fixed. The apparatus was used both in the horizontal and vertical plane.

Six experienced female workers (mean age 37 years, range 19-58 years) drove ten screws in 24 different test settings in a random order. The settings were performed on two days and the worker had a rest of two minutes between each test setting. Screws were driven into three different materials: the wall of the trailer and two types of round strip of wood. Four different types of screws were driven into the trailer wall: long (34 mm) and short (19 mm) self-tapping and normal sharp screws. Each material-screw combination was tested on the vertical (height 114 cm) and horizontal surface (height 75 cm) both with an in-line and pistol handle screw driver. The work load was calculated as exposure:

$$(1) \qquad \text{exposure} = \int_{to}^{tf} F(t)dt$$

where t_0 = initial time of driving a screw or drilling

t_f = final time of driving a screw or drilling

$F(t)$ = force as a function of time.

The first screw of each setting was considered as training and was dropped out of the analysis. Differences between the exposures in different settings were tested with ANOVA.

RESULTS

The short self-tapping screw required a higher work load compared to a similar sharp point screw for both work levels and with both types of tools ($p<0.0001$) (Fig. 1). In case of long screws the situation was the same: sharp screws penetrated more easily

than self-tapping screws ($p<0.004$) in all test settings. There was a statistically significant difference between the two materials ($p<0.0001$) of the round strip of wood. For both types of wood, working with the pistol driver imposed lower exposure on the upper limb than with the in-line driver ($p<0.0005$). The use of pistol driver was less loading also in all other test settings, even though the differences in the exposures were smaller.

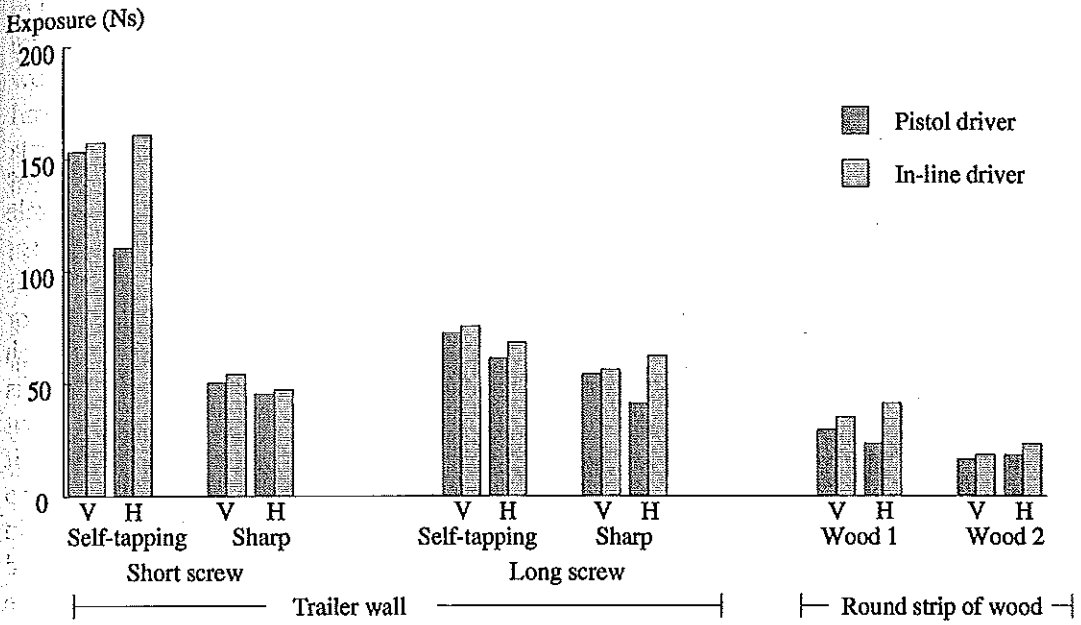

Figure 1. Average exposures (Ns) imposed on the upper limb in driving nine screws in different work settings (V=Vertical, H=Horizontal) (n=6).

DISCUSSION

Prior to this experiment a self-tapping screw mostly used in the assembly was supposed to be less force demanding than a sharp screw especially when penetrating hard materials, such as the trailer wall. The workers had complained about the difficult penetration of the short self-tapping screws and the experiment showed that the type of screw was a major determinant for the exposure. The point of the self-tapping screw was too dull to stick properly into the material in the beginning of driving the screw. Therefore the worker had to press down hardly and the screw had to be driven slowly to avoid its slipping away from the tip of the driver. Due to the long duration of driving the short self-tapping screws the exposure imposed on the upper limb was higher than the one of the long screws. Long screws could be supported with fingers in the beginning of driving a screw, which shortened the time needed for the penetration.

The lower exposure with the pistol driver in each test setting could be explained by the better control of the tool-screw combination by the workers.

Based on this experiment the self-tapping screws were replaced by the sharp ones and the material of the round strip of wood was replaced by the softer one. This lowered the daily exposure of the workers.

REFERENCES

Silverstein, B.A., Fine, L.J. and Armstrong T.J. 1986, Hand-wrist cumulative trauma disorders in industry, British Journal of Industrial Medicine, **43**, 779-784.

NEUROMUSCULAR ADAPTATIONS DURING BILATERAL VERSUS UNILATERAL STRENGTH TRAINING IN MIDDLE-AGED AND ELDERLY MEN AND WOMEN

K.Häkkinen[1], M. Kallinen[2], V. Linnamo[1], U-M. Pastinen[1], R. Newton[3] and W.J. Kraemer[4]

[1]Department of Biology of Physical Activity, University of Jyväskylä, Finland
[2]Peurunka - Medical Rehabilitation and Physical Exercise Centre, Laukaa, Finland
[3]Centre for Exercise Science, Southern Cross University, Lismore, Australia
[4]Centre for Sports Medicine, Penn State University, University Park, USA

INTRODUCTION

It is well known that the aging process, usually associated with a decline in the intensity of normal daily physical activity, leads to a great decrease in human muscle strength, especially at the onset of the sixth decade in both sexes. Age-related decreases in strength seem to be related to a great extent to the reduction in muscle mass which is thought to be mediated by a reduction both in the size of individual muscle fibres and / or a loss of individual fibres, especially of the fast twitch types. The extent to which voluntary neural drive to the muscles would probably decrease with increasing age is obviously much smaller than peripheral changes and may vary between the different muscles in relation to their decreased use in daily physical activities. On the other hand, it has been well established that considerable strength increases take place due to progressive strength training not only in young but also in older people. The increase in strength results both from increased motor unit activation of trained muscles and hypertrophy of muscle fibres, when the overall training intensity and the duration of the training period are sufficient (Frontera et al 1988, Charette et al 1991, Häkkinen & Pakarinen 1994). The purpose of the present study was to further investigate neuromuscular adaptations in middle-aged and elderly men and women during strength training. Our special interest was to compare adaptations of bilateral training for the leg extensors to those produced by training utilizing only unilateral exercises.

METHODS

Twelve middle-aged men and 12 middle-aged women in the 50-year age group (M50; range 44-57, W50; range 43-57), 12 elderly men and 12 elderly women in the 70-year age group (M70; range 59-75, W70; range 62-75) volunteered as subjects for the study. All subjects gave their written informed consent to participate in the investigation approved by the Ethics Committee of the University of Jyväskylä, Finland. The subjects were healthy and habitually physically active but they had no background in regular strength training. In this study the subjects participated in supervised strength training two times a week for 12 weeks. The training loads were 40 to 50 % of 1RM (1 repetition maximum) (10-12 reps for 3-4 sets) during the first four weeks, 60 to 80 % of 1RM (6-8 reps for 3-5 sets) during the next four weeks, and 70 to 90 % of 1RM (3-6 reps for 4-6 sets) during the last four weeks of training. Each session the subjects performed knee extension, knee flexion, trunk extension and flexion and two upper extremity exercises. One half of the subjects in each group performed the knee extension and flexion exercises bilaterally (BIL), while another half performed the exercises unilaterally (UNIL). The measurements taken two weeks before (-2), immediately before training (0), and 12 weeks after the training (12) included the recording of concentric 1RM for the knee extensors on a variable resistance David 210 machine both bilaterally and unilaterally. Electromyographic activity was recorded from the vastus lateralis (VL), vastus medialis (VM) and rectus femoris (RF) of both legs by surface electrodes and integrated to obtain maximum IEMG averaged for the knee extension and expressed for 1 s. The cross-sectional areas (CSA) of the quadriceps femoris muscles of the right and left leg were measured by ultrasonography (Aloka 190 LS).

RESULTS AND DISCUSSION

The present results are well supported by previous findings (Frontera et al 1988, Charette et al 1991, Häkkinen & Pakarinen 1994) and demonstrated that the progressive strength training led to great increases in maximal dynamic strength of the trained muscles both in the middle-aged and elderly men and women (Table 1). The increases observed in the voluntary maximum IEMG of the trained muscles indicate that considerable training-induced adaptations took place in the nervous system (Table 2). The enlargements noted in the CSA of the trained muscles in all groups suggest that considerable training-induced muscular hypertrophy may also take place both in middle-aged and elderly men and women, when the training intensity and the duration of the training period are sufficient. Interestingly, a strong specificity effect was observed so that the increases in bilateral strength were greater in BIL than in UNIL trained subjects (19% vs. 13%), while the increases in unilateral strength tended to be greater in UNIL than in BIL trained subjects. Although none of the present subject groups demonstrated a bilateral deficit as such (Archontides & Fazey 1993), the Bil/Unil strength ratio increased in BIL trained subjects, while UNIL trained subjects showed a slight decrease in this ratio. This specificity in strength development seemed to be related primarily to specific training-induced neural adaptations, because the increases in maximum IEMG during the bilateral contractions were greater in BIL than in UNIL trained subjects, while the increases in the maximum unilateral IEMG tended to be greater in UNIL than in BIL trained subjects. The degree of muscular hypertrophy did not differ significantly between BIL and UNIL trained subjects. In conclusion, one can suggest that to minimize effects of aging on the neuromuscular system, strength training could well be recommended as a part of an overall physical training program to maintain functional capacity of elderly people at as high a level as possible. Both bilateral and unilateral exercises are effective to produce neuromuscular adaptations but the magnitude of strength increase is specific to the type of exercise used.

Table 1 Percentage changes (± SD) in maximal concentric bilateral and unilateral strength (1RM) in bilaterally and unilaterally trained groups during the 12-week training

	Bil 1 RM	Unil 1 RM, right	Unil 1 RM, left	Bil/Unil r+l
BIL W50	18±9**	11±1***	27±13**	0±6
UNIL W50	12±5***	14±10**	17±10**	-2±6
BIL M50	22±12**	14±11*	13±7**	8±10
UNIL M50	17±9**	21±12**	17±10	-1±6
BIL W70	21±16*	11±9*	3±7	*[12±13
UNIL W70	12±9**	19±13**	16±21	-4±8
BIL M70	14±11*	6±7	6±5*	8±14
UNIL M70	12±10*	15±12*	7±5*	3±5
BIL All	*[19±12***	*[10±8***	11±11***	**[7±11**
UNIL All	13±8***	17±11***	14±14***	-2±6

Table 2 Percentage changes (±SD) in maximum IEMG (VL, VM, RF) and in cross-sectional area (CSA) of quadriceps femoris muscle during the 12-week training

	Bil. max IEMG	Unil; right, max IEMG	Unil; left, max IEMG	CSA
BIL All	*[19±19***	7±11*	8±22	14±12***
UNIL All	10±17*	9±15*	11±18*	11±6***

REFERENCES

Archontides, C. & Fazey, J. Inter-limb interactions and constraints in the expression of maximum force: A review, some implications and suggested underlying mechanisms. J. Sports Sci., 11: 145-158, 1993.

Charette, S., McEvoy, L., Pyka, G., Snovharter, C., Guido, D., Wiswell, R. & Marcus, R. Muscle hypertrophy response to resistance training in older women. J. Appl. Physiol. 70: 1912-1916, 1991.

Frontera, W., Meredith, C., O'Reilly, K., Knuttgen, H. & Evans, W. Strength conditioning in older men: skeletal muscle hypertrophy and improved function. J. Appl. Physiol. 64: 1038-1044, 1988.

Häkkinen, K. & Pakarinen A. Serum hormones and strength development during strength training in middle-aged and elderly males and females. Acta Physiol. Scand. 150: 211-219, 1994.

Acknowledgements:This study was supported in part by a grant from the Ministry of Education, Finland.

THE FORMULATION OF CONGRUITY AND THE PREDICTION OF THE RANGE OF MOTION OF A JOINT FROM BONE AND CARTILAGE MORPHOLOGY.

Hamilton, G. R., Thorne, C., Buckley, R. E., Vellet, D. A., Nigg, B. M., and Wyvill, B.

The University of Calgary, Calgary, Canada

INTRODUCTION

Joint congruity and range of motion (ROM) are two variables which are clinically relevant in the assessment of joints. Congruity is often a good predictor of joint recovery after trauma (Paley and Hall, 1989). ROM is often included in outcome measures of joint rehabilitation (Crosby and Fitzgibbons, 1990). Joints with an abnormal ROM or congruity have a higher incidence of osteoarthritis, pain and aberrant kinematics than normal joints (Paley and Hall, 1989).

Despite the general agreement of the importance of these two variables, there are problems in their implementation. First, an adequate formulation of congruity is not available. Second, an indication of the rehabilitated ROM cannot always be assessed post-trauma.

The ***purpose*** of this paper is to present an adequate formulation of congruity and to use this formulation to develop a method to predict and image the rehabilitated ROM for selected joints. The proposed method is applied to the subtalar joints of ten patients with unilateral calcaneal fractures.

The ***relevance*** of the developed method for predicting the rehabilitated ROM lies in the fact that it can be used in situations where other techniques cannot be used. The method uses one 3-D data set of the joint of interest. The method does not require the patient to move painful, swollen or temporarily immobilized joints since the rehabilitated ROM is predicted using theoretical calculations.

METHODOLOGY

The methodology requires the formulation of congruity for joints with two bones. For the purpose of this paper, congruity is defined as the area of cartilage contact under the constraints that the volume of bone and cartilage deformation are equal to zero and a constant (V_o) respectively. A joint may therefore exhibit high congruity in one position and low congruity in another position.

Some joints exhibit a high congruity between opposing articular surfaces only within their physiologic range of motion (ROM). Outside of the physiologic ROM for these joints, the congruity is small. This behavior is exploited to image these joints moving through a predicted ROM.

First, a high resolution 3D data set of the joint is obtained by CT or MRI. The structures of interest (namely the bones and cartilage) are extracted from the 3D data set with the help of an interactive program. Using this simplified data set, one bone can be computationally repositioned with respect to the other. Congruity is defined in those joint positions in which the volume of cartilage-cartilage deformation is equal to V_o and the volume of bone-bone overlap is equal to zero.

The six dimensional space which registers the relative position of the bones contains the true ROM of the joint. The predicted ROM is found by optimizing with respect to congruity in successive slices through this six dimensional space. The choice of the dimension and orientation of the slices depends on the joint studied (Figure 1). The extreme joint positions are identified by either a small, threshold congruity or a high congruity gradient (Figure 2).

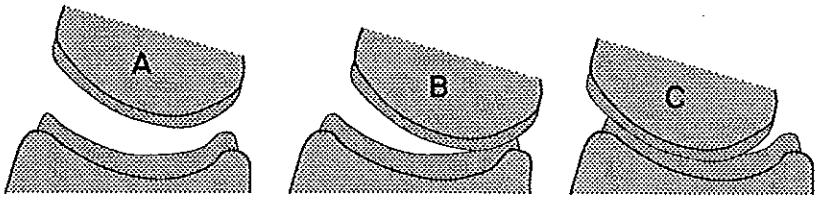

Figure 1. For this joint, ROM is predicted by optimizing congruity for different relative rotations of the two bones. (A), (B) and (C) all have the same relative rotation. Congruity is not defined for (A), but is defined for (B) and (C). (C) is a position in the predicted range of motion because its congruity is maximal for its relative rotation.

The final step is the imaging of the predicted range of motion which can be accomplished by standard techniques in computer graphics. Validation of this range of motion is obtained by making sure that the joint position at which the CT or MRI was taken (a point in the true ROM) is close to some point in the predicted ROM.

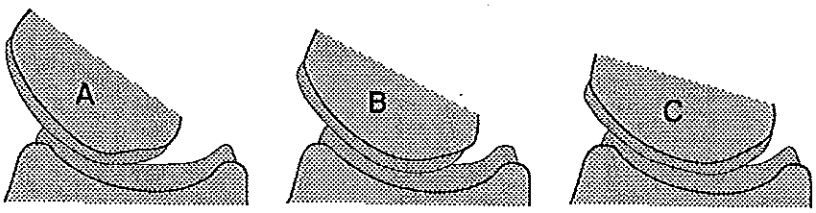

Figure 2. (A), (B) and (C) are three joint positions for which congruity is maximal (see Figure 1). (A) exhibits less congruity than (B) which exhibits less congruity than (C). The predicted ROM of the joint may exclude position (A) if the threshold congruity is chosen large enough.

APPLICATION

The methodology was applied in vivo to 10 patients with a unilateral displaced intra-articular calcaneal fracture. Each patient was managed conservatively. Both the injured and uninjured joints had a high resolution MRI taken within 7 weeks of the injury.

RESULTS

The rehabilitated ROM of the subtalar joint was calculated and imaged for the 10 injured and 10 uninjured subtalar joints. Each patient's recovery was predicted based upon the rehabilitated ROM of their injured subtalar joint relative to their uninjured joint. The 10 patients are currently being followed. In an upcoming clinical paper, each patient's predicted recovery will be compared to their actual recovery as reflected in standard outcome measures of the injury.

REFERENCES

Paley, D.; Hall, H. (1989) Calcaneal fracture controversies: can we put Humpty Dumpty together again? *Orthop. Clinics of North America* **20**, 665-677.

Crosby, L. A.; Fitzgibbons, T. (1990) Computerized tomography scanning of acute intra-articular fractures of the calcaneus. *J. Bone and Joint Surgery* **72-A**, 852-859.

MULTI-MEDIA TECHNOLOGY FOR MOVEMENT ANALYSIS TO ASSIST CLINICAL DECISION MAKING

J. Harlaar, E.H. Hautus

Dept. Rehabilitation Medicine / Dept. Clinical Physics & Engineering
Free University Hospital, Amsterdam, Netherlands

INTRODUCTION

It has been the subject of many discussions why the useful clinical applications of biomechanical movement analysis for individual patients are scarce (e.g. Brand [1993]). In the scientific context of biomechanics, movement analysis is aimed at a complete mechanical description of the movement, e.g. gait. This includes time courses of the kinetics and the kinematics of the joints, regarding the human body as a model of linked rigid segments.

In our approach, the clinical problem is taken as a starting point. In clinical practice the movement of the patient is analyzed by observation. Doing so, many implicit assumptions are made about the function of not directly observable variables, e.g. joint load and muscular co-ordination. As therapeutic alternatives might be aimed at changing impairments of these functions, an explicit expression of them potentially serves clinical decision making.

INSTRUMENTATION

The patient's movement is recorded using a video-camera and a videocassette recorder. Simultaneously, depending on the specific analysis, the foot reaction forces and/or surface EMGs are recorded. Off-line, the video recordings are transferred to a computer (i.e digital video), by using Motion-JPEG compression hardware. A specialized multi-media application program (called 'SYBAR') was developed to display the video-recordings together with the synchronized display of foot reaction-vector (see also [Lanshammer 1988]) or the actual EMG-values (see also Goodwin [1991]) or both. The analysis of the movement can be done interactively, by the clinician, in slow motion or frame-by-frame, to carefully assess the impairments

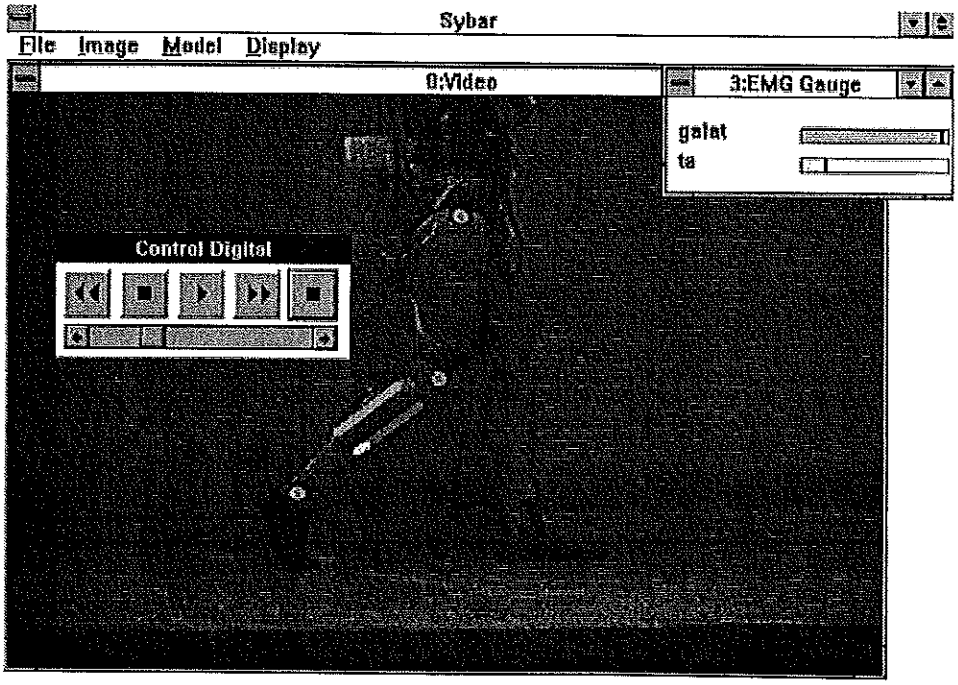

Fig.1 *Display of SYBAR, showing the digital video with two EMG activation levels, in a separate window, as well as superimposed at the location of the muscles.*

considered for treatment. Furthermore, after image processing each of the frames of the video-recording (automatically performed by SYBAR), the EMG activation levels of several muscles are displayed at the location of the specific muscle. So muscle activation is visualized in a way that clinicians really can 'see' contracting muscles (see fig.1)

EVALUATION

SYBAR was subjected to evaluation in clinical practice. The system showed several advantages over tape recorded registrations. The system is much more versatile in its possibilities to display the variables of interest, in relation to the recorded movement. Especially the annotation of the video recording with the muscle and joint functions at relevant anatomical locations was appreciated. Also during playback the recording can be randomly accessed, enhancing both the interactive analysis of the motion, as well as the retrieval of patient-records.

DISCUSSION

The clinical appreciation of this system is owed to the fast and clear description of muscle and joint function within the familiar observational analysis. The annotation of biomechanical parameters to each subsequent image of the video-recording is both resembling and extending current clinical practice. Even more important is that through the visualization, biomechanics gets an apparent meaning for clinicians. Multi-media technology serves as a language to communicate between biomechanics versus rehabilitation medicine, orthopaedics, neurology etc.. This opens up the possibility that clinical problems, will be stated in terms of certain physical parameters, that can be measured using a biomechanics approach, see also Andriacchi [1992]. It is to be expected that a biomechanical assessment that pinpoints the clinical problem, will yield a greater rate of clinical success (when subjected to the acid tests, see Brand [1993]), than an assessment that starts with a complete full 3D movement analysis. Fortunately, it has also been shown that systems based on video are almost equally accurate as full 3D movement analysis systems, regarding the most clinical applications [Lanshammer 1993].

The system will be elaborated to be applied on several clinical problems. Typical applications already reported in literature: the selection of surgical planning (i.e. tendon-releases, -lengthening or -transfers) [Perry et al. 1974] e.g. correcting equinovarus during gait; indication for high tibial osteotomy [Promodos et al. 1985]. These are readily available, future applications are the assessment of functional cocontraction for active knee stabilisation, and evaluation of the alignment of prosthesis.

CONCLUSION

Biomechanical assessment of impaired functions using visualization through multi-media technology has a great potential in assisting clinical decision making.

REFERENCES

Andriacchi TP (1992) Clinical applications of gait analysis *Proc. of NACOB II.* pp. 295-298

Brand RA (1993) Biomechanical assessments for clinical decisions *Book of abstracts, XIV Int. Congr. Biomechanics* (ed: S Metral) pp: 44-45

Goodwin J, et al. (1991) A novel EMG/video system for the analysis of movement. *Int. Disabil. Studies* **13**, 23-25

Lanshammer H (1993) Force vector visualization versus full 3D gait analysis. *Book of abstracts, XIV Int. Congr. Biomechanics* (ed: S Metral) pp: 754-755

Lanshammer H (1988) VIFOR - A system for force line visualization. In: *Biomechanics XI-B*, ed: G de Groot, P Hollander, P Huijing, GJ vanIngen Schenau, Free Univ. Pr., Amsterdam, pp. 984-988

Perry, J. et al. (1974) Gait analysis of the triceps surea in cerebral palsy. A preoperative and postoperative clinical and electromyographic study. *J Bone Joint Surg* **56A** 511-520

Promodros, CC et al.(1985) A relationship between knee joint loads and clinical changes following high tibial osteotomy *J Bone Joint Surg* **67A** 1188-1194

THE SPRINT START: A KINETIC AND KINEMATIC COMPARISON OF SLOW VERSUS FAST STARTERS

M. J. Harland, J. R. Steele and M. H. Andrews
Department of Biomedical Science, University of Wollongong, Wollongong, Australia

INTRODUCTION

Track coaches advocate a good start as being essential to winning sprint races. In the 100 m, 200 m and 400 m track sprints, the start is a crucial skill that must be refined if one is to maximise the sprinters performance over the race distance. Tellez & Doolittle (1984) reported that clearance time from the starting blocks accounted for approximately 5% of the total time of a 100 m race. However, a good start can contribute much more to a race than merely reducing block clearance times. Efficient acceleration over the first portion of the race is also influenced by the way the sprinter is positioned in the blocks at the set command, and the mechanics displayed as the athlete leaves the blocks at the sound of the gun (Tellez & Doolittle, 1984). High performance levels over 100 m have been related to correspondingly high performance levels in the block start and acceleration phase of a race up to 20 m (Baumann, 1976). Identifying variables that distinguish fast from slow starters can better direct the improvement of sprinters learning the skill of block starting. Therefore, the purpose of the present study was to compare selected kinematic and kinetic variables, displayed by slow starters versus fast starters performing a sprint start to identify which variables contributed to a faster start technique.

METHODS

Twenty six male 100 m sprinters (mean age = 23.1 ± 4.1 years) performed three maximal sprint starts, accelerating 15 m, from a set of blocks instrumented to record force-time histories (1000 Hz). Motion was filmed from a lateral view (100 Hz) with a 16 mm LOCAM high speed camera, time-synchronised to the instrumented blocks. From the high speed film, the time taken for each subject's total body centre of gravity (TBCG) to displace 2.5 m from initial force production was determined using their fastest trial. This criterion was then used to identify the 12 fastest starters (Group A) and the 12 slowest starters (Group B). The film data was digitised into cartesian coordinates and smoothed using a fourth order Butterworth filter (10 Hz). Several kinetic and kinematic variables were then calculated for the time the subjects were in contact with the blocks (Block Phase) and during the Post Block Phase to toe-off of the second stride. *T*-tests for independent means were applied to the data to identify any significant ($p < 0.05$) differences in the starting technique displayed by subjects in Group A compared to Group B.

RESULTS

The mean time taken for Group A to displace their TBCG 2.5 m (0.90 s) was significantly faster (t = -7.270; p = 0.000) than that displayed by Group B (0.98 s). During Block Phase, mean horizontal block impulse normalised to body weight (also block velocity in the units of m.s) was significantly higher for Group A (3.54 ± 0.25 $N.s.kg^{-1}$; t = 2.534; p = 0.019) than Group B (3.21 ± 0.38 $N.s.kg^{-1}$). Total block time was found to be significantly less for Group A (0.351 ± 0.023 s; t = -2.948; p = 0.007) compared to Group B (0.381 ± 0.028 s). Block acceleration for Group A was found to be significantly higher (10.16 ± 1.22 $m.s^{-2}$; t = 3.622; p = 0.002) than Group B (8.46 ± 1.09 $m.s^{-2}$). In the Post Block Phase, Group A was found to have their TBCG significantly further ahead of the toe of the support foot at the beginning of first ground

contact (0.065 ± 0.059 m; t = -2.155; p = 0.042) compared to Group B (0.015 ± 0.56 m). During this first ground contact after leaving the blocks Group A elevated their TBCG significantly less (0.029 ± 0.020 m; t = -2.197; p = 0.039) than Group B (0.052 ± 0.030 m). At the beginning of the second ground contact, Group A was found to exhibit significantly greater knee flexion of the contacting lower extremity (112.1 ± 7.5°; t = -3.542; p = 0.002) compared to Group B (121.6 ± 5.5°). In addition, it was found that Group B displayed a significantly smaller rear hip angle (swing leg) (69.4 ± 10.7°) at loss of contact of the front block of the contralateral leg as compared to Group A (81.9 ± 9.4°; t = 3.027; p = 0.006). Of this 12.5° difference observed at loss of contact of the front foot, 8.5° was present at loss of contact of the rear foot (ipsilateral leg) with 1° being present at the set position (84.0° vs 85.0° for Group A and Group B respectively).

DISCUSSION

Subjects in Group A were able to displace their TBCG in less time over 2.5 m due largely to being able to leave the blocks sooner and at a higher velocity than could subjects in Group B. The significant difference in rear hip angle (swing leg) at front foot off block was due to increased rear hip flexion during the Block Phase for Group B. This may indicate that Group B lacked rear hip extension, extension which is necessary to facilitate force production on the rear block. This assertion appeared to be supported by the fact that Group B produced a lower, although nonsignificant, mean normalised impulse (0.96 ± 0.44 N.s.kg^{-1}) than Group A (1.26 ± 0.30 N.s.kg^{-1}; t = 1.988; p = 0.059). It is possible that the slower starters began to recover the rearward thrusting lower extremity before it was fully utilised to produce force. Gagnon (1978) reported a similar lack of rear foot force generation in slower sprint starters.

By maintaining a more anteriorly positioned TBCG with respect to their support foot at first ground contact potentially allowed subjects in Group A to reduce horizontal braking forces and maximise horizontal propulsive forces compared to subjects in Group B. An increased vertical TBCG displacement during the first ground contact for Group B indicated that vertical propulsive forces created during this phase for Group B were excessive, leading to a potential decrease in horizontal propulsive forces.

CONCLUSIONS

It was concluded that faster starters were characterised by the ability to exert a greater average horizontal force (normalised to body weight) while on the blocks, in less time compared to the slower starters. This enabled the faster starters to leave the blocks with a higher acceleration compared to the slower starters. Combined with a more effective alignment of their TBCG at first contact, this increased impulse created a superior start performance compared to the slower starters.

REFERENCES

Baumann, W. (1976). Kinematic and dynamic characteristics of the sprint start. In P.V. Komi (Ed.), Biomech. V-B, (pp. 194-199). Baltimore: University Park Press.

Gagnon, M. A. (1978). Kinetic analysis of the kneeling and the standing starts in female sprinters of different ability. In E. Asmussen & K. Jorgensen (Eds.), Biomech.V1-B (pp. 46-50). Baltimore: University Park Press.

Tellez, T., & Doolittle, D. (1984). Sprinting from start to finish. Track Technique, 88, 2802-2805.

LEG SPRING LINEARITY IN FORWARD HOPPING AND RUNNING JUMPING BY HUMANS

Michael J. Harwood[1], David G. Kerwin[2] and John H. Challis[3]

[1]Department of PE, Sport and Leisure, De Montfort University Bedford, UK
[2]Department of Sports Science, Loughborough University of Technology, UK
[3]School of Sport and Exercise Sciences, University of Birmingham, UK

INTRODUCTION

Research into the ground contact phase of running and hopping by humans has demonstrated a linear relationship between the mass centre vertical displacement and the vertical component of ground reaction force (Cavagna, Franzetti, Heglund, and Willems, 1988). This has been used to justify the use of a linear spring in simple mass-spring models of locomotion (for example McMahon and Cheng, 1990). However it has not been demonstrated that there is a linear relationship between the ground reaction force and the mass centre to foot distance, which could then be used to justify a linear mass-spring model for forward sagittal plane motion of the mass centre in these activities. Furthermore forward motion is generally asymmetrical in the sagittal plane; that is to say the body leaves the ground at a different velocity and inclination than that at which it touches down. This asymmetry has not previously been considered.

The purpose of this study was to investigate the relationship between sagittal plane ground reaction forces and mass centre to mid toe distance during a variety of forward hopping motions, and thus to determine the suitability of using a linear spring in a model of these activities.

METHODS

Film (Locam II model 51 at 50 frames per second) and sagittal plane force data (Kistler 9281-B12 at 1000 Hz) were recorded for a single bare-footed male subject performing: a) two footed forward hopping (symmetrical ground contact), and b) two footed jumps from the force plate onto a 0.3 m platform following a short run up (asymmetrical ground contact). Eight trials for each condition were recorded. In each trial a 2D Direct Linear Transformation was used to reconstruct the 14 body landmarks defining an 11 segment model of the subject. These data were then combined with the body segment inertial parameters of Dempster (1955) (summarized in Winter, 1990) to locate the subject's mass centre position in the first and last frames where the subject was airborne during the flight onto the force plate. From these two positions and knowing the time interval between them, the horizontal and vertical components of the mass centre velocity at force plate contact were calculated using the equations of constantly accelerated motion.

Using the initial mass centre position and velocity as determined from film, the mass centre position during plate contact was computed by numerical double integration of the force data. A simple mass-spring model of these activities was proposed, having a spring from the ground to the mass centre, therefore the mid-toe to mass centre distance was calculated to represent the 'spring length'. The ground reaction force magnitude was then determined and plotted against spring length during the plate contact period. The suitability of a linear spring model was assessed by computing the linear correlation coefficient between the force and length data.

RESULTS

Figures 1 and 2 show the force-length relationships and correlation coefficients found for the forward hopping and running two-footed jump conditions respectively. The directions of the arrows indicate the loading and unloading portions of the curves.

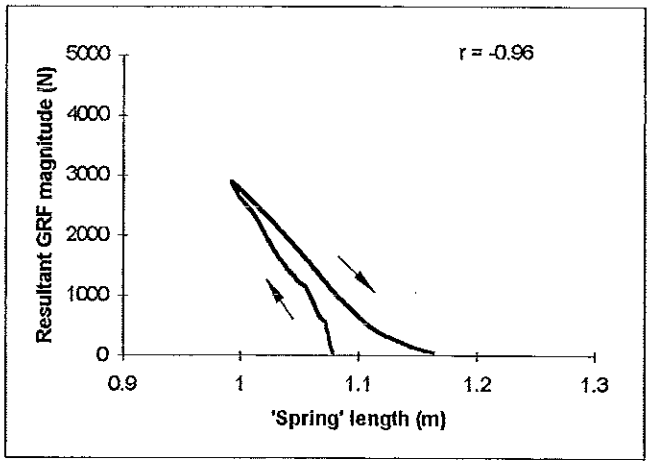

Figure 1: Resultant GRF magnitude-spring length relationship, and linear correlation coefficient (r) for force plate contact in forward two-footed hopping.

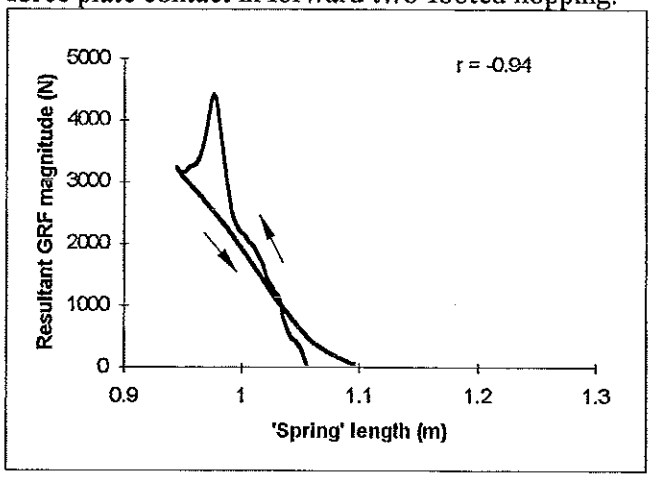

Figure 2: Resultant GRF magnitude-spring length relationship, and linear correlation coefficient (r) for force plate contact in a running two-footed jump.

DISCUSSION

Despite the complexity of the musculo-tendinous and skeletal structures involved in supporting the body, it has previously been demonstrated (Cavagna *et al.*, 1988) that a linear spring adequately represents the vertical rebound of the body from the ground. In this study the high linear correlation coefficients found between 'spring length' and ground reaction force supported the adoption of a linear spring for models of the sagittal plane mass centre motion. This was for both forward hopping and running jumping, i.e. symmetrical and asymmetrical ground contacts.

It was interesting that the early impact peak evident in the jump condition did not greatly affect the resulting correlation coefficient. In activities where a more compliant surface is used or compliant shoes are worn, for example gymnastic tumbling and vaulting or jogging, the fit of a linear spring would be expected to be even better, since the initial impact peak would be attenuated or nonexistent.

REFERENCES

Cavagna, G.A., Franzetti, P., Heglund, N.C. and Willems, P. (1988). The determination of the step frequency in running, trotting and hopping in man and other vertebrates. *Journal of Physiology*, 399, 81-92.

McMahon, T.A. and Cheng, G.C. (1990). The mechanics of running: How does stiffness couple with speed? *Journal of Biomechanics*, 23, 65-78.

Winter, D.A. (1990). *Biomechanics and Motor Control of Human Movement (Second edition)*. John Wiley and Sons.

ELECTROMYOGRAPHIC MANIFESTATIONS OF FATIGUE DURING REPETITIVE BRIEF MAXIMAL EXERCISE ON CYCLE ERGOMETER

C.A. Hautier, L.M. Arsac, A. Belli, J. R. Lacour
Laboratoire de Physiologie - GIP exercice, Univ. Lyon I, France

INTRODUCTION

Several authors have studied the influence of fatigue on Electromyographic (EMG) parameters during isometric and isokinetic contractions and stretch-shortening cycles. Kirsch and Rymer (1987) investigated the role of reflex regulation in neural compensation for muscular fatigue whereas Psek and Cafarelli (1993) studied the activation of coactive muscles during fatigue. The aim of the present study was to investigate neural modification caused by sprint repetition on a friction loaded cycle ergometer. The changes in activation level and coordination pattern of six muscles involved in explosive cycling task were studied.

MATERIAL AND METHODS

Ten subjects (8 males and 2 females) well trained in cycling sprint exercise volunteered to participate in this study (age, 20.2 ± 0.8 years [mean ± sd]; height 175.6 ± 7.2 cm; body mass 65.7 ± 8.5 kg).

Each subject performed on a friction loaded cycle ergometer series of 15 maximal sprints of 5 s duration with a 25 s rest period between each sprint. Sprints were performed without toe-clips and the frictional force was ordered to permit subjects to reach a maximal velocity of 150 rpm during the first sprint. Loads had been determined previously with several force-velocity tests and setted at 33.8 (± 11.8) N. Before and after the serie of 15 sprints, subjects performed a sub maximal cycling period of 2 min duration at constant velocity (60 RPM) with the load determined for the sprints. Mechanical and EMG data were recorded and analyzed during the first and the 13^{th} sprint and during constant velocity periods.

Mechanical measurements Cycle ergometer (Monark 818E, Stockholm, Sweden) was equipped with a strain gauge (200 N) for measurement of frictional force and an optical encoder (11815 points per pedal revolution) for measurement of the flywheel displacement. Force and displacement signals were sampled (200 Hz) and stored on a PC computer (386sx) via a 12 bits analog to digital interface card. First and second order derivatives of the flywheel displacement were calculated to obtain flywheel velocity and acceleration. External force produced by the subject was calculated as the sum of frictional (given by the strain gauge) and inertial (dependant of the flywheel acceleration) forces. Power output was computed as the product of instantaneous velocity by total force.

EMG measurements EMG signals from the Gluteus Maximus (GM), Rectus Femoris (RF), Vastus Lateralis (VL), Gastrocnemius Lateralis (GL), Soleus (SL) and Biceps Femoris (BF) muscles were recorded by use of bipolar Ag-AgCl surface electrodes (Biochip, Elmatek S.A., Crolles, France) including an amplifier (gain 600) and a pass band filter (6-600Hz) fixed longitudinally over the muscle belly. Raw EMG was electronicaly root mean squared (RMS) with a time averaging period of 25 ms and then converted and stored on the PC computer at the same resolution and sampling frequency than mechanical data (12 bits, 200 Hz).

Values were compared using Student's t-test with a significance level of 5%.

RESULTS

Sprint measurements The maximal force was obtained during the first downstroke. It was significantly ($p < 0.05$) decreased by sprint repetition (579.4 ±97.3 N vs. 553.5 ±96.7 N). Similarly, maximal power decreased significantly ($p < 0.01$) after the sprints (957.1 ±217.3 W vs. 849.3 ±199.3 W). EMG signal was constant during a sprint bout whatever the downstroke and the force recorded. There was significantly ($p < 0.01$) less RMS EMG for BF, GL and SL muscles. On the other hand, there was no difference in the activation level of the GM, VL and RF. The pattern of activation of these muscles was modified after sprint repetition. They were activated respectively 14.5, 13.7 and 16.9 degrees latter ($p < 0.05$) in regard with he crank angle. Other muscles coordination pattern was not modified at the end of exercise (figure 1).

Constant velocity measurements Power output and cycling velocity during the submaximal exercise were unaltered by sprint repetition ($p > 0.05$). RMS EMG

decreased significantly ($p < 0.01$) after sprint repetition for BF, SL and GL. On the other hand, there was no difference in the EMG level of the GM, VL and RF.
The pattern of activation of two muscles was modified by sprint repetition: VL and RF muscles were activated respectively 11.2 and 9.4 degrees latter ($p<0.05$) in regard with the crank angle. Other muscles coordination pattern was not modified.

figure 1 : Inter-muscular coordination pattern modifications relative to crank position (0 degree is the top dead center)

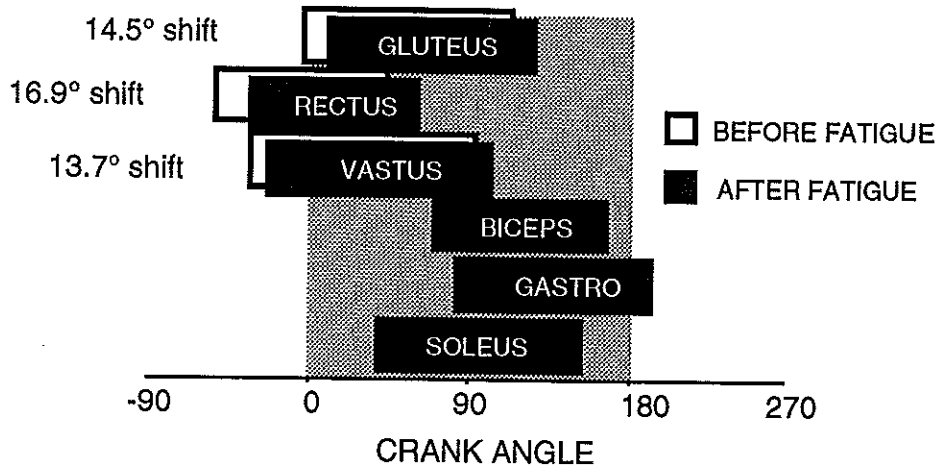

DISCUSSION

The main result of this study is that sprint repetition altered the mechanical properties of power producing muscle group and modified the co-activation level and inter muscular coordination pattern. The decrease of force and power associated with a constant EMG level (GM, VL, RF) is in line with the results of Greig et al. (1985). The EMG modifications observed during the sprints could be attributed to power and force changes but constant cycling period results (in which force and power are unchanged) confirmed the hypothesis that these changes are the manifestation of fatigue. Van Ingen Schenau (1992) proposed that mono articular muscles are responsible of power production and Broker and Gregor (1994) demonstrated that knee joint is the main contributor of total system energy. Therefore, it seems reasonable to conclude that GM, VL and RF muscles were selectively fatigued by sprint repetition. Moreover, this study showed that GL, SL and BF are less activated after fatigue. Such a regulation in activation level is line with the results of Kirsch and Rymer (1987) who demonstrated a neural compensation for muscular fatigue. It can be argued that GL, SL and BF muscles are less activated in order to prevent them to interfere in fatigued agonists muscles power production. However, Psek and Cafarelli (1993) obtained an increase co-activation with fatigue in an untrained subjects group.
The change in activation pattern observed in relation with fatigue can be attributed to a decrease in muscle fibre conduction velocity (MFCV). However, the decrease in MFCV can't explain the important time shift observed in this study. Such changes could be an adaptation of the coordination pattern to the fatigue status of power producing muscles in order to better use the other muscles. Moreover, changes in the time history of neural activation could be an original manifestation of the central fatigue reported by Gandevia (1992).

REFERENCES

Broker J. P., and Gregor R. J. (1994) Med. Sci. Sports Exerc., vol. 26, No. **1**, 64-74
Gandevia S. C. (1992) Sports Med. **13** (2), 93-98
Greig G., Hortobagyi T. and Sargeant A.J. (1985) J. Physiol. **369**, 180*P*
van Ingen Schenau G. J., Boots P. J. M., de Groot G., Snackers R. J. and van Woelsen W. W. L. M. (1992) Neurosci. vol. **46**, No **1**, 197-207
Kirsch R. F. and Rymer W. Z. (1987) J. Neurophysiol. vol. **57**, No. **6**, 1893-1910
Psek J. A. and Cafarelli E. (1993) J. Appl. Physiol. **74** (**1**), 170-175

THE EFFECTS OF RUNNING SPEED AND SURFACE ON MUSCLE ACTIVITY - A FIELD STUDY IN ORIENTEERING

E. HAVAS[1] and O-P. KÄRKKÄINEN[2]
1) LIKES-Research Center, Jyväskylä, Finland; 2) Danish Orienteering Federation, Kolding, Denmark.

INTRODUCTION

Orienteering is a popular outdoor sport in which the competition environment changes continuously. To evaluate the effects of varying running surface on the muscular work we measured the electromyographic activity of the leg muscles under different competition like circumstances in terrain.

METHODS AND SUBJECTS

Five danish international class orienteers ran at four self adjusted speeds in path (hard, even surface) and at three speeds in terrain (soft, uneven surface). The speed range was designed so that the last speed was maximum, and others competition and training speeds respectively.

Surface EMG was measured by a portable ME3000P device (MEGA ELECTRONICS, Kuopio, Finland) from *m. gastrocnemius* (GN) , *m. biceps femoris* (BF), *m. vastus lateralis* (VL) and *m. rectus femoris* (RF). The sampling frequency was 1000 Hz, each measurement lasted about 15 sec. Memory capacity of the device (1 Mb) allowed totally 2 minutes recording at time. Stored signal was processed and analyzed by the system included software. Raw signal was integrated (for 10 ms), and the integrated signal (IEMG) was used in analysis. The IEMG data was related to contraction time and the values from path and terrain were related to IEMG of maximal effort during a short steep uphill running.

RESULTS

A typical IEMG recording is presented in figure 1. It shows six consecutive steps in path (left) and terrain (right) at same running speed. The variation between steps is considerable in terrain but rather similar steps follow each other in path.

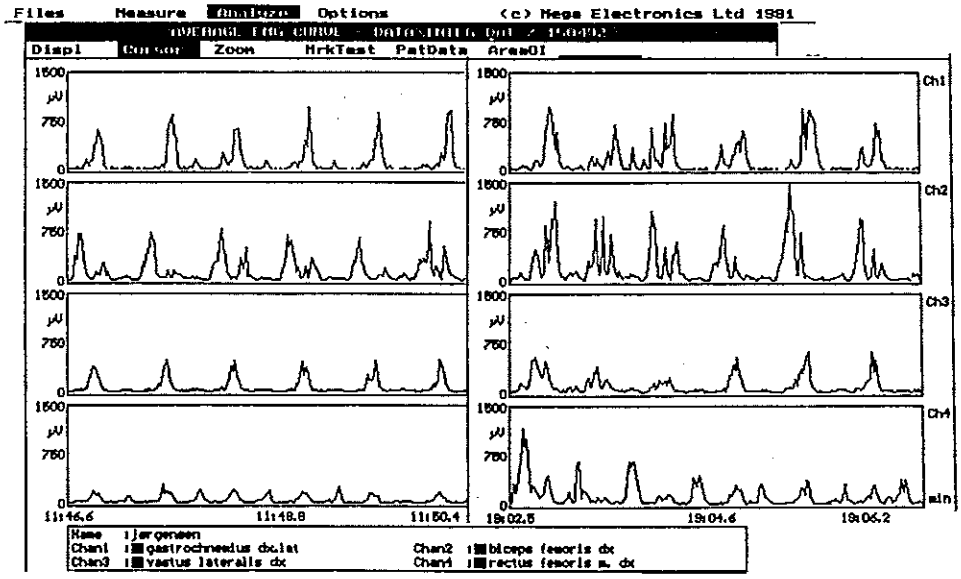

Figure 1. A typical IEMG in path (v=4.3 m/s) (left) and terrain (v=4.4 m/s) (right).

The increase in IEMG as function of running speed is presented in figure 2. The EMG activities in path running were 55-94 % and in terrain 55-80 % of those in the steep uphill. Except GN the muscle activities at same running speed were 5-10 % higher in terrain. The maximal IEMGs of VL and RF were the same in path and terrain, but those of GN and BF were 15-20 % higher in path.

The increase in speed in path was mainly due to the increasing activity of GN and BF, whereas the activities of VL and RF increased remarkably only when the speed was increased from 89 % to maximum. In terrain the activity of GN did not increase as much as did the activity of BF. VL and RF showed very similar patterns of increasing activity in path and terrain. Individual differences were remarkable in all muscles studied.

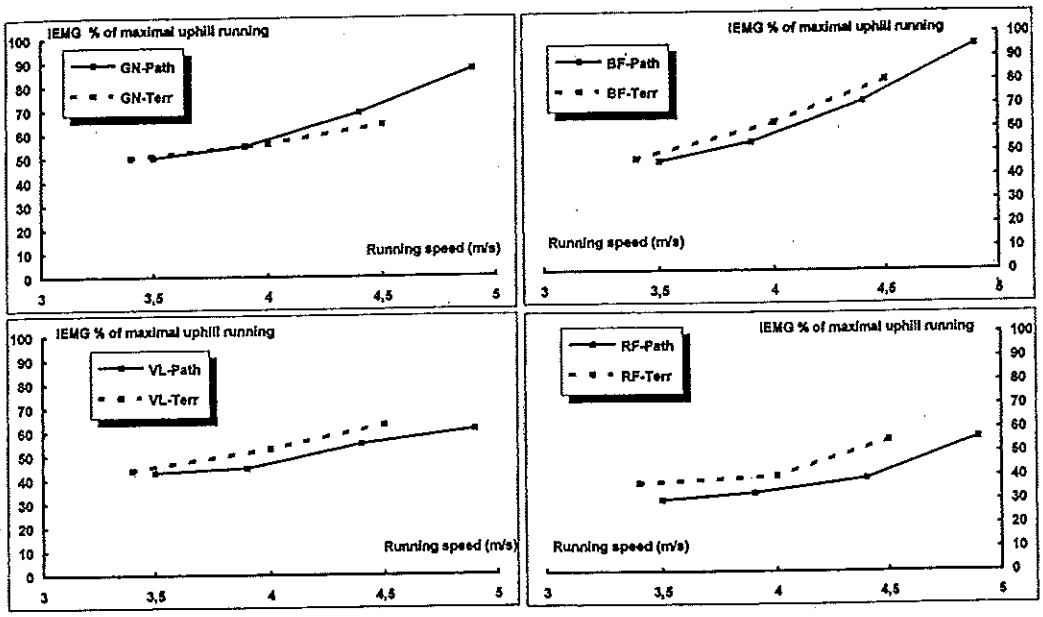

Figure 2. To maximal uphill running related IEMGs of individual muscles at different running speeds in path and terrain (average data of 5 subjects).

DISCUSSION

We found the portable ME3000P EMG-measurement device very suitable for field measurements, mainly because of it's light weight, feasibility and good quality of EMG signals.

The main finding of this study was that at maximal speed the IEMGs of VL and RF were about the same in path and terrain but those of GN and BF about 20 % units higher in the path. The lower maximal IEMG of GN and BF in terrain could be due to the the unability to "push" properly at the end of a step in terrain. This concept is supported by the small increase in GN activity in terrain suggesting diminished contribution to the increase in running speed. On the contrary the increase in the activities of BF, VL and RF was similar in path and terrain indicating similar contribution to the increase in running speed. It is unclear if that is due to the uneven ground itself or if it is just a matter of learning the "proper recruitment model".

The greater IEMG of quadriceps muscles at same speed in terrain may be due to the small continuous height differences in the ground. The balancing task during each step may effect the muscle recruitment in terrain, too.

The differences in IEMGs emphasize the need for sport specific training instead of just level running in orienteering. It is suggested that the ability to use GN and BF muscles may limit the maximal running speed in terrain.

SWIMMING TECHNIQUES USED IN A FLUME DIFFER FROM THOSE USED IN A POOL.

James G. Hay and Jake do Carmo.

University of Iowa, Iowa City, Iowa, U.S.A. and Universidae de Brasilia, Brasilia, Brazil

INTRODUCTION

The use of flumes in studies of swimming has increased steadily in recent years. As with the use of other devices for the simulation of human motions -- devices like walking and running treadmills; bicycle, rowing and canoeing ergometers; and cross-country skiing machines -- the use of a swimming flume raises the inevitable question "Is the motion used when swimming in a flume the same as that used when swimming in a pool?"

The purpose of this study was to compare characteristics of the techniques used when swimming in a flume with those used when swimming in a pool. The characteristics chosen were the mean stroke length (MSL), the mean stroke frequency (MSF), the mean pull time (MPT) and the mean recovery time (MRT) for five consecutive stroke cycles of freestyle, backstroke and butterfly; and the MSL and MSF for five consecutive stroke cycles and the backward phase time (BPT) and the forward phase time (FPT) for one stroke cycle of breaststroke.

METHODS

Data Collection. Eighteen male competitive swimmers performed four trials at each of three speeds (fast, medium and slow) for each of the four competitive strokes -- first in a pool and then in a flume. For trials in the pool, the subjects were paced by a pacing system placed on the bottom of the pool. Two video cameras were used to gather data. The first was placed in the pool balcony and was panned to follow the subject's performance over the entire trial. The second was placed on the pool deck the and used, together with an inverse half-periscope system, to record the above- and below-water motions of the subjects when they performed their breaststroke trials.

For trials in the flume, the speed of swimming was determined by the flow rate of the water. The performance of each trial was recorded using a video camera placed opposite the middle of the test section.

Data Reduction. For the freestyle, butterfly and backstroke trials, the locations of the subject's right hand at entry for the first and sixth strokes were determined. For breaststroke, the locations of the vertex of the subject's head at its highest point in the first and sixth strokes were determined. These coordinate data, and the corresponding temporal data, were used to calculate the MSL and MSF for the trials performed in the pool. The number of fields between entry and exit (pull phase) and between exit and entry (recovery phase) of the hand were counted to determine MPT and MRT, respectively; and between corresponding events in the motion of the hands to determine BPT and FPT. Similar procedures were followed in determining these same variables for the trials performed in the flume.

Data Analysis. Eight multiple analyses of variance with repeated measures were used to evaluate differences in the mean values for the two conditions, pool and flume.

RESULTS

Significant F-values were found between conditions for all four variables when the subjects were swimming freestyle and breaststroke, and for three variables when they were swimming butterfly, at the slow and medium speeds. With two exceptions, no significant F-values was found between conditions when the subjects were swimming backstroke. This was attributed to difficulties experienced with the modified pacing method used when swimming that stroke. With one exception, no significant F-values were found between conditions for trials conducted at the fast speeds. This was attributed to difficulties in performing at the fast speeds selected and the consequent reduction in the number of subjects for whom data could be included in the analysis.

Post-hoc t-tests revealed significant differences between conditions for the means of all four variables when the subjects were swimming freestyle and breaststroke, and for three variables when they were swimming butterfly, at the slow and medium speed. These significant findings indicated that the MSL, MPT and MRT were shorter and the MSF was higher for the trials performed in the flume than for the corresponding trials performed in the pool.

DISCUSSION

The significant differences found were probably related to the strategy adopted when swimming in the flume. For the trials in the flume, the subject was instructed to remain in the same position relative to the oncoming flow throughout each trial. Similar instructions are commonly given when flumes are used for testing or training and, even if this were not the case, it seems likely that swimmers would naturally tend to adopt this strategy to avoid the disconcerting backward and forward oscillation that would otherwise be experienced.

When swimming in a pool, a swimmer perceives intra-cycle fluctuations in velocity as decreases and increases in speed. When swimming in a flume, these fluctuations are manifested as backward and forward oscillations of the body relative to the flume. It is hypothesized that the swimmer eliminates (or minimizes) these unwelcome oscillations when swimming in a flume by increasing SF and thereby decreasing the time between propulsive impulses; and that this increase in frequency is produced by decreases in MPT (or BPT) and MRT (or FPT), and is accompanied by a decrease in MSL.

The smaller MSL and larger MSF observed when a swimmer is asked to maintain a stationary position relative to the flume appears to compromise the value of using a flume for training purposes. To remedy this, use of a flume should probably include initial practice sessions designed to train the swimmer to accept backward and forward oscillation of the body relative to the oncoming flow. This oscillation must be preserved if the technique used by a swimmer in the pool is to be maintained when swimming in a flume.

NON-INVASIVE DEVICE FOR APPLICATION IN BIOMECHANICS
MEASUREMENTS OF MATERIAL AND GEOMETRICAL PROPERTIES OF THE HUMAN LOCOMOTOR SYSTEM

J. Heidjann, C. Bohn, H. Lohrer and K. Nicol
Institut für Bewegungswissenschaften, Universität Münster, Germany

INTRODUCTION

For diagnosing injuries and overstress reactions in the active and passive locomotor system as well as for attaining material and geometrical properties a high frequency (HF) measuring method called Antroposkop is used since two years.

METHODS

A generator induces an electric field (350 kHz, 1.2 kHz modulated in amplitude, 7 V, 0.5 mA) to the human body and the local field strength on the surface of the human body is measured by a capacitance type receiver-electrode (Figure 1).

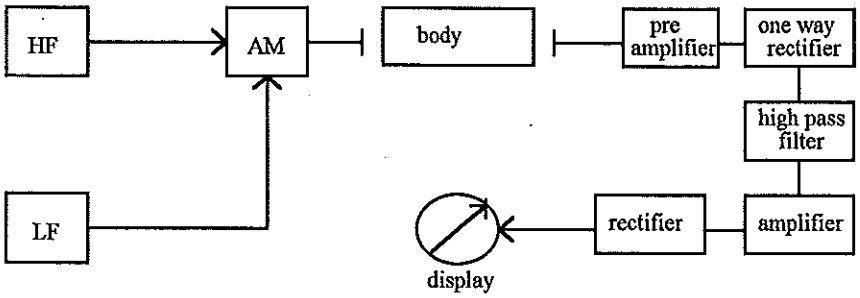

Figure 1: Principle of the HF device

The electric field is applied to the human body by two special electrodes so that a condensator is formed. The received signal is basically influenced by the dielectric constant in a small area around the receiver electrode. The course of the electric field in the body depends on the dielectric properties of the specific tissue.

Table 1. Dielectric constant of human tissue by an external electric field of 350 kHz

tissue	blood	fat	bone marrow	bone tissue	muscle
DC @ 350 kHz	2500	13300	5000	230	10000

Every kind of human tissue has a characteristic dielectric constant (DC) so that biological structures can be determined by this way with the Anthroposkop. As seen in table 1 the dielectric constant of different types of tissue is very different (Foster & Schwan, 1989). Moreover the dielectric constant is influenced by the metabolic processes with the result that inflammations and necroses can be diagnosed.

The interaction of an external electric field with the human body is simulated by a software package (IGUN, Becker 1991). The course of the electric fieldlines are simulated for a modell of a long bone with a local spot of increased admittivity, for example stress fracture or bone bruise. The simulations by solving Maxwell's Equations lead to understanding the influence of metabolic processes on the signal.

APPLICATIONS

The device was used in the orthopaedic diagnosis and for controlling the course of a disease parallel to other technical methods for diagnosis in orthopaedics like x-rays, ultrasound and computer tomography. Especially, a high number of measurements of stress-fractures of the Os metatarsale and Os naviculare were carried out.

Applications are:

- diagnosing of injuries and overstress reactions of the active and passive locomotor system
- supervision of healing process
- influence of local anaesthetics and antiphlogistics.

A second area of application is the study of the biomechanical structure of the lower leg. Data of multiple measurements are fit into the IGUN for attaining material data and geometrical data to be used in a Finite Element Analysis.

RESULTS

Figure 2 shows the results of measurements of various damages of the movement system. There are 28 measurements in total. The signals picked up by the receiver varies between - 17 and +12 units. The measurements of stress fractures split into a group with positive and negative signals. By reason of the increased local metabolism the dielectric constant of acute stress fractures is high and the received signal is positive. In contrast to the acute stress fracture the signal of the chronic one is negative because the dielectric constant of the degenerative material is quite low. Measurements of capsular stimulations form positive osteosynthesis and anaesthetics negative groups of signals.

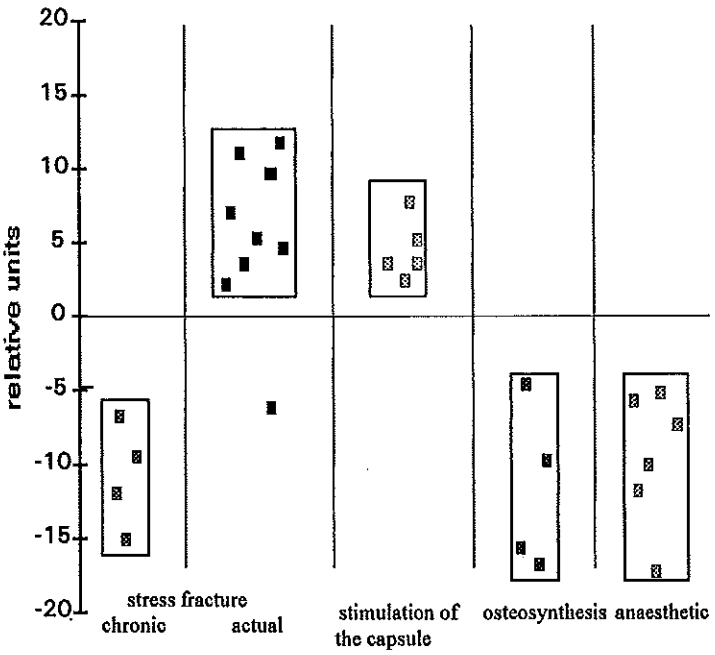

Figure 2: Measurements with the HF-device

CONCLUSION

A large variety of injuries and overstress reactions of the movement system were studied using the device. In any case unaffected, inflammatory and necrotic tissue could be discriminated in accordance with the orthopaedic diagnosis. To date, the number of measurements is not sufficient to discriminate in terms of nature, stadium or strength of the damage. Considering the great differences of the dielectric constant we expect that the high frequency device will become an alternative for diagnosis of inflammatory and necrotic processes and damages of the active and passive locomotor system.

REFERENCES

1. Foster, K.R. & Schwan, H.P. (1989): Dielectric Properties Of Tissue And Biological Materials: A Critical Review, In: Critical Reviews in Biomedical Engineering, Volume 17, Issue 1
2. Becker, R. (1991): IGUN, Programm zur teilchenoptischen Simulation von Elektronenstrahlen in Elektronenkanonen, Institut für Angewandte Physik, J.W. Goethe Universität Frankfurt

NEW METHOD FOR MEASUREMENT OF LIMB WEIGHT-BEARING

L.M. Heikkinen[1], H.E. Panula[2], T. Lyyra[3], I. Kiviranta[3], H. Olkkonen[1], H.J. Helminen[3].

[1] Department of Applied Physics, [2] Department of Surgery, [3] Department of Anatomy, University of Kuopio, P.O.Box 1627, FIN-70211, Kuopio, Finland.

INTRODUCTION

Determination of the forces acting across the limbs of experimental animals have usually been carried out using force-plate measurements (Budsberg *et al.* 1987, Dueland *et al.* 1977). In this work we introduce a new simple and reliable method for the measurement of dynamic forces using a sensor inserted under the limb. We utilized electromechanicalfilm (EMF), which is a new type of sensor material for force measurements (Räisänen *et al.* 1992, Siivola *et al.* 1993). The method was applied on beagle dogs exercising on the treadmill.

METHODS

The EMF-sensor consists of foamized, permanently polarized plastic film, which is about 1 mm thick and has a conductive electrode on the surface (Kirjavainen 1987). Vertical force directed towards the film sensor generates an electrical charge, which is proportional to the force. To measure forces under the limbs of beagle dogs, we used sensors with size 2 cm x 10 cm. The sensors were fixed to the undersurface of the paw with adhesive elastic bandage. The current signal from the sensors was measured using a commercial integrator circuit, which acts as a current-to-voltage converter. Voltage signals were interfased with a multiplexer and an analog-to-digital converter installed to a PC computer. Sensors were calibrated with known weights between 1 - 4.5 kg by using a mechanical apparatus. The calibration curve was computed from the least square approximation of the experimental data. Experiments with beagle dogs were carried out on a treadmill with speed varying from 2.5 km/h to 7.5 km/h and with both 15° uphill and 15° downhill inclination.

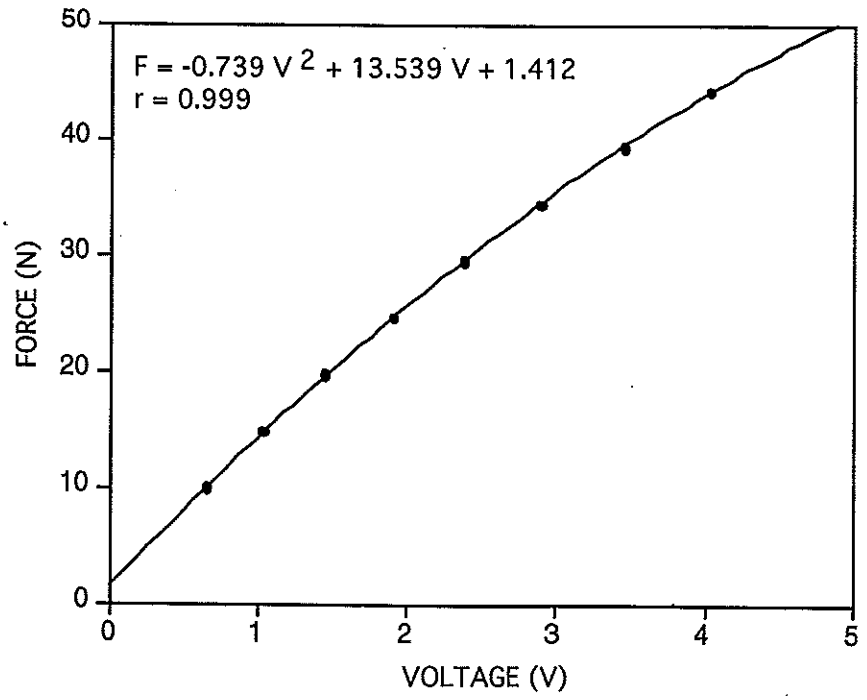

Fig. 1. Calibration curve for EMF-sensor.

RESULTS

The calibration curve appeared to almost linear (Fig.1). Figure 2 shows force signals from the forelimbs of a beagle dog. Repeatability of the force measurements was determined using the intraclass correlation coefficients (ICC). Correlations were calculated for all of the inclinations and speeds of treadmill, separately for fore- and hindlimbs. The correlations (n=18) varied between 0.85 and 0.91, which indicates good repeatability of the measurements.

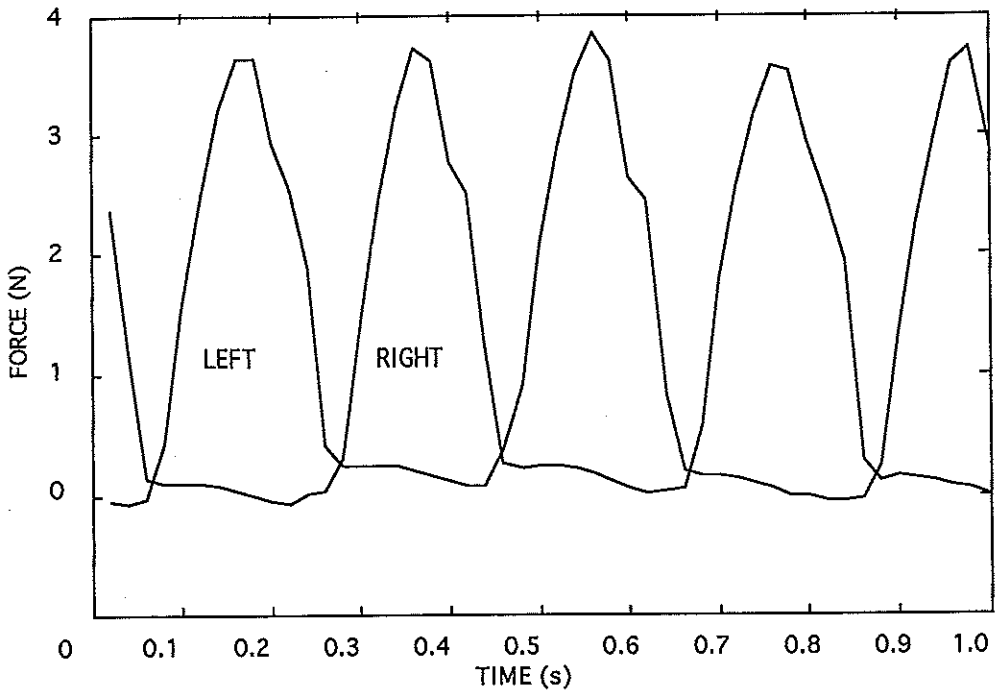

Fig. 2. The EMF-force sensor signals from the beagle forelimbs.

DISCUSSION

According to ICC-analysis, the repeatability of the method was excellent under experimental conditions. Since a sensor could be attached beneath each limb of the animal at the same time, the measurements proved to be simple in practice and also the signal analysis was easy to perform separately for each limb. Measurements could be carried out from animals running on treadmill at different velocities and treadmill inclinations. According to our experience on the EMF-sensor, we found it inherently reliable and convenient probe in the measurement of forces acting on limbs of the beagle dog.

REFERENCES

Budsberg S. *et al.* (1987) Force plate analysis of the walking gait in healthy dogs. *Am. J Vet Res.* 48, 915-918; Dueland R. *et al.* (1977) Force-plate technique for canice gait analysis of the total hip and excision arthoplasty. *J. Am. Animal Hospital Ass.* 13, 647-652; Kirjavainen K. (1987) Electromechanical film and procedure for manufacturing same. U.S. Patent 4654546; Räisänen L. *et al.* (1992) A new method for the measurement of spontaneous motor activity of laboratory animals. *Pharmacology & Toxicology.* 70, 230-231; Siivola J. *et al.* (1993) ETMF-polymer transducer as a detector of respiration in humans. *Medical & Biological Engineering & Computing.* 31, 634-635.

GAIT ANALYSIS ON THE UTKNEE, A PROSTHETIC KNEE FOR FUNCTIONAL AND STABLE FLEXION DURING THE PUSH-OFF PHASE.

P.J.H. Hendriks, H.J. Grootenboer, J. de Vries and H.F.J.M. Koopman

Laboratory of Biomedical Engineering, University of Twente

Enschede, **The Netherlands**

INTRODUCTION

With the present kneehinges there is no or a very limited possibility to make a stable kneeflexion during the stance phase, while none of the kneemechanisms allow for a functional kneeflexion during the push-off.

Research on the biomechanics of the gait of prosthetic walkers has resulted in a concept for a new type of kneemechanism, the UTKnee. From computer simulations was found that with this new kneemechanism walking should cost less energy while symmetry increases. The new kneehinge is based on a four-axial kneehinge with an inverted trajectory of the momentary rotation centres. When the prosthetic knee is flexed, the rotation centre moves posteriorly thus increasing the stability. This means that flexion of the new knee during the push-off phase is stable: The hipextensors need to generate less energy to stabilise the prosthetic knee in comparison with other kneehinges. Because it is expected that the prosthetic leg is lengthening when flexing the knee, the push-off time of the prosthetic leg increases as well. The hipflexors are now able to generate more energy during push-off.

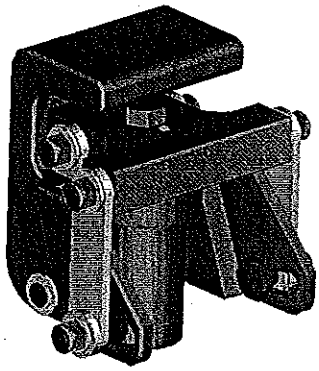

Figure 1: The UTKnee

METHODS

A first prototype of the UTKnee was tested on a single subject. Analysis of the kinematic and dynamic gait parameters has been done by measurements with a Vicon video system. An average cycle is calculated from 10 walking trials, which is analysed with an inverse dynamics model (Koopman, 1989).

The purpose of these measurements was to indicate the differences between the normal prosthetic leg of the subject with a regular four-axial kneehinge and the prosthetic leg with the UTKnee. Because there was no information available about the optimal trajectory of the polar curves of the UTKnee, different adjustments of the UTKnee have been tried out to find this. So the first Vicon measurement has been done with a normal four-axial kneehinge. In the next four measurements, the trajectory of the momentary rotation centres has been varied, whereby the momentary rotation centre at zero degree knee flexion moved from 0.27m to 0.15m above the prosthetic knee (steps: 0.27m, 0.20m, 0.17m, 0.15m).

Further measurements have been done with an Oxycon system to measure the oxygen expenditure during walking.

RESULTS

One of the most significant parameters is the push-off time with the prosthetic leg. Normally this double stance time is shorter for the prosthetic leg than for the sound leg. This is also the case for the measurement with the normal prosthesis of the subject, see

Figure 2: Indicted with *Normal.* In this figure the time duration of the double stance phase with the push off with the sound leg (SPO = Sound Push-Off) is considerably larger than the time duration of the other double stance phase (PPO = Prosthetic Push-Off). For all different settings of the UTKnee (1 indicates the largest polar curve, 4 the smallest) the prosthetic push-off time increases significantly, whereas the normal push-off time with the sound leg remains the same.

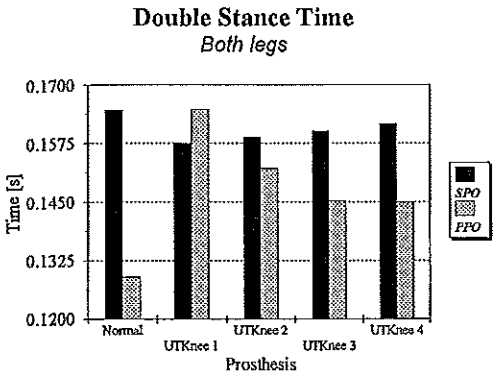

Figure 2: Double stance time for both legs

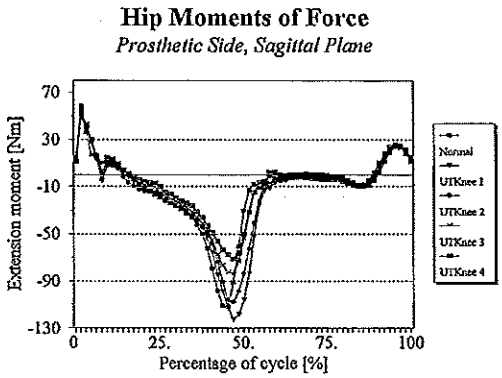

Figure 3: Moments of Force from the Right Hip

An interesting dynamic parameter is the hip moment of force on the prosthetic side. Figure 3 shows these moments for the normal four-axial prosthetic knee and the different adjustments of the UTKnee, where the cycle starts with prosthetic heel contact. Except for setting 1, the moments needed to flex the knee during push-off are smaller for the UTKnee than for the normal prosthesis.

DISCUSSION

From computer simulations was expected that the prosthetic push-off time would increase, and therefor the energy generation by the hip flexor muscles would increase as well. The measurements show that the model was right in the predicting the increase of the double stance time. However, the hip energy generation did not increase as much as expected. Instead, the hip moments of force were reduced during late stance, which indicates that it is easier to control the kneeflexion with the UTKnee. Walking with the UTKnee resulted in a better left- right symmetry.

REFERENCES

Koopman, H.F.J.M. (1989) *The three-dimensional analysis and prediction of human walking.* Dissertation, University of Twente, Enschede.

REST LENGTH AND PASSIVE COMPLIANCE OF IMMOBILISED RABBIT SOLEUS MUSCLE AND TENDON

Robert D. Herbert and Jack Crosbie
School of Physiotherapy, University of Sydney, Australia.

INTRODUCTION

When a muscle-tendon unit is lengthened, as occurs when joints move, its tendinous and muscular parts increase length in proportion with their compliances. Numerous studies have investigated the relative compliance of tendons and contracting muscle, but there is very little data on the relative compliance of tendon and resting muscle, so it is not clear whether length increases in resting muscle-tendon units occur primarily in muscle or tendon. The first aim of this study was to determine the relative compliance of muscle and tendon components of the rabbit soleus muscle-tendon unit over a physiological range of resting tensions.

Immobilisation of muscle-tendon units in a shortened position causes the muscle-tendon unit to become shorter and less compliant. Theoretically such adaptations could occur either in the muscle fascicles or in the tendon. The second aim of this study was, therefore, to determine whether immobilisation-induced decreases in muscle-tendon rest length are mediated primarily by muscle or tendon.

METHODS

One ankle joint of each of eight rabbits was immobilised with a cast in a plantarflexed position for either 14 days (five rabbits) or 28 days (three rabbits). After the period of immobilisation, soleus muscle-tendon units were excised from both hindlimbs. Markers were placed on the surface of the muscle at the ends of both tendons and tendon plates, defining the lengths of proximal and distal tendons, tendon plates and muscle fascicles. The muscle-tendon unit was mounted in a tensile-testing system as previously described (1). Muscle-tendon length and tension were measured as the muscle-tendon unit was stretched from short of its slack length to more than 1400 mN - a range of lengths slightly greater than that likely to be attained by normal muscle-tendon units in vivo. Simultaneously, three-dimensional marker kinematics were recorded from three video cameras.

The lengths of proximal and distal tendons, tendon plates and muscle fascicles were computed off-line from three-dimensional marker coordinates and multiplied by the cosine of the angle which they made with the long axis of the muscle, giving tendon, tendon plate and muscle fascicle lengths projected onto the long axis of the muscle. By measuring a muscle model of known dimensions it was shown that the measurement procedures provide unbiased and reliable measures of muscle-tendon component lengths.

RESULTS

Non-immobilised muscles: Comparisons of tendon and muscle fascicle compliance were made on soleus muscle-tendon units from the non-immobilised (contralateral) hindlimb.

At all tensions, tendon strain was less than fascicle strain. Mean total tendon strain at 1100 mN, the greatest tension studied, was 6.0% (± 1.1) and 7.4% (± 1.1) for tendon in series with proximal and distal muscle fascicles respectively, compared to 28.4% (± 4.0) and 31.3% (± 4.0) for proximal and distal muscle fascicles,

respectively. Increasing tension from 20 mN to about 200 mN (or fascicle strains of about 15%) produced a large increase in the ratio between fascicular and tendon strains. Above 200 mN the ratio of muscle fascicle strain to total tendon strain was nearly constant at approximately 4.5:1.

Muscle fascicles constituted only 22% of muscle-tendon rest length at muscle-tendon rest length. Therefore, even though muscle fascicles strains greatly exceeded tendon strains, tendon contributed nearly half of the total changes in muscle-tendon length. For most of the range of tensions investigated, between 40 and 50% of the change in muscle-tendon length was attributable to changes in the length of tendinous components, the remainder being due to changes in muscle fascicle length. This relationship was remarkably constant at tensions greater than about 200 mN. At tensions less than 200 mN changes in muscle-tendon length were primarily attributable to tendon.

Effects of immobilisation: On average, 14-day immobilised muscles were 8.4 mm shorter than non-immobilised contralateral muscle-tendon units ($p = 0.007$). The rest length of distal muscle fascicles of 14-day immobilised muscles was 2.3 mm less than the rest length of distal fascicles from contralateral muscles. This decrease accounted for 27% of the difference in immobilised and contralateral muscle-tendon rest lengths, but was not statistically significant ($p = .11$). The remaining 73% was due to a decrease in the length of the tendon which lies in series with the distal muscle fascicles ($p = 0.008$). In contrast, the proximal muscle fascicles were no shorter than proximal fascicles from contralateral muscles, so shortening of the tendinous components in series with the proximal muscle fascicles accounted for all of the decrease in muscle-tendon length ($p = 0.003$). The contributions of 28-day immobilised muscle fascicle and tendon to total muscle-tendon length changes were similar to those in 14-day immobilised animals. There were large decreases in the length of both tendon plates in 28-day immobilised muscles, suggesting that the area of insertion of muscle fibres onto tendon decreases with prolonged immobilisation.

DISCUSSION

The first finding of this study was that, while tendon strains were much smaller than muscle fascicle strains, changes in tendon length accounted for more than 40% of the total muscle-tendon length changes. This is because, in rabbit soleus muscle, the tendons have a much greater rest length than the muscle fascicles. The rabbit soleus muscle is not unusual in this respect, and it is likely that tendon contributes substantially to passive muscle-tendon compliance in many other muscles with relatively long tendons.

Immobilisation at short lengths caused rabbit soleus muscle-tendon units to become shorter. These length changes occurred primarily in the tendon. To our knowledge, adaptations of tendon rest length have not previously been described, although Heslinga and Huijing have shown a decrease in the "active slack length" of the proximal tendon plate of the rat gastrocnemius with four weeks of immobilisation (2). These changes may be of considerable functional significance.

REFERENCES

1. Herbert, R.D. and Balnave, R.J. (1993). *J. Orthop. Res.* **11**, 358-366.
2. Heslinga, J.W., and P.A. Huijing (1993). *Eur. J. Appl. Physiol.* **66**, 289-298.

SOLEUS FORCES AND SOLEUS FORCE POTENTIAL DURING UNRESTRAINED CAT LOCOMOTION

W. Herzog, T.R. Leonard
The University of Calgary, Calgary, Canada

INTRODUCTION

Direct muscle force measurements in freely moving animal preparations have become standard in the past two decades (e.g., Walmsley et al., 1978). The most frequently measured muscle forces are those of the cat ankle extensor group, particularly the soleus, either head of the gastrocnemius, and the plantaris. Force-sharing among these muscles has been studied extensively for a variety of activities; however, one of the stumbling blocks for explaining the force-sharing among soleus, gastrocnemius, and plantaris comprehensively has been the soleus force-time histories. Soleus (peak) forces remain approximately constant for a large range of demands of ankle extensor moments (e.g., Hodgson, 1983; Walmsley et al., 1978).

The reason why soleus peak forces remain about constant for a large range of locomotor speeds is unknown, but two basic theories have prevailed. In the first theory, it is assumed that the activation of the soleus muscle is maximal for most movements, therefore, the fact that peak forces remain about constant for many different situations must be explained with the contractile conditions and the contractile properties of the soleus exclusively (e.g., Walmsley et al., 1978). In the second theory, it is argued that the contractile conditions of the soleus and the remaining ankle extensors (particularly the medial head of the gastrocnemius) are similar during locomotion, therefore, the fact that soleus forces do not increase with increasing demands (as do the gastrocnemius and plantaris forces) must be explained primarily with the activation of the muscle (e.g., Hodgson, 1983). In the second theory, the soleus is considered to be activated submaximally for any movement.

The purpose of this study was to test the force potential of the cat soleus during unrestrained locomotion, and to determine if the soleus was maximally activated during step cycles at different speeds of walking.

METHODS

In order to assess the force potential of the soleus muscle during locomotion, the soleus nerve was stimulated supramaximally (square wave pulses of 0.1 ms duration, 100 Hz, 100 ms, 1.5-2.0 times the stimulation threshold level) at systematic instants during the step cycle using a chronically implanted nerve cuff electrode. Soleus forces were measured using "E"-shaped, home-made tendon transducers. Measurements were obtained from a total of three animals, walking at nominal speeds of 0.4, 0.8, and 1.2 m/s on a motor-driven treadmill. Supramaximal stimulations were performed approximately every tenth step. For each animal, a minimum of 70 supramaximal stimulations were performed at each speed of walking for a total of more than 630 assessments of the soleus force potential (3 animals · 3 speeds · 70 assessments).

RESULTS

Figure 1 shows 14 selected step cycles following supramaximal stimulation of the soleus for one animal walking at a nominal speed of 0.4 m/s. Figure 2 shows the corresponding results from another animal walking at a nominal speed of 1.2 m/s. The supramaximal stimulations in both figures were performed in such a way that the effects of the stimulation (through an increase in soleus force) should be seen throughout the step cycle.

For 0.4 m/s, the effects of the supramaximal stimulation of the soleus can be seen throughout the swing phase (time = 0.0 s-0.25 s, Fig. 1), and again from approximately the occurrence of peak force until near the end of the stance phase (zero force, Fig. 1). For 1.2 m/s, force enhancement following supramaximal soleus stimulation could only be observed during the swing phase (time = 0.0 s-0.22 s, Fig. 2), but not the stance phase, of the step cycle.

DISCUSSION

From the results of this study, it appears that force enhancement through supramaximal stimulation of the soleus is not possible in the early parts (from paw contact to approximately the occurrence of peak forces) and the very late parts of the stance phase for slow walking (0.4 m/s Fig. 1). Furthermore, no force enhancement appears to be possible during any part of the stance phase for walking at 1.2 m/s (Fig. 2). It appears, therefore, that soleus forces are maximal for big parts of the stance phase for slow walking, and for all of the stance phase for fast walking. These results are in agreement with the hypothesis proposed by Walmsley et al. (1978); they do not agree with most of the literature (e.g., Hodgson, 1983) in which soleus activation, and the corresponding soleus forces, were (implicitly or explicitly) considered to be submaximal.

The mechanisms of force-sharing among the cat ankle extensors during locomotion, and the mechanisms of control of ankle movements during voluntary movements in the cat must be re-evaluated to a large extent based on the findings presented here.

REFERENCES

Hodgson, J.A. (1983). The relationship between soleus and gastrocnemius muscle activity in conscious cats - a model for motor unit recruitment? J. Physiol. 337, 553-562.

Walmsley, B., Hodgson, J.A. and Burke, R.E. (1978). Forces produced by medial gastrocnemius and soleus muscles during locomotion in freely moving cats. J. Neurophysiol. 41, 1203-1216.

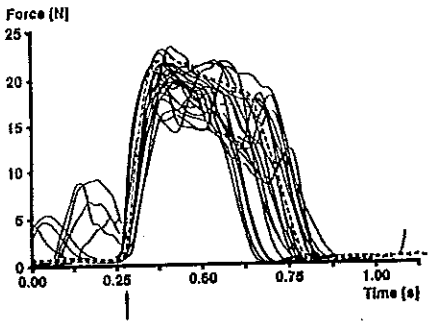

Fig. 1 14 step cycles following perturbation at a speed of walking of 0.4 m/s.

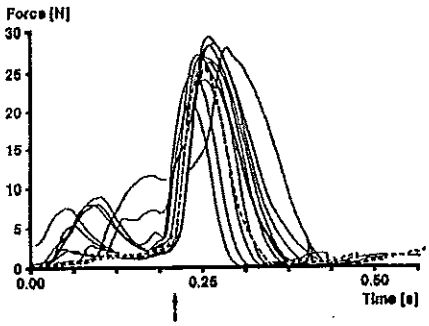

Fig. 2 11 step cycles following perturbation at a speed of walking of 1.2 m/s.

THE IMPORTANCE OF KNEE JOINT MOMENTS DURING GAIT IN TIBIAL COMPONENT LOOSENING IN KNEE ARTHROPLASTY.

M. B. Hilding, H. Lanshammar †, L. Ryd ‡.
Department of Orthopedics, Central Hospital, Västerås + Karolinska Institute, Stockholm, Sweden. † The Systems and Control Group, Department of Technology, Uppsala University, Sweden. ‡ Department of Orthopedics, University Hospital, Lund, Sweden.

INTRODUCTION: Artificial joint surgery has by virtue of the good results expanded into a very large operation. The long-term results are, however, still marred by component loosening, in knee arthroplasty especially by the tibial component. The ethiology is not fully understood. Much attention has lately been focused on wear debris particles as initiators of cell reactions leading to loosening. Mechanical factors are also considered, like initial implant stability, alignment and activity level, but there is still limited knowledge of the stresses and strains that an artificial joint is exposed to and to what extent individual differences in these forces exist. To test the hypothesis of joint load as an ethiologic factor, a prospective clinical study was conducted, where tibial component fixation was monitored by roentgen stereophotogrammetry and dynamic load was assessed by gait analysis.

MATERIAL AND METHODS: 45 patients, aged 60-75 years, scheduled for knee replacement due to gonarthrosis, were included in a prospective study after informed consent. Three different cementless prosthesis designs, the Tricon stem, the Tricon-M and the PCA resurfacing, were randomized before the operations into groups of 15 patients in each. These groups were equal with respect to age, weight, gender, degree of deformity and arthrosis stage. Two patients, from the Tricon-M group, died before two years of follow-up and were the only ones lost.

Roentgen Stereophotogrammetry (RSA): Tantalum balls were placed in the tibial metaphysis and the plastic part of the tibial component at the operations, to enable measurements of the relative movements between these parts, by RSA. The three-dimensional coordinates of the markers were obtained by digitization of pairs of radiograms, exposed simultaneously. Reference markers with known positions were located in a plexiglass cage surrounding the knee. The mathematical evaluation was performed by rigid-body kinematics. For the purpose of this study, results are expressed as maximum total point motion (MTPM), the three-dimensional vector-sum of the motion of the marker that moves the most. The accuracy of RSA applied to knee arthroplasty is 0,2 mm. From previous long-term follow-up by RSA, different patterns of migration have been identified (1). Tibial components that migrate only the first postoperative year and thereafter stabilize have a good prognosis, in contrast to components that continue to migrate, which is an indication of instability and a poor prognosis. The limit of migration has been established at 0,2 mm MTPM the second year (1). The results from RSA were used for prediction of future component loosening.

Gait analysis. Pre- and postoperatively, at six months and two years, gait analysis was done with a videobased system, Vifor (2), with a synchronized force-plate (Kistler). Recordings were made with self-selected walking speed on a 10 m. walkway. Markers were not used, the positions of the ground reaction force vector and the center of the ankle, knee and hip joints during the stance phase were digitized, from frames with 40 ms intervals. Gravitational and inertial forces were omitted in the calculation of moments due to their small contribution at the ankle and knee joint at slow walking speed. Three to six trials were pooled together and analyzed as ensemble averages. For

the purpose in this study, to assess joint load, the moments in the frontal and sagittal planes were analyzed, both the mean value from all observations in the gait cycle and the single peak values. The standard deviation of the difference between two measurements for moments, peak and mean, frontal and sagittal, were all between 1.8 and 5.0 Nm. Statistics: Repeated measurements ANOVA.

RESULTS: 15 of the tibial components migrated >0,2mm the second year, thereby denoted unstable by RSA and at risc for future loosening. The good prognosis group was formed by 28 cases with less migration. The prosthesis design types were equally distributed. Mean moment levels in the frontal plane were not significantly different between the two prognosis groups, but the reduction by the operation was more pronounced in the unstable group (peak adduction: p=0.025, mean adduction: p=0.014). In the sagittal plane a significantly larger peak flexion moment was found in the group with poor prognosis, both before and two years after the operation (Fig. 1). The mean moment was also significantly different, both pre- and postoperatively in the two prognosis groups (Fig. 1). Peak extension moments, as well as other parameters investigated, radiographic and clinical and obtained from gait analysis, did not discriminate between the groups.

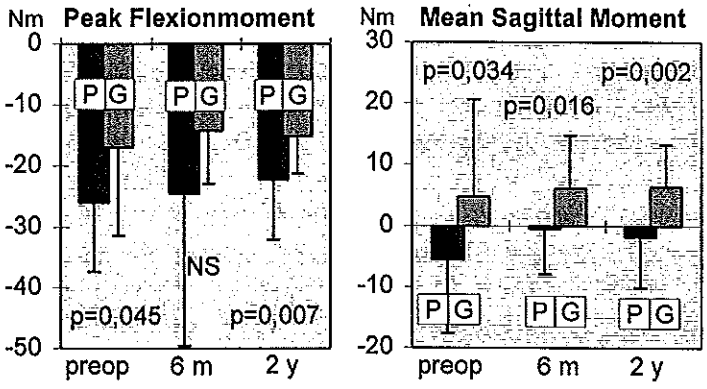

Figure 1. Moments ±SD in P=poor G=good prognosis groups

DISCUSSION: Roentgen stereophotogrammetric analyses of the migratory pattern of the tibial component have shown that the process of tibial component loosening can be detected already the second year after the operation (1). This early onset of loosening made us call in question the hypothesis of debris as primary causative agents, in favour of mechanical factors, which, in contrast to wear debris, exist already peroperative. In the frontal plane, a difference between prognosis groups in the level of reduction of moments by the operation was found. In the sagittal plane a strong relationship between increased flexion moments during gait before and after the operation and poor prognosis for the tibial component was demonstrated. Individual gait patterns with substantially different forces in the knee joint may play a role in the process of tibial component loosening. Possibly by directing the differentiation of the interface tissue, by the balance created between generated forces and the ability of the implant/bone system to withstand these forces. Differences in joint forces during gait require further evaluation, concerning the ethiology of prosthetic loosening and possible interventions.

References: (1) Ryd L, Albrektsson B, Carlsson L, Herberts P, Lindstrand A, Regnér L, Dansgaard F, Toksvig-Larsen S. Roentgen stereophotogrammetric analysis (RSA) as a predictor of mechanical loosening. J Bone Joint Surg (Br) 1995. In press.

(2) Lanshammar H. Vifor- a system for force line visualization. In *Biomechanics XI-B,* pp.984-988. Edited by de Groot, Hollander, Huijing, van Ingen Schenau. Amsterdam, Free University Press, 1988.

THE DESIGN OF A BELOW KNEE PROSTHESIS USING BIOMECHANICAL ANALYSIS TECHNIQUES.

S.C. Hillery*, E.S. Wallace*, R. McIlhagger*, P Watson^
*University of Ulster at Jordanstown, Belfast, N. Ireland.
^Musgrave Park Hospital, Belfast, N. Ireland.

INTRODUCTION

A Dynamic Elastic Response (DER) below knee prosthesis which attempts to simulate the energy of the intact foot and shank segments for natural and fast walking gaits is being designed. In 1991, a prototype dynamic elastic response, (DER), prosthesis was developed at Musgrave Park Hospital, Belfast. The biomechanical analysis that led to the identification of a number of variables which can be altered to improve performance is described. The recent developments in DER feet have resulted in limbs that are expensive or do not offer any significant biomechanical or energy conservation benefits to the active amputee (Gitter et al, 1991, Anzel et al, 1992-1993). In prosthetic gait, the intact limbs and the hip on the prosthetic side strive to compensate for the functional loss of the below knee musculature of the amputated limb. In walking, the missing musculature is responsible for (i) assisting in the forward rotation of the shank over the foot during midstance through the anterior tibial muscles, and (ii) the generation of crucial quantities of the mechanical power by the plantar flexors needed to "push off" in the terminal stance and preswing phases.

METHODS

The aim of this research is to develop a prosthesis that will reduce the gait asymmetries and increase the range of cadences possible by the amputee by inducing a segmental energy balance within the system. A full three dimensional biomechanical analysis of the prosthesis was carried out using a five camera VICON motion analysis system linked with an Advanced Mechanical Technologies Inc. (AMTI) force plate. The forceplate is placed in the middle of a 12m walkway. Results were processed using the AMASS software and the VICON VX Clinical Manager. The patient walked five times over the forceplate at each cadence for the right (intact) and left legs. The cadences were self-selected and proved to be consistent.

RESULTS

Results revealed that the primary compensations for the below knee muscle loss take place at the hip on both the prosthetic and intact sides. When the prosthetic limb is in stance, the hip extensors of the prosthetic side have to produce more power to pull the body over the prosthesis. The compensatory effect is also transferred to the intact limb, with the plantarflexors producing more power than normal in terminal stance and the hip flexors producing more power in preswing and early swing in order to increase the inertia of the swinging leg to push the system up into midstance. When the intact leg is in stance, the hip flexors of the prosthetic side produce more power than normal in preswing and early swing to compensate for a below average function of the plantarflexor type action of the prosthesis in terminal stance. The intact limb is also affected with the hip extensors generating up to 2.5 times the power than normal to compensate for the reduced "push" from the swinging leg. The Vertical Ground Reaction Force (VGRF) revealed that the prosthesis fails to push off the ground, rather the hips pull the affected limb. The prosthetic foot action is slow to achieve foot flat due to the delayed plantar flexor moment at initial contact which further disturbs the movements at the hip by the muscles trying to pull the body over

the foot at midstance. Also the momentum of the body is not being used effectively at midstance due to the absence of the plantarflexion action. These pathological actions can be minimised be altering the design of the prosthesis.

DISCUSSION

From this analysis, the design and development of a further prototype using strength of materials, Finite Element and composite materials techniques is underway. The present design stores energy at terminal stance and releases energy at preswing when it cannot be used effectively. The suggested new design (Fig1) should solve the problem by storing the energy earlier and releasing it at Terminal Stance. The aim of this second prototype is to design, into the geometry and to the material from which it is made, a means whereby the initial deflection due to the weight of the user can be stored as strain energy and then released to accelerate the limb at preswing. A further aim is to design a dynamic prosthesis which is not expensive.

Variables:

W:	Determined by the force and necessary absorption at Initial Contact and Load Response
X:	Determined by the moment at Terminal Stance
Y:	Determined by the Shoe Length
Z:	Determined by the moment at Initial Contact
L,R,o,b,d:	Determined by the deflection necessary for the stored strain energy
M:	Mass of the prosthesis
CoG:	Centre of Gravity of the prosthesis
I:	Moment of Inertia of the prosthesis
E:	Modulus of Elasticity of the material

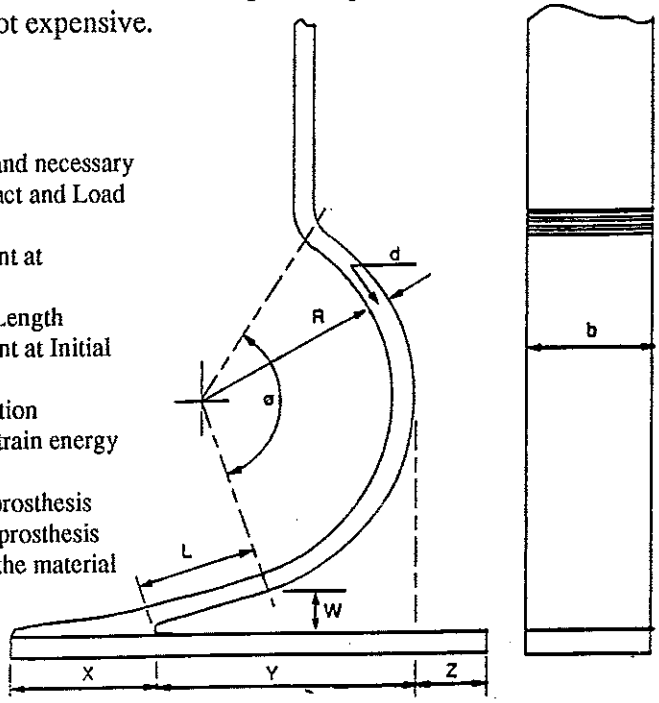

Fig.1 Design Variables for a Dynamic Elastic Response Below Knee Prosthesis.

A strength of materials approach is being used to optimise the geometry of the prosthesis and a computer programme is being written to facilitate the varying of the variables, such as the length of the cantilevers, the radius of curvature and the material properties. These variables can only be altered within biomechanical constraints, so that the compensatory mechanisms in operation at present will be assisted by the improved mechanical design. A finite element analysis (FEA) model is being constructed to optimise the material selection and lay-up, to attempt to induce a segmental energy balance between the prosthetic and intact limbs.

REFERENCES

Anzel, S., Perry, J. Ayyappa, E., Torburn, L. and Powers, C.M. (1992-1993) Efficiency of Dynamic Elastic Response Feet. *Rehabilitation R&D Progress Reports,30-31,* Veterans Health Administration, Rehabilitation Research and Development Services, pp27-28.

Gitter, A., Czerniecki, J.M. and DeGroot, D.M. (1991) Biomechanical analysis of the influence of prosthetic fee on below-knee amputee walking. *Am J Phys Med Rehabil* **70,** 142-148.

MECHANICAL DIFFERENCES IN THE BATTING MOTION BETWEEN CUBAN AND JAPANESE BASEBALL PLAYERS

Y. Hirano

Lab. for Exercise Physiology and Biomechanics, Faculty of Educatin, The University of Tokyo, Tokyo, Japan

INTRODUCTION

The speed of the bat-head at impact can be varied considerably by the player through his arm-swing mechanics (Sprigings et al., 1994). Muscle torque, the generator of arm-swing, is dependent on the joint angle through which the muscle exerts the force (Kulig et al., 1984). This implies the optimal position in which the joint should be placed when large torque is required. As Cuban baseball players are recognized to generate high speed of the bat-head, their batting motions are worthy to be analyzed for inspecting this implication.

The purpose of the present study was to examine the mechcanical factors required for the high speed of the bat-head by comparing the batting motions between Cuban and Japanese baseball players.

METHODS

Batting motions of Cuban and Japanese elite baseball players were recorded during the exhibition match with 2 phase-locked high speed video cameras (HSV-400, Nac, Tokyo) operating at 200fps. Only these motions in which the ball was hit successfully to the same-field were analyzed. Points for the joints of the body and both ends of the bat in each video image were manually digitized by using the motion analyzer (Movias-2000, Nac, Tokyo) and 3D coordinates of them were determined by the DLT method. The data points were filtered using the second order Butterworth-type low-pass filter, which was set the cut-off frequency of 5Hz (Winter, 1979).

RESULTS AND DISCUSSION

Cuban players indicated the larger increase in the angular velocity of the bat in the horizontal plane at the beginning of the swing than Japanese players (Fig. 1). This increase was considered to decrease the time lags between the body and the bat horizontal rotations. At the end of the swing, Cuban players showed the smaller horizontal angle of the linked line between both shoulders but larger one of the bat than Japanese players (Fig. 2). This means that the movement of arm-swing contributed more to the horizontal rotation of the bat. From these results, it was suggested that for shoulder horizontal abductors and elbow flexors in the lead arm, optimal joint angles were maintained for Cuban players when large torques produced by these muscles were required.

References

Kulig, K., Andrews, J. G., and Hay, J. G. (1984) Human strength curves. In R. L. Terjung (Ed.), Exercise and sport sciences reviews Vol. 12, Macmillan, New York, pp417-466.

Springings, E., Marshall, R., Elliott, B., and Jennings, L. (1994) A three-

dimensional kinematic method for determining the effectiveness of arm segment rotations in producing recquet-head speed. J.Biomech., 27(3): 245-254.
Winter,D.A.(1979) Biomechanics of human movement, John Wiley & Sons, New York, pp25-39.

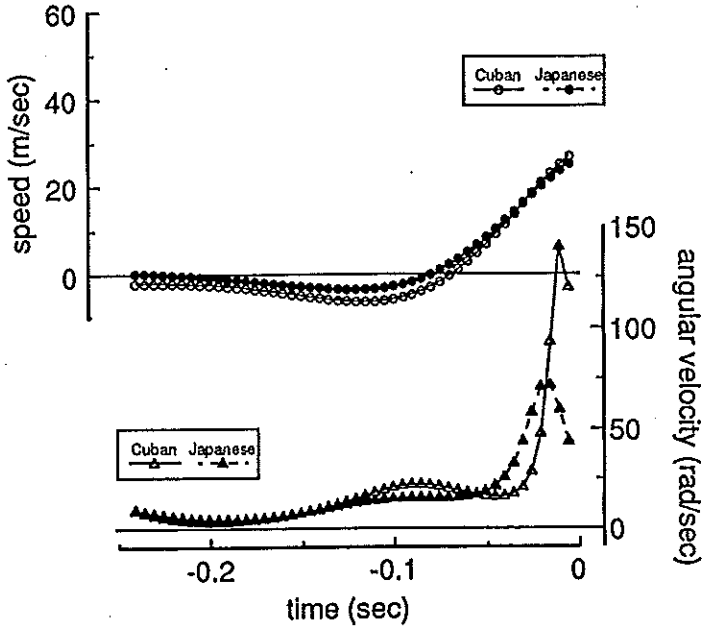

Fig.1 The speed of the bat-head in the pitcher-catcher direction and the angular velocity of the bat in the horizontal plane (typical data).

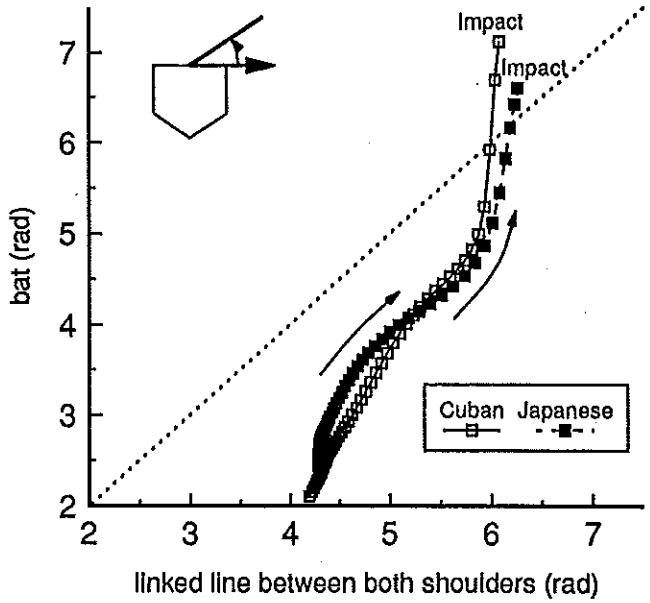

Fig.2 The relationship between angles of the bat and of the linked line between both shoulders during the swing (typical data).

MEASUREMENT AND ANALYSIS OF STRAIN DISTRIBUTION IN THE CRUCIATE LIGAMENT

Shunji Hirokawa and Reiji Tsuruno†
Faculty of Engineering, Department of Graphic Science, Kyushu University,
†Department of Visual Communication Design, Kyushu Institute of Design,
Fukuoka, Japan

INTRODUCTION

Although many studies on the tensile characteristics of the cruciate ligaments, especially of the anterior cruciate ligament (ACL) have been performed, the differential function and the length patterns of the ACL fibers are still a controversial issue. The non-uniform distribution of strain on the fibers within the ACL has not been fully studied. Discrepancies among previously performed experiments on the ACL elongation are partially due to the fact that strain distribution varies, even along the fiber direction, from portion to portion. Ligaments should not be considered as a bundle of separate fibers such as a Venetian blind-like structure, but as a bundle of fibers which are glued to each other. Therefore even though both anterior and posterior fibers stay isometric, tension may arise in either of the diagonal directions when a "belt-shaped" ligament is deformed. Also, a belt-like ligament becomes slender in the middle portion when considerably elongated, which would lead to noticeable error in the distance measurement between the attachments.

The objectives of this study are to experimentally measure and to theoretically analyze the change in shape and stress distribution over the entire surface of the ACL when its attachment sites are moved in the threedimensions associated with knee flexion.

MATERIALS AND METHODS

To determine stress distribution over the entire region in the ACL, experiments were carried out to measure the change in shape and strain distribution over the entire surface of a pseudo ligament (a special rubber plate with an extremely large stretch: $600\%_{max}$) when the attachment sites were moved in threedimensions. An elaborate instrument (knee motion simulator) was developed, to which the pseudo ligament was attached. Both of the attachments could be moved in several directions and could be rotated on several axes, resulting in six-degrees of motion to simulate knee motion. An outline of the measurement apparatus is shown in **Fig.1**. The three-dimensional positions of 272 markers on the ligament were measured by *the Stereo-Photogrammetric Method* to compute the components of the Lagrangian strain tensor for each element. Instead of using two cameras, one was used, and the pseudo ligament was moved in threedimensions at known distances relative to the position of the camera; consequently, no control and/or fiducial makers were used. The data of three-dimensional displacement of the attachment as a function of knee angle had been obtained in another project. This data was applied in the present study.

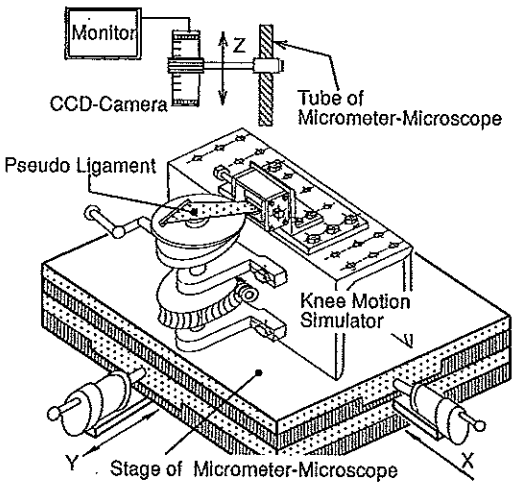

Fig.1 Outline of measuring apparatus

The Lagrangian strain tensor **E** was calculated by the following equation:

$$(dS)^2 - (ds)^2 = 2d\mathbf{x}.\mathbf{E}.d\mathbf{x} \qquad (1)$$

where dS and ds are the deformed and undeformed lengths of a vector between two of the points, dx is the undeformed vector.

Next, stress analysis using the finite element method for a noncompressive hyper-elastic material was performed. The non-linear stiffness relation between the node force, P_{NK} and the node displacement, U_{MK} for a special triangular element, was introduced as follows:

$$P_{NK}=2V_0\{C_1(\delta_{\eta\zeta}-\lambda^4 f_{\eta\zeta})+C_2[f_{\eta\zeta}(1-2\lambda^4-2\lambda^4 E_{\xi\xi})+\lambda^2\delta_{\eta\zeta}]\}B_{N\alpha}(\delta_{\beta K}+B_{M\beta}U_{MK})$$

$$E_{\xi\xi}=B_{J\xi}(U_{J\xi}+\frac{1}{2}B_{Q\xi}U_{JP}U_{QP}),$$

$$f_{\eta\zeta}=\delta_{\eta\zeta}+e_{\mu\eta}e_{\pi\zeta}(B_{J\mu}U_{J\pi}+B_{J\pi}U_{J\mu}+B_{J\pi}B_{Q\mu}U_{JP}U_{QP}) \quad (2)$$

$$\lambda^2=(1+2E_{\eta\zeta}+2e_{\eta\zeta}e_{\pi\mu}E_{\eta\pi}E_{\zeta\mu})^{-1}$$

where, V_0: volume of the triangular element

P_{NK}: generalized node forces of node N, direction K, in local coordinates

$B_{N\alpha}$: node displacement coefficients of node N, direction α, in local coordinates

U_{MK}: element node displacement of node M, direction K in local coordinates

$E_{\alpha\beta}$: Lagrangian strain tensor

λ: extension ratio (the thickness ratio between the deformed and the undeformed membranes)

C_1, C_2: the material constants for Mooney-Rivlin material (rubber)

δ_{ij}: Kronecker delta

$e_{\alpha\beta}$: two-dimensional permutation symbol ($e_{12}=1$, $e_{21}=-1$, $e_{11}=e_{22}=0$)

In eq.(2), Latin and Greek indices range from 1 to 3, and 1 to 2 respectively, and Einstein's rule (the symbol, $\sum$ is dropped) is applied to all indices except M, N and K. The Newton-Raphson method was used to solve the nonlinear equations associated with finite element representations of the pseudo ligament.

RESULTS

Both the measurement and theoretical results were in good agreement. **Figure 2** shows a typical example of the measurement results from the longitudinal(E_{yy}), transverse(E_{xx}) and shear(E_{xy}) components of the strain tensor in the pseudo ligament at 90° of knee flexion. Special attention was paid for the distribution of longitudinal strain as a function of the knee flexion angle, and the following results were obtained. On the anterior side, the region near the femoral bone attachment stretched noticeably at 60° of knee flexion, and almost the entire region along the fiber direction stretched at 90° of knee flexion. On the posterior side, the strain in the region near the femoral bone attachment was noticeable but not near the tibial bone attachment. The strain pattern on the central side showed a decrease from full extension to a minimum value near 30°, a continuation of almost the same value at 60°, then an increase up to 120° of flexion but not full recovery of strain at full extension.

CONCLUSIONS

Stress analysis on the entire surface of the ACL was performed by the measurement for the pseudo ligament and by an application of the finite element method for an noncompressible hyper elastic material. Strain distribution varied, even along the fiber direction, and large strain gradients were observed in the regions near the bone attachments.

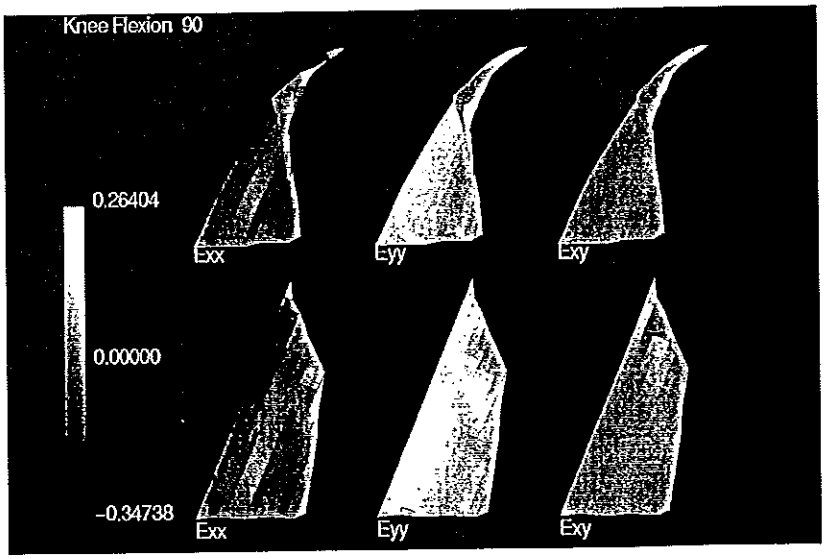

Fig. 2 Distribution of Lagrangian strain tensors of the pseudo ligament at 90° of knee flexion.

DETECTION OF SUDDEN MOVEMENTS OF THE TRUNK DURING A WORKDAY

[1] Hirvonen Mikko , [1] Leskinen Timo, [2] Grönqvist Raoul , [1] Viikari-Juntura Eira
[3] Riihimäki Hilkka. Finnish Institute of Occupational Health, [1] Department of Physiology, [2] Department of Physics, [3] Department of Epidemiology, Vantaa, Finland

INTRODUCTION

Unexpected sudden movements which occur during slips and falls are considered to be one of the causal factors for work-related low-back pain. According to Stobbe and Plummer (1988) slipping and tripping caused 25% of low-back pain in three examined branches of industry (mining, health care, and tyre manufacturing). Manning et al. (1988) found out that slipping accounted for 62% and tripping for 17% of various underfoot accidents.

The purpose of the study was to measure the frequency and intensity of sudden movements during a workday and to investigate their causes. The method of measurement was based on the assessment of the horizontal acceleration of the trunk. A portable device was developed for recording sudden movements at worksites.

METHODS

Horizontal accelerations in medio-lateral and antero-posterior directions were recorded by a two-dimensional accelerometer (Entran EGA125) taped to a subject's lumbar region. The accelerometer was connected to a battery-operated signal conditioning unit including pre-amplifiers and second-order Butterworth bandpass filters for 5 Hz - 100 Hz. The lower frequency limit of the filter was chosen to attenuate most of the acceleration signals during normal gait. The pre-amplifier was connected to a pocket computer (PSION Organizer). The system was equipped with an automatic peak detection and an alarm buzzer. The computer continuously monitored the level of acceleration signals and gave an audible alarm and stored the data if the level of 1 g ($9.81 m/s^2$) was exceeded. The level of 1 g was chosen on the basis of walking experiments on a slipping track which showed that this level was exceeded in most of the slipping incidents (Hirvonen et. al. 1994). As a receipt notification the subjects were asked to press a receipt button after hearing an alarm.

The subjects were selected from a postal inquiry made in 1993 among workers in a large forestry company. From about 7 000 respondents a sample of 18 male subjects were picked, their ages varying from 30 to 40 years, who reported walking more than 5 kilometres during the workday, and who worked mainly indoors. The subjects were given pocket-size forms with questions about the causes of the alarm, and they were asked to fill in a form each time the pocket computer gave an alarm.

RESULTS

During the 18 workdays, 297 incidents were recorded during which the horizontal acceleration exceeded the level of 1 g. The most common causes of reported alarms were jerking (33), walking on stairs (30), walking (26), bounding (17) and lifting (16). Only two of the alarms were caused by slipping.

A third (100) of the alarms were not notified by the subjects. Almost half of the non-receipted alarms (43) occurred to only two persons. According to the subjects they did not always hear the buzzer sound because of the noise of machines and the use of hearing protectors.

DISCUSSION

The results showed that sudden movements similar to those occurring during slips and falls were usual during normal work tasks. The method of measurement of acceleration could not discriminate slips from the sudden movements due to other causes. The causes of high acceleration of the trunk were manifold. Jerks - e.g. when opening the door - were the most common. The acceleration peaks caused by jerks in this study were as high as those recorded during slipping in our previous laboratory study (Hirvonen et al. 1994).

Slips and trips were very unusual: Only two cases were detected in this study consisting of one-day recordings of 18 subjects. Long follow-up times would therefore be needed in an epidemiologic study to investigate the role of slipping in the etiology of low back pain.

REFERENCES

1. Manning, D.P., Ayers, I., Jones, C., Bruce, M. and Cohen, K. (1988) The incidence of underfoot accidents during 1985 in a working population of 10,000 Merseyside people. J. of Occup. Accid. , 10, 121-130.
2. Stobbe, T.J. and Plummer, W. (1988) Sudden movement/unexpected loading as a factor in back injuries. In: F. Aghazadeh (Ed.), Trends in Ergonomics/Human Factors V. , p. 713-720.
3. Hirvonen M., Leskinen T., Grönqvist R., Saario J., 1994. Detection of near accidents by measurement of horizontal acceleration of the trunk. Int. J. of Ind. Erg., 307-314.

MEASUREMENT OF HUMAN POSTURE AND MOVEMENT WITH A SYSTEM BASED ON INDUCTIVE SENSORS

[1] Hirvonen Mikko, [1] Haijanen Jari , [1] Laitinen Heikki , [2] Hietanen Maila
[2] von Nandelstadh Patrick. Finnish Institute of Occupational Health,
[1] Department of Safety, [2] Department of Physics, Vantaa, Finland

INTRODUCTION

New devices based on the use of a magnetic field and inductive coils have been developed to measure human motion. They have the advantage, compared to optical measurement systems, of not having to have a clear line of vision to the measured object.

The aim of the study is to evaluate the precision and usability of one magnetic measurement device, the Flock of Birds (Fob), in measuring human position, orientation and movement. The strength of magnetic fields caused by the Fob transmitter is also evaluated. Previously, Samuelsson et al. (1987) assessed the precision of the Selspot optical infra-red camera system in a respective study.

METHODS

The Fob system is based on the transmitter which sends a pulsed DC-magnetic field and receivers which contain inductive coils for sensing the transmitted magnetic field. The receiver is connected via cable to the control unit which computes the location and orientation of the receiver. Each receiver has its own control unit. One of the control units is defined as a master unit and it controls other units and the transmitter. The whole system is operated and data collected by connecting the master unit to a host computer.

The examined version of the Fob was equipped with an extended range transmitter, the usable measuring range of which is up to 2.4 meters. Each receiver can theoretically make up to 144 measurements per second of its orientation and position but this value is decreased significantly when using an ordinary PC with a single RS232 -port. In this study we used a microcomputer (PC-386SX) which was connected to the Fob system through a single RS-232 cable to control and collect the data.

The static accuracy of the system was measured by using a feeding table (accuracy better than 0.1 mm) to which the Fob sensor was attached. The sensor was moved parallel to the examined axis and the data given by the Fob were compared with the values of the feeding table.

The orientation accuracy was assessed with a lathe chuck made for gearwheel manufacturing (accuracy > 0.25 degrees). A pendulum was used to evaluate the dynamic properties of the system.

The strength of the magnetic field was measured with a magnetic field meter (MFM 10). The measurements were taken from the surface of the cubic-shaped extended range transmitter (ERT) and at regular intervals from 10 to 300 cm. The meter indicates magnetic flux densities in microteslas (μT).

RESULTS

Table 1. Measured mean deviations (N=10) of Fob position and orientation data from the actual values of the feeding table and lathe chuck. *Sensor distance from varied between 70-110 cm .

	Sensor distance 100 cm		Sensor distance 230 cm	
Axis direction	Rotation (degrees)	Position (mm)	Rotation (degrees)	Position (mm)
x *	0.3	1.8	-----	-----
y	0.1	1.9	-----	18.8
z	0.1	2.4	0.4	-----

Dynamic tests showed that the Fob system could measure slow motion of the used pendulum (T=2.4 s) reliably.

The flux density of measured magnetic field varied from 1.4 mT on the surface of the ERT to the 0.5 μT at a distance of 300 cm.

DISCUSSION

The static accuracy of the Fob measurement system is good. Its orientation accuracy is even better than that of optical measurement systems. The orientation can be measured with only one sensor unlike optical measurement systems which normally require two separate sensors attached to the object.

The dynamic measurement rate of the Fob system is quite moderate (our system 45 Hz with two sensors). It is not enough for studying rapid movements like jumping. Fob can be used in measuring slower movements and static measurements like studying working postures. Attachment of the Fob's quite large sensors might be difficult especially for small flexible surfaces like the palm of the hand. The connecting cables of the sensors are an other restriction of the system because they limit the test person's movements.

The Fob system can also be connected directly to human modeling software called "Jack" which runs in an effective graphical workstation environment. This gives the system a lot of new possibilities for animation and analysis purposes.

The magnetic field caused by the transmitter is quite strong near the equipment. Comparable fields can be found close to inductive ovens or welding machines in industrial plants. According to ACGIH recommendations for an extremely-low-frequency (ELF) magnetic field, the magnetic flux density should not exceed 0.59 mT (102 Hz). Due to the lack of exact knowledge on the biological effects of ELF-fields, it is advisable that exposure to magnetic fields should not exceed 0.01 mT constantly. This corresponds to the strength of the magnetic field at a distance of one metre from the ERT.

REFERENCES

1. ACGIH - American Conference of Governmental Industrial Hygienist : 1994-1995 Threshold Limit Values for Chemical Substances and Physical Agents and Biological Exposure Indices.
2. Samuelsson B., Wangheim M., Wos H. (1987) A device for three-dimensional registration of human movement, Erg. , vol. 30, no.12, 1655-1670.

Mathematical Analysis of Errors Inherent in the Use of Euler Angles in Measuring Joint Motion

Hollerbach K, Hollister AM
Lawrence Livermore National Laboratory, Livermore, California USA

Introduction

Measurements of human joint motion should include measurement of movements of the joints' mechanisms. Euler angles calculated from anatomic coordinates have been used to describe joint motion and to calculate forces and moments [2]. Accurate placement of the observer coordinates on human limbs is difficult, resulting in misalignment of the reference frame with the joint mechanism. Furthermore, several human joints have been shown to move about fixed revolutes that are not parallel to anatomic coordinates [1, 3, 4, 5, 6]. In both cases, errors will be introduced, because the Euler coordinates are not coincident with the joint's axes of rotation. These errors can be evaluated by comparing the rotations about arbitrary axes with different offsets to calculated Euler angles for the movements, resulting in the net rotation matrix, $R_{k\theta}$.

Methods

Rotations of a body moving about an arbitrary axis in a reference frame are determined by the axis' α and β angles of offset from the reference frame and the θ_k angle of rotation about the arbitrary axis, k (Fig. 1). The rotation about the arbitrary axis may be obtained by first rotating the axis into one of the reference axes, then rotating about the reference axis, and then undoing the first rotation by rotating the arbitrary axis back into its original position.

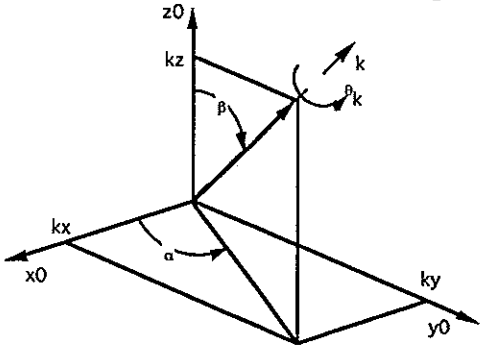

$$R_{k\theta} = \begin{bmatrix} k_x^2 v_\theta + c_\theta & k_x k_y v_\theta - k_z s_\theta & k_x k_z v_\theta + k_y s_\theta \\ k_x k_y v_\theta + k_z s_\theta & k_y^2 v_\theta + c_\theta & k_y k_z v_\theta - k_x s_\theta \\ k_x k_z v_\theta - k_y s_\theta & k_y k_z v_\theta + k_x s_\theta & k_z^2 v_\theta + c_\theta \end{bmatrix}$$

where $v_\theta = 1 - c_\theta$

Figure 1: Rotation about an arbitrary axis.

Euler angles are rotations of the reference frame (Fig. 2); results are dependent on the sequence of coordinate rotations. The orientations of the body in space relative to the reference frame can be calculated, and the Euler angles for the reference frame can be determined and compared to demonstrate the anticipated errors due to misalignment of the reference coordinates with the joint mechanism.

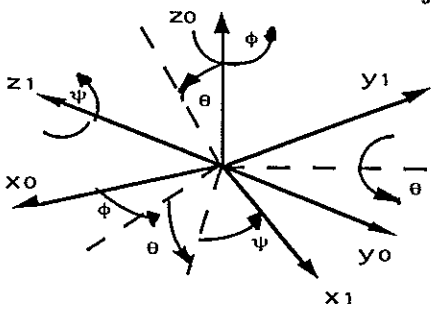

$$R_E = \begin{bmatrix} C\phi C\theta C\psi - S\phi S\psi & -C\phi C\theta S\psi - S\phi C\psi & C\phi S\theta \\ S\phi C\theta C\psi + C\phi S\psi & -S\phi C\theta S\psi + C\phi C\psi & S\phi S\theta \\ -S\phi S\psi & S\phi C\psi & C\theta \end{bmatrix}$$

Figure 2: Euler angle representation.

The matrices for rotation about an arbitrary axis and the resulting Euler angle determinations were performed with programs written with LabView 3.0 (National Instruments) on a Macintosh Quadra 840. The programs allowed changes to be made in the α and β offset angle for the axis and calculated the rotations for 180° of θ_k rotation about the axis. Euler angles were calculated and displayed as a function of θ_k.

Results

With 0° α and β offsets, the Euler angles correspond with the θ_k rotations. With rotation about a single arbitrary axis with 10° this relationship breaks down: α and β offset angles produces rotations about all three Euler coordinates, and the relationships are nonlinear (Fig. 3).

Different results are obtained if the α and β offsets are 80°, even though the axis lies within 10° of a reference coordinate (Fig. 4). However, rotations about all three Euler coordinates are seen again for rotation about a single offset revolute. 30° α and β offsets produce even larger differences than do 10° offsets (Fig. 5). Even 5° of α and β offsets produce significant error (Fig. 6).

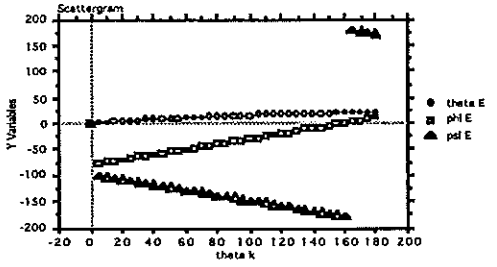

Figure 3: α and β = 10°

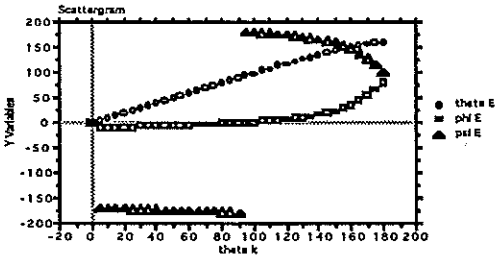

Figure 4: α and β = 80°

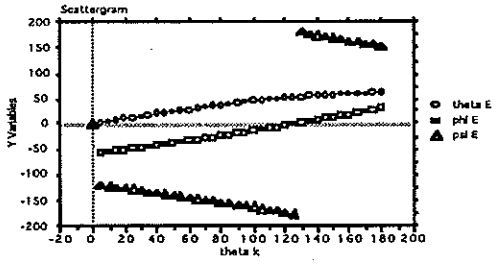

Figure 5: α and β = 30°

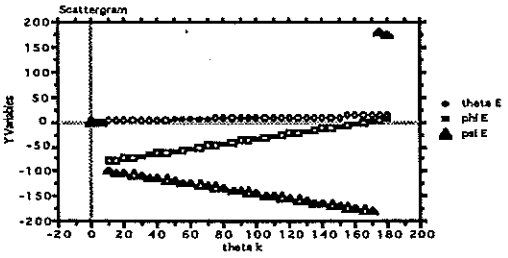

Figure 6: α and β = 5°

Discussion

There are many sources of error in the measurement of human joint movements. Minimizing these errors is important since the measurements are used to model human limb motion and calculate joint forces and moments. If Euler angles are used to represent joint rotations, proper alignment of the coordinate reference frame with the joint mechanism is essential. Even small offsets will introduce significant error. Misalignment of the coordinates with the joint axis produces errors in the displacement observed as well. The nature of the joint mechanism must also be understood. If the joint motion is about a single offset revolute, such as the tibiotalar joint or the elbow, Euler angles can be used to accurately represent the motion, if the first Euler coordinate is aligned with the joint's axis of rotation. Joints with more than degree of freedom, such as the thumb carpometacarpal joint, pose a more serious problem. These joints do not have a single path but have an envelope of motion defined by motion about both axes simultaneously. If the axes are not perpendicular or do not intersect, simple Euler angle calculations cannot represent the movements of the joint mechanism.

References

[1] Fick A (1854) Die Gelenke mit sattelformigen Flachen. Zeitschrift fur Rationelle Medizin. Heidelberg, Akadem Verlagshandlung v C. F. Winter, 314-21.

[2] Grood ES, Suntay WJ (1983) A joint coordinate system for the clinical description of three-dimensional motions: application to the knee. J Biomech Eng, **105(2)**:136-44.

[3] Hollister A, Buford, WL, Myers, LM, Giurintano, DJ, Novick, A, (1991) The axes of rotation of the thumb carpometacarpal joint, J Orth Res, **10**:445-460.

[4] Hollister AM, Jatana S, Singh AK, Sullivan WS, Lupichuk,A (1993) The axes of rotation of the knee, Clin Orthop, **290**:259-268.

[5] Inman VT (1976) The joints of the ankle. New York, Williams and Wilkins

[6] London JT (1981) Kinematics of the elbow, J Bone Joint Surg, **63-A**:529-35.

COMPUTER MODEL OF THE KNEE WITH TWO FIXED OFFSET REVOLUTES FOR TIBIOFEMORAL MOTION

Anne Hollister, Rancho Los Amigos, Downey, California, Mari Truman, Arthromotion, Warsaw, Indiana and Louise Focht, Sutter Corporation, San Diego, California USA

Recent publications have suggested that knee motion occurs about two fixed offset axes of rotation. The flexion-extension axis is in the femur under the epicondyles and is directed distal and posterior from medial to lateral. The longitudinal rotation axis is fixed relative to the tibia and exits through the anterior cruciate ligament insertion. These axes are not perpendicular to the bones or to each other and do not intersect.

Bearing surfaces of mechanisms which move about axes of rotation are surfaces of revolution of those revolutes. The revolutes of most man made mechanisms are perpendicular to each other and parallel to the surfaces. With modern computer aided design (CAD) and engineering (CAE) technology, it is possible to produce surfaces of revolution for offset revolutes. Surfaces of revolution for the two tibiofemoral revolutes and the patellofemoral axis were made using a HP 9000 series workstation and Structural Dynamics Research Corporation's Ideas Master Series CAD/CAE software. The femoral surface includes a tibiofemoral surface, a patellofemoral surface and a transition zone between the patellofemoral and tibiofemoral joints. The lateral femoral condyle is smaller than the medial and the posterior condyles are circular when sectioned perpendicular to the FE axis. The tibia has a swept surface including motion about both tibiofemoral revolutes and an anterior portion to articulate with the femoral transition zone when the knee is in extension. This surface resembles a combination of both tibial bone and menisci.

CAE analysis of the joint model shows a range of FE from -5 to 120°. There is no internal (IR) or external (ER) rotation in extension and 20° IR to 10° ER at 60° of knee flexion. Movements of the tibia on the femur include varus and valgus, internal and external rotation as well as flexion and extension. The screw home mechanism described by Grood occurs as the joint is extended. The joint has AP and lateral stability in both flexion and extension and is very congruous. Bezier curvature analysis of the medial femoral condyle sagittal plane curvature give similar results to anatomic studies. The surface of the medial condyle includes the tibiofemoral and patellofemoral curves. Both of these curves are elliptical since their rotation axes are not perpendicular to the sagittal plane.

This mathematical representation of the knee should aid in understanding knee joint mechanics and the functions of its anatomic structures.

References

(1) Elias, S.G., Freeman, M.A.R., and Gokcay, E.I.: A Correlative Study of the Geometry and Anatomy of the Distal Femur. Clin. Orth. and Rel. Res. 260:98-103, 1990.
(2) Goodfellow
(3) Hollister, A., Jatana, S., Singh, A., Sullivan, W., and Lupichuk, A.: The Axes of Rotation of the Knee, Clinical Orthopaedics and Related Research, No. 290; 259-268, 1993a.
(4) Piegel, L., Tiller, W., Curve and Surface Construction Using Rational B-splines, Computer Aided Design, 1987 Vol. 19, No. 9, pp. 485-498.
(5) Tiller, W., Geometric Modeling Using Non-uniform Rational B-splines: Mathematical Techniques, SIGGRAPH'86 Tutorial Notes, Dallas, USA, 1986.

(6) Tiller, W., Rational B-splines for Curve and Surface Representation, IEEE Comput. Graph Applic., 1983, Vol. 3, No. 6, pp. 61-69.

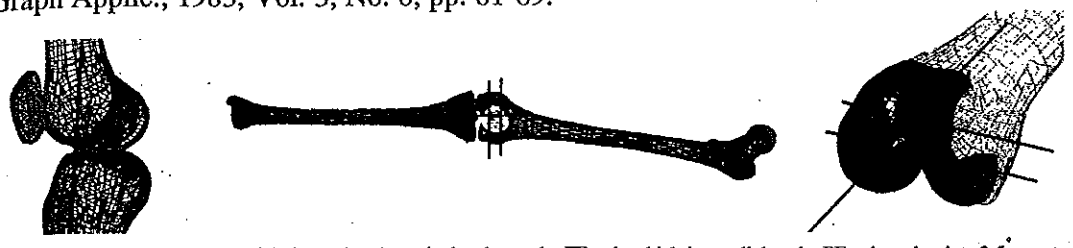

Figure 1 There are three axes which determine the articular shape, the FE axis which is parallel to the PF axis and points 3.5° posterior and inferior from medial to lateral. The tibiofemoral joint moves about the longitudinal rotation axis (LR) and the FE axis. The axes are shown here in the bones.

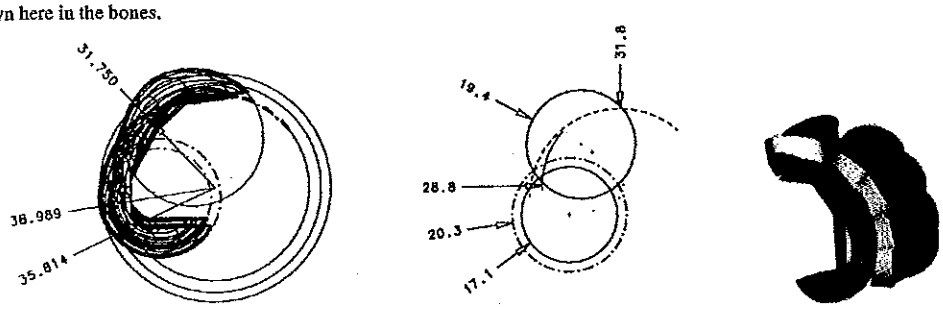

2a 2b 2c

Figure 2a & 2b The femoral surface includes curvatures of both the PF and the TF joints. These wire frames show projections of the primary curves (normal to the FE axis) in the femur. Note that the patella articulates with different regions of the femur, yet still maintains a fixed FE axis of motion as it dips into the intercondylar notch region during deep flexion maneuvers. 2c Patellar model transitioning from lateral and central articular contact to medial and lateral contact during flexion motion (medial-to -lateral isometric view).

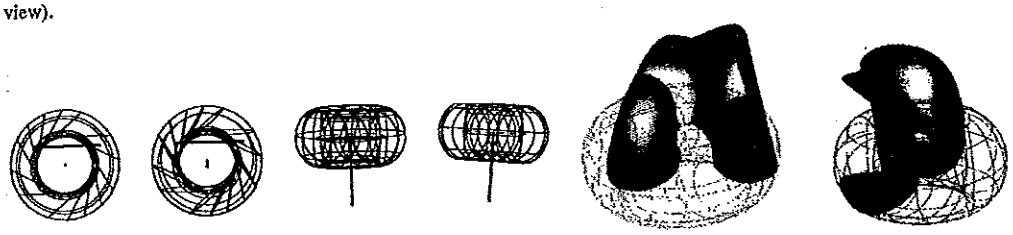

3a 3b

Figure 3 Tibio-femoral spacial motion: 3a The tibio-femoral surfaces are torroidal, and reflect the revolutes for the joint shown here (4 views of medial revolute for left knee). The torriods are rather flat because the axes are nearly perpendicular to, and offset from each other. 3b The revolutes for tibio-femoral motion superimposed about each posterior femoral condyle.

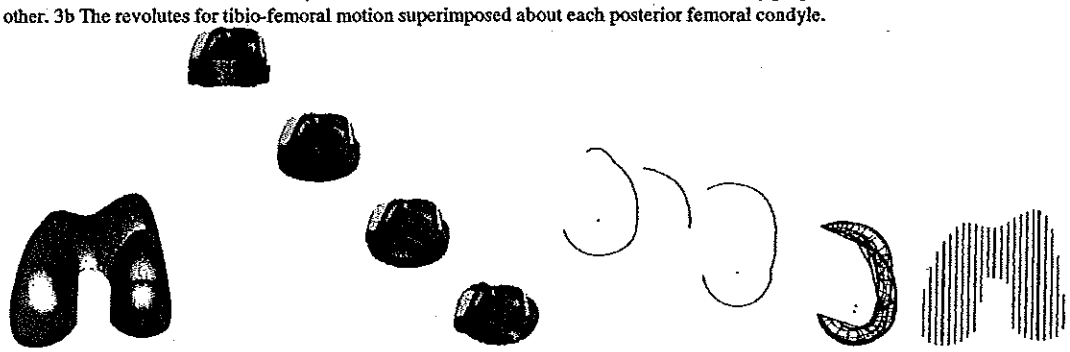

4a 4b 4c

Figure 4 Femoral shape: 4a The joint surfaces are shown with the tibio femoral, patellofemoral and transition zones highlighted. Figure 4b The screw home mechanism with external rotation of the tibia with knee extension. 4c Bezier curvature analysis of the midportion medial femoral condyle in the sagittal plane shows good correlation with published data[2].